

In compliance with the
Canadian Privacy Legislation
some supporting forms
may have been removed from
this dissertation.

While these forms may be included
in the document page count,
their removal does not represent
any loss of content from the dissertation.

Characterization and Regulation of the Early Secretory
Pathway by the p24 proteins

Jennifer Nicole Gushue

Department of Anatomy and Cell Biology
McGill University, Montreal

November 2002

A thesis submitted to the Faculty of Graduate Studies and Research in partial fulfillment
of the requirements of the degree of Doctor of Philosophy

©Jennifer Nicole Gushue 2002



National Library
of Canada

Bibliothèque nationale
du Canada

Acquisitions and
Bibliographic Services

Acquisitions et
services bibliographiques

395 Wellington Street
Ottawa ON K1A 0N4
Canada

395, rue Wellington
Ottawa ON K1A 0N4
Canada

Your file Votre référence

ISBN: 0-612-88483-X

Our file Notre référence

ISBN: 0-612-88483-X

The author has granted a non-exclusive licence allowing the National Library of Canada to reproduce, loan, distribute or sell copies of this thesis in microform, paper or electronic formats.

L'auteur a accordé une licence non exclusive permettant à la Bibliothèque nationale du Canada de reproduire, prêter, distribuer ou vendre des copies de cette thèse sous la forme de microfiche/film, de reproduction sur papier ou sur format électronique.

The author retains ownership of the copyright in this thesis. Neither the thesis nor substantial extracts from it may be printed or otherwise reproduced without the author's permission.

L'auteur conserve la propriété du droit d'auteur qui protège cette thèse. Ni la thèse ni des extraits substantiels de celle-ci ne doivent être imprimés ou autrement reproduits sans son autorisation.

Canada

Table of Contents

Abstract	7
Resumé.....	8
Preface – Contribution of Authors	9
Acknowledgments.....	11
List of Figures	12
List of Tables	14
Abbreviations	15
Introduction.....	21
Literature Review.....	26
1. The Secretory Pathway	27
1.1. The Endoplasmic Reticulum.....	27
1.1.1. The Rough Endoplasmic Reticulum	28
1.1.1.1. Sugar Modifications.....	29
1.1.1.2. Retrieval Sequences.....	30
1.1.1.3. Misfolding.....	30
1.1.2. The Smooth Endoplasmic Reticulum	31
1.1.3. The Transitional Endoplasmic Reticulum	31
1.1.4. ER Cargo Exit Sites	32
1.2. The Intermediate Compartment	32
1.2.1. Roles of the Intermediate Compartment	33
1.3. The Golgi Apparatus.....	34
1.3.1. Golgi Structure.....	34
1.3.2. Golgi Composition.....	35
1.3.3. Golgi Lipids	36
1.3.4. Disease	37
2. The <i>Saccharomyces cerevisiae</i> Secretory Pathway	38
2.1. The Yeast Endoplasmic Reticulum.....	38
2.2. The Yeast Golgi Apparatus.....	40

2.2.1. Glycosylation	41
2.2.2. Biochemical distinctions	42
3. Membrane Biogenesis and Regulation	44
4. Components of the Secretory Pathway	47
4.1. COPI	47
4.2. COPII	49
4.3. SNAREs, NSF and Rabs	50
4.3.1. SNAREs	50
4.3.2. NSF	51
4.3.3. Rabs	52
4.4. The p24 Family	53
4.4.1. Mammalian	53
4.4.2. <i>Saccharomyces cerevisiae</i>	56
4.4.3. <i>Caenorhabditis elegans</i>	59
4.4.4. <i>Xenopus laevis</i>	60
4.4.5. <i>Fugu rubripes</i> , <i>Anguilla anguilla</i> and <i>Cyprinus carpio</i>	61
4.4.6. <i>Polyphondylium pallidum</i> and <i>Dictostelium discoideum</i>	61
4.4.7. Other Species	62
4.4.8. Cell Free Systems	62
5. The p24s and the Secretory Pathway	66
CHAPTER 1.	68
Calnexin and rp24 α 2 Associate with the Ribosome	68
1.1. Abstract	69
1.2. Introduction	70
1.3. Results	72
1.3.1. Calnexin and rp24 α 2 are ribosome associated proteins	72
1.3.2. Morphology and morphometry of the isolated membranes	72
1.3.3. Calnexin's association with the ribosome is independent of the nascent peptide chain, while rp24 α 2's association is dependent on newly synthesized cargo	78
1.4. Discussion	81

1.5. Materials and Methods.....	83
1.5.1. Reagents and antibodies.....	83
1.5.2. Subcellular fractionation.....	83
1.5.3. Immunoprecipitations	84
1.5.4. Analysis of ribosome-associated membrane proteins.....	84
1.5.5. Electron Microscopy.....	85
CHAPTER 2.	86
Reconstitution of the Morphological	86
Changes of the Early Secretory Pathway.....	86
2.1. Abstract.....	87
2.2. Introduction.....	88
2.3. Results.....	90
2.3.1. Distribution of soluble cargo and integral membrane proteins in reconstituted ER system.....	90
2.3.2 Localization of p97 and Syntaxin 5	91
2.4. Discussion.....	97
2.5. Materials and Methods.....	99
2.5.1. Preparation and Characterization of Microsomes.....	99
2.5.2. Cell-free Incubation Conditions.....	99
2.5.4. Analysis of Gold Label Distribution.....	100
2.5.5. Antibodies.....	101
CHAPTER 3.	102
The p23 Compartment is the Site of Golgi Enzyme Retrieval	102
3.1. Abstract.....	103
3.2. Introduction.....	104
3.3. Results.....	105
3.3.1. Immunoisolation of ER/Golgi intermediates with p23 antibodies ...	105
3.3.2. Co-immunoisolation of VSV-G and Golgi enzymes with p23.....	108
3.4. Discussion.....	111
3.5. Materials and Methods.....	112
3.5.1. Cell Growth.....	112

3.5.2. VSV Infection	112
3.5.3. Pulse–Chase Labeling.....	112
3.5.4. Preparation of Cisternal wt Golgi Membranes	113
3.5.5. Electron Microscopy.....	113
3.5.6. Immunoisolation of Membranes	114
CHAPTER 4.	115
Identification of Novel Golgi Membrane Proteins and Cargo Concentration in Pre-Golgi Compartment.....	115
4.1. Introduction.....	116
4.2. Abstract.....	117
4.3. Results.....	118
4.3.1. Morphometric analysis of Golgi fractions	118
4.3.2. Immunoisolation of novel membrane proteins	118
4.4. Abstract.....	125
4.5. Results.....	126
4.5.1. The Major Site of Cargo Concentration in Hepatocytes is Within the Golgi Apparatus	126
4.5.2. β -COP Localization is Largely Distinct from that of Secretory Cargo In Rat Liver Golgi Apparatus in situ.....	127
4.5.3. Analysis of β -COP, Albumin, rp24 α 2, and ERD2 in Purified Golgi Fractions.....	128
4.6. Discussion	138
4.7. Materials and Methods.....	140
4.7.1. Isolation of Golgi Fractions	140
4.7.2. Antibodies	140
4.7.3. EM Immunolocalization and Morphometry	141
4.7.4. Preparation of Liver Samples for Cryoimmune EM.....	141
4.7.5. Antibody Dilutions.....	142
4.7.6. Analysis of Gold Label.	142
CHAPTER 5.	144
Morphological Analysis of p24 Mutants	144

5.1. Introduction.....	145
5.2. Results.....	147
5.2.1. The p24 Family.....	147
5.2.2. Morphological Analysis of p24 Mutants	151
5.2.3. Morphological Analysis of p24 Overexpressors.....	151
5.2.4. Cryo-immunolabeling of Overexpressors with Anti-Erv25p	157
5.2.5. Cryo-immunolabeling Analysis of the Overexpressors.....	157
5.2.6. Plasmid Instability	159
5.2.7. Quantitation of ERV25 Overexpressors	160
5.3. Discussion.....	173
5.4. Materials and Methods.....	176
5.4.1. Strains, Plasmids and Growth Media.....	176
5.4.2. Antibodies	176
5.4.3. Yeast Transfection	176
5.4.4. Routine Electron Microscopy	177
5.4.5. Cryoimmune Electron Microscopy.....	177
5.4.6. Plasmid Stability	178
CHAPTER 6.	180
Genetic Expression Profiles of p24 Mutants	180
6.1. Introduction.....	181
6.2. Results.....	183
6.2.1. Yeast ORF Microarrays	183
6.2.2. The DNA Microarray System.....	183
6.2.3. Quality Control and Statistical Analysis.....	191
6.2.4. Microarray Analysis.....	209
6.2.5. Gene Deletion Analysis	219
6.2.6. Over expression of ERV25	220
6.3. Discussion.....	232
6.4. Materials and Methods.....	234
6.4.1. Strains, Plasmids and Growth Media.....	234
6.4.2. Microarrays	234

6.4.3. Cell Cultures for RNA Isolation	234
6.4.4. RNA Isolation for DNA Microarrays	235
6.4.5. cDNA Synthesis and Hybridization of Microarrays.....	236
6.4.6. Scanning of Microarray Slides and Analysis.....	237
Discussion	238
The p24 proteins: from the ER to the Golgi and back	238
The Endoplasmic Reticulum.....	239
Exit from the Endoplasmic Reticulum.....	240
The Intermediate Compartment	241
The Golgi Apparatus.....	242
<i>Saccharomyces cerevisiae</i>	244
Proposed Role of the p24 Proteins.....	246
Conclusions.....	249
Original Contributions	251
References	253
Appendix 1.....	294

Abstract

The secretory pathway of dog pancreas, liver parenchyma, cultured CHO cells and yeast has been analyzed with reagents focusing on the p24 family of membrane proteins. The results show that at least one of the p24s is ribosome associated in a nascent chain dependent manner. The cell free reconstitution of the endoplasmic reticulum (ER) cargo exit sites has demonstrated that the p24s are involved in the generation of both the cargo exit sites and vesicular tubular clusters (VTCs) in a COPI dependent manner. Work done *in situ* and in isolated subcellular fractions has indicated that the p24-enriched *cis* Golgi compartment is the primary site of retrieval of Golgi resident enzymes during membrane maturation as well as being the boundary for the major site of cargo (albumin) concentration. The morphogenic properties of the p24s were studied in yeast, with DNA chip analysis revealing 160 genes whose expression was altered coincident with the perturbation of members of the p24 family. Over expression of one of the members of the p24 family has led to the increase in ER membranes and a p24 enriched VTC compartment. Taken together, these data indicate that the p24s are present both when newly synthesized cargo enter and exit the ER and that the p24s are involved in the morphological transitions of the early secretory pathway.

Resumé

La voie sécrétrice du pancréas canin, du parenchyme hépatique, de cellules CHO cultivées et de la levure a été analysée à l'aide de réactifs visant la famille de protéines membranaires p24. Les résultats indiquent qu'au moins une des p24 présente un lien ribosomal dépendant d'une chaîne naissante. La reconstitution acellulaire des sites de sortie de cargo du réticulum endoplasmique (RE) a montré que les p24 interviennent dans la formation des sites de sortie du cargo et des groupes vésiculo-tubulaires (GVT) de façon COPI-dépendante. Des travaux réalisés *in situ* et sur des fractions subcellulaires isolées ont indiqué que le compartiment cis golgien enrichi en p24 est le principal lieu de récupération des enzymes résidentes de l'appareil de Golgi pendant la maturation membranaire et forme la bordure du principal site de concentration de cargo (albumine) du parenchyme hépatique. Les propriétés morphogéniques des p24 ont été étudiées dans la levure; des analyses réalisées à l'aide de puces à ADN ont révélé une modification de l'expression de 160 gènes compatible avec la perturbation de membres de la famille p24. La surexpression d'un des membres de cette famille a entraîné l'expansion du RE et la formation d'un compartiment à GVT enrichi en p24. Ensemble, ces résultats indiquent que les p24 sont présentes lorsque le cargo nouvellement synthétisé entre dans le RE et en sort et que les p24 interviennent également dans les transitions morphologiques des premières étapes de la voie sécrétoire.

Preface – Contribution of Authors

The work presented in this thesis is my own original contribution with the exception of:

1. The work presented in Chapter 1 is part of a paper published by Oxford University Press (Chevet E, Wong HN, Gerber D, Cochet C, Fazel A, Cameron PH, Gushue JN, Thomas DY, and Bergeron JJ. Phosphorylation by CK2 and MAPK enhances calnexin association with ribosomes. *EMBO J.* 1999 Jul 1;18(13):3655-66.). The isolation of microsomes, immunoblots and quantitation of ribosomes from isolated fractions were performed by Dr. Eric Chevet.
2. The work presented in Chapter 2 is part of a paper published by the Rockefeller University Press (Lavoie C, Paiement J, Dominguez M, Roy L, Dahan S, Gushue JN, and Bergeron JJ. Roles for $\alpha 2p24$ COPI in endoplasmic reticulum cargo exit site formation. *J Cell Biol.* 1999 Jul 6;146(2):285-99) and a paper published by the American Society for Cell Biology (Roy L, Bergeron JJ, Lavoie C, Hendriks R, Gushue J, Fazel A, Pelletier A, Morre DJ, Subramaniam VN, Hong W, Paiement J. Role of p97 and syntaxin 5 in the assembly of transitional endoplasmic reticulum. *Mol Biol Cell.* 2000 Aug;11(8):2529-42). The isolated membrane fraction that was used for the electron microscopy was obtained from Dr. Christine Lavoie and Ms. Line Roy.
3. The work presented in Chapter 3 is part of a paper published by the Rockefeller University Press (Lin CC, Love HD, Gushue JN, Bergeron JJ, Ostermann J. ER/Golgi intermediates acquire Golgi enzymes by brefeldin A-sensitive retrograde transport in vitro. *J Cell Biol.* 1999 Dec 27;147(7):1457-72). The immuno-isolated membranes used for electron

microscopy were obtained from Dr. Harold Love. The phosphorimaging and Western blot were done by Dr. Chung-Chih Lin.

4. The first part of the work presented in Chapter 4 is part of a paper published by the American Society for Biochemistry and Molecular Biology (Bell AW, Ward MA, Blackstock WP, Freeman HN, Choudhary JS, Lewis AP, Chotai D, Fazel A, Gushue JN, Paiement J, Palcy S, Chevet E, Lafreniere-Roula M, Solari R, Thomas DY, Rowley A, and Bergeron JJ. Proteomics characterization of abundant Golgi membrane proteins. J Biol Chem. 2001 Feb 16;276(7):5152-65). The second study presented in Chapter 4 is part of a manuscript to be submitted. The *in situ* work and quantitations were carried out by both Dr. Sophie Dahan and J.N. Gushue. The WNG fraction was isolated for both studies by Mr. Ali Fazel.
5. The PCR and test for plasmid toxicity in Chapter 5 were performed by Ms. Edith Garneau.
6. The hierarchical clustering, Venn diagrams and spreadsheets for statistical manipulations were produced by Dr. Andre Nantel (Chapter 6).

Acknowledgments

I would like to thank Dr. John Bergeron for the opportunity to work in his laboratory and for launching my scientific career. His enthusiasm and fervor for science as well as his vast knowledge of the field has been most appreciated.

I would like to thank Dr. Sophie Dahan and Ms. Jennifer Hassard for spending many hours teaching me scientific techniques and for providing insight.

I would like to acknowledge my collaborators Dr. Eric Chevet, Mr. Ali Fazel, Dr. Michel Dominguez, Dr. Andre Nantel, Dr. Sandrine Palcy, Ms. Pamela Cameron, Dr. Jaques Paiement, Ms. Line Roy, Dr. Christine Lavoie, Dr. Joachim Ostermann, and Dr. Alexander Bell who have all shared scientific insights. I would also like to acknowledge Ms. Edith Garneau and Ms. Jeannie Mui for their meticulous work.

Thank you to Dr. David Thomas, Dr. Gordon Shore, Dr. Malcolm Whiteway, Mr. Daniel Tessier, Dr. Charles Barlowe, and Dr. Adele Rowley for sharing their knowledge and time to help advance this project.

Financial assistance was provided by the McGill Department of Medicine Studentship and the Fonds pour la Formation de Chercheurs et l'Aide à la Recherche Scholarship.

To my family, without their support this would not have been possible. I am deeply indebted to Mr. Mark Barrell, Mr. Michael Gushue, and Ms Micheline Gushue.

List of Figures

Figure i. Summary the effects of the p24s on the secretory pathway.....	65
Figure 1.1. rp24 α 2 and calnexin association with ribosomes.....	74
Figure 1.2. Ribosome removal from canine pancreatic rough microsomes.....	76
Figure 1.3. Characterization of rp24 α 2 and calnexin association with ribosomes	80
Figure 2.1. Concentration of albumin, transferrin, rp24 α 2, ribophorin, and calnexin in tER.....	93
Figure 2.2. Localization of syntaxin 5 within reconstituted tER.....	96
Figure 3.1. Immunoisolation of the p23 compartment.....	107
Figure 3.2. Immunoisolation of VSV-G and Golgi marker enzymes with p23 cytoplasmic tail antibodies.....	110
Figure 4.1. Electron micrograph of WNG fraction.....	121
Figure 4.2. Localization of GPP34 in the Golgi fraction.....	124
Figure 4.3. Mean labeling density of albumin in the rough ER, smooth ER, Golgi- associated tubular compartment and the Golgi apparatus.....	131
Figure 4.4. <i>In situ</i> distribution of albumin and β -COP within liver hepatocyte Golgi apparatus.....	133
Figure 4.5. Distribution of albumin, β -COP, and rp24 α 2 in purified rat liver Golgi fraction.....	135
Figure 4.6. Percent distribution of β -COP, rp24 α 2, ERD2 and albumin in the WNG Golgi fraction.....	137
Figure 5.1. Alignments of cytosolic tails of p24s.....	149
Figure 5.2. Morphological Analysis of the p24 deletion strains of <i>Saccharomyces cerevisiae</i>	154
Figure 5.3. Morphological Analysis of <i>S. cerevisiae</i> Overexpressing ERV25.....	156
Figure 5.4. Erv25p localization in ERV25 expressing cells.....	163
Figure 5.5. Immunolabeling of ER profiles in ERV25 overexpressing cells.....	165

Figure 5.6. Quantitation of ER membrane proliferation and Erv25p labeling....	168
Figure 5.7. Cell section without membrane network.....	170
Figure 5.8. Quantitation of the incidence of nuclei in cell section.....	172
Figure 6.1. Schematic representation of the preparation of DNA microarrays....	186
Figure 6.2. RNA isolation for gene expression analysis.....	188
Figure 6.3. Confocal laser image of a DNA microarray.....	190
Figure 6.4. Schematic representation of data analysis.....	196
Figure 6.5. QuantArray Image of DNA Microarrays.....	198
Figure 6.6. Enlarged image of subarray.....	200
Figure 6.7. Intensity Scatter Plot of ERV25 Overexpressor (36h).....	202
Figure 6.8. Expression profiles of the p24 genes.....	204
Figure 6.9. PCR analysis of the p24 deletion strains.....	206
Figure 6.10. Inherent variability in DNA microarrays.....	208
Figure 6.11. GeneSpring Analysis.....	212
Figure 6.12. Hierarchical clustering of 160 p24-modulated genes	214
Figure 6.13. Schematic of modulated genes for the single deletion strain.....	223
Figure 6.14. Schematic of modulated genes for the quadruple deletion strain.....	225
Figure 6.15. Schematic of modulated genes for the complete deletion strain.....	227
Figure 6.16. Schematic of modulated genes for 24h ERV25 overexpressor.....	229
Figure 6.16. Schematic of modulated genes for the 36h ERV25 overexpressor.....	231

List of Tables

Table 1.1. Quantitation of membrane-bound ribosomal particles at the surface of ER microsomes.....	77
Table 2.1. Amount of Soluble Cargo and Integral Membrane Proteins in Reconstituted tER.....	94
Table 4.1. Morphometric Analysis of the WNG fraction.....	122
Table 5.1. Species containing p24 genes.....	150
Table 5.2. Stability of the p426-ERV25 plasmid.....	166
Table 5.3. Yeast Strains.....	179
Table 6.1. RNA preparations.....	194
Table 6.2. Genes Modulated in the Deletion Strains.....	215
Table 6.3. Genes Modulated in the ERV25 Overexpressors.....	216
Table 6.4. Degree of Conservation of the Modulated Genes	217
Table 6.5. Gene list from Figure 6.12.....	218

Abbreviations

A – Alanine

a.a. - Amino acids

AAA - ATPase associated with various cellular activities

AD - Alzheimer's disease

Ala – Alanine

ALS - Amyotrophic Lateral Sclerosis

Anp1 - Aminonitrophenyl propanediol

APP - Amyloid precursor protein

ARF – Adenosine diphosphate ribosylation factor

Arg – Arginine

Asn – Asparagine

ATP – Adenosine triphosphate

ATPase – Adenosine triphosphatase

BACE - β -site APP cleaving enzyme

BFA – Brefeldin A

BiP – Binding protein

BST - Bypass of SEC13

COP – Coatamer protein

cDB - EST database for *Dictostelium discoidem*

cDNA – Complementary deoxyribonucleic acid

CGN – Cis-Golgi network

CMP – Cytidine monophosphate

CNX – Calnexin

CPY – Carboxy peptidase Y

CTX - Cholera toxin

Cy - Cyanine

Cys – Cysteine

d - day

dCTP - Deoxy-cytosine triphosphate

DGT1 - Delayed GPI-anchored protein transport
DEPC – Diethyl pyrocarbonate
DPBS - Delbosco's phosphate buffered saline
DTT - Dithiothreitol
EDTA – Ethylenediamine tetra-acetic acid
EM – Electron microscopy
EMP24 - Endomembrane protein of the precursor of 24 kDa
ER - Endoplasmic reticulum
ERAD – ER-associated degradation
ERGIC – ER to Golgi intermediate compartment
ERK1 – Extracellular-signal regulated kinase-1
ERO1- ER oxidoreductin 1
ERp – Endoplasmic reticulum protein
Erp - Emp24p- and Erv25p-related proteins
ERS-24 – Endoplasmic Reticulum SNARE of 24 kDa
Erv25p – ER vesicle protein of 25 kDa
Erv29p – ER vesicle protein of 29 kDa
EST – Expressed Sequence Tags
EsRM – EDTA striped rough microsomes
FALS - Familial amyotrophic lateral sclerosis
FKB2- FK506 binding
G1 – Growth phase 1
GA - Golgi apparatus
GalT - Galactosyl transferase
GAP – GTPase-activating protein
Gas1p - Glycophospholipid-anchored surface protein
GDI – GDP dissociation inhibitor
GDP – Guanosine diphosphate
GEF - Guanine nucleotide exchange factor
GERL – Golgi-endoplasmic reticulum-lysosome
Glc – Glucose

GlcNac – N-acetylglucosamine
 Glu – Glutamic acid
 gp25L – Glycoprotein of 25 kDa low
 GP27 - Glycoprotein of 27 kDa
 GPI - Glycosylphosphatidyl inositol
 GRASP – Golgi reassembly stacking protein
 GTP – Guanine triphosphate
 GTPase – Guanine triphosphatase
 GTP γ S – Guanosine 5'-3-O-(thio)triphosphate
 h - hour
 HCl – Hydrogen chloride
 HDEL – Histidine-Aspartic acid-Glutamic acid-Leucine
 HMG-CoA – 3-hydroxyl-3-methyl-glutaryl coenzyme A
 Hoc1p - Homologous to OCH1
 ^{125}I – Iodine isotope 125
 IC – Intermediate compartment
 IgG – Immunoglobulin heavy chain gamma
 Ile – Isoleucine
 IR – Inositol response
 K - Lysine
 KAR – Karyogamy
 KCl – Potassium chloride
 kDa - KiloDalton
 KDEL – Lysine-Aspartic acid-Glutamic acid-Leucine
 Kex2p – Kexin 2 protein
 kV – Kilovolts
 LAG1 – Longevity-assurance gene 1
 LAS21 - Local Anesthetics Sensitive 21
 LbrA - Long branch A
 Ldb - Low dye binding
 LDM - Low density microsome

Leu – Leucine
LHS1 – Luminal HSP70
LV - Lysine-valine
Lys – Lysine
M1 – Membrane fraction 1
M2 – Membrane fraction 2
Man – Mannose
min - Minute
mM - Millimolar
Mnn - Mannan
mRNA – Messenger RNA
MSH – Melanophore-stimulating hormone
N-terminus – Amino terminus
NAC – Nascent polypeptide-associated complex
NADH – Nicotinamide adenine dinucleotide, reduced form
NaF – Sodium fluoride
NAGT – N-acetylglucosamine transferase
NaOH – Sodium hydroxide
NE – Nuclear envelope
NEM – N-ethylmaleimide
Ngd - N-linked glycosylation defective
nm – Nanometer
NMR - Nuclear magnetic resonance
NSF – N-ethylmaleimide-sensitive factor
Och - Outer chain
O-linked - Linkage between N-acetylgalactosamine and a serine or threonine residue via oxygen
p23 - Protein of 23 kDa
p24 - Protein of 24 kDa
p25 - Protein of 25 kDa
p27 - Protein of 27 kDa

p58 - Protein of 58 kDa
p97 – Protein of 97 kDa
p450 – Protein of 450 kDa
PBS - Phosphate buffer saline
PC – Phosphatidylcholine
PDI – Protein disulfide isomerase
pH – Negative logarithm of proton concentration
Phe – Phenylalanine
PI – Phosphatidylinositol
PM – Plasma membrane
PMSF – phenylmethylsulfonyl fluoride
POMC – Pro-opiomelanocortin
PS1 – Presenilin gene
Q – Glutamine
R – Arginine
rER – Rough endoplasmic reticulum
RM – Rough microsomes
RNA – Ribonucleic acid
RNAi – RNA interference
RNC – Ribosome-nascent chain complex
rp24 α 2 – Rat protein of 24 kDa of the alpha subfamily, number 2
r.p.m. - revolutions per minute
S - Serine
S phase – Stationary phase
SAR - Secretion-Associated Ras-related
SCAMP – Secretory carrier-associated membrane protein
SDS-PAGE – Sodium dodecyl sulfate polyacrylamide gel electrophoresis
SEC - Secretory
SEL – Suppressors/enhancers of LIN-12
Ser - Serine
sER – Smooth endoplasmic reticulum

SNAP – Soluble NSF attachment protein
SNARE – Soluble NSF-attachment protein receptor
SR – Signal recognition particle receptor
SRP - Signal recognition particle
t-SNARE – Target- soluble NSF-attachment protein receptor
TC – Transport complex
tER – Transitional endoplasmic reticulum
TGN – Trans-Golgi network
Thr – Threonine
TRAP – Translocon associated protein
tRNA – Transfer RNA
Tyr – Tyrosine
UAS – Upstream activating sequence
UGGT - UDP-glucose:glycoprotein glucosyl transferase
UDP – Uridine diphosphate
UPR – Unfolded protein response
VAMP - Vesicle-associated membrane protein
Van1p - Vanadate resistance protein 1
VPS – Vacuolar sorting protein
v-SNARE – Vesicle-soluble NSF-attachment protein receptor
VSV-G – Vesicular stomatis virus glycoprotein
VTC – Vesicular-tubular cluster
WT – Wild type
X – Any amino acid
Y – Tyrosine
Yps1p – Yaspin 1 protein
 μ Ci - Microcurie
 μ g - Microgram

Introduction

Many key components of the secretory pathway have been identified (e.g., COPI, COPII, NSF, SNAREs, Rabs) through in vitro, biochemical and genetic studies (Novick *et al.*, 1980; Rothman, 1994). Subcellular fractionation coupled with mass spectrometry has also provided the means to study the protein constituents of purified organelles (Bell *et al.*, 2001; Gagnon *et al.*, 2002). The identification and characterization of individual components of the secretory pathway has allowed a dissection of this system and has led to a resolution of several of the mechanisms of this highly regulated system.

Despite all of these findings, a very fundamental mechanism of this pathway, how proteins and membranes move, has yet to be resolved. Some of the early models that were proposed were the membrane flow and cisternal maturation models (Morre and Ovtracht, 1977; Morre and Keenan, 1997). These models used electron microscopy to describe a fluid movement for the Golgi apparatus. Specifically, cisternae would continually form at the cis face of the Golgi, progress or mature until the cisternae reached the trans side, where the cisternal membrane would vesiculate and shuttle the proteins via vesicles to their next destination (Grasse, 1957). A major concern with this type of study is that it uses static images to describe a dynamic view of the system. Furthermore, the long half-life of resident proteins of the secretory pathway (hours and days) versus the short half-life of cargo transport (less than 1 hour) was considered incompatible with the cisternal maturation or membrane flow models (Meldolesi, 1974; Franke *et al.*, 1971; Becker *et al.*, 1995). Indeed, a more stable view of the organelle was soon favored (Jamieson and Palade, 1968) and the vesicular transport model was proposed (Jamieson and Palade, 1967a; Jamieson and Palade, 1967b; Palade, 1975).

Unlike the maturation model, the vesicular model viewed the organelles as stable structures through which proteins are transported. The movement of these proteins was predicted to occur through transport vesicles. In 1967, a pulse-chase study in pancreatic exocrine cells showed that transport of secretory proteins occurred from the ER to the Golgi apparatus via small membrane bound vesicles (Jamieson and Palade, 1967a). Indeed, the discoveries of COPI (Orci *et al.*, 1986) and COPII (Salama *et al.*, 1993; Barlowe *et al.*, 1994) vesicles seemed to prove that the vesicular model was the true mechanism for protein transport through the secretory pathway. COPII vesicles transport cargo from the ER (Barlowe *et al.*, 1994) while COPI vesicles move cargo through the successive cisternae of the Golgi (Ostermann *et al.*, 1993; Malhotra *et al.*, 1989). Indeed, COPI vesicles were shown to contain the cargo protein VSV-G and to be devoid of Golgi enzymes (Orci *et al.*, 1997; Orci *et al.*, 2000).

Recently, however, the fundamental aspects of this model have been questioned. The distribution of the Golgi enzymes as a gradient over the stacks of the cisternae (Nilsson *et al.*, 1993; Rabouille *et al.*, 1995) rather than each enzyme in its own cisternae indicated that the Golgi cisternae are not discrete entities. The movement and maturation of large macromolecules such as algae scales (Brown, 1969; Melkonian *et al.*, 1991) or procollagen (Marchi and Leblond, 1984; Bonfanti *et al.*, 1998), which can not fit into transport vesicles also favored the cisternal maturation model. In addition, previous studies that had appeared to give value to the vesicular model were put into question. One such study used a cell free assay to describe the anterograde movement of cargo (Balch *et al.*, 1984), however, the re-evaluation of the assay has indicated that it in fact reconstitutes the retrograde flow of Golgi enzymes in a COPI-dependent fashion (Lin *et al.*, 1999 discussed in Chapter 3). Other studies has used the non-hydrolysable GTP γ S to isolate COPI vesicles and analyze their content (Melancon *et al.*, 1987; Malhotra *et al.*, 1989). However, when more physiological conditions were used (i.e., GTP hydrolysis was allowed to occur), COPI vesicles had low amounts of cargo and large amount of Golgi enzymes (Lanoix *et al.*, 1999). This effect was

further supported by in vivo work (Pepperkok *et al.*, 2000) and electron microscopy studies (Dahan *et al.*, 1994; Martinez-Menarguez *et al.*, 2001), where no cargo was found in COPI vesicles. These results are in contrast to the work of Orci (Orci *et al.*, 1997; Orci *et al.*, 2000) who found the vesicular stomatitis virus glycoprotein (VSV-G) cargo protein in COPI structures.

Indeed the bulk flow hypothesis, once thought to be the mechanism through which proteins were secreted was also rejected. It had been proposed that the flow of proteins through the secretory occurs through a bulk flow model (Pfeffer and Rothman, 1987; Rothman, 1987). This model predicts that, by default, proteins are transported through the secretory pathway and secreted. Sorting is only required for proteins destined to other parts of the cell. However, not all proteins are secreted at the same rate (reviewed in Lodish, 1988; Rose and Doms, 1988). In fact, not all proteins exit the ER at the same rate (Fries *et al.*, 1984; Fitting and Kabat, 1982; Lodish *et al.*, 1983; Ledford and Davis, 1983; Scheele and Tartakoff, 1985; Williams *et al.*, 1985). The reason for the different rates of exit is unclear. Some propose that differences in folding rates may be responsible or proteins may be retarded due to interactions with resident ER proteins or sorting factors (Pfeffer and Rothman, 1987; Pelham, 1989; Hurtley and Helenius, 1989; Rose and Doms, 1988). Others have hypothesized that cargo receptors are responsible for the differing rates of secretion (Lodish, 1988; Schimmöller *et al.*, 1995). In yeast, it has been shown that sorting of cargo occurs in the ER, before cargo enters COPII vesicles (Campbell and Schekman, 1997; Muniz *et al.*, 2001). Indeed, not all proteins are packaged into the same ER-derived vesicles, but that there is a segregation or sorting of proteins before they leave the endoplasmic reticulum (Muniz *et al.*, 2001). Erv29p is one component of this sorting machinery. It is required for the packaging of glycosylated pro-alpha-factor into COPII vesicles (Belden and Barlowe, 2001a). Emp24p was proposed as a candidate cargo receptor (Schimmöller *et al.*, 1995). Deletion of EMP24 causes a delay in the kinetics of a subset of proteins. In addition, Muniz and colleagues have shown that Emp24p is required for efficient packaging of

certain proteins (Gas1p and Yps1p) into ER-derived vesicles (Muniz *et al.*, 2000; Muniz *et al.*, 2001).

Thus the vesicular transport model is now in question and the cisternal maturation model has re-emerged (reviewed in Storrie and Nilsson, 2002). However, neither has been completely proven or rejected. The fact remains that COPI and COPII vesicles exist and that there is some controversy as to the contents of the vesicles. It has yet to be proven if the Golgi is a pre-existing structure or whether it is self-forming. Some in vitro work has shown that VTCs can be derived from ER membranes (Lavoie *et al.*, 1999; Roy *et al.*, 2000; Chapter 2). However, attempts to reconstitute the Golgi have so far been unsuccessful (Pelletier *et al.*, 2000). Another element to this field is the fact that there are continuities within the Golgi stack (Rambourg and Clermont, 1990; Hermo *et al.*, 1991; Hermo and Smith, 1998). It is also relevant that the fragmentation of the Golgi renders it more active in an intra-Golgi transport assay (Dominguez *et al.*, 1999). Indeed, there are several ways to fragment a Golgi: mechanically (Dominguez *et al.*, 1999), with the phosphatase inhibitor okadaic acid (Lucocq *et al.*, 1991; Reaven *et al.*, 1993), with 1-butanol (Siddhanta *et al.*, 2000; Sweeney *et al.*, 2002), with the sea sponge metabolite ilumaquinone (Takizawa *et al.*, 1993), with Brefeldin A (Fujiwara *et al.*, 1988; Lippincott-Schwartz *et al.*, 1989), nocadazole (Rogalski and Singer, 1984) or when the cell goes through mitosis (Lucocq *et al.*, 1987). It is unclear whether the re-formation of the Golgi (e.g., after wash out or telophase) is due to a de novo formation or if the Golgi elements converge upon a pre-existing matrix. In addition, a third model proposes that movement of proteins occurs through tubular elements (reviewed in Lippincott-Schwartz, 2001).

In order to distinguish between these models, we chose to characterize the p24 proteins. This group of proteins was chosen because they are of high abundance in the secretory pathway and they are linked to protein secretion (Dominguez *et al.*, 1998; Schimmöller *et al.*, 1995). To characterize the p24

proteins we wanted to determine (1) what types of interactions the proteins had (Chapter 1), (2) if the proteins had a role in cargo exit site formation (Chapter 2), (3) to isolate the p24-compartment (Chapter 3), (4) to look at protein content of the p24 compartment (Chapter 4), and (5) to perform mutational analyses of the p24s in *Saccharomyces cerevisiae* (Chapters 5 and 6). The following thesis describes the characterization of the p24 proteins.

Literature Review

Eukaryotic cells contain a considerable amount of internal organization. They possess a dynamic system of membranes that forms all of the internal compartments of the cell (Palade, 1975). The introduction of electron microscopy into biological sciences was instrumental in defining the morphology of the cell and the membrane compartments within. For the first time, researchers were able to see that the interior of the cell was filled with membrane bound organelles. The secretory (biosynthetic or exocytic) pathway is one of the membrane systems contained within the cell. It is involved in the production and transport of proteins.

The secretory pathway of all eukaryotic cells is composed of distinct membrane bound organelles. It is these organelles that provide the machinery for the synthesis, folding, modification and delivery of cargo proteins. The organelles of the secretory pathway consist of the endoplasmic reticulum (ER), the intermediate compartment (IC), the Golgi apparatus (GA) and the plasma membrane (PM). This text deals predominantly with the early secretory pathway that is composed of the endoplasmic reticulum, the intermediate compartment and the Golgi apparatus.

Each of the membranous compartments of the secretory pathway has a multitude of functions. The endoplasmic reticulum is involved in protein synthesis (Hedge and Lingappa, 1999), lipid synthesis (Helms *et al.*, 1991; van Meer, 1993), proteolytic processing (Blobel and Dobberstein, 1975; Lyko *et al.*, 1995), protein folding (Zapun *et al.*, 1999; Chevet *et al.*, 2001), N-linked oligosaccharide modification of proteins (Kornfeld and Kornfeld, 1985), packaging of newly synthesized proteins (Pryer *et al.*, 1992; Herrman *et al.*, 1999), and calcium storage (Meldolesi and Prozzan, 1998). The intermediate compartment is the site of recycling of escaped ER proteins and concentration of cargo proteins (Martinez-Menarguez *et al.*, 1999). The Golgi apparatus is the site

where sphingolipid synthesis (van Meer, 1993; Fang *et al.*, 1998), phosphorylation of cargo proteins (Bingham *et al.*, 1972; Rosa *et al.*, 1992; Swift, 1996; Vegh and Varro, 1997), sulfation (Neutra and LeBlond, 1966), sorting and further modifications occurs (Jamieson, 1998; Fullekrüg and Nilsson, 1998).

Below is a description of various elements of the secretory pathway for both multicellular (mammalian) and unicellular (*Saccharomyces cerevisiae*) systems. This text will also discuss the models that predict how these various elements are linked and attempt to unravel pieces of the molecular framework of this pathway.

1. The Secretory Pathway

The secretory pathway is a system of organelles whose function is to aid and monitor the maturation of proteins and lipids and deliver them to their proper destination. The organelles of this system also face the challenge of maintaining their resident protein and lipid content, and thus their functional integrity, while a host of newly synthesized proteins and lipids is passed through them. Below are descriptions of various components of the secretory pathway, the functions associated with them and their regulation of membrane and protein movement.

1.1. The Endoplasmic Reticulum

The endoplasmic reticulum was identified by Keith Porter in 1945 (Porter, 1945). The term endoplasmic means within the cytoplasm, while reticulum is a Latin term meaning little net. Indeed, the ER forms an internal network of membranes within the cell. This organelle is generally seen as the most extensive membrane system in the cell. The membrane of the ER is composed of a phospholipid bilayer that is approximately 5-8 nm thick (DePierre and Dallner, 1975). The endoplasmic reticulum is synonymous with protein synthesis, but this organelle is also involved in lipid synthesis, signal transduction, detoxification

and stress response. Along with its many functions, the ER has many subcompartments (Sitia and Meldolesi, 1992). This text will address four of these ER subcompartments: the rough endoplasmic reticulum (rER), the smooth endoplasmic reticulum (sER), the transitional endoplasmic reticulum (tER) and the ER exit sites.

1.1.1. The Rough Endoplasmic Reticulum

The endoplasmic reticulum is designated as the beginning of the secretory apparatus. It is on the surface of the ER that proteins are synthesized by ribosomes (complexes of RNA and protein that compose the machinery for protein synthesis). Numerous ribosomes stud the surface of the ER, thus the term rough ER. Only a subset of proteins passes through to the secretory pathway. Specifically, proteins that contain a signal sequence (usually at the N-terminus) are targeted to the ER membrane. The targeting process is effected by a signal recognition particle (SRP) that recognizes the hydrophobic sequence and halts the synthesis of the protein. The ribosomal-nascent chain complex (RNC) is then targeted to a specific site on the ER membrane where the SRP receptor (SR) and the translocon are located (Rapoport *et al.*, 1996). The binding of the SRP-RNC to the SR causes a dissociation of the signal sequence from the SRP in a GTP-dependent fashion (Connolly *et al.*, 1991) and the nascent polypeptide is then transferred to the Sec 61 α subunit of the translocon. The nascent polypeptide-associated complex (NAC) is present as a quality control measure to prevent the association of the SRP molecule with ribosome associated peptides that do not possess a hydrophobic signal sequence. Protein synthesis resumes once the ribosome is associated with the ER membrane. As the protein is being synthesized by the ribosome, it is passed through the trimeric Sec61 protein complex (composed of Sec61 α , β and γ , termed the translocon) that forms a pore in the ER membrane and gains access to the ER lumen.

The lumen of the ER provides newly synthesized proteins with an oxidizing redox milieu conducive to the folding of these proteins (Frand *et al.*, 2000; Hwang *et al.*, 1992; Braakman *et al.*, 1992). In addition, there are numerous ER resident proteins, termed chaperones, that aide these proteins to attain their correct structural conformation (Zapun *et al.*, 1999; Chevet *et al.*, 2001). The chaperones can be classed into two subgroups based on the manner in which they function. The chaperones can either function by catalyzing protein folding reactions (e.g., protein disulfide isomerase and cis-trans prolyl isomerase) or by maintaining proteins in a folding competent state (e.g., calnexin, BiP, GRP78) (Zapun *et al.*, 1999). These molecules form part of the quality control machinery of the endoplasmic reticulum.

1.1.1.1. Sugar Modifications

Some proteins receive N-linked or O-linked oligosaccharide modifications. N-linked glycosylation occurs in the endoplasmic reticulum while O-linked glycosylation occurs in the Golgi or pre-Golgi compartment. The oligosaccharide moieties are synthesized in the ER on a lipid dolichol phosphate and subsequently transferred to the asparagine (Asn– X – Ser/Thr motif) of newly synthesized proteins (reviewed in Kornfeld and Kornfeld, 1985). The oligosaccharides are then processed and trimmed and further modified in the Golgi apparatus. The glycosylation of proteins may provide various roles, including stability, proper folding and protease resistance. The sugar moieties are essential for a group of chaperones that are lectins (e.g., calnexin, calmeglin, and calreticulin). These chaperones bind to the oligosaccharide portion of the glycoprotein. Calnexin, for example, interacts specifically with the monoglucosylated form of the oligosaccharide (Hammond *et al.*, 1994; Ou *et al.*, 1993; Zapun *et al.*, 1999).

1.1.1.2. Retrieval Sequences

Resident ER proteins must be distinguished from cargo proteins and must be maintained at steady state in the ER compartment. One way this is achieved is by the presence of a motif of short stretches of amino acids on the cytosolic tail of ER membrane proteins. This motif, usually a KDEL sequence (HDEL for yeast for ER luminal proteins) or a di-lysine motif (K(X)KXX) for the cytosolic terminus of transmembrane proteins, serves as a retrieval signal for escaped ER proteins (Pelham, 1989; Munro and Pelham, 1987). A KDEL receptor (ERD2), mainly located in the cis Golgi network (CGN), recycles the escaped ER proteins. The affinity of ERD2 for the KDEL motif is pH sensitive and has been proposed to be increased in the Golgi, a slightly acidic environment, and reduced in the ER, which has a neutral pH (Wilson *et al.*, 1993).

1.1.1.3. Misfolding

Misfolded proteins can accumulate in the ER for various reasons, e.g., calcium depletion, exposure to certain metabolites, over expression of proteins. When this accumulation occurs, the cell initiates an unfolded protein response (UPR). The UPR in turn induces the synthesis of many ER resident proteins (see Table 1, Kaufman, 1999). This is one of the many ways the ER ensures the proper processing of proteins through its quality control.

The quality control of the ER is in place to regulate the processing of proteins. It is a stringent mechanism and proteins that fail the quality control are retained and/or degraded. The quality control system of the ER is not only important for maintaining the proper operation of the secretory pathway and protein maturation, it also prevents defects in the cell that can lead to the death of the cell or disease of the organism (reviewed in Ellgaard *et al.*, 1999; Aridor and Balch, 1999).

1.1.2. The Smooth Endoplasmic Reticulum

The rough endoplasmic reticulum and the smooth endoplasmic reticulum are a continuous unit of membrane (DePierre and Dallner, 1975). Although there is a continuity between the two membrane systems, the two are segregated into distinct masses (reviewed in Bruni and Porter, 1965). Syntaxin 17, which is a SNARE involved in membrane trafficking, specifically localizes to the smooth ER (Steegmaier *et al.*, 2000). The sER in rat liver hepatocytes, which is involved in glycogen metabolism, is predominately found in regions that are rich in glycogen. The tubular anastomosing networks of the smooth ER are postulated to increase in surface area for drug detoxification via the cytochrome p450. Indeed the sER specifically proliferates in response to drug challenge (e.g., phenobarbital, 3-methylcholanthrene) in order to accommodate more detoxification enzymes (Jones and Fawcett, 1966; Bolender and Weibel, 1973; Baron *et al.*, 1982).

The smooth ER is the site of lipid and sterol synthesis, including the synthesis of cholesterol, diacylglycerol-based phospholipids, the sphingolipid backbone, ceramide and galactosylceramide. In addition, many of the enzymes involved in this process, like hydroxymethylglutaryl-CoA reductase, are localized to the sER (Rodwell *et al.*, 1976).

1.1.3. The Transitional Endoplasmic Reticulum

The transitional endoplasmic reticulum is a portion of the ER that is continuous with the rER but does not have the abundance of ribosomes. The morphology of the tER is also distinct from that of the rER. Instead of long regular cisternae, it has a more convoluted form. The tER has been reconstituted in vitro in a nucleotide-dependent step (Lavoie *et al.*, 1996; Lavoie *et al.*, 1999; Chapter 2) that requires the actions of the AAA ATPase p97 and the t-SNARE syntaxin 5 (Roy *et al.*, 2000 discussed in Chapter 2).

1.1.4. ER Cargo Exit Sites

It is in this part of the ER that COPII coats are seen to concentrate on the membrane, forming a coat complex for a budding vesicle. The buds contain newly synthesized proteins that have passed the quality control check points of the ER system and are competent to travel to the next compartments to receive further modifications. It is at this site that cargo proteins must be segregated from ER proteins in order to prevent the escape of resident proteins. From the ER, the newly synthesized proteins will travel to the IC, to the Golgi apparatus and will then be targeted to their resident organelle, stored in secretion vesicles or transported to the plasma membrane.

1.2. The Intermediate Compartment

The intermediate compartment is a membranous network that closely opposes the Golgi apparatus. This smooth tubular membrane system is distinct from the ER and the Golgi and has received a battery of names and morphological definitions. It has been described as the intermediate compartment (IC) (Schweizer *et al.*, 1990), vesicular tubular clusters (VTCs) (Balch *et al.*, 1994; Bannykh and Balch, 1997), the ER to Golgi intermediate compartment (ERGIC) (Schweizer *et al.*, 1991; Hauri and Schweizer, 1992), the salvage compartment (Warren, 1987), export complexes (Bannykh *et al.*, 1996) and transport complexes (TCs) (Scales *et al.*, 1997). In addition, some investigators confuse or combine the IC with the cis Golgi network (CGN). The intermediate compartment has been widely described with little coherency and much diversity among descriptions, including where this structure begins and ends (Pelham, 1995; Scales *et al.*, 1997). No attempt to consolidate these terms will be made here rather this section will point out the similarities and discuss the possible role that this membrane compartment plays.

1.2.1. Roles of the Intermediate Compartment

That the intermediate compartment is a distinct compartment from the ER and Golgi apparatus was evident through its isolation from Vero cells. The isolated compartment was composed of smooth membrane bound vesicles with an average diameter of 89 nm (Schweizer *et al.*, 1991). This study revealed a distinct protein pattern for the IC from that of the ER and Golgi apparatus. This indicated that the intermediate compartment is distinct from both ER and Golgi and thus has a distinct role.

Some of the proteins that have been shown to concentrate in or cycle through the intermediate compartment include $\text{p24}\alpha 2$ (Dominguez *et al.*, 1998), COPI (Griffiths *et al.*, 1995; Oprins *et al.*, 1993), the small GTPases, Rab1 and Rab2 (Pind *et al.*, 1994; Chavrier *et al.*, 1990), the v-SNARE SEC22/ERS-24 (Zhang *et al.*, 1999) and ERGIC-53, which is involved in the proper processing of cargo (Nichols *et al.*, 1998).

One of the widely used characteristics of this compartment is that it accumulates cargo proteins at 15°C. At this reduced temperature, the compartment becomes significantly enlarged and accumulates secretory products (reviewed in Kuismanen and Saraste, 1989).

One of the proposed roles of the IC is that it is a site of retrieval of escaped ER proteins. Proteins possessing a retrieval sequence of KDEL are sequestered by the KDEL-receptor (ERD2) and returned to the ER through vesicular intermediates. In addition, the IC has been shown to be a site of cargo protein concentration, possibly effected through the recycling of membrane by COPI vesicles (Balch *et al.*, 1994; Bannykh *et al.*, 1996; Martinez-Menarguez *et al.*, 1999). Thus the intermediate compartment is the compartment where ER proteins are segregated from cargo proteins, the latter of which will move forward to the Golgi apparatus.

1.3. The Golgi Apparatus

The Golgi received its name from the man who first identified this organelle, Camillo Golgi. In an attempt to achieve better pictures, Camillo Golgi treated neural cells with silver nitrate. The result was a “reazione nera”, a black reaction, which occurred in the Golgi apparatus (GA) (reviewed in Droscher, 1998). Camillo Golgi described this in 1898 as the “apparato reticolare interno”, an internal reticular network that is now referred to as the Golgi apparatus. The Golgi apparatus consists of tightly stacked membrane subunits (Mollenhauer and Morre, 1991). The stacked subunits are generally referred to as saccuoles or cisternae (Latin for “collecting vessels”). The Golgi apparatus is the site where further maturation and sorting of proteins and lipids occurs.

1.3.1. Golgi Structure

The initial description of the Golgi apparatus was at the light microscope level, but it was electron microscopy that truly revealed the complex structure of the Golgi apparatus. The structure of the Golgi apparatus varies dramatically from cell type to cell type. Generally, secretory cells or cells that produce a lot of glycoproteins/lipids, exhibit a well-developed Golgi apparatus. Those cells that do not express a large amount of protein generally have a less extensive Golgi apparatus.

This organelle is divided into the cis Golgi network (CGN), the cis, medial and trans cisternae, and the trans Golgi network (TGN). The CGN is located in the forming side of the Golgi stack. It is a network of anastomotic tubules (Rambourg and Clermont, 1990). The CGN opposes the stack of the Golgi cisternae. The Golgi stack is formed of adjacent saccuoles that generally appear to be separate membrane units but that are in fact interconnected by dilated tubules

(Rambourg and Clermont, 1990; Hermo *et al.*, 1991; Hermo and Smith, 1998). There are also wells that form within the stacked structure. This is believed to be a site for vesicular interaction (Hermo and Smith, 1998). These interconnections and wells are not obvious in all sections, but they have been widely described (Rambourg and Clermont, 1990; Hermo *et al.*, 1991; Mollenhauer and Morre, 1991; Thorne-Tjomsland *et al.*, 1998; Hermo and Smith, 1998; Dominguez *et al.*, 1999; Ladinsky *et al.*, 1999). The Golgi is indeed a continuous organelle with both compact (Golgi cisternae) and non-compact (interconnecting tubules) zones.

The sorting of secretory proteins occurs in the TGN (Griffiths and Simons, 1986). The TGN was first described as part of the Golgi-endoplasmic reticulum-lysosome system (GERL) (reviewed in Novikoff, 1976) or the trans tubular network (Rambourg *et al.*, 1979). The TGN is located at the mature side of the Golgi, where proteins have been processed and are ready to be targeted to their final destination. The TGN is not directly connected with the Golgi stack. It is a fenestrated network of tubules with dilations filled with secretory proteins. Clathrin coated buds can be seen on the membranes of the TGN. Specifically, AP-1 directs traffic from the TGN to the endosome while AP-3 directs traffic from the TGN to the lysosome or vacuole (Cowles *et al.*, 1997). The release of secretory vesicles from the TGN is effected by phospholipase D (Chen *et al.*, 1997) indicating a role for modified phospholipids in trafficking.

1.3.2. Golgi Composition

The Golgi apparatus can be described as a compartment intermediary between the ER and the plasma membrane. As such, there are both ER and PM components found in the Golgi apparatus. The ER enzymes are associated with the dense portion of the Golgi apparatus and the PM enzymes are associated with the less dense, electronegative GA (Bergeron *et al.*, 1973). This compartment also contains nucleotide mono-, di- and tri-phosphatases, acid phosphatase, glucose-6-phosphatases, arylsulfatases, NADH dehydrogenases, enzymes for lipid

biosynthesis, endo- α -mannosidase, tyrosyl protein sulfontransferase, and furin (an endoprotease). Possibly the best known enzymes are mannosidases I and II, which remove the mannose residues from the $\text{Glc}_{1-3}\text{Man}_{4-9}\text{GlcNac}_2$ -N-linked oligosaccharide chains (Tabas and Kornfeld, 1979; Tulsiani *et al.*, 1982).

The Golgi apparatus also contains specific transporters for UDP-galactose, UDP-N-acetylglucosamine, UDP-N-acetylgalactosamine, GDP-fructose and CMP-sialic acid (Hirschberg *et al.*, 1998).

1.3.3. Golgi Lipids

The lipid content of the Golgi membranes is about 54% phospholipid and 46% neutral lipids (Keenan and Morre, 1970). About 45% of the total phospholipids are phosphatidylcholine (PC) and about 12% sphingomyelin. The Golgi apparatus is seen as the intermediate in the lipid gradient that goes from the ER to the plasma membrane (Keenan and Morre, 1970). While the ER is rich in phosphatidyl choline and phosphatidylinositol (PI), the PM is rich in sphingomyelin, cholesterol, and phosphatidylserine (reviewed in Nickel *et al.*, 1998). In rat liver cells, 58% of the total phospholipids of the ER are phosphatidylcholine and 3% sphingomyelin. 39% of the total phospholipids in the PM are phosphatidylcholine and 16% sphingomyelin (van Meer, 1998). On the other hand, phosphatidylinositol and phosphatidylethanolamine are about the same percentage in the three membrane systems, accounting for approximately 10% and 22% of the total phospholipid, respectively (van Meer, 1998)

Unsaturated fatty acids form a gradient from highest abundance in the ER to the lowest abundance in the PM (Keenan and Morre, 1970). The reverse is true for cholesterol, which is low in the ER and high in the PM.

Biosynthesis of phosphatidyl inositol occurs in the Golgi apparatus (Jergil and Sundler, 1983). In fact the Golgi contains many enzymes required for lipid

biosynthesis and whose specific activity is about 45% that of the ER enzymes (Jelsema and Morre, 1978).

1.3.4. Disease

The Golgi also plays a role in the disease pathology of ALS (Amyotrophic Lateral Sclerosis), AD (Alzheimer's disease) and ricin intoxication (reviewed in Gonatas *et al.*, 1998). For example, the trans-Golgi is the site of cleavage of the amyloid- β protein by the β -site APP-cleaving enzyme (BACE) which is associated with Alzheimer's disease (Huse *et al.*, 2002).

2. The *Saccharomyces cerevisiae* Secretory Pathway

Since the compartmentalization of the secretory pathway is conserved from yeast to humans, then the application of yeast genetics has been a powerful tool to categorize constituents and compartments of the secretory pathway (Schekman and Orci, 1996). Indeed the SEC mutants have been instrumental in discovering many aspects of the secretory pathway (including COPII) (Novick *et al.*, 1980). Importantly, many of the genes discovered have homologues in other organisms, including humans.

2.1. The Yeast Endoplasmic Reticulum

Similar to the mammalian system, the yeast endoplasmic reticulum is composed of long cisternae that are in continuity with the nuclear membrane (Preuss *et al.*, 1991). In yeast, the ER cisternae are poorly fenestrated, flat sheet-like structures. The cisternae can be peripheral, just under the plasma membrane, or located within the cytoplasm. The latter type links the subplasmalemmal ER to the nuclear membrane. The yeast ER is also biochemically similar to the mammalian ER. The translocation of secretory proteins across the ER membrane into the lumen is effected by the translocon (Sec61p complex), Kar2p and Sec63p (Young *et al.*, 2001).

Translocation of proteins into the ER in yeast may occur in two ways (Ng *et al.*, 1996). The protein can be targeted co-translationally, as in the mammalian secretory pathway, where the ribosome-peptide complex is targeted to the ER membrane, or posttranslationally, where peptides are inserted into the ER after the protein is synthesized. As in mammalian systems, co-translational targeting to the ER membrane requires the proteins to have a signal sequence. The peptide is targeted to the membrane through SRP (reviewed in Walter and Johnson, 1994). SRP is recruited to the membrane by the SRP receptor (a heterodimeric protein). The ribosome-peptide complex is docked onto a pore complex, the translocon. In

the posttranslational (or SRP-independent) pathway, translation occurs in the cytoplasm. The nascent protein is kept in an unfolded state and is targeted to the Sec62p/Sec63p complex (composed of Sec62p, Sec63p, Sec71p and Sec72p) and the translocon (Sec61p complex). The protein is then translocated across the ER membrane (Ng *et al.*, 1996). Yeast proteins may follow the SRP-independent pathway, the SRP-dependent pathway, or both. CPY, α -factor, Gas1p and PDI are all SRP-independent. Kar2p and Och1p can use either pathway and Pho8 and DRAP B are SRP-dependent (Ng *et al.*, 1996).

As in mammalian cells, many ER resident proteins are involved in the processing of polypeptides and in assisting the newly synthesized proteins to attain their correct configuration. Among these are Kar2p, Pdi1p, Mpd1p, Lhs1p, Ero1p, Fkb2p, and Eug1p (Normington *et al.*, 1989; Rose *et al.*, 1989; LaMantia *et al.*, 1991; Partaledis and Berlin, 1993; Tachibana and Stevens, 1992; Craven *et al.*, 1996; Baxter *et al.*, 1996; Tachikawa *et al.*, 1995; Norgaard *et al.*, 2001).

In the ER, newly synthesized proteins undergo further modifications such as signal sequence cleavage, side chain glycosylation, disulfide bond formation, and addition of glycosylphosphatidyl inositol (GPI) membrane anchor. Proteins that are destined to undergo GPI modification possess a peptide motif at the C-terminal end. This C-terminal peptide signal is removed and replaced with a GPI anchor (Englund, 1993). Las21p (Gpi7p) is among the proteins proposed to be involved in the addition of the GPI anchors (Benachour *et al.*, 1999). The GPI anchor is required for the exit from the ER (Nuoffer *et al.*, 1993; Doering and Schekman, 1996). Two genes, LAG1 and DGT1, are postulated to be involved in ER to Golgi transit of GPI-anchored proteins (Barz and Walter, 1999).

HMG-CoA reductase (3-hydroxy-3-methyl-glutaryl-coenzyme A reductase) is a resident membrane protein of the ER. It catalyzes the production of mevalonate, an intermediate of sterols and nonsterol isoprenoid compounds.

Yeast cells have two HMG-CoA reductase enzymes, Hmg1p and Hmg2p (Basson *et al.*, 1986).

Sec12p is associated with the ER cargo exit sites. This is the site where COPII vesicle formation and cargo exit occurs. Sec12p is a type II transmembrane glycoprotein that recruits Sar1p-GDP to the ER membrane (Nakano *et al.*, 1988; d'Enfert *et al.*, 1991a; Barlowe and Schekman, 1995). In *S. cerevisiae*, Sec12p is distributed throughout the ER, indicating that COPII vesicle formation is not restricted to specific subregions of the ER, but may in fact form vesicles throughout the ER (Rossanese *et al.*, 1999).

2.2. The Yeast Golgi Apparatus

In the budding yeast, *Saccharomyces cerevisiae*, the Golgi apparatus is not composed of closely stacked cisternae, as in the mammalian system, rather, the Golgi cisternae are dispersed throughout the cytoplasm. (Preuss *et al.*, 1992; Rambourg *et al.*, 1993; Rambourg *et al.*, 1995). The morphology of the *S. cerevisiae* Golgi apparatus has not been described as extensively as the mammalian Golgi. It is seen by some as a disk-like structure surrounded by vesicles (Preuss *et al.*, 1992) and by others as tubular networks with nodular dilations (Rambourg *et al.*, 1996), or even as membrane profiles (<400nm) that are often curved and sometimes arranged in stacks of two cisternae (Wooding and Pelham, 1998). The difficulty of describing the yeast Golgi apparatus is due to its physical nature (a single membrane profile) and the scarcity of good fixation and staining techniques (Preuss *et al.*, 1992; Rambourg *et al.*, 1993).

Certain mutants, such as the *sec7* and *sec14* mutants, when grown at a restrictive temperature disrupt glycoprotein traffic and accumulate Golgi membranes into a stack resembling those found in mammalian cells (Rambourg *et al.*, 1996; Novick *et al.*, 1980; Franzusoff *et al.*, 1991). Both SEC7 and SEC14 are essential genes. Sec7p is found in both cytosolic (soluble) and membrane

(pelleted) pools (Frauzusoff *et al.*, 1991). In addition, the *sec7* mutant disrupts the traffic of proteins destined for the cell surface as well as to the vacuole and is possibly involved at a late stage in maturation. Sec7p contains a stretch of approximately 200 amino acids, referred to as the *sec7* domain. This domain is involved in the guanine nucleotide exchange for ARF (Sata *et al.*, 1998). Sec14p is a phosphatidylinositol/phosphatidylcholine transfer protein. It is required to control the phosphatidyl content of the Golgi (McGee *et al.*, 1994; Bankaitis *et al.*, 1990).

2.2.1. Glycosylation

Part of the function of the Golgi apparatus is to modify glycoproteins with sugar residues. In yeast, the type and amount asparagine-linked (N-linked) oligosaccharide can be divided into two general classes. The glycoproteins associated with the outer surface (e.g., invertase) have a large glycan structure of up to 200 mannose residues. Those of the inner compartments (e.g., CPY) are much smaller, with a single α -1,6-mannose attached to the core oligosaccharide to which 2-3 more mannoses may be added (reviewed in Herscovics and Orlean, 1993; Trimble and Atkinson, 1986; Ballou *et al.*, 1990). The sugars of the glycoproteins associated with the outer surface of the cell are thought to act as a shield to protect the cell, to give the cell wall integrity and to act in cell-cell associations (Klis, 1994; Stratford, 1992). The glycosylation of proteins is also important for the folding and the function of certain proteins (Varki, 1993). The initial addition of the sugar moiety ($\text{Glu}_3\text{Man}_9\text{GlcNAc}_2$) occurs in the ER, where the core N-linked glycan is attached to newly synthesized proteins. Before leaving the ER, the oligosaccharide is trimmed to $\text{Man}_8\text{GlcNAc}_2$ (Esmon *et al.*, 1984). Once in the Golgi, the extent to which the glycoprotein is modified is dependent on the individual protein. As mentioned above, some glycoproteins will undergo extensive modification while others will only have a few residues added. The mannosyltransferase Och1p is responsible for the addition of the α -1-6-mannose to the core oligosaccharide (Nakayama *et al.*, 1992). Two protein complexes

effect further elongation of the mannose residues. The first complex is composed of Mnn9p and Van1p. The second is a complex of Mnn9p, Anp1p, Hoc1p and Mnn11p (Jungmann and Munro, 1998). Both complexes possess α -1,6-mannosyltransferase activity. Mnn2p and Mnn5p are α -1,2 mannosyltransferases that act sequentially to form and extend the mannan branches even further (Raynor and Munro, 1998). Mnn1p adds the terminal α -1,3-linked mannose residues to the sugar chains (Raschke *et al.*, 1973; Yip *et al.*, 1994; Wiggins and Munro, 1998). Mnn6p is required for the addition of a phosphomannan (Wang *et al.*, 1997).

A separate family of proteins has been identified for serine/threonine-linked (O-linked) glycans. Mnt1p (Kre2p), Ktr1p, Yur1p and Ktr3p are α -1,2-mannosyltransferase that attach the second and third mannoses (Lussier *et al.*, 1996; Hausler *et al.*, 1992). GPI anchors also exhibit α -1,2-linked mannose residues (Sipos *et al.*, 1995).

2.2.2. Biochemical distinctions

The single, dispersed cisternae of the yeast Golgi are biochemically distinct compartments. The specific regions of these Golgi compartments (i.e., cis versus trans) can be defined by the enzymes that reside within them. The Mnn9p complexes are located in the first (cis-most) element of the Golgi. Mnn2p is in the second. Mnn1p is in the third and Kex2p, an endoprotease, is in the fourth (trans-most) element (Wooding and Pelham, 1998; Brigance *et al.*, 2000).

The postranslational processing of pro- α -factor has also been used to describe the functional compartments of the Golgi apparatus. The ER-core glycosylation of pro- α -factor is sequentially modified from the α 1,6-mannosylated form, to the α 1,2-mannosylated form, to the α 1,3-mannosylated form. The α 1,3-mannosylated form is then proteolytically processed by Kex2p

and exocytosed as the mature peptide (Graham and Emr, 1991; Redding *et al.*, 1991). The *sec18* mutants were used to show that each modification step was in a distinct membrane bound compartment (Brigance *et al.*, 2000). Thus four distinct, biochemical compartments (cis, medial, trans, TGN) have been described in *S. cerevisiae*.

3. Membrane Biogenesis and Regulation

The membrane systems of eukaryotic cells are as diverse in composition as they are in function. Exactly how these membranes are regulated, coordinated and established is not clear. Indeed, the molecular mechanisms that drive membrane biogenesis are poorly understood. Since the structure, lipid content and protein content of the various membranes of the cell are quite distinct, membrane biogenesis requires careful orchestration of the synthesis and assembly of membranes. In many cell types, over expression of certain membrane proteins induces the proliferation of internal membrane systems.

3-hydroxy-3-methylglutaryl coenzyme A (HMG-CoA) reductase is an ER membrane protein that is involved in mevanolate production. It catalyzes the rate-limiting step in sterol biosynthesis (Shapiro and Rodwell, 1971; Rodwell *et al.*, 1976). Over expression of this protein in yeast or mammalian cells leads to membrane proliferation (Wright *et al.*, 1988; Kochevar and Anderson, 1987; Anderson *et al.*, 1983; Orci *et al.*, 1984; Chin *et al.*, 1982). There are two isozymes for HMG-CoA reductase in yeast, Hmg1p and Hmg2p (Basson *et al.*, 1986). Increased expression of the isozymes creates distinct and dramatic membrane proliferations that reflect the localization of the particular protein (Wright *et al.*, 1988; Koning *et al.*, 1996). Hmg1p is associated with nuclear associated ER. Over expression of Hmg1p causes proliferation of membranes (karmellae) which are associated with the nuclear membrane. Hmg2p is also associated with nuclear associated ER, but when over expressed, it has a more peripheral localization. Indeed, peripheral karmellae are seen when this isozyme is over expressed. The protein composition of these two membranes systems is also distinct, possibly revealing two subregions of the ER involved in sterol synthesis (Koning *et al.*, 1996). Although subregions in the ER membrane are not obvious in yeast, some evidence suggests that they exist (Wright *et al.*, 1988; Koning *et al.*, 1996; Nishikawa *et al.*, 1994).

The other proteins that led to membrane structures when over expressed include: (1) cytochrome hydroxylases, which are involved in sterol biosynthesis (Vergeres *et al.*, 1993; Schunk *et al.*, 1991); (2) the peroxisomal membrane protein, Pex15p (Elgersma *et al.*, 1997); (3) the ER membrane protein, Sec12p (Nishikawa *et al.*, 1994); (4) the canine ribosome receptor (Wanker *et al.*, 1995; Becker *et al.*, 1999); (5) the protease B negative 1 protein (Naik and Jones, 1998); (6) ARF (Deitz *et al.*, 2000); (7) the cycling protein, p23 (Rojo *et al.*, 2000) and (8) the prosequence derivative of RNAP-I (Umebayashi *et al.*, 1997). Conversely, depletion or deletion of certain proteins has also led to new membrane structures. In the *vps45Δ* mutant there is an accumulation of vesicles. VPS45 is a member of the Sec1p/Sly1p/Vps33p family and is thought to be involved in the transport of vesicles to the vacuole (Cowles *et al.*, 1994). Depletion of Sec24p, a COPII component, leads to an extensive membrane system, specifically, an amplification of ER membranes (Kurihara *et al.*, 2000). In addition, phenobarbital treatment has also been reported to induce membrane formation (Jones and Fawcett, 1966; Bolender and Weibel, 1973).

Incidences of membrane proliferation in prokaryotes have also been documented. In *Escherichia coli*, ATP synthase and fumarate reductase over expression produces intracellular membrane tubules (Weiner *et al.*, 1984). Thus, both eukaryotes and prokaryotes possess mechanism involved in de novo membrane biosynthesis.

Some of the factors involved in membrane morphogenesis have recently been elucidated through the use of cell free assays. COPI, rp24α2, the AAA ATPase p97 and the SNARE syntaxin 5 are all required for the transformation of membrane structures *in vitro* (Lavoie *et al.*, 1999; Roy *et al.*, 2000; Chapter 2).

In yeast, the volume of the ER changes in response to the accumulation of proteins. This is controlled by the unfolded protein response (UPR) and the inositol response (IR). The UPR increases the amount of chaperones (*e.g.*, KAR2,

PDI, EUG1) while the IR induces membrane synthesis (*e.g.*, INO1, CHO1). These two pathways are activated through the actions of the transmembrane kinase Ire1p and the transcription factor, Hac1p (Cox *et al.*, 1997).

Increase in ER membrane structures may also occur in systems where trafficking is perturbed. This is seen when SEC12 is over expressed (Nishikawa *et al.*, 1994), when ARF1 is over expressed in an $\Delta arf1 \Delta arf2$ background (Deitz *et al.*, 2000), or when Sec24p is depleted (Kuirihara *et al.*, 2000).

4. Components of the Secretory Pathway

Although morphologically different, the mammalian and yeast systems have many common factors. Genetic and biochemical studies have revealed that *S. cerevisiae* and higher eukaryotes both utilize the same basic mechanisms for the proper secretion of proteins and the overall functioning of the secretory pathway (Novick *et al.*, 1980; Schekman, 1985; Rothman and Orci, 1992). Indeed, many components in one eukaryotic system are interchangeable with those of another eukaryotic system (Wilson *et al.*, 1989; Griff *et al.*, 1992; Ferro-Novick and Jahn, 1994; Minard *et al.*, 1998; Li *et al.*, 1997). The sharing of the basic machinery by many organisms has allowed us to use a wide variety of systems to study the mechanisms of the secretory pathway. This text will concentrate on the yeast and the mammalian systems, which have been instrumental in the discovery of the molecular components of this the secretory pathway.

4.1. COPI

COPI is a protein complex that is involved in vesicular transport (Rothman and Wieland, 1996; Schekman and Orci, 1996). This protein complex is recruited to membranes and forms a coat that surrounds the budding transport vesicle. It was first identified in isolated Golgi membranes through the use of electron microscopy (Orci *et al.*, 1986). The protein complex was seen as a fuzzy coat over the membrane. This study also identified a cargo protein (a viral G protein, VSV-G) in the COPI coated structures, thus implicating COPI in anterograde transport (Orci *et al.*, 1986). COPI coated vesicles were then isolated with the use of GTP γ S (Melancon *et al.*, 1987; Malhotra *et al.*, 1989). The COPI components were identified and found to be composed of seven protein subunits (α , β , β' , γ , δ , ϵ and ζ) (Waters *et al.*, 1991; Serafini *et al.*, 1991a; Stenbeck *et al.*, 1993; Duden *et al.*, 1991) and the small GTP-binding protein ARF (ADP-ribosylation factor) (Serafini *et al.*, 1991b). The largest subunit is α (~150 kDa)

and the smallest subunit is ζ (~21kDa) (for the size of all subunits see Table 1 in Gaynor *et al.*, 1998). In a mammalian *in vitro* assay, COPI was found to bind to Golgi membranes and induce the formation of functional transport vesicles (Malhotra *et al.*, 1989). In yeast, the COPI subunits were identified as sec and ret mutants (Hosobuchi *et al.*, 1992; Duden *et al.*, 1994; Letourneur *et al.*, 1994; Cosson *et al.*, 1996).

The formation of COPI vesicles is proposed to occur with the initial binding of ARF-GTP to the membrane (Donaldson *et al.*, 1992). Once the membrane is primed, the coat protein self-assembles or polymerizes onto the membrane (Palmer *et al.*, 1993). The coat is released when ARF-GTP is hydrolyzed to ARF-GDP and Pi, allowing the vesicle to fuse with target membranes (Tanigawa *et al.*, 1993).

As mentioned, initial studies implicated COPI in anterograde transport (Pepperkok *et al.*, 1993; Peter *et al.*, 1993), however, many subsequent studies have implicated COPI in a retrograde pathway (Gaynor and Emr, 1997; Letourneur *et al.*, 1994; Pelham, 1994; Schekman and Orci, 1996; reviewed in Aridor and Balch, 1996). Indeed, COPI has the ability to bind to a di-lysine (KKXX) retrieval motif. This retrieval signal is found on the type I membrane proteins of the secretory pathway (Jackson *et al.*, 1993; Gaynor *et al.*, 1994; Townsley and Pelham, 1994; Cosson and Letourneur, 1994). Resident proteins that escape the ER and contain a retrieval motif are cycled back to the ER in COPI vesicles. Indeed, COPI is not essential for the anterograde transport of all secretory proteins (Gaynor and Emr, 1997). Mutants in γ -COP (sec21) cause a block in only a subset of proteins, which may in fact be a disruption in retrograde transport rather than a direct effect on anterograde transport (Gaynor and Emr, 1997).

It appears that COPI has yet another role. A recent study has shown that COPI binds to and dissociates from membranes in a continuous manner. The

transient association of COPI is significantly longer than that of ARF1 and is independent of vesicle formation. The proposed model is that coatomer generates separate membrane domains prior to the formation of transport structures, whether in coated vesicles or larger transport intermediates (Presley *et al.*, 2002).

4.2. COPII

COPII is the membrane coat that is involved in cargo exit from the ER. COPII was initially identified in yeast (Novick *et al.*, 1980). It is a complex composed of a Sec23p/Sec24p subunit (Hicke and Schekman, 1989; Hicke *et al.*, 1992), a Sec13p/Sec31p subunit and the small GTP-binding protein Sar1p (Salama *et al.*, 1993; Barlowe *et al.*, 1994; see Table 1 in Barlowe, 1998).

Unlike the ambiguity associated with the role of COPI, the role of COPII in vesicular transport is much more clear. The subunits of COPII, Sar1p, Sec13p and Sec23p localize to the ER exit sites, the location where this complex effects its role (Orci *et al.*, 1991; Shaywitz *et al.*, 1995; Kuge *et al.*, 1994). Essentially, COPII is required for the formation of ER-derived anterograde transport vesicles (Barlowe *et al.*, 1994; Bednark *et al.*, 1995). Coat formation is proposed to be initiated by the recruitment of Sar1p to the membrane by Sec12p in a process that requires a guanine nucleotide exchange (d'Enfert *et al.*, 1991a; d'Enfert *et al.*, 1991b). Sar1p then recruits the Sec23p/Sec24p complex, followed by the Sec13p/Sec31p complex. Once the vesicle is released from the ER membrane it will lose its coat, thus making the vesicle fusion competent and able to interact with its target membrane (reviewed in Barlowe, 1998).

Two other proteins are potentially involved in the coat formation. Sec16p has been suggested to be associated with Sec23p (Espenshade *et al.*, 1995). It may provide a scaffold on which the coat complex is formed (Gimeno *et al.*, 1996). Alternatively, it may be involved in cargo selection (Campbell *et al.*, 1997).

Sec4p is another potential component of COPII budding. Sec4p shares 45% identity with Sec12p, and Sec4p binds directly to Sec16p (Gimeno *et al.*, 1995).

4.3. *SNAREs, NSF and Rabs*

Once a transport vesicle is formed it must be able to find its target organelle and fuse with it. The machinery that dictates this specificity and allows the two membrane bilayers to fuse consists in part of SNAREs (soluble N-ethylmaleimide-sensitive factor attachment protein receptors), NSF (N-ethylmaleimide-sensitive factor), SNAPs (soluble N-ethylmaleimide-sensitive factor attachment proteins) and Rabs.

SNAREs are molecules that are intimately involved in the targeting of membrane fusion events. In fact, they define the vesicle (v) and target (t) membranes (hence, v- and t-SNAREs). They function by forming fusion complexes between v-SNAREs and t-SNAREs to bridge the vesicle and target membranes (Rothman and Warren, 1994; Sutton *et al.*, 1998). NSF and SNAP are required to disrupt the SNARE complex. Rabs are small GTP-binding proteins that are also involved in targeting and fusion events. These proteins are discussed in greater detail below.

4.3.1. *SNAREs*

SNAREs are integral membrane proteins that are involved in various membrane fusion events within the cell. In fact there are important commonalities between the structural motifs of SNAREs and viral fusion proteins (Skehel and Wiley, 1998). This indicates that the mechanism for membrane fusion is highly conserved.

SNAREs associate to form complexes that consist of bundles of four parallel helices. Three of the SNAREs are located on the target membrane while

the fourth SNARE is on the vesicle membrane (Parlati *et al.*, 2000). The syntaxin and SNAP-25 families make up the target-SNAREs, while synaptobrevins or VAMPs (vesicle-associated membrane proteins) make up the vesicle-SNAREs. Recently, SNAREs have been divided into Q- (glutamine containing) and R- (arginine containing) SNAREs. This designation is based on the highly conserved central amino acids (Q or R) (Fasshauer *et al.*, 1998). It is not clear what the precise role of the SNAREs are, whether they are involved in the docking or fusion events (reviewed in Chen and Scheller, 2001) or even what level of specificity they contribute to the targeting of vesicles (Pelham, 2001). The SNARE hypothesis initially predicted that the v- and t-SNAREs provide the complete specificity for the targeting of the vesicle to the target organelle and that the interactions between the v- and t- SNAREs served to dock the vesicle onto the target membrane (Sollner *et al.*, 1993). Recent studies, however, question the role of SNAREs in docking (Hunt *et al.*, 1994; Broadie *et al.*, 1995) and provide evidence that Rabs may be the molecules involved in vesicle docking (Cao *et al.*, 1998). Thus SNAREs may be directly involved in membrane fusion, and the formation of the SNARE complex may be the driving force (Chen and Scheller, 2001).

4.3.2. NSF

NSF is a hexameric AAA (ATPase associated with various cellular activities) ATPase that is required to dissociate the SNARE complexes. This process also requires the presence of α -SNAP. Both NSF (Block *et al.*, 1988; Malhotra *et al.*, 1989) and SNAPs (Clary *et al.*, 1990) were initially identified using a cell free system. The yeast homologue for NSF is Sec18p (Wilson *et al.*, 1989) and α -SNAP is Sec17p (Griff *et al.*, 1992).

NSF uses the energy from ATP hydrolysis to drive the dissociation of the complexes. α -SNAP interacts with the SNARE complex and with the ATP bound form of NSF to form a 20S complex (Wilson *et al.*, 1993). Initially, it was thought

that NSF and α -SNAP provide the driving force for membrane fusion through the disassembly of the SNARE complexes (Sollner *et al.*, 1993). However, it has been postulated that NSF and α -SNAP act after membrane bilayers have fused and are required instead to disassemble the SNARE complexes to allow recycling and further rounds of fusion to occur (Littleton *et al.*, 2001).

4.3.3. Rabs

Rabs are small GTP-binding proteins that have been implicated in various steps of vesicular traffic (reviewed in Zerial and McBride, 2001). Generally, Rabs are associated with the docking or tethering events of the vesicle to the target membrane, however, Rabs are also involved in vesicle formation, as a mutated form of rab1 inhibits protein export from the ER (Nuoffer *et al.*, 1994). In addition, a yeast two hybrid screen identified kinesin as a Rab interacting protein, thus implicating Rabs in vesicle motility (Echard *et al.*, 1998).

Rabs associate with a membrane through a prenylation on their carboxyl termini. Once heterotypic fusion of membranes has occurred, the Rab GDP dissociation inhibitor (Rab GDI) retrieves the Rab, which is now in a GDP-bound state, and returns it to its resident membrane (Pfeffer *et al.*, 1995).

Due to the large number of Rabs that have been identified (>60; reviewed in Zerial and McBride, 2001; Segev, 2001; Pereira-Leal and Seabra, 2000) these proteins have recently been proposed to help define organelles by creating unique protein scaffolds (Pfeffer, 2001). In addition to the large number of Rabs GTPases there is also a large number of effector proteins to which they bind. The diversity of these effector proteins appears to lend new functions to the Rabs (Segev, 2001).

4.4. The p24 Family

One of the major protein constituents of the secretory pathway is a group of type I transmembrane proteins termed the p24 family. These proteins are major constituents of COPI vesicles, COPII vesicles and the organelles of the early secretory pathway (Wada *et al.*, 1991; Stamnes *et al.*, 1995; Sohn *et al.*, 1996; Belden and Barlowe, 1996; Dominguez *et al.*, 1998). They are found in a wide variety of organisms, ranging from yeast to human. The p24 proteins have been grouped into four categories (α , β , γ , and δ) based on their amino acid sequence (Dominguez *et al.*, 1998). Below is a description of the data obtained on the p24 family from various species.

4.4.1. Mammalian

The first p24 protein (gp25L) was initially cloned in 1991 through its co-isolation with calnexin, TRAP α and TRAP β (Wada *et al.*, 1991). In 1999, a second paper recorded its relationship with calnexin (Chevet *et al.*, 1999; Chapter 1) and demonstrated that gp25L, now termed rp24 α 2, (Dominguez *et al.*, 1998), is a ribosome-associated protein. More specifically, rp24 α 2 requires a nascent polypeptide chain to form an association with the ribosome (Chevet *et al.*, 1999; Chapter 2).

The p24 proteins are abundant proteins of the early secretory pathway (Dominguez *et al.*, 1998; Fullekrüg *et al.*, 1999). They are mainly localized to the Golgi apparatus and intermediate compartment, but are also found in the endoplasmic reticulum and in phagosomes (Rojo *et al.*, 1997; Dominguez *et al.*, 1998; Fullekrüg *et al.*, 1999; Lavoie *et al.*, 1999; Emery *et al.*, 2000; Bell *et al.*, 2001; Garin *et al.*, 2001). Indeed the different p24s possess various degrees of glycosylation corresponding to their cycling pathway (Fullekrüg *et al.*, 1999).

The p24s have been proposed to be involved in both membrane structure and the transport of the secretory proteins through the early secretory pathway (Rojo *et al.*, 1997). The expression of exogenous p23 in mammalian cells causes p23 (both the endogenous and exogenous form) to relocate to the ER and generates a smooth ER membrane structure (Rojo *et al.*, 2000). Significantly, protein transport was not blocked, although minor delays were seen. In addition, the morphology of the Golgi was changed (Rojo *et al.*, 2000). It is postulated that the relocation of p23 to the ER may be a consequence of titration. That is, p23 may require a partner in order to exit the ER. If this partner is not as abundant as the p23 molecule, then the p23 protein may be trapped in the ER. Indeed, other members of the p24 family did not relocate to the ER (Rojo *et al.*, 2000). In fact, when at least 2 members of the p24 family are over expressed in mammalian cells the exogenous p24s are detected in the CGN (Dominguez *et al.*, 1998; Fullekrüg *et al.*, 1999; Emery *et al.*, 2000).

The relationship between the p24s and COPI is not clear. Some believe that the p24s are COPI receptors while others believe that no association is present. Initially p24s were isolated as abundant constituents of COPI vesicles (Sohn *et al.*, 1996; Stamnes *et al.*, 1995), predicting a role for the p24s as either sorting constituents or COPI receptors. Indeed, many have found that the p24s can bind COPI (Dominguez *et al.*, 1998; Sohn *et al.*, 1996). However, others have stated that they find no association of the p24s and COPI (Rojo *et al.*, 1997). The differences in the experiments used to create these conclusions are significant. Briefly, Sohn and colleagues added CHO cell lysates to p24 peptides linked to thiopropyl Sepharose 6B via their NH₂-terminal cysteine residues (Sohn *et al.*, 1996). Coatamer subunits were detected by Western blot. Likewise, Dominguez and colleagues used peptides corresponding to the cytosolic domain of five different p24s (Dominguez *et al.*, 1998). The peptides were coupled to thiopropyl Sephrose beads via cysteines and added to a pre-cleared HeLa lysate. The presence of COPI or COPII was detected through Western blots. These two experiments test for only the interactions between the p24 peptide tails and COPI

or COPII. The experiment that draws a different conclusion is one that uses membrane fractions. Briefly, two membrane fractions (M1, essentially devoid of p23; M2, high amounts of p23) were incubated with cytosol and nucleotides. COP and p23 were detected by Western blot. Since both membrane fractions appeared to recruit comparable amounts of COP, the authors concluded that the p24s do not contribute to COPI binding. It is significant to note that the COPI-binding motif of the p24s is K(X)KXX, a motif found on a large number of membrane proteins. The authors neglect the fact that the M1 fraction may contain membrane proteins with a COPI binding motif (including other members of the p24 family). It can be concluded that the p24s are not essential for COPI recruitment, nor are they the only proteins able to recruit coatomer. Recent work has shown that COPI has a short, yet continuous interaction with the membrane (Presley et al., 2002). It is possible that the p24s are able to enhance the COPI association with membrane. Thus the p24s do bind to COPI, but it is unlikely that they are true COPI receptors.

The p24 proteins cycle throughout the early secretory pathway and their localization is interdependent (Dominguez *et al.*, 1998; Fullekrüg *et al.*, 1999; Rojo *et al.*, 2000; Emery *et al.*, 2000). In fact, these proteins have been shown to be in a complex (Dominguez *et al.*, 1998; Fullekrüg *et al.*, 1999; Marzioch *et al.*, 1999). Initially, rp24 α 2 was found to co-sediment in a complex with a peak distribution around 35S (Dominguez *et al.*, 1998). Immunoprecipitation experiments reveal an interaction between p24 and p23 (Gommel *et al.*, 1999) and between p27, p25, p24 and p23 (Fullekrüg *et al.*, 1999). As mentioned above and consistent with the fact that the p24s form a complex, the exogenous expression of only one member of the p24 family leads to a mislocalization to the ER (Rojo *et al.*, 2000). Only when two p24s are co-expressed (*i.e.*, a member from the delta/p23 and beta/p24 subfamilies), is the exogenous p24 able to exit the ER (Dominguez, *et al.*, 1998; Fullekrüg, *et al.* 1999; Rojo, *et al.*, 2000; Emery, *et al.*, 2000). In fact, one member from each of the four subfamilies (alpha, beta, gamma

and delta) must be expressed for the proper sorting/trafficking of the p24s to occur (Fullekrüg *et al.*, 1999; Emery *et al.*, 2000).

The expression of the p24s is tissue specific as well as being regulated by various signaling pathways (Blum *et al.*, 1996; Baker and Gomez, 2000; Rötter *et al.*, 2002). p23 is developmentally regulated in the kidney and ureter development of Sprague-Dawley rats (Baker and Gomez, 2000). When embryonic day 14 (E14), newborn and adult kidneys were compared, p23 was found to be the most pronounced in the nephrogenic zone of the kidneys of newborn rats. Indeed, the role of p23 in development is significant since p23 null mice are embryonic lethal (Denzel *et al.*, 2000). Thus the p24s are spatially and temporally regulated.

4.4.2. *Saccharomyces cerevisiae*

An N-terminal sequence for the first yeast p24 protein was initially obtained from a partially purified endosomal fraction that was known to contain ER and Golgi (Singer-Kruger *et al.*, 1993). The gene for this protein was then cloned and sequenced in 1995 (Schimmöller *et al.*, 1995). It was termed EMP24 (endomembrane protein of the precursor of 24kD). Subcellular fractionation studies revealed that EMP24 mainly co-localizes with the ER marker Wbp1p, but also with the Golgi marker Och1p (Schimmöller *et al.*, 1995). EMP24 was also localized to COPII vesicles. The deletion of EMP24 causes a delay in the kinetics of a subset of proteins, specifically, periplasmic invertase and Gas1p, while alpha-factor, acid phosphatase, carboxypeptidase Y and alkaline phosphatase are secreted normally (Schimmöller *et al.*, 1995). The delay was found to occur in the transport of Gas1p and invertase to the Golgi rather than due to a delay in processing/modification of the proteins (Schimmöller *et al.*, 1995). Indeed, the p24s are implicated in the sorting/concentration of a specific subset of secretory proteins (Schimmöller *et al.*, 1995; Muniz *et al.*, 2000). In addition, the secretion of two resident ER proteins (Kar2p and Pdi1p) was increased (Schimmöller *et al.*, 1995; Elrod-Erickson and Kaiser, 1996). Seven more p24 proteins were later

identified, Erv25p (ER vesicle protein of 25 kDa) and Erp1p-Erp6p (Emp24p- and Erv25p-related proteins) (Belden and Barlowe, 1996; Marzioch *et al.*, 1999). Deletion of ERV25 (but not ERP1-6) also resulted in reduced invertase secretion (Marzioch *et al.*, 1999). Deletion of ERV25, ERP1 and ERP2 (but not ERP3-6) resulted in reduced rate of Gas1p secretion and increased Kar2p secretion (Belden and Barlowe, 1996; Marzioch *et al.*, 1999). The increase in Kar2p secretion appears to be due to the activation of the unfolded protein response pathway (UPR) in the deletion strains (Belden and Barlowe, 2001b). In fact, the *erv25Δ ire1Δ* and *emp24Δ ire1Δ* strains showed a reduction in growth rate, indicating a partial dependence of the p24s on this stress response pathway (Belden and Barlowe, 2001b). Further experiments showed a modest UPR response in the single knock out and that Kar2p secretion is dependent on IRE1 (Belden and Barlowe, 2001b). In addition, defects in the rate of incorporation of certain secretory proteins into COPII vesicles were found (Muniz *et al.*, 2000). As mentioned previously, a subset of proteins has altered kinetics in p24 deletion strains (Schimmöller *et al.*, 1995; Belden and Barlowe, 1996). One of these proteins, Gas1p, has been found to cross link with Erv25p and Emp24p (Muniz *et al.*, 2000). These data have led to the proposed role of cargo receptors for the p24s (Schimmöller *et al.*, 1995; Muniz *et al.*, 2000).

Belden and Barlowe (1996) first documented an association between ERV25 and EMP24. Later, an association was shown between ERV25, EMP24, ERP1 and ERP2 (Marzioch *et al.*, 1999). Knockouts of the p24 proteins in yeast are not lethal and show no distinct morphological changes. In fact a complete deletion of all eight (8) p24s shows no increase in the secretion defects from the most dramatic single knock outs (*erv25Δ* or *emp24Δ*) (Schimmöller *et al.*, 1995; Belden and Barlowe, 1996; Springer *et al.*, 2000). This result implies that a single knock out is sufficient to perturb the function of the p24s. Indeed, the quadruple and single knockouts show a perturbation in the stability/expression of the other p24s, thus implying a destabilization of the p24 complex (Belden and Barlowe, 1996; Marzioch *et al.*, 1999; Ciufo and Boyd, 2000).

The p24s are also postulated to be intimately involved with COPII. The p24s are abundant constituents of COPII vesicles (Belden and Barlowe, 1996), in addition, EMP24 was identified as BST2 (bypass of SEC13) (Elrod-Erickson and Kaiser, 1996). Thus an EMP24 deletion rescues the lethality of *sec13Δ*. This property is exclusive to SEC13 and BSTs will not rescue other null mutants such as SEC12, SEC23 and SEC31 (Elrod-Erickson and Kaiser, 1996). In addition, all three *bst sec13Δ* mutants exhibit an increase in Kar2p and Pdi1p secretion and a reduction in the release of invertase from the ER while CPY is only slightly affected (Elrod-Erickson and Kaiser, 1996). This data shows that the phenotype exhibited by the p24 deletions is not exclusive to this protein family. In fact *erd* mutants are also characterized by an increase in Kar2p secretion (Hardwick *et al.*, 1990; Semenza *et al.*, 1990). Two other p24s, ERV25 and ERP1, were later shown to also rescue the null phenotype of *sec13Δ* (Marzioch *et al.*, 1999). In a study that classified protein-protein interactions in yeast, Emp24p was found to form interactions with Sar1p, Sec23p and Sec24p (Schwikowski *et al.*, 2000). Erv25p was found to interact with Ylr124w (Schwikowski *et al.*, 2000). Emp24p, Erv25p and Erp1p have also been localized to Sed5p membrane vesicle fraction (Cho *et al.*, 2000). This fraction was identified as an early Golgi compartment fraction (Cho *et al.*, 2000).

The defects in secretion and retention appear to be due to exit from the ER. Other data indicate that the p24 deletions have no effect on COPI or COPII budding (Belden and Barlowe, 1996; Springer *et al.*, 2000). Thus the p24s may be involved in protein sorting, protein packaging or may just be a non-essential component of the COPI/COPII recruitment machinery.

The rate at which Emp24p cycles through the early secretory pathway is affected by the hydrophobic LV (lysine-valine) residues located at the terminal end of the cytoplasmic tail of the protein (Nakamura *et al.*, 1998). These hydrophobic residues, which are somewhat conserved among the p24s, accelerate

the forward movement of the proteins (Nakamura *et al.*, 1998). Glutamine residues in the transmembrane domain on the other hand, act to reduce the transport rate of the proteins and counteract the accelerated anterograde movement of the LV motif (Nakamura *et al.*, 1998). Exactly how Emp24p is recycled back to the ER is not clear because it does not contain a known retrieval signal. Emp24p does, however, interact with Erv25p, which does have a KK retrieval signal, and may be cycled back to the ER in this manner (Belden and Barlowe, 1996; Nakamura *et al.*, 1998). The interaction between p24 proteins appears to be in the luminal domain (Ciuffo and Boyd, 2000). The specificity for Emp24p lies between Cys-99 and Lys-147, which encompass the coiled-coil region of the protein (Ciuffo and Boyd, 2000).

The p24s are regulated during the cell cycle. Several studies have demonstrated an increase in the expression level of EMP24 during G1 and of ERV25 during S phase (Cho *et al.*, 1998; Spellman *et al.*, 1998). ERV25 expression is also increased during the unfolded protein response (UPR) (Travers *et al.*, 2000).

4.4.3. *Caenorhabditis elegans*

In *Caenorhabditis elegans*, there are at least five p24 genes (Wen and Greenwald, 1999; Kuiper and Martens, 2000). The first p24 gene, SEL-9, was discovered through screens for suppressors/enhancers of LIN-12 (SEL genes) (Sundaram and Greenwald, 1993; Wen and Greenwald, 1999). This genetic screen looks for genes that enhance or suppress the activity of the LIN-12/NOTCH family of proteins. The mutations in the luminal domain or deletion of the cytosolic and part of the transmembrane domains in the *sel-9* gene increased the activity of both *lin-12* and *glp-1* (genes that have mutations in the extracellular domain of LIN-12 and GLP-1, respectively). The increased activity of *lin-12* and *glp-1* was due to the increased amount of *lin-12* and *glp-1* that reached the plasma membrane. The *sel-9* mutant allowed the escape of mutated

proteins that would otherwise accumulate in the cell, presumably in the ER. Through database searching, four more p24 genes were identified in *C. elegans* in this study (W02D7, F47G9.1, F57B10.5, and 08E4.6). RNAi experiments were done with *sel-9* and F47G9.1. This also produced an increased *lin-12* and *glp-1* activity (Wen and Greenwald, 1999).

Hence, SEL-9 and F47G9.1 appear to be negative regulators of LIN-12 and GLP-1 transport. The mutated gene, *sel-9*, relieved some of the rigidity of the quality control of the ER, allowing proteins that would otherwise fail quality control to escape. This led the investigators to predict a functional role in quality control and cargo selection within the secretory pathway for SEL-9 and the p24s. Specifically, the p24s may act as cargo receptors for the LIN-12 and GLP-1 genes in *C. elegans*.

4.4.4. *Xenopus laevis*

In the amphibian *Xenopus laevis*, the first member of the p24 family to be identified (Xp24 δ_2) was found to be coordinately expressed with the translocon associated protein TRAP δ and pro-opiomelanocortin (POMC) in the melanotropes of the intermediate pituitary during black background adaptation (Holthuis *et al.*, 1995). These neuroendocrine cells possess a highly specialized secretory pathway and control various physiological aspects of the organism through neuropeptide and peptide hormone release (reviewed in Kuiper and Martens, 2000). Black background adaptation causes an increase in protein synthesis and depletion of melanophore-stimulating hormone (MSH). The opposite was seen for white background adaptation (Jenks *et al.*, 1977). In 2000, a second p24 from *Xenopus*, Xp24 δ_1 , was identified (Kuiper *et al.*, 2000). The Xp24 δ_1 , however, is not induced in melanotropes in coordination with POMC. These two p24 proteins appear to be tissue specific, which may account for the differences in expression levels with respect to POMC. Recently, Martens has recently identified six more p24s in *Xenopus laevis* through screening of cDNA

libraries (Rötter *et al.*, 2001). Thus *Xenopus* have at least eight different p24 proteins: two alpha subfamily members (p24 α_2 and p24 α_3), one beta subfamily member (p24 β_1), three gamma subfamily members (p24 γ_1 , p24 γ_2 and p24 γ_3), and two delta subfamily members (p24 δ_1 and p24 δ_2). In the amphibian, *Xenopus laevis*, only six of the eight p24s are expressed in melanotrope cells, of which only four are induced in active melanotropes (Rötter *et al.*, 2002). This same group has also shown that the subcellular location of the p24s within the melanotrope is dependent of its biosynthetic activity (Kuiper *et al.*, 2001).

4.4.5. *Fugu rubripes*, *Anguilla anguilla* and *Cyprinus carpi*

In fish, as in humans, the p24s have been identified in association with the neural degenerative condition, Alzheimer's disease. This disease is characterized by the deposition of amyloid- β , which forms plaques in neural tissue. In pufferfish (*Fugu rubripes*), the p24 gene, S31iii125, was identified due to its location at the AD3 locus (a chromosomal region associated with Alzheimer's disease) (Trower *et al.*, 1996). In a screen for G-protein coupled receptors from eel (*Anguilla anguilla*) retinal cDNA, a clone was found that showed similarities to the p24 gene S31iii125 of pufferfish and human. This knowledge was then used to screen for an orthologue in carp retina. In 1998, the carp (*Cyprinus carpio*) p24 was identified. The discovery of this gene was in conjunction with the identification of a presenilin gene PS1 (which is associated with Alzheimer's disease). To this point, the only association of the p24s with this disease is purely on the basis of its chromosomal location.

4.4.6. *Polyphondylium pallidum* and *Dictostelium discoideum*

The p24 LbrA (long branch A) was identified in slime mold (*Polyphondylium pallidum*) through an insertional mutagenesis system, restriction-enzyme-mediated integration (REMI) (Kawabe *et al.*, 1999). The LbrA gene was identified because the mutant strain M2323 (with a vector insertion site

near the LbrA gene) produced a strain with altered morphology (longer branches). Disruption of the *lbrA* gene produced the same changes in structure and for the first time implicates the p24s in morphogenesis. The investigators proposed that the role of the p24s in morphogenesis may not necessarily be a direct role, but rather an indirect role in the transport and/or sorting of protein factors that are involved in morphogenesis.

In addition, four potential p24 genes for *Dictostelium discoideum* were found in the Dicty cDB (an EST database for *Dictostelium discoideum*). One of which has 69% identity to LbrA, the other three with about 30% identity.

4.4.7. Other Species

The genomic sequencing projects have provided databases with complete and incomplete genomes of various species. These databases have provided the means to identify numerous p24s in other species, including *Drosophila melanogaster*, *Schizosaccharomyces pombe*, *Arabidopsis thaliana*, *Bos taurus*, *Neurospora crassa* and *Salmo salar*. In fact, the p24s have sequence related gene products in at least fifty-four different species, with over a hundred p24 genes identified (Chapter 5).

4.4.8. Cell Free Systems

In cell free systems, the p24 tails have been shown to bind to the coat proteins COPI and COPII (Dominguez *et al.*, 1998). More specifically, a peptide with the amino acid sequence of the cytoplasmic tail of p23 (YLRRFFKAKKLIE) has been shown to bind specifically to the γ subunit of COPI (Harter and Wieland, 1998). p23 is highly enriched in COPI vesicles. It is present in a ratio of 4:1 (Sohn *et al.*, 1996). The tail of p23 (and p24) has also been shown to be required for COPI vesicle formation from lipid bilayers, along with ARF, coatamer and GTP (Bremser *et al.*, 1999). The binding of coatamer to p23 and vesicle

formation is abolished by the mutation of the FF motif to AA and the KK motif to SS (Dominguez *et al.*, 1998; Bremser *et al.*, 1999). Nuclear magnetic resonance (NMR) spectroscopy studies revealed that p23 tails form tetrameric α -helix structures (Weilder *et al.*, 2000).

The p24s are abundant proteins of the secretory pathway and are somehow involved in the morphology and protein transport, whether through direct or indirect means. A clear functional role, however, has remained elusive.

There are indeed many more molecular components essential to the secretory pathway that are not described in this text. Noteworthy are the proteins involved in nucleotide exchange, structural integrity, the cytoskeleton, recycling and the regulation of all of these factors.

Figure i. Summary of the effect of the p24s on the secretory pathway. A collection of the data is presented in a schematic that represents the early secretory pathway.

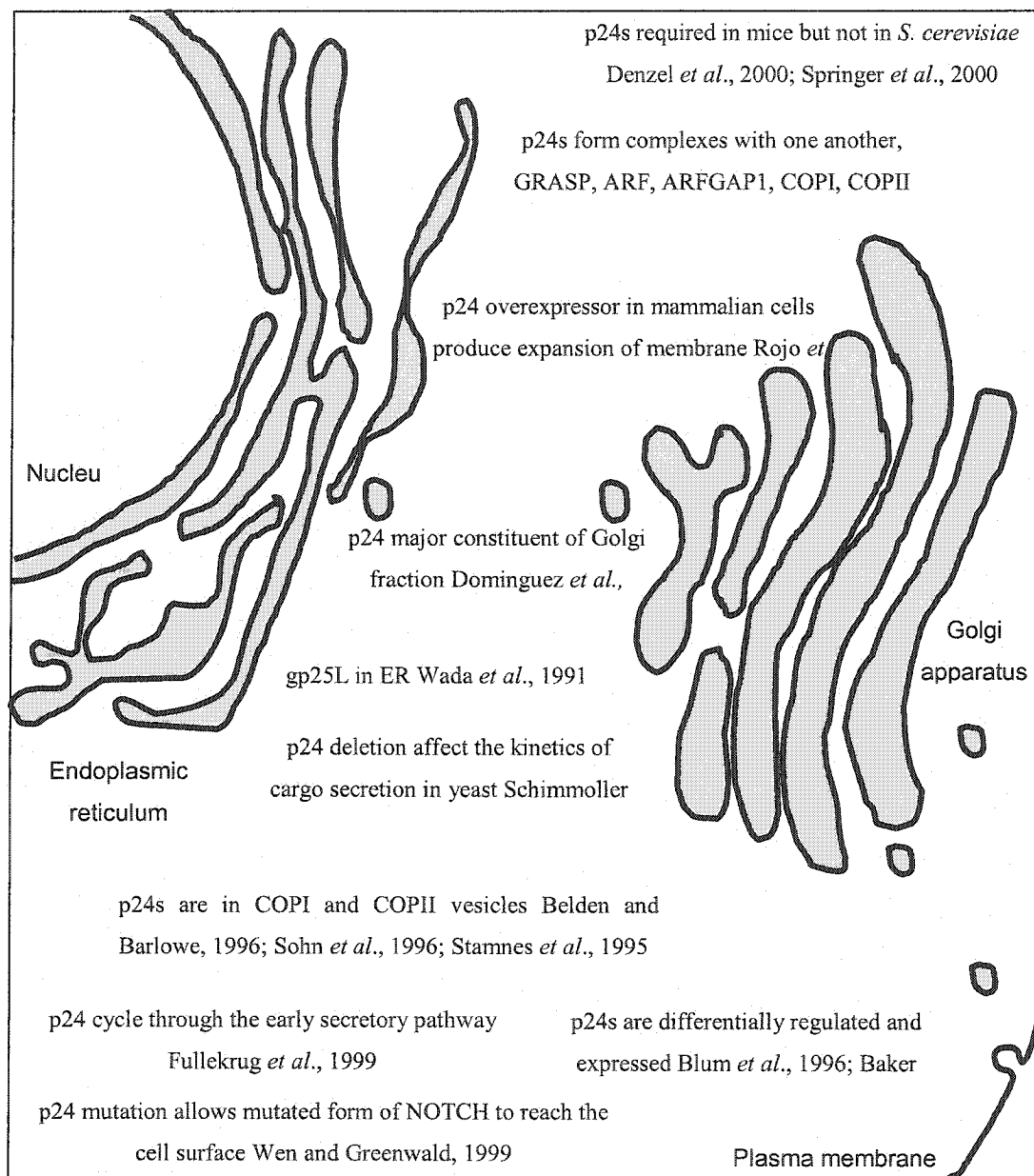


Figure i.

5. The p24s and the Secretory Pathway

This thesis proposes to resolve some of the mechanisms of the early secretory pathway by focusing on one of its abundant constituents, the p24 family of transmembrane proteins. It is interesting that an increase in p23 protein elicits the formation of large membrane structures (Rojo *et al.*, 2000). In addition to the formation of this novel membrane structure, there is a fragmentation of the Golgi into mini-Golgi stacks. Microinjection of antibodies to p23 into mammalian cells inhibits both the anterograde transport of the VSV ts045-G protein to the plasma membrane (Rojo *et al.*, 1997) and the retrograde transport of the cholera toxin mutant (CTX-K63) from the Golgi to the ER (Majoul *et al.*, 1998). It is clear that the p24s are involved in both protein transport and morphogenesis.

In addition to their associations with coatomer, the p24s have been found to associate with ArfGAP1, Sec23p (Sar1pGAP) and ARF1 (Lanoix *et al.*, 2001; Dominguez *et al.*, 1998; Gommel *et al.*, 2001). These associations may contribute to the recruitment of COPI and COPII. A recent study has found that COPI associates/dissociates in a rapid and continuous manner with the membrane (Presley *et al.*, 2002). Presley and colleagues have also found that COPI generates membrane domains (Presley *et al.*, 2002). An increase in a p24 protein may enhance the association of coatomer to the ER membranes, thus producing new membrane domains as seen in the over expression studies (Rojo *et al.*, 2000). Since the p23 molecules appear to be unable to leave the ER in the p23 overexpressors and there is a delay in transport kinetics, it is possible that p23 causes a partial depletion of the pools of COPI/COPII/ARF1 to the extent that ER transport is delayed. If p23 is tying up much of the coatomer/ARF, the effect is somewhat reminiscent of a mild BFA response, where the Golgi becomes fragmented. In light of these and other data we predict that the p24s may contribute to the stability of the Golgi structure, the organization of the membranes of the IC/CGN and the kinetics of protein transport through their interactions with other components of the secretory pathway. Thus, the p24s may

act to enhance the association of COPI/COPII/ARF to membranes and have an indirect role in both transport and morphogenesis.

CHAPTER 1.

Calnexin and rp24 α 2 Associate with the Ribosome

1.1. Abstract

Calnexin and gp25L (rp24 α 2) were initially identified as endoplasmic reticulum (ER) type I integral membrane proteins, where calnexin was phosphorylated on its cytosolic domain by ER-associated protein kinases. Although the role of the ER luminal domain of calnexin has been established as a constituent of the molecular chaperone machinery of the ER, less is known about the role of the cytosolic domain of calnexin. On the other hand, the cytosolic tails of the p24s have been associated with COPI and COPII binding, however, their association with calnexin, TRAP α and TRAP β remains unclear. Isolation of rough microsomes was used to assay the associations of calnexin and rp24 α 2. It was determined that both proteins are ribosome associated proteins, however, the association of rp24 α 2 is dependent on the newly synthesized polypeptide chain, while the ribosome-association of calnexin is not. This indicates that calnexin has a direct association with the ribosome, while rp24 α 2 does not.

1.2. Introduction

The endoplasmic reticulum (ER) is a highly regulated multifunctional organelle. This organelle has several subdomains that are responsible for varying roles. The rough endoplasmic reticulum (rER), so named for its ribosome-studded surface, is responsible for the synthesis and conformational folding of secretory proteins. The smooth endoplasmic reticulum (sER), which is devoid of ribosomes and continuous with the rER, is responsible for detoxification and glycogen synthesis. A third subdomain, the transitional ER (tER) is the site where newly synthesized and folded proteins (cargo) are concentrated. The ER is also responsible for the quality control of these processes, especially to ensure proper folding and sorting of secretory proteins into cargo exit sites.

The ER has a plethora of resident proteins that carry out the various roles of the organelle. One such group of proteins is the ER chaperones. These proteins are responsible for ensuring the correct conformation of newly synthesized proteins. Secretory proteins contain a signal sequence that targets the peptide chain and attached ribosome to the ER membrane. The secretory protein enters the ER lumen through a protein pore, consisting of Sec61 trimeric protein complex. The peptide chain is captured by various resident ER proteins that are intrinsic in the maturation of the protein. One such protein is calnexin.

Calnexin was initially identified as a kinase substrate in isolated rough ER microsomes (Wada *et al.*, 1991). It was co-purified with TRAP α and TRAP β (translocon-associated proteins) and the founding member of the p24 family, gp25L (Wada *et al.*, 1991). Calnexin was speculated to be involved in protein translocation. Mass spectrometry was used to identify three phosphorylation sites for the human sequence of calnexin (Ser534, Ser544 and Ser563; Wong *et al.*, 1998). The role of gp25L (rp24 α 2) has yet to be resolved.

Calnexin is a type I transmembrane protein that is responsible for the proper folding of glycoproteins. Specifically, calnexin interacts with monoglucosylated moiety $\text{Glc}_2\text{Man}_9\text{GlcNac}_2$. ERp57 is then recruited to this complex to further assist in the folding of the newly synthesized glycoprotein (Zapun *et al.*, 1998). Once the oligosaccharide is released from calnexin the terminal glucose is available for hydrolysis by α -glucosidase II (Zapun *et al.*, 1997; Trombetta and Helenius, 1998). When a glycoprotein does not possess the correct conformation it may both be hydrolyzed by ER mannosidase I and targeted for degradation or reglucosylated by the UDP-glucose:glycoprotein glucosyl transferase (UGGT). The reglucosylation allows calnexin to bind once again (Cannon and Helenius, 1999) in an attempt to achieve the proper conformational folding, thus creating the Calnexin Cycle.

rp24 α 2 is also a type I transmembrane protein. It is the founding member of the p24 family (Wada *et al.*, 1991; Dominguez *et al.*, 1998). The p24 proteins are major constituents of the early secretory pathway (Dominguez *et al.*, 1998; Fullekrüg *et al.*, 1999). They cycle through the early secretory pathway, they appear to be involved in cargo transport and they have been linked to membrane morphogenesis (Schimmöller *et al.*, 1995; Fullekrüg *et al.*, 1999; Rojo *et al.*, 2000). The p24 proteins have been shown to associate with many of the protein constituents that make up the machinery that is responsible for cargo movement. They have been found to interact with COPI, COPII, ArfGAP1, Sec23p (Sar1pGAP) and ARF1 (Lanoix *et al.*, 2001; Dominguez *et al.*, 1998; Gommel *et al.*, 2001). In spite of what is known about the p24 proteins, a mechanistic role has yet to be described.

The following chapter details the analysis of the associations of rp24 α 2 and calnexin in the rough ER. In particular, it reveals the interactions of calnexin and rp24 α 2 with the ribosome.

1.3. Results

1.3.1. Calnexin and rp24 α 2 are ribosome associated proteins

Calnexin and gp25L were both initially co-isolated with the translocon-associated proteins (TRAP) α and β (Wada *et al.*, 1991). TRAP α and TRAP β are ribosome-associated membrane proteins. In order to determine whether calnexin and gp25L were also associated with the ribosome a methodology employed by Görlich *et al.* (1992) was used. Rough ER microsomes isolated from canine pancreas were solubilized with 1% Triton X-100, 1.5% digitonin or 1% CHAPS. A 1.5M sucrose cushion was then used to purify the ribosome-associated proteins. Calnexin was found to be ribosome-associated when digitonin or CHAPS was used as a detergent. rp24 α 2 was found to be ribosome-associated whether Triton X-100, digitonin or CHAPS was used to solubilize the membrane (Figure 1.1.).

1.3.2. Morphology and morphometry of the isolated membranes

In order to assess the association of calnexin and rp24 α 2 with the ribosome, the isolated rough microsomes were treated with 750 mM potassium chloride and 1 mM puromycin, 2mM EDTA or 25 mM potassium chloride and 1 mM puromycin (Figure 1.2.). The efficiency of ribosome removal from the membranes was assessed by quantifying electron micrographs of treated and untreated membranes. 750 mM KCl and 2 mM EDTA were comparable in their removal of ribosomal particles from the membrane. 25 mM KCl did not remove the ribosomal particles from the membranes (Table 1.1.).

Figure 1.1. The associations of calnexin and rp24 α 2 with ribosomes. Canine pancreatic rough microsomes (RM) were solubilized with 1% Triton X-100 (T), 1.5% digitonin (D) or 1% CHAPS (C). Ribosome-associated protein fractions were purified through a 1.5 M sucrose cushion, the pellet was suspended in SDS-PAGE Laemmli sample buffer, resolved by SDS-PAGE, transferred onto nitrocellulose and immunoblotted with anti-CNX-C1, anti-Sec61, anti-TRAP α or anti-rp24 α 2 antibodies, followed by [125 I]goat anti-rabbit IgG and visualized by radioautography using Kodak X-OMAT AR film.

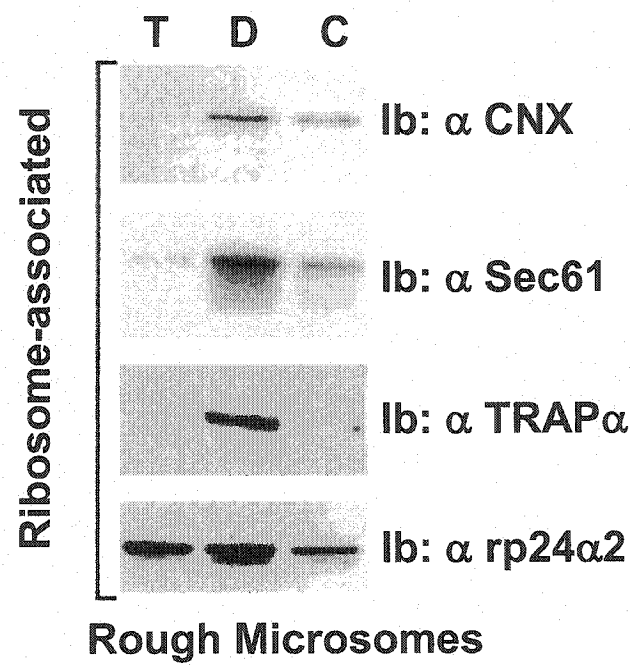


Figure 1.1.

Figure 1.2. Ribosome removal from canine pancreatic rough microsomes.

Canine pancreatic rough microsomes were isolated as described in the Materials and methods and treated with (A) 750 mM KCl + 1 mM puromycin (K750), (B) 2 mM EDTA (EsRM), (C) 25 mM KCl + 1 mM puromycin (K25) or (D) untreated (control). Membranes were fixed with 2.5% glutaraldehyde in 0.1 M cacodylate buffer with 0.05% calcium chloride pH 7.4, filtered onto 0.45 μ M pore size filters and processed for electron microscopy as described in the Materials and methods.

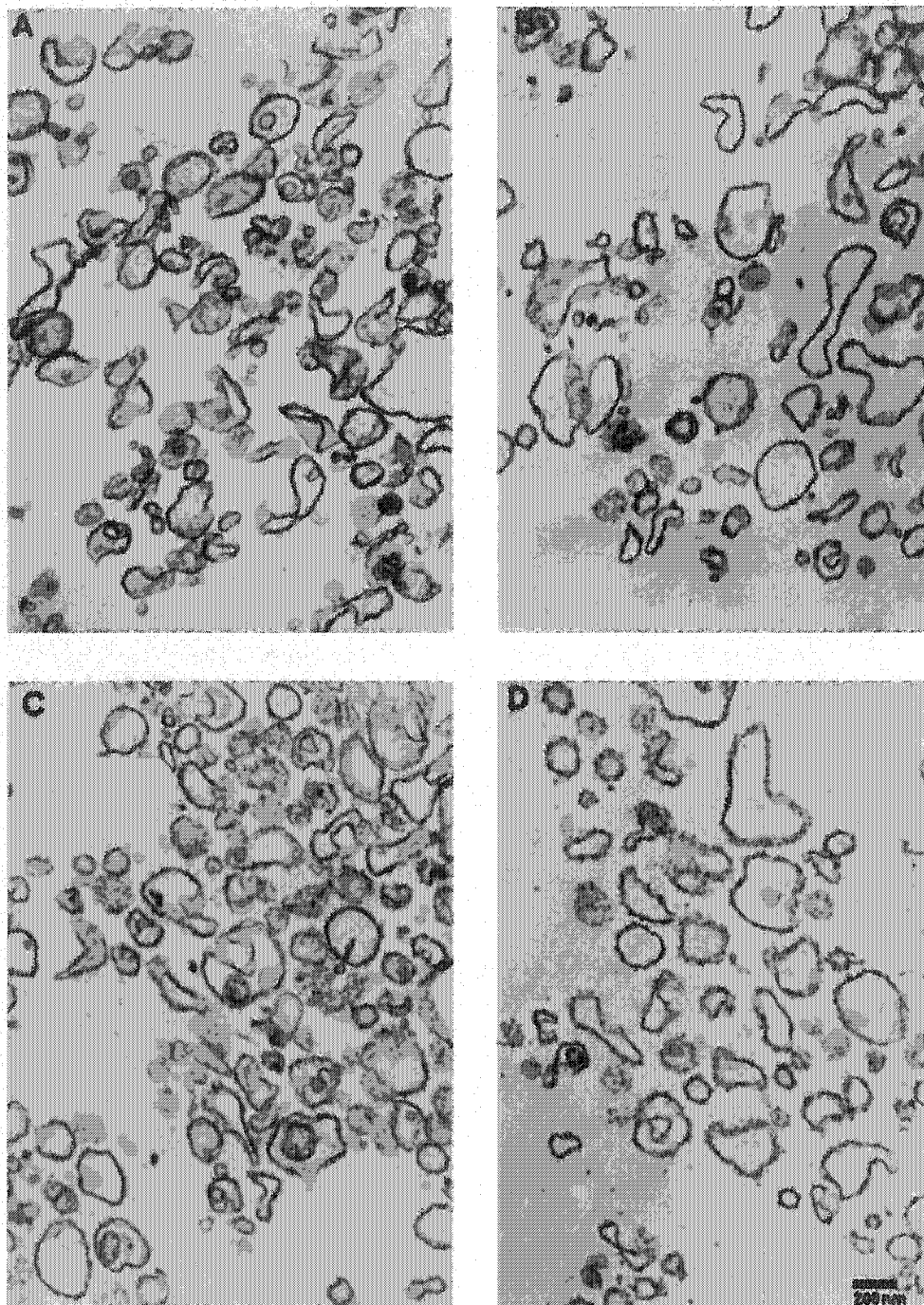


Figure 1.2.

Table 1.1. Quantitation of membrane-bound ribosomal particles at the surface of ER microsomes

	Ribosomes/vesicles	No. of vesicles analyzed
750 mM KCl + puromycin	2 ± 2	66
EDTA	3 ± 1	92
25 mM KCl + puromycin	37 ± 5	110
Control	43 ± 3	124

Canine pancreatic RM (control) were stripped as described by Adelman *et al.* (1973). Membranes were then analyzed by electron microscopy as described by Baudhuin *et al.* (1967). The number of ribosomal particles per vesicle was determined by counting on electron micrograph pictures.

1.3.3. Calnexin's association with the ribosome is independent of the nascent peptide chain, while rp24 α 2's association is dependent on newly synthesized cargo

To test whether the association of calnexin and rp24 α 2 was dependent on the nascent peptide chain, ribosome sedimentation experiments were carried out on the membranes described in Figure 1.2. and Table 1.1. Calnexin remained bound to the ribosome in isolates from rough membranes (untreated) or membranes treated with 25 mM potassium chloride and 1 mM puromycin. rp24 α 2 remained bound to the ribosome in isolates from rough membrane (untreated) but not to membranes treated with 25 mM potassium chloride and 1 mM puromycin. (Figure 1.3.). This result indicates that the association of calnexin with the ribosome is independent of the removal of the nascent chain by puromycin. rp24 α 2, however, requires the nascent peptide chain in order to be associated with the ribosome. The calnexin-ribosome association is likely to be direct while the p24 association is dependent of the nascent peptide chain.

Figure 1.3. Characterization of calnexin association with ribosomes. Canine pancreatic rough microsomes (RM) were stripped with EDTA (EsRM) or 1 mM puromycin + 750 mM KCl (K750) or 1 mM puromycin + 25 mM KCl (K25) and were immunoblotted with anti-ribosomal L4 antibodies. Ribosome-associated proteins from membranes which had received the above treatments were purified and analyzed by immunoblotting with anti-CNX-C4 or anti-rp24 α 2 antibodies and visualized by enhanced chemiluminescence.

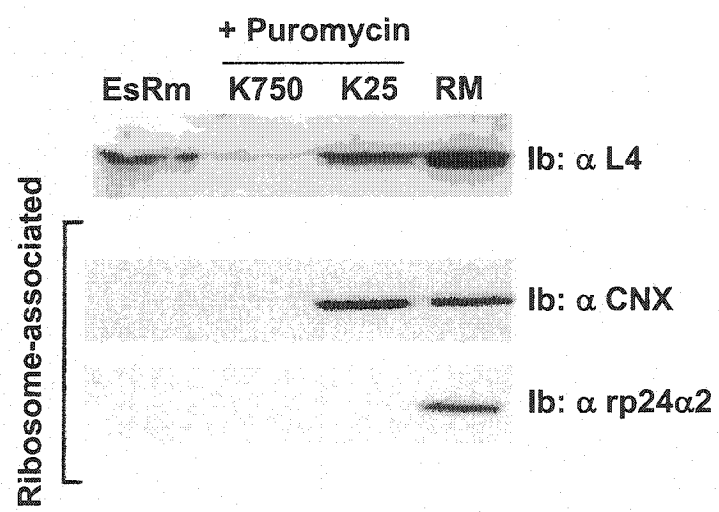


Figure 1.3.

1.4. Discussion

This study revealed that calnexin and rp24 α 2 are both found to associate with the ribosome. The association of calnexin is independent of the nascent polypeptide chain but enhanced by ERK1 phosphorylation (Chevet *et al.*, 1999). Thus calnexin's association is mediated by its phosphorylation state and the interaction is with the ribosome itself. rp24 α 2, on the other hand, has an association that is dependent on the presence of a peptide chain, suggesting its interaction is not directly with the ribosome but may be with the newly synthesized polypeptide or with an accessory protein(s) that in turn interact with the newly synthesized protein.

The association of rp24 α 2 with the ribosome in a manner dependent on the presence of a nascent peptide chain is significant. It implies that the p24 protein may, in part, act as a sensor for protein synthesis. Several roles can be proposed for the p24s. (1) The p24s may act as a type of sorting mechanism. They may identify particular proteins and sort them away from other proteins. In fact, Emp24p has been established as the cargo receptor of GPI-linked proteins for ER exit in yeast, while Erv29p has been documented to be the cargo receptor for ER exit for pro-alpha-factor (Muniz *et al.*, 2000; Belden and Barlowe, 2001a). (2) The p24s may guide all newly synthesized proteins through the ER. The role of the p24s would be to identify cargo proteins and guide them through the molecular chaperone and then to the ER cargo exit sites. p24s and Erv29p are both enriched in COPII derived vesicles in yeast (Otte *et al.*, 2001), and must thus be present at the ER cargo exit sites. (3) The p24s may detect the presence of newly formed cargo proteins and create cargo-specific exit sites as a consequence. It has been documented that GPI-linked proteins and alpha factor can be segregated before exit from the ER, thus different cargo exit sites must exist in yeast (Muniz *et al.*, 2001). (4) Alternatively, the p24 protein may be part of a signaling pathway that recruits the machinery for cargo exit. Essentially, it is known that the p24s are at the site of cargo exit. This study has revealed that the

p24s are also located at the site of polypeptide entry into the ER. It can thus be extrapolated that the p24s may have a role linking cargo entry with cargo exit.

Unlike calnexin, a protein whose association with newly synthesized proteins has been proven, it is not clear why the p24s interact with the ribosome. This study, however, clearly shows that while in the rER, both calnexin and rp24 α 2 have an association with the ribosome. It is also of interest and importance to note that the association of the p24s and the ribosome is dependent on the presence of a nascent polypeptide chain. This lends further support to the idea that the p24s are intimately involved in the processing or shuttling of newly synthesized proteins. This study also confirms the presence of the p24s in the rER and maintains the original link of the p24s to calnexin and TRAP α and TRAP β (Wada *et al.*, 1991). Further studies will have to be undertaken to identify the true nature of the association of the p24s with the ribosome and the nascent peptide chain. Indeed, it may be discovered that the role of the p24s begins as soon as a peptide becomes associated with the endoplasmic reticulum.

1.5. Materials and Methods

1.5.1. Reagents and antibodies

Rabbit anti-sera were raised against three synthetic peptides corresponding to amino acids 30-48 (anti-CNX-C1), 487-505 (anti-CNX-C3) and 555-573 (anti-CNX-C4) of canine calnexin (Ou *et al.*, 1995). Anti-rp24 α 2 antibodies have been previously described in Dominguez *et al.*, 1998. Anti-Sec61 and L4 antibodies were generously provided by Dr C. Nicchitta (Duke University Medical Center). Anti-TRAP α antiserum was raised against the C-terminal domain of TRAP α and kindly provided by Dr G. Kreibich (NYU Medical Center). [¹²⁵I]goat anti-rabbit IgG (sa: 15 μ Ci/ μ g) were from ICN Biomedicals (Mississauga, ON). All other reagents were of the highest grade commercially available

1.5.2. Subcellular fractionation

Translocation competent canine pancreatic rough microsomes were prepared and stripped as described previously (Walter and Blobel, 1983). Stripping was performed with 2 mM EDTA or 1 mM puromycin and 750 mM KCl (Adelman *et al.*, 1973). Microsomes (10-12 mg/ml) were stored in aliquots frozen at -80°C in 20 mM HEPES-NaOH, pH 7.4, 50% glycerol, 1 mM dithiothreitol (DTT). The MLP fraction from rat liver homogenate was separated on linear sucrose gradients (0.5-2.3 M) as described previously (Amar-Costesec *et al.*, 1974). ER-associated ribosomes were purified from cells as described previously (Loftus *et al.*, 1997).

1.5.3. Immunoprecipitations

Cells or microsomal membranes were solubilized for 30 min on ice in 30 mM Tris-HCl pH 8.0, 150 mM NaCl, 1 mM phenylmethylsulfonyl fluoride (PMSF), 1 mM NaF, 1 µg/ml leupeptin, 5 KIU/ml aprotinin containing 1% CHAPS (buffer A). The lysate was centrifuged at 100 000 r.p.m. in a Beckman TLA-100.2 rotor for 20 min at 4°C, and the supernatant was incubated overnight at 4°C with the indicated antibody. Protein A-Sepharose beads were added for 1 h at 4°C with rotation then pelleted and washed four times with buffer A. Beads were either directly resuspended in Laemmli sample buffer or subjected to sequential immunoprecipitations. For this, the beads were resuspended in 50 µl of 30 mM Tris-HCl pH 8.0 containing 1% SDS and heated for 10 min at 95°C, followed by centrifugation for 10 min at top speed in a Brinkmann microfuge. The supernatant was diluted 15× with 30 mM Tris-HCl pH 8.0, 150 mM NaCl, 1 mM PMSF, 1% Triton X-100 and subjected to immunoprecipitation with the indicated antibody overnight at 4°C. Protein A-Sepharose beads were added for 1 h at 4°C with rotation, following by washing and resuspension in Laemmli sample buffer.

1.5.4. Analysis of ribosome-associated membrane proteins

The association of membrane proteins with ribosomes was assayed as described previously (Görlich *et al.*, 1992; Kalies *et al.*, 1994) except that five equivalents of canine pancreatic microsomes were solubilized in 75 µl of 50 mM Tris-HCl pH 7.6, 400 mM K acetate, 10 mM Mg acetate, 15% glycerol, 5 mM β-mercaptoethanol, protease inhibitors and 1.5% digitonin, or 1% CHAPS or 1% Triton X-100. After incubation for 30 min on ice, the ribosomes were centrifuged through a 100 µl cushion of 1.5 M sucrose in the same buffer, containing only

0.1% of the corresponding detergent. Membrane proteins in the ribosomal pellet were analyzed by immunoblotting after SDS-PAGE. The trypsin protection assay was performed as described previously (Kalies *et al.*, 1994).

1.5.5. Electron Microscopy

Membranes were diluted to reach 0.25 M sucrose final concentration. Samples were fixed with 2.5% glutaraldehyde in 0.1 M cacodylate buffer with 0.05% calcium chloride pH 7.4 for 2.5 h, and filtered onto 0.45 μ M pore-size filters (Baudhuin *et al.*, 1967), and washed with 0.1 M cacodylate buffer overnight. Samples were treated with a 1:1 solution of 3% potassium ferrocyanide and 2% osmium tetroxide for 1 h on ice (Karnovsky, 1971), and then washed with 0.1 M maleate buffer, pH 5.7, and stained with 5% uranyl acetate for 2 h on ice. After two washes with 0.1 M maleate buffer and one with 0.1 M cacodylate buffer, samples were dehydrated with a graded series of ethanol washes followed by 100% propylene oxide and then placed in a 1:3 mixture of Epon and propylene oxide for 1 h. This was followed by a 1:1 mixture for 1 h and then 100% Epon for 1 h. Samples were then placed in a 60°C oven for polymerization. Thin sections were cut, stained for 2 min in lead citrate and 5 min in uranyl acetate, and micrographs were taken at 37 500 magnification on a JEOL JEM-2000FX electron microscope operating at 80.0 kV; prints were magnified a further 1.8x.

CHAPTER 2.

**Reconstitution of the Morphological
Changes of the Early Secretory Pathway**

2.1. Abstract

A two-step reconstitution system for the generation of ER cargo exit sites from starting ER-derived low-density microsomes (LDMs; 1.17 g/cc) is described. The first step is mediated by the hydrolysis of Mg^{2+} ATP and Mg^{2+} GTP, leading to the formation of a transitional ER (tER) with the soluble cargo albumin, transferrin, and the ER-to-Golgi recycling membrane proteins rp24 α 2 and p58 (ERGIC-53, ER-Golgi intermediate compartment protein) enriched therein. The transitional endoplasmic reticulum (tER) consists of confluent rough and smooth endoplasmic reticulum (ER) domains. The ATPase associated with different cellular activities, p97, has been identified as the relevant ATPase. The t-SNARE syntaxin 5 was observed within the smooth ER domain of tER. The successful reconstitution of the transitional ER along with protein sorting has been achieved. In addition, the AAA ATPase p97 and syntaxin 5 are involved in the regulation of the assembly of the smooth ER domain of tER and hence one of the earliest membrane differentiated components of the secretory pathway.

2.2. Introduction

The organelles of the secretory pathway provide a milieu in which proteins and lipids can mature. These organelles are also involved in the movement and delivery of these lipids and proteins to their proper destination. The organelles of this system must maintain their functional integrity while a host of newly synthesized proteins and lipids is passed through them.

Newly synthesized secretory proteins attain their correct conformational state in the endoplasmic reticulum (ER). Once this is achieved, the proteins must then continue to travel through the secretory pathway. The mechanism through which this is achieved has been the subject of much controversy. Two popular models are the maturation model and the vesicular model. The maturation model predicts that both membrane and cargo move in an anterograde direction while resident proteins cycle in a retrograde manner (Morre and Keenan, 1997). Thus a maturation of cargo and the compartment in which it resides occurs. The vesicular model predicts that cargo is shuttled between pre-existing static organelles via small vesicular carriers (Rothman and Wieland, 1996). In this case, only the cargo matures. A third and more recent model has been proposed whereby transport between the ER and Golgi occurs in tubular structures (Lippincott-Schwartz *et al.*, 1998). Another characteristic of this model is that it describes the Golgi apparatus as one compartment, not as a set of discrete, separate cisternae. Indeed, the interconnections between the Golgi saccuoles have been identified (Clermont *et al.*, 1994). In order to distinguish among these models, careful analysis of the secretory pathway must be undertaken. Indeed, many efforts have been put forth to identify the proteomes of various organelles (Bell *et al.*, 2001), to analyze the mutants of the secretory pathway (Novick *et al.*, 1980), to visualize *in vivo* transport (Presley *et al.*, 1997) and to study cell free systems that reconstitute certain aspects of the secretory pathway (Rothman, 1994).

The following chapter is a description of the faithful reconstitution of the ER in an in vitro system. ER derived low-density microsomes were used to reconstitute transitional ER and ER cargo exit sites. Immunocytochemical analysis revealed that both the morphology and protein segregation were reconstituted in this assay. In addition, p97 is identified as the ATPase involved in the ATP-depend step of the formation of tER. Syntaxin 5 and rp24 α 2 were also identified as requirements for the tER formation.

2.3. Results

2.3.1. Distribution of soluble cargo and integral membrane proteins in reconstituted ER system

The cell-free reconstitution of the rough and smooth regions of the endoplasmic reticulum has previously been documented (Lavoie *et al.*, 1996). This was achieved by incubating an isolated fraction of low-density microsomes (LDMs) with magnesium GTP and magnesium ATP. The structures that are generated consist of an array of rough ER cisternae continuous with a smooth transitional region, which corresponds to the tER. In order to determine the protein distribution of the reconstituted networks gold immunolabeling was performed (Figure 2.1.).

The luminal cargo proteins albumin and transferrin were assessed for their localization in the reconstituted ER compartment. Albumin is an abundant protein of the blood plasma. Transferrin is a glycoprotein with the ability to bind ferric iron. Both of these secretory proteins were found to be more concentrated in the smooth ER than in the parallel rough cisternae (Figure 2.1. A and B; Table 2.1.). The membrane proteins ribophorin, calnexin, rp24 α 2 and p58 were also assessed. Ribophorin is a subunit of the oligosaccharyltransferase of the ER (Kelleher *et al.*, 1992). Calnexin is an ER lectin that is involved in the protein folding of glycoproteins. rp24 α 2 and p58 are membrane proteins that cycle through the secretory pathway but that are concentrated in the ER-to-Golgi-intermediate-compartment (Dominguez *et al.*, 1998; Saraste and Kuismanen, 1992; Tisdale *et al.*, 1997; Fullekrüg *et al.*, 1999). Ribophorin was found to be more concentrated in the rough cisternae (Figure 2.1.E; Table 2.1). rp24 α 2 and p58 were both more concentrated in the sER compartment (Figure 2.1. C and D; Table 2.1). Surprisingly, calnexin was also concentrated over the SER compartment (Figure 2.1. F; Table 2.1).

These results indicate that, despite the continuity between the rough and smooth membrane systems, there is a sorting of luminal and membrane proteins. It is also noteworthy that the ribosome distribution also exhibits a distinct segregation, thus producing areas of rough and smooth membrane.

Protein concentrations in the starting material were calculated as a control. Labeling densities for calnexin and rp24 α 2 were calculated to be each 1.2x more concentrated in the smooth microsomes than over the rough microsomes in the LDM fraction. In the reconstituted networks, rp24 α 2 was concentrated 2.1x and calnexin 1.6x over the sER as compared to the rough ER. This clearly indicates that the reconstitution of the ER networks also causes a concentration or sorting of proteins.

2.3.2 Localization of p97 and Syntaxin 5

Syntaxin 5 and p97 were determined to be key factors in the formation of the sER portion of the reconstituted ER networks (Roy *et al.*, 2000). Cryo immunolabeling was performed on the ER networks with antibodies to p97 and syntaxin 5. No detectable labeling was found for p97 (results not shown). This is consistent with the idea that p97 dissociates from the membranes during the in vitro reconstitution, after the membranes have formed. Immunoblots with p97 revealed that it was found in the cytosol and microsomal fraction (Figure 6A of Roy *et al.*, 2000). In contrast, syntaxin 5 labeling was readily visualized (Figure 2.2.). Gold particles were detected over the smooth interconnecting tubules, with some labeling over the rough portions of the membrane. In fact, syntaxin 5 was concentrated 1.4x on the smooth ER as compared to the surrounding rough ER.

Figure 2.1. Concentration of albumin, transferrin, rp24 α 2, p58, ribophorin, and calnexin in tER. LDMs were incubated in the presence of mixed nucleotides to form tER. Antibodies to albumin (**A**), transferrin (**B**), rp24 α 2 (**C**), p58 (**D**), ribophorin (**E**), and calnexin (**F**) were applied to ultrathin cryosections. Gold particle labeling is predominantly distributed over interconnecting ER tubules for all antigens studied, except in the case of ribophorin (**E**), where gold particle labeling is mainly over rough ER. Inset in **C** shows rp24 α 2 labeling over a bud in the tER. rer, Parallel rough ER cisternae; ser, interconnecting smooth ER tubules. Bars, 0.2 μ m.

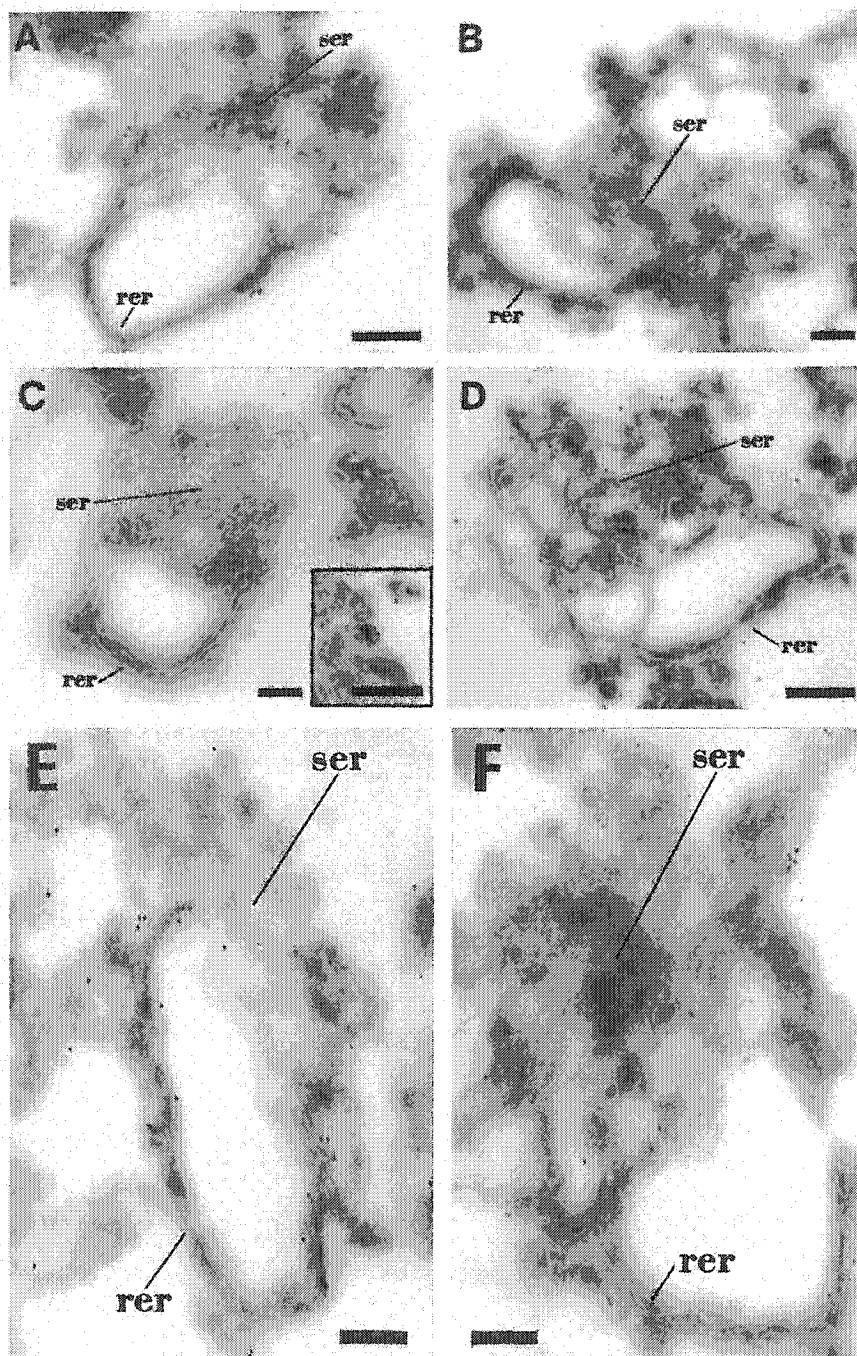


Figure 2.1.

Table 2.1. Amount of Soluble Cargo and Integral Membrane Proteins in Reconstituted tER

Protein	Networks	Gold particles	Surface area of SER*	Labeling over SER	Concentration in SER [§]
	n	n	%	%	
Albumin	26	319	60.6	73	1.6x
Transferrin	15	131	57.9	64.9	1.2x
rp24 α 2	20	395	66.4 [‡]	76.7	2.1x
p58	12	303	76.0 [‡]	82.8	1.6x
Calnexin	17	185	61.7 [‡]	74.6	1.6x
Ribophorin	19	332	61.6 [‡]	42.5	0.5x

* SER corresponds to the smooth ER tubules of the reconstituted tER.

[‡] Surface area of tER excludes the lumen of the central cisternae of the rough ER compartment.

[§] To calculate concentrations, percent antigen labeling densities were determined for the rough and smooth ER compartments, and these values were compared to the relative amounts of surface areas occupied by each compartment as described in Materials and Methods.

Figure 2.2. Localization of syntaxin 5 within reconstituted tER. LDM were incubated in the presence of mixed nucleotides to form tER. Antibodies to syntaxin 5 were applied and gold immunolabeling studied using the post embedding immunolabeling procedure described in the Materials and Methods. Gold particle labeling (arrows) is predominantly distributed over interconnecting smooth tubular portions of tER. Structures labeled rm correspond to parallel rough ER membranes, and those labeled st correspond to smooth ER tubules. Large arrows point to clusters of gold particle labeling, whereas small arrows point to single gold particle label. Scale bars represent 200 nm.

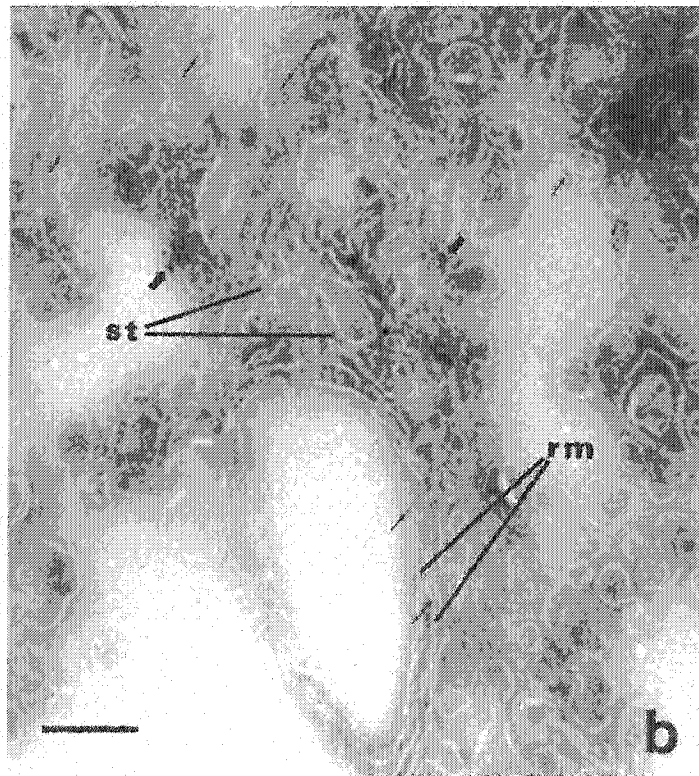


Figure 2.2.

2.4. Discussion

This chapter details the reconstitution of the morphological and molecular changes of the early secretory pathway. This is achieved through the use of low-density microsomes and the addition of magnesium and nucleotides. This produces a membrane system consisting of arrays of rough ER cisternae that are continuous with a network of smooth membranes. The cargo proteins albumin and transferrin are concentrated in the sER along with the membrane proteins rp24 α 2, p58, calnexin and syntaxin 5. The ER protein ribophorin is more concentrated in the rER network.

rp24 α 2 was found to be involved in the morphological changes of this system as the addition of antibodies to rp24 α 2 affected the morphogenesis of the membrane system (Figure 4, Lavoie *et al.*, 1999). β -COP, likewise, is involved in the morphogenic transformation of the membranes. Addition of BFA or partial depletion of β -COP from the cytosol both affected the generation of VTCs (Lavoie *et al.*, 1999).

The membrane fusion events of this system are highly specific and involve different sets of molecular machinery for the fusion between rough membranes and the fusion between smooth membranes. Indeed, p97 and syntaxin 5 are essential for the formation of the smooth ER membranes, but are not required for the formation of the rough ER networks (Roy *et al.*, 2000). Antibodies to either protein greatly affected the formation of sER networks. Thus rp24 α 2, β -COP, p97 and syntaxin 5 are part of the molecular machinery involved in the morphogenesis of smooth membranes of the early secretory pathway.

The assay described in this chapter clearly demonstrates the ability of the membranes of the early secretory pathway to undergo morphological changes and to mature. In fact, the analysis of this cell free assay has led to the identification

several constituents that are necessary for this process to occur. p97, syntaxin 5, rp24 α 2 and β -COP are all required for the reconstitution and morphological transitions of the early secretory pathway (Lavoie *et al.*, 1999; Roy *et al.*, 2000). These data are consistent with the model where the entire membrane compartment is dynamic and can undergo morphological change. Indeed, vesicular structures were accompanied by tubular structures when cytosol is added to this system (Lavoie *et al.*, 1996; Lavoie *et al.*, 1999). This data would be consistent with either a maturation model or a model where movement occurs in tubular structures.

2.5. Materials and Methods

2.5.1. Preparation and Characterization of Microsomes

Total microsomes were obtained by differential centrifugation of rat liver homogenates (Paient and Bergeron 1983). They were suspended in sucrose to give a final concentration of 1.38 M, placed under a step-gradient of 1.0, 0.86, and 0.25 M sucrose, and centrifuged using a Beckman SW 60 rotor at 300,000 g_{av} for 60 min. A subfraction containing smooth microsomes and low density rough microsomes (1.17 g/cm^3) was obtained from the upper half of the 1.38 M sucrose step above the residual pellet after centrifugation. This fraction, characterized as LDMs, was washed once by centrifugation and resuspension in 0.25 M sucrose at 100,000 g_{av} (Lavoie *et al.*, 1996). High density rough microsomes were prepared as previously described (Paient and Bergeron 1983). These fractions have been shown by electron microscope cytochemistry to contain a uniform distribution of the ER marker glucose-6-phosphatase. Further biochemical characterization for UDP-galactose:ovomucoid galactosyltransferase enzyme activity revealed a 2.2-fold increase over the homogenate for these microsomes, while that of a Golgi apparatus fraction prepared by the method of Dominguez *et al.*, 1998 revealed a 138-fold enrichment in galactosyl transferase activity. Hence, LDMs were at the most 1.6% contaminated by Golgi elements.

2.5.2. Cell-free Incubation Conditions

Unless otherwise indicated, the medium consisted of 0.25 ml of buffer containing 150 μg microsomal protein, 100 mM Tris-HCl, pH 7.4, 5 mM MgCl_2 , 1 mM GTP, 2 mM ATP, an energy regenerating system (7.3 IU/ml creatine kinase, 2 mM creatine phosphate), 0.1 mM DTT, 0.02 mM PMSF, 1 $\mu\text{g/ml}$ leupeptin, and 50 mM sucrose. Incubations were carried out at 37°C for 180 min. For studies on the effect of cytosol, 750 μg of rat liver cytosolic protein (in the presence or absence of 1 mM $\text{GTP}\gamma\text{S}$) was added to the medium described above

after 180 min and the incubation was continued for 5–60 min. To assess the effect of Brefeldin A (BFA; 200 μ M final concentration), this reagent was added to the medium 10 min before addition of cytosol. For fusion of classical rough ER, high density rough microsomes were incubated at 37°C in the presence of Mg^{2+} GTP (Palement and Bergeron 1983). For the effects of antibodies, 20 μ g (protein) of affinity-purified anti-rp24 α 2 or anti-calnexin was added where indicated.

2.5.3. Immunogold Labeling of Cryosections.

After incubation of membranes under assembly conditions, membranes were fixed using 4% paraformaldehyde and 0.1% glutaraldehyde in 0.1 M cacodylate buffer (pH 7.4) at 4°C. Cryoprotection, freezing, sectioning, immunolabeling, and contrasting were carried out as previously described by Dahan *et al.* (1994).

2.5.4. Analysis of Gold Label Distribution.

Rough membrane cisternae were defined as large cisternal profiles limited by ribosome-studded membranes. SER were defined as branching and anastomosing tubules limited by membrane devoid of associated ribosomes. The number of gold particles over rough ER membranes, as well as those over the SER that made up the reconstituted networks, were expressed as average number of gold particles per ER membrane network. Counts were compared for different membrane incubation conditions.

For quantification of rp24 α 2, p58, albumin, transferrin, calnexin, ribophorin and p97 labeling on cryosections, gold particles associated with rough membranes and SER comprising the ER networks were counted. Gold particles were counted over parallel juxtaposed ER cisternae (representing rough ER cisternae) and over the adjacent continuous mass of interconnecting membranes (corresponding to interconnecting smooth ER tubules). Surface area

measurements of each compartment comprising the reconstituted ER networks were measured as previously described for ER membranes in situ (Paiement *et al.*, 1988). Gold particle densities were calculated as number of particles per compartment of ER network and concentrations expressed in each category of membranes were then expressed as average number of gold particles per surface area for each ER network.

2.5.5. Antibodies

Rabbit polyclonal antibodies against calnexin (Ou *et al.*, 1993) and rp24 α 2 (Dominguez *et al.*, 1998) have been previously described. Polyclonal antibodies against p58 were a gift from Dr. J. Saraste (Ludwig Institute for Cancer Research, Stockholm, Sweden). Antibodies to rat albumin and rat transferrin were obtained from Cappel Laboratories (Organon Teknika Inc.). Rabbit polyclonal antibodies against p97 used in the in vitro assays have been previously described (Zhang *et al.*, 1994). Rabbit polyclonal antibodies against heat-denatured p97 from dog pancreatic cytosol, described above, were used in immunoblot studies. Affinity purified rabbit polyclonal antibodies against recombinant C-terminally HisX6-tagged cytoplasmic domain of syntaxin 5 were previously described (Subramaniam *et al.*, 1997). Rabbit polyclonal antibodies against ribophorin II were a gift from G. Kreibich (Department of Cell Biology, New York University, School of Medicine, New York, NY).

CHAPTER 3.

**The p23 Compartment is the Site of Golgi Enzyme
Retrieval**

3.1. Abstract

Secretory proteins exit the ER in transport vesicles that fuse to form vesicular tubular clusters (VTCs) which move along microtubule tracks to the Golgi apparatus. Using the well-characterized in vitro approach to study the properties of Golgi membranes, we determined whether the Golgi enzyme NAGT I is transported to ER/Golgi intermediates. Secretory cargo was arrested at distinct steps of the secretory pathway of a glycosylation mutant cell line, and in vitro complementation of the glycosylation defect was determined. Complementation yield increased after ER exit of secretory cargo and was optimal when transport was blocked at an ER/Golgi intermediate step. The rapid drop of the complementation yield as secretory cargo progresses into the stack suggests that Golgi enzymes are preferentially targeted to ER/Golgi intermediates and not to membranes of the Golgi stack. Two mechanisms for in vitro complementation could be distinguished due to their different sensitivities to brefeldin A (BFA). Transport occurred either by direct fusion of preexisting transport intermediates with ER/Golgi intermediates, or it occurred as a BFA-sensitive and most likely COP I-mediated step. Direct fusion of ER/Golgi intermediates with cisternal membranes of the Golgi stack was not observed under these conditions.

3.2. Introduction

This chapter discusses the next stage of the secretory pathway: from ER/Golgi intermediates to the Golgi. The p24s have previously been shown to cycle in the early secretory pathway and are particularly concentrated in the cis Golgi network (CGN) (Dominguez *et al.*, 1998). This study takes advantage of this fact by using an antibody to p23 to isolate the pre-Golgi and early Golgi compartment. These structures in turn are used to confirm the pre-Golgi location of VSV-G. In addition, a cell free assay was used in order to determine where glycosylation of a viral cargo protein (VSV-G) occurs and how the appropriate Golgi enzymes gain access to this compartment. This is significant with regard to the molecular mechanism of transport through the secretory pathway. Specifically, to distinguish between the vesicular model of protein transport (Farquhar, 1985; Orci *et al.*, 1997), the cisternal maturation model (Beams and Kessel, 1968; Becker and Melkonian, 1996; Bonfanti *et al.*, 1998) and an alternative view where the continuities seen in the Golgi stacks are involved in the flow of cargo and/or enzymes within the organelle (Rambourg *et al.*, 1993; Clermont *et al.*, 1994; Dominguez *et al.*, 1999). If the vesicular model holds true, cargo is delivered to the pre-existing Golgi cisternae that contain the required processing enzymes. The cisternal maturation model, however, predicts that the cargo moves forward in larger membrane structures while the enzymes are cycled backwards to these anterograde moving structures.

This chapter relies on isolated fractions and cell-free assays to distinguish the molecular mechanisms whereby cargo becomes modified by Golgi enzymes. Specifically, cells deficient in the Golgi enzyme N-acetylglucosamine transferase I (NAGT I) and transfected with the vesicular stomatis virus glycoprotein (VSV-G) were subjected to various temperature blocks to accumulate cargo at various stages of the secretory pathway. Membranes were isolated and a complementation assay was performed to determine the optimum location for cargo to receive glycosylation by the Golgi enzymes of membranes isolated from control cells.

3.3. Results

3.3.1. *Immunoisolation of ER/Golgi intermediates with p23 antibodies*

The in vitro complementation assay used to measure intra-Golgi transport in the study by Lin *et al.*, 1999 uses a combination of Golgi enriched membranes isolated at various temperature block in VSV-G-transfected glycosylation-deficient cells and isolated membranes from WT cells. The goal of this study is to determine the cellular compartment in which VSV-G is located when it accesses glycosylation enzymes in the in vitro assay. It was determined that enzymatic modifications still occurred when VSV-G was accumulated in the ER/Golgi intermediate compartment by a 15°C block (Lin *et al.*, 1999).

In order to isolate the ER/Golgi compartment, p23 antibodies were conjugated to magnetic beads in order to pull down p23 enriched membranes. p23 is known to be concentrated in the ER/Golgi intermediate compartment, but also extends into the Golgi. Isolated membranes were analyzed by electron microscopy in order to visualize the compartment that was sedimented by p23. Figure 3.1. (A-F) are samples of membrane that were brought down with p23 antibodies conjugated to magnetic beads with an anti-rabbit IgG antibody. These membranes are enriched in anastomosing sectioned tubules characteristic of the ER/Golgi intermediates. In some instances, cisternae reminiscent of the Golgi cisternae were present. Figure 3.1. (G-H) are controls where no p23 antibody was present. No membranes were conjugated to the magnetic beads in the absence of the p23 antibody. Overall, the p23 derived fraction was enriched in anastomosing tubular element reminiscent of pre-Golgi structures as well as some Golgi cisternae.

Figure 3.1. Immunoisolation of the p23 compartment. Elements of the cis-Golgi network are prominent. Partial stacks of Golgi cisternal also observed (Gc) as well as pleiomorphic tubular structures (ps). The magnification bars (500 nm) are indicated as are the sectioned magnetic beads themselves. Control beads (**G** and **H**) are indicated. The variation in two separate experiments is shown (**A**, **B**, **C**, **D**, and **G** are from one experiment; **E**, **F**, and **H** are from a separate experiment).

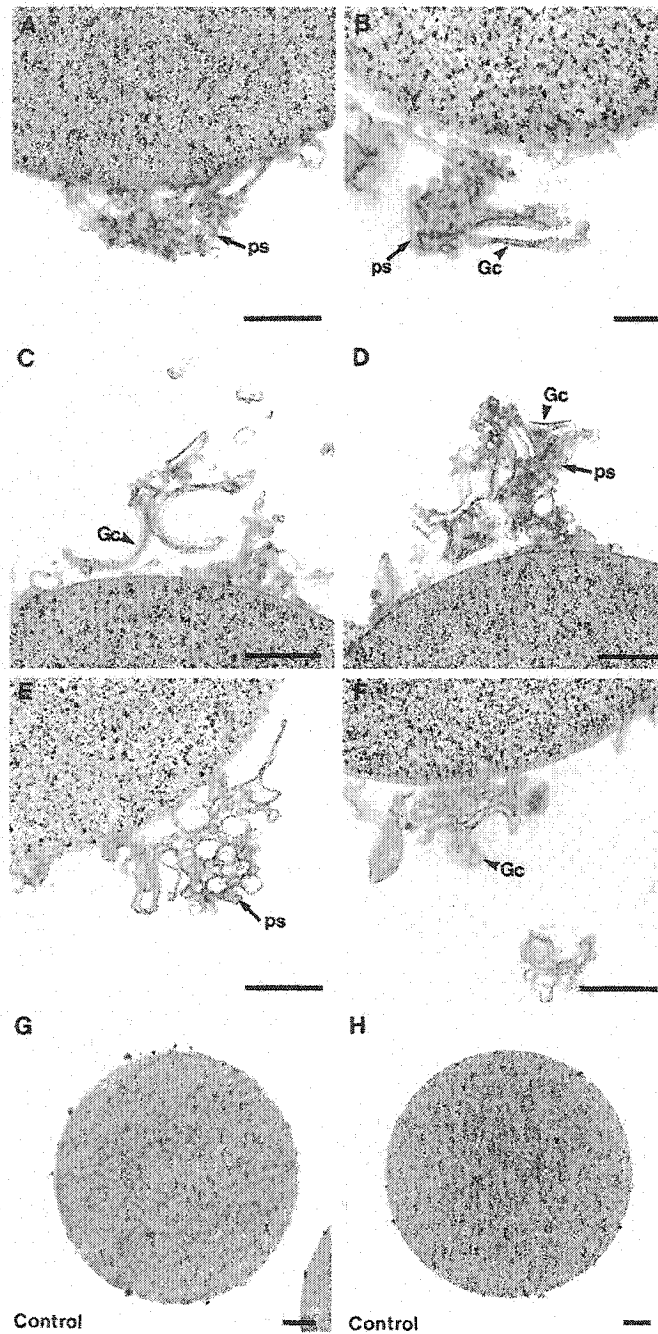


Figure 3.1.

3.3.2. Co-immunoisolation of VSV-G and Golgi enzymes with p23

In order to further assess the location of the VSV-G protein, Golgi-enriched membrane were isolated from cells with radiolabeled VSV-G in the 15°C compartment and cells that had been chased for 20 minutes at 37°C. Thus in the former fraction VSV-G should be in the ER/Golgi intermediate compartment and in the latter the VSV-G should have reached the Golgi. These membranes were then incubated with magnetic beads with and without antibodies to p23. The membranes were then analyzed for their content of p25 (another p24 protein) and VSV-G (Figure 3.2.). p25 was completely removed from the supernatant in fractions isolated with p23 antibody-coated beads. The majority of the VSV-G that had been accumulated in the 15°C compartment was precipitated with p23 antibody-coated beads. When the p23 antibody was omitted, both VSV-G and p25 remained in the supernatant, and very little binding to the beads was detectable. When cells were incubated after the 15°C chase for an additional 20 min at 37°C, then only approximately one-third of VSV-G was recovered with p23 antibodies. The immunoisolation of p25 was unaffected.

The percentage of different Golgi enzyme activities that was precipitated with p23 antibodies was also assessed. Approximately 30% of the total mannosidase activity was immunoisolated with p23 antibodies, which is a yield similar to the recovery of VSV-G after release of the 15°C block. When p23-containing membranes were immunoisolated from wt cells, an average of 38% of N-acetylglucosamine (GlcNAc) transferase (NAGT) and 23% of galactosyl transferase (GalT) activities were immunoprecipitated. This indicates that by the end of the 15°C incubation, VSV-G was in ER/Golgi intermediate and cis-Golgi network membranes, but after a 20-min chase at 37°C, it entered the Golgi stack. It also indicates that there is a significant amount of Golgi enzymes in the p23 fraction.

Figure 3.2. Immunoisolation of VSV-G and Golgi marker enzymes with p23 cytoplasmic tail antibodies. Magnetic beads were coated with p23 antibodies and incubated with membranes isolated from VSV-infected 15B cells containing labeled VSV-G in the 15°C compartment. Beads were recovered with a magnet and membranes that remained in the supernatant were pelleted by ultracentrifugation. When indicated, cells were incubated for 20 min at 37°C before homogenization of cells and isolation of membranes. A fraction of membranes bound to beads and membranes that were pelleted by ultracentrifugation were dissolved in electrophoresis sample buffer, and another fraction was dissolved in mannosidase assay buffer. VSV-G was visualized by phosphorimaging, p25 by Western blotting, and mannosidase activity was determined using a fluorescent substrate.

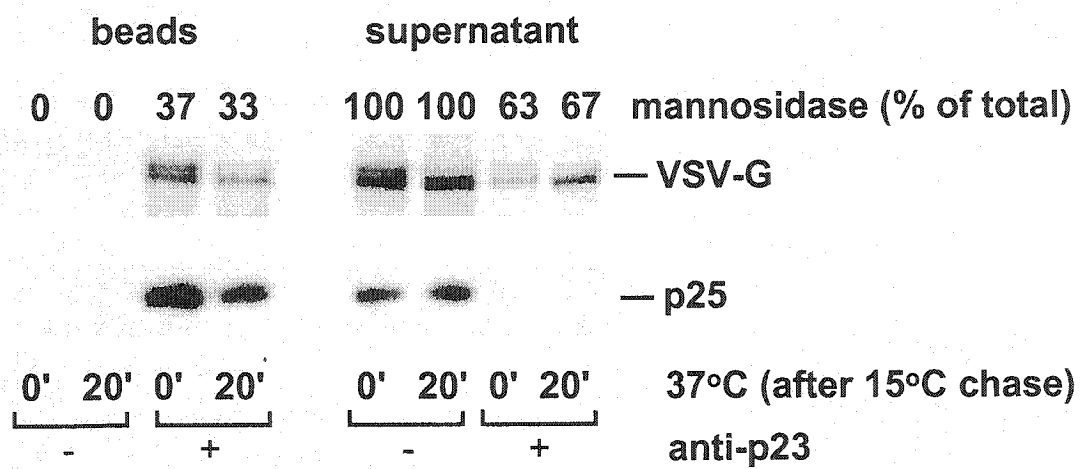


Figure 3.2.

3.4. Discussion

This study has shown that the glycosylation of the cargo protein VSV-G is most efficient in the ER/Golgi or 15°C compartment. This is significant and surprising, since the glycosylation efficiency of VSV-G was reduced once it had reached the Golgi apparatus, the site where the majority of the NAGT I enzyme is located.

This study has also determined that the ER/Golgi or 15°C compartment is identical to the p24 compartment. In fact, the p24 compartment was isolated for the first time in this study. This newly identified compartment is composed of anastomosing tubules and some elements of the Golgi stack. It accounts for approximately 30% of the Golgi enzyme activity. Thus Golgi enzymes are not restricted to the stacked cisternae of the Golgi apparatus.

In addition, this study has also revealed that glycosylation in the complementation assay is not due to fusion of Golgi membranes, but through another method. It appears that COPI vesicles are the mode of retrograde transport for Golgi enzymes from the Golgi apparatus to the ER/Golgi intermediate compartment. This finding is of great importance as it provides further evidence for the mechanisms through which cargo, membranes and enzymes are transported through the early secretory pathway. Indeed, this data is consistent with the maturation model. This model predicts that enzyme movement occurs in a retrograde fashion. These enzymes are predicted to fuse with anterograde moving structures that contain secretory cargo (Lin *et al.*, 1999).

This Chapter describes the site where glycosylation by the NAGT I enzyme is most efficient with respect to the VSV-G cargo protein. Further studies will have to be undertaken to identify where and how cargo modifications that occur at a later stage are carried out.

3.5. Materials and Methods

3.5.1. Cell Growth

CHO wt and 15B cells were grown on tissue culture plates in MEM α supplemented with 10% fetal calf serum plus penicillin and streptomycin in a 5% CO₂ atmosphere at 37°C and split 1 to 10 every 2 d. For large scale production of cells for isolation of membrane fractions or cytosol, cells were grown in spinner flasks until confluent.

3.5.2. VSV Infection

15B cells from a confluent spinner culture were pelleted, resuspended in 50 ml of infection media (serum free media, 1 ml VSV, 0.1 mg/ml actinomycin D, 25 mM Hepes, pH 7.2), and incubated for 45' at 37°C in a small spinner flask. 200 ml of media with serum were added, and the infection was continued for an additional 2 h 15 min.

3.5.3. Pulse-Chase Labeling

Cells were pelleted by centrifugation, washed once, and resuspended in 10 ml of methionine-free media per 1 ml of cell pellet. After 5 min at 37°C, 0.1 to 0.5 mCi per ml of ³⁵S-methionine/cysteine were added, and cells were incubated for an additional 5 min at 37°C (pulse). The labeling mixture was then diluted into a spinner flask containing a large volume of methionine-containing media in a water bath set to the desired temperature to be incubated for the indicated times (chase). For an additional chase at 37°C, aliquots were withdrawn and incubated for the indicated times in a water bath at 37°C.

3.5.4. Preparation of Cisternal wt Golgi Membranes

To prepare Golgi-enriched membranes, homogenate was centrifuged for 5 min at 1,000 g. The supernatant was loaded on a 1-ml cushion of 40% sucrose in 10 mM Tris, pH 7.2, and Golgi membranes were pelleted on this cushion by a 10-min centrifugation at 17,500 g. The bottom 2 ml were collected, mixed in an SW40 tube with 62% sucrose to ~40% final, and overlaid with 4 ml of 35% and 3 ml of 29% sucrose. After 90 min centrifugation at 40,000 rpm, Golgi membranes were harvested at the interface between 29% and 35% sucrose. For small scale preparations of Golgi membranes from cells after pulse-chase incubations, homogenates were mixed with 62% sucrose to 37.5% sucrose final and were overlaid with 2 ml 35% and 1 ml 29% sucrose in an SW55 centrifuge tube. After 90 min centrifugation at 50,000 rpm, Golgi membranes were harvested at the interface between 29% and 35% sucrose. To prepare salt-washed Golgi membranes, Golgi membranes harvested after flotation were diluted with 4 volumes of 10 mM Tris, pH 7.2, and KCl was added to 250 mM final concentration. After 20 min incubation on ice, the mixture was loaded on 1 ml 40% and 3 ml 20% sucrose in an SW40 centrifuge tube. Golgi membranes were pelleted through the 20% layer on the 40% cushion by 20 min centrifugation at 15,000 rpm and were harvested at this interface.

3.5.5. Electron Microscopy

Membrane fractions were prepared for routine electron microscopy using a filtration apparatus for random sampling exactly as described previously by Dominguez *et al.*, 1999. Membranes associated with magnetic beads were processed identically to the conditions described in Dominguez *et al.* 1999, except that the material was retained by magnets throughout the washing and fixation procedures.

3.5.6. Immunoisolation of Membranes

M450 (for gel electrophoresis and enzyme assays) or M500 (for electron micrographs) magnetic beads were cross-linked with anti-rabbit IgG according to the manufacturer's instructions. Typically, 10 and 40 μ l of the bead suspension was used per immunoisolation. Beads were preincubated with affinity-purified p23 cytoplasmic tail antibodies and re-isolated with a magnet. Antibody coated magnetic beads were incubated with membranes in immunoisolation buffer (KHM buffer plus 0.2 M sucrose and 0.5 mg/ml milk powder) for ~2 h in the cold room with gentle agitation. Beads were re-isolated with a magnet and washed repeatedly in buffer (last wash without milk powder). Beads were either extracted with electrophoresis buffer (for gel electrophoresis and Western blotting) or in NAGT, GalT, or mannosidase assay buffers. Membranes that remained in the supernatant after immunoisolation were pelleted by ultracentrifugation. For EM analysis, samples were frozen for shipment and storage.

CHAPTER 4.

Identification of Novel Golgi Membrane Proteins and Cargo Concentration in Pre-Golgi Compartment

4.1. Introduction

To extend the work done to distinguish between the various models for the molecular mechanisms of protein and membrane movement, two further studies were performed. The first was to gain insight into the workings of the Golgi apparatus by sequencing the entire set of membrane proteins of the Golgi apparatus (Bell *et al.*, 2001). Mass spectrometry of a Golgi fraction has previously been used to identify additional members of the p24 family (Dominguez *et al.*, 1998). Indeed many of the mechanisms of this pathway have been elucidated by analyzing the protein constituents of the secretory pathway (Novick *et al.*, 1980; Rothman, 1994; Gagnon *et al.*, 2002). The first study in this chapter details the analysis of the entire proteome of membrane proteins of an isolated Golgi fraction.

The second study consists of a rigorous immunocytochemical study of rat liver hepatocytes and Golgi fractions. In an attempt to define more clearly the role of COPI-coated compartments in cargo concentration through the secretory pathway, we have undertaken a quantitative analysis of the distribution of the cargo protein albumin relative to that of COPI coatomer protein β -COP. This was undertaken in both ultrathin cryosections of liver and isolated liver Golgi fractions. The abrupt concentration of albumin at the RER/SER boundary, between the COPI decorated *cis*-Golgi network and stacked flattened Golgi cisternae and diminishment of albumin in intercisternal COPI vesicles renders unlikely a vesicular transport model of anterograde cargo secretion.

In this chapter we have identified and characterized the key trafficking proteins as well as novel proteins of the Golgi apparatus. Thus defining, in part, the protein machinery available in this organelle. We have also identified the stages of cargo concentration and protein localization in order to define the morphological and molecular boundaries of this organelle.

4.2. Abstract

A mass spectrometric analysis of proteins partitioning into Triton X-114 from purified hepatic Golgi apparatus (84% purity by morphometry, 122-fold enrichment over the homogenate for the Golgi marker galactosyl transferase) led to the unambiguous identification of 81 proteins including a novel Golgi-associated protein of 34 kDa (GPP34). The membrane protein complement was resolved by SDS-polyacrylamide gel electrophoresis and subjected to a hierarchical approach using delayed extraction matrix-assisted laser desorption ionization mass spectrometry characterization by peptide mass fingerprinting, tandem mass spectrometry to generate sequence tags, and Edman sequencing of proteins. Major membrane proteins corresponded to known Golgi residents, a Golgi lectin, anterograde cargo, and an abundance of trafficking proteins including KDEL receptors, p24 family members, SNAREs, Rabs, a single ARF-guanine nucleotide exchange factor, and two SCAMPs. Analytical fractionation and gold immunolabeling of proteins in the purified Golgi fraction were used to assess the intra-Golgi and total cellular distribution of GPP34, two SNAREs, SCAMPs, and the trafficking proteins GBF1, BAP31, and rp24 α 2 identified by the proteomics approach as well as the endoplasmic reticulum contaminant calnexin. Although GPP34 has never previously been identified as a protein, the localization of GPP34 to the Golgi complex, the conservation of GPP34 from yeast to humans, and the cytosolically exposed location of GPP34 predict a role for a novel coat protein in Golgi trafficking.

4.3. Results

4.3.1. *Morphometric analysis of Golgi fractions*

This study identified 81 proteins isolated from a Golgi fraction. The Golgi fraction that was selected is highly enriched in galactosyl transferase, a Golgi marker, and had low endosomal contamination (Dominguez *et al.*, 1999). The morphology of this Golgi fraction was also analyzed. Morphometry was done using a random sampling method (Baudhuin and Berthet, 1967). Electron microscopy of the filtered Golgi fractions revealed, as deduced from the point hit method (Weibel, 1979), that 84% of the profiles were Golgi complexes. The remaining profiles were endoplasmic reticulum or plasma membrane (14%), mitochondria (1%), or peroxisomal cores (1%), as based on the analysis of 100 micrographs ($\times 27,000$ final magnification) and a point hit methodology employing 42 points per grid (per micrograph) (Figure 4.1; Table 4.1).

4.3.2. *Immunoisolation of novel membrane proteins*

Included among the 81 proteins identified in this study is a novel protein that is conserved from yeast to humans, GPP34. The absence of a signal sequence and transmembrane domain predicts that GPP34 is a peripheral membrane protein. To assess whether selected trafficking proteins were indeed in Golgi membranes or contaminants, an immunolocalization study was effected. We elected to study the intra-Golgi and cellular distribution of selected trafficking proteins and GPP34 by electron microscope immunolabeling of the Golgi fraction.

Antibodies were raised to GPP34. Western blotting confirmed that the antigen was membrane-associated as well as cytosolic (data not shown). Immunolabeling of cryosections of the WNG fraction with the peptide-specific antibody to GPP34 revealed specific labeling at the periphery of the Golgi stack. Antigenicity was found on the cis and trans sides as well as at the lateral edges of

stacked cisternae (Figure 4.2. *arrowheads*). Controls without primary antibody but with secondary antibody conjugated to gold revealed no detectable gold labeling in the fraction (data not shown).

Figure 4.1. Electron micrograph of WNG fraction. Golgi fractions were isolated as described in Dominguez *et al.*, 1999. Samples were processed for routine electron microscopy. Quantitation of the contaminating organelles was effected by using the point hit method. Essentially a 42-point grid was superimposed over the electron micrographs (as shown) and the number and type of organelle that appeared under each point or hit was recorded. Endoplasmic reticulum (ER), peroxisome (p), mitochondrion (m). The bar represents 250 nm.

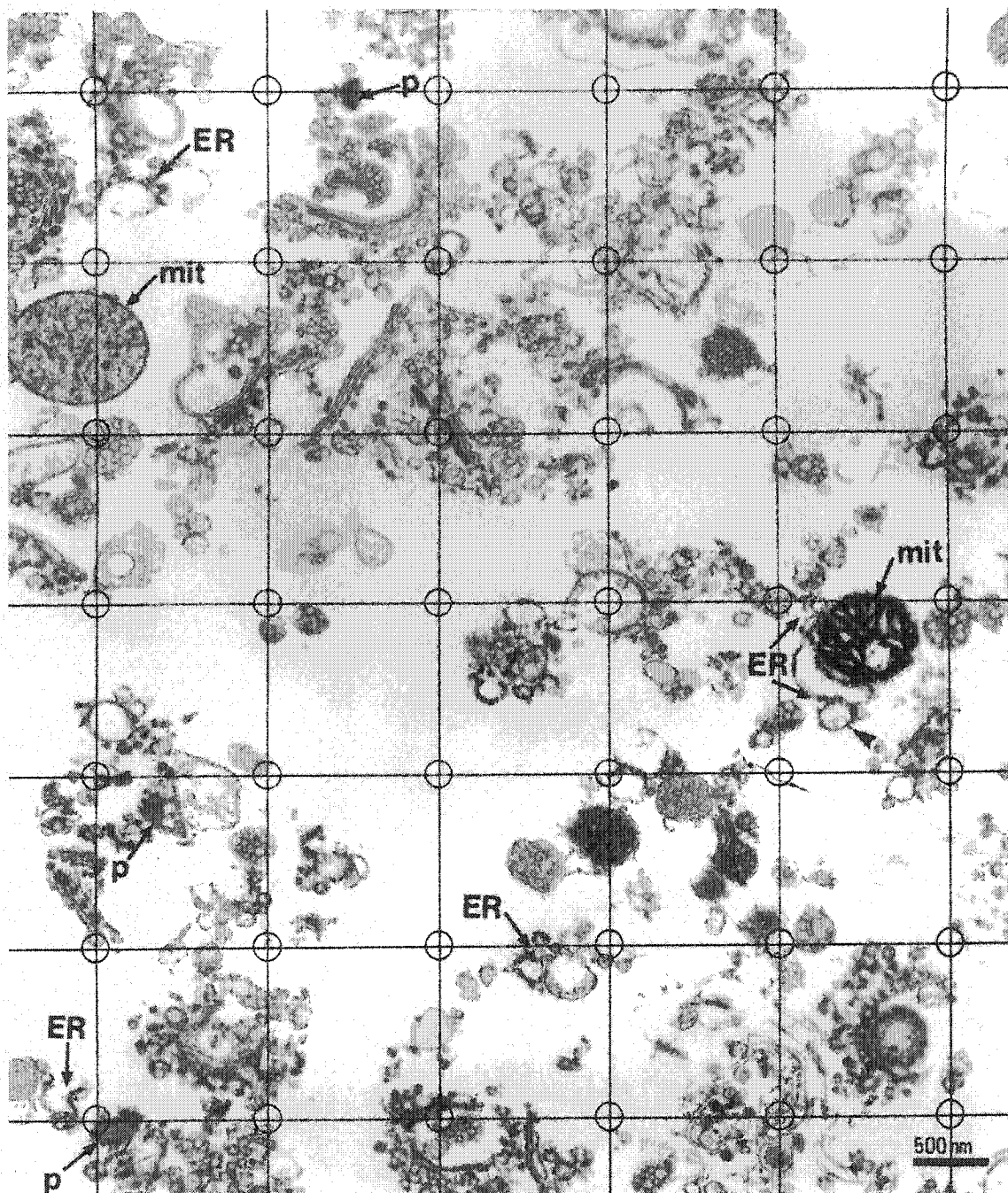


Figure 4.1.

Table 4.1. Morphometric Analysis of the WNG fraction.

Organelle	Total Hits	Mean \pm Standard Deviation	% Purity
Golgi elements	1772	17.7 ± 4.9	84
Peroxisomal cores	22	0.2 ± 0.7	1
ER & plasma membrane	288	2.9 ± 2.7	14
Mitochondria	31	0.3 ± 0.7	1

Morphometric assessment of contamination by relative volume distribution was carried out on the WNG fraction. Random views of the WNG fraction, as prepared for electron microscopy by filtration, were evaluated by the point hit method for contaminants. Based on the analysis of 100 micrographs and 42 points per grid, Golgi elements are the major component of the fraction. Not shown is the proportion of free space in the micrographs (50%).

Figure 4.2. Localization of GPP34 in the Golgi fraction. Cryosections of the Golgi fraction were labeled with anti-peptide antibodies to GPP34. Gold particle (10 nm) labeling is seen at the periphery of stacked Golgi flattened cisternae on both cis and trans sides. *Arrowheads* indicate gold particles; *Gc*, Golgi cisternae. *Bar*, 100 nm.

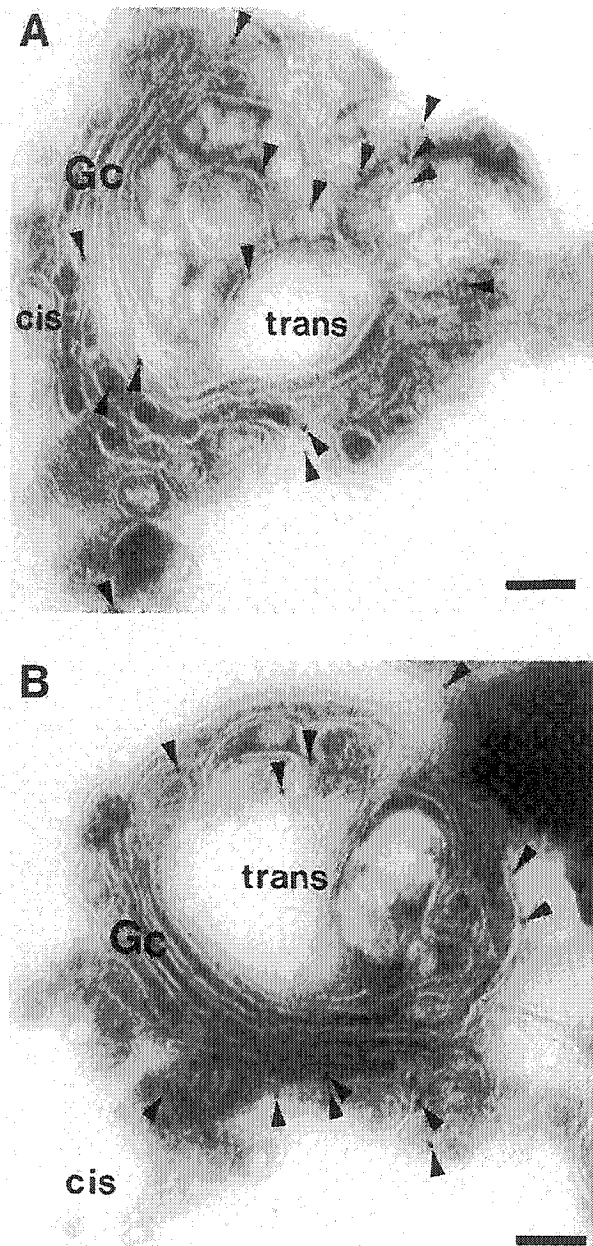


Figure 4.2.

4.4. Abstract

The steady state distribution of the small monomeric soluble protein, albumin, has been assessed in rat liver parenchyma and isolated Golgi fractions by quantitative immunogold labeling. Two concentration steps were observed with the first (2-fold concentration) at the continuity between the rough and smooth ER. The second (6.3-fold concentration) was found at the interface between the *cis*-Golgi network (CGN) and the tightly apposed Golgi flattened cisternae (G). Throughout the Golgi, cargo content was found to be uniform from the *cis* to *trans* cisternal compartments. A detailed analysis of COPI decorated vesicular profiles of 50-90 nm at the periphery of stacked Golgi cisternae revealed negligible labeling for albumin *in situ*. COPI-positive vesicular profiles were similarly weakly labeled for albumin in a purified Golgi fraction isolated following gentle homogenization and low speed differential centrifugation. Taken together, the data indicate a major concentration step for albumin in liver parenchyma between the CGN and the stacked Golgi cisternae coinciding with a sorting away of COPI coatomer and $\text{rp24}\alpha 2$ into the intercisternal vesicular profiles devoid of albumin and presumably other soluble cargo.

4.5. Results

4.5.1. The Major Site of Cargo Concentration in Hepatocytes is Within the Golgi Apparatus

That albumin is concentrated as it migrates from the ER to the Golgi apparatus was evident in many micrographs, one example of which is shown in Figure 4.3. An apparent uniform distribution of immunoreactive albumin was observed throughout the stacked flattened cisternae of the Golgi complex and in dilated lipoprotein-filled distensions (Figure 4.3. A and B; Figure 4.4.A). Vesicular profiles of approximately 50-60 nm in diameter (*arrowheads*) are clearly seen at the lateral edges of Golgi cisternae and occasionally in apparent continuity with Golgi cisternae (Figure 4.4.). These are predominantly devoid of immunoreactive albumin.

The high abundance and distribution of albumin throughout all major compartments of the secretory pathway greatly facilitated a detailed quantitative analysis of cargo concentration sites. Quantitative analysis of gold particle density of albumin in the secretory apparatus compartments revealed an apparent concentration step of 2- to 3-fold within anastomosing tubular networks (DTP) distal to the Golgi complex compared to albumin content in the rough ER cisternae (Figure 4.3.). Remarkably, at the Golgi apparatus, albumin concentration increased 5-fold relative to levels detected in adjacent tubules of the CGN (Figure 4.3.). In contrast, albumin concentration appeared to be similar at all levels of the Golgi stack and along the length of individual Golgi flattened cisternae. Indeed, separate quantitation of albumin labeling in the *cis*, medial and *trans* cisternae revealed no significant differences in concentration between these compartments (1176 gold particles scored in n=34 Golgi apparatus revealed a $p < 0.7$ for $G = 5.288$ in a Goodness of Fit Test for > 2 classes). The large increase in albumin density in the Golgi did not result from aggregation of gold conjugates or signal amplification due to multiple antibody binding since each gold cluster on

sections, which accounted for less than 16% of the total gold particles, was scored as a single hit (for details see Dahan *et al.*, 1994 and Materials and Methods). It should be noted that qualitative analysis of the distribution of another soluble cargo protein, apoE, and an integral membrane protein, the polymeric IgR, revealed a similar low concentration in pre-Golgi compartments relative to stacked cisternae (not shown). The difference in cargo concentration between pre-Golgi structures and flattened cisternae is important as it facilitates identification of the COPI-labeled structures.

4.5.2. β -COP Localization is Largely Distinct from that of Secretory Cargo In Rat Liver Golgi Apparatus in situ

Previous studies on the presence of anterograde secretory cargo in small vesicles near Golgi stacks have yielded conflicting results (Dahan *et al.*, 1994; Orci *et al.*, 1997). Vesicular structures at the edges of flattened cisternae were found to be decorated with β -COP (Figure 4.4. B-D). Out of these β -COP-labeled vesicular structures, $8.5 \pm 0.8\%$ also labeled for albumin. Moreover these vesicular profiles accounted for less than 0.2% of all albumin labeling relative to that present over Golgi flattened cisternae. Quantitation of 10 nm gold labeling density measurements for albumin in Golgi cisternae compared to that measured within vesicular profiles around Golgi stacks revealed that albumin content was approximately 4.4-fold depleted in vesicular profiles compared to Golgi cisternae (labeling densities: $176.4 \text{ particles}/\mu\text{m}^2$ cisternal profile area, $n=57$ cisternae vs. $40.1 \text{ particles}/\mu\text{m}^2$ vesicular profile area, $n=558$ vesicular profiles). Hence β -COP-decorated intercisternal vesicular profiles were largely devoid of albumin cargo (Figure 4.4. B-D). Those containing cargo may likely be interdigitations within Golgi flattened cisternae of the CGN rather than true vesicular profiles.

4.5.3. Analysis of β -COP, Albumin, rp24 α 2, and ERD2 in Purified Golgi Fractions

A protocol for the isolation of a hepatic fraction that is highly enriched in Golgi marker enzyme content and greatly diminished in endosomal contamination has been documented (Dominguez *et al.*, 1999). This Golgi fraction reveals coats over the flattened cisternae as well as in bud-like profiles abutting Golgi stacks in cryosections (Figure 4.5.A, *arrowheads*) and in Epon-embedded sections (Figure 4.5.A, inset, *arrowheads*). Few free small intercisternal vesicles were observed in this fraction by electron microscopy (Figure 4.5.A and Figure 2 in Dominguez *et al.*, 1999). This was expected since the low speed centrifugation step used to sediment the starting material to isolate this fraction from liver homogenates would have excluded any untethered free vesicles (Dominguez *et al.*, 1999). However, this fraction does contain stacked Golgi apparatus with the closely associated CGN compartment. Notably, this fraction might allow for a better visualization of the immunogold signal for our proteins of interest owing to the greater accessibility of cytoplasmic epitopes in fractions compared to whole cells.

Gold immunolabeling revealed β -COP and albumin to be heterogeneously distributed with most albumin labeling over Golgi flattened cisternae while most β -COP labeling was in the CGN (Figure 4.5. B-E). A similar distribution to that of β -COP was found in fractions for COPI binding protein, rp24 α 2 (Figure 4.5. F and G), and the KDEL receptor, ERD2 (Figure 4.5. H and I), two ER-Golgi recycling proteins. Remarkably, 75-85% of gold particle labeling for β -COP, rp24 α 2, and ERD2 was scored within the CGN, compared with only 15-25% within Golgi stacks (Figure 4.6. A). Albumin, in contrast, was found to be more abundant in Golgi flattened cisternae.

These apparent protein enrichment patterns were confirmed by more rigorous gold particle labeling density measurements in Golgi fraction cryosections that were double-labeled for albumin and β -COP, to rule out

subjectivity in distinguishing between the tubular CGN and the tubular TGN (Figure 4.6.). This was a necessary precaution since albumin is in higher abundance within the TGN than in the CGN *in situ*. The results with double-labeled fractions revealed a higher concentration of albumin in the Golgi cisternae as opposed to the β -COP-decorated CGN. β -COP, in contrast, was at a higher density in the CGN (Figure 4.6.). The ratio of albumin labeling in Golgi flattened cisternae over that in the CGN was 2.4-fold, while for β -COP, the ratio was 0.56. This compares with a quantitation done with cryosections of rat liver parenchyma. The *in situ* work revealed a 5.1-fold ratio for albumin and 0.42 for β -COP.

Finally, the quantitative analysis was extended to p24 α 2 and ERD2 in single-labeling studies of Golgi-enriched fractions. As was observed for β -COP in the double-labeling studies above (Figure 4.6), p24 α 2 and ERD2 were 3- and 1.8-fold enriched in labeling density in the CGN over the Golgi cisternae, respectively (86 and 213 gold particles were evaluated, for p24 α 2 and ERD2, respectively). Hence, the analyses of fractions as well as the *in situ* results demonstrate that a concentration step for albumin occurs between the CGN and the closely apposed stacked Golgi flattened cisternae. Importantly, this concentration step coincides with depletion of β -COP as well as p24 α 2 and ERD2.

Figure 4.3. Mean labeling density of albumin in the rough ER, smooth ER, Golgi-associated tubular compartment and the Golgi apparatus. A. The profile area of the Golgi apparatus is indicated by the *thick dashed lines* and that of the Golgi-associated tubular compartment (CGN) is indicated by the *thin dashed lines*. Gold particles were scored as shown in the CGN compartment (*circles*) where aggregates of 2 or 3 particles were scored as a single 'hit' (see Materials and Methods). In this particular micrograph 249 particles were found over 1.16 μm^2 profile area of Golgi apparatus versus 161 particles over 1.18 μm^2 profile area of CGN; this represents a 6.3-fold increase in albumin concentration between the CGN and Golgi apparatus. *cis* and *trans* indicate the polarity of the stack. Bar, 400 nm. B. Liver cryosection labeled for albumin showing examples of the CGN and distal tubular profiles (DTP) in relation to the Golgi apparatus (G). Although similar in morphology and albumin content, the CGN appears to be a tighter network of tubules than the DTP. These compartments were defined by their relative distance (CGN tubules being within a 750 nm radius at the *cis* side of the Golgi, and the DTP tubules being at least 750 nm away from the Golgi apparatus in the Golgi region) (see Materials and Methods). Gold labeling for albumin in the DTP and CGN is indicated by *arrowheads* and *arrows*, respectively. L, lysosome; P, peroxisome. Bar, 400 nm. C. Ultrathin liver cryosections (n=36 micrographs from 4 animals) were immunolabeled with anti-albumin followed by goat anti-rabbit IgG 10 nm gold and the labeling density (particles/ μm^2) was estimated as described in Materials and Methods. Golgi stacks in which secretory vesicles were observed, were quantitatively analyzed to enable the identification of the *cis* vs. *trans* sides of the Golgi apparatus. Background labeling (as evaluated by labeling density measurements over mitochondria and peroxisomes) was subtracted from labeling densities over secretory compartments in albumin-labeled cryosections to yield the values presented. The numbers (n) in the bars of the graph represent the absolute number of gold particles counted.

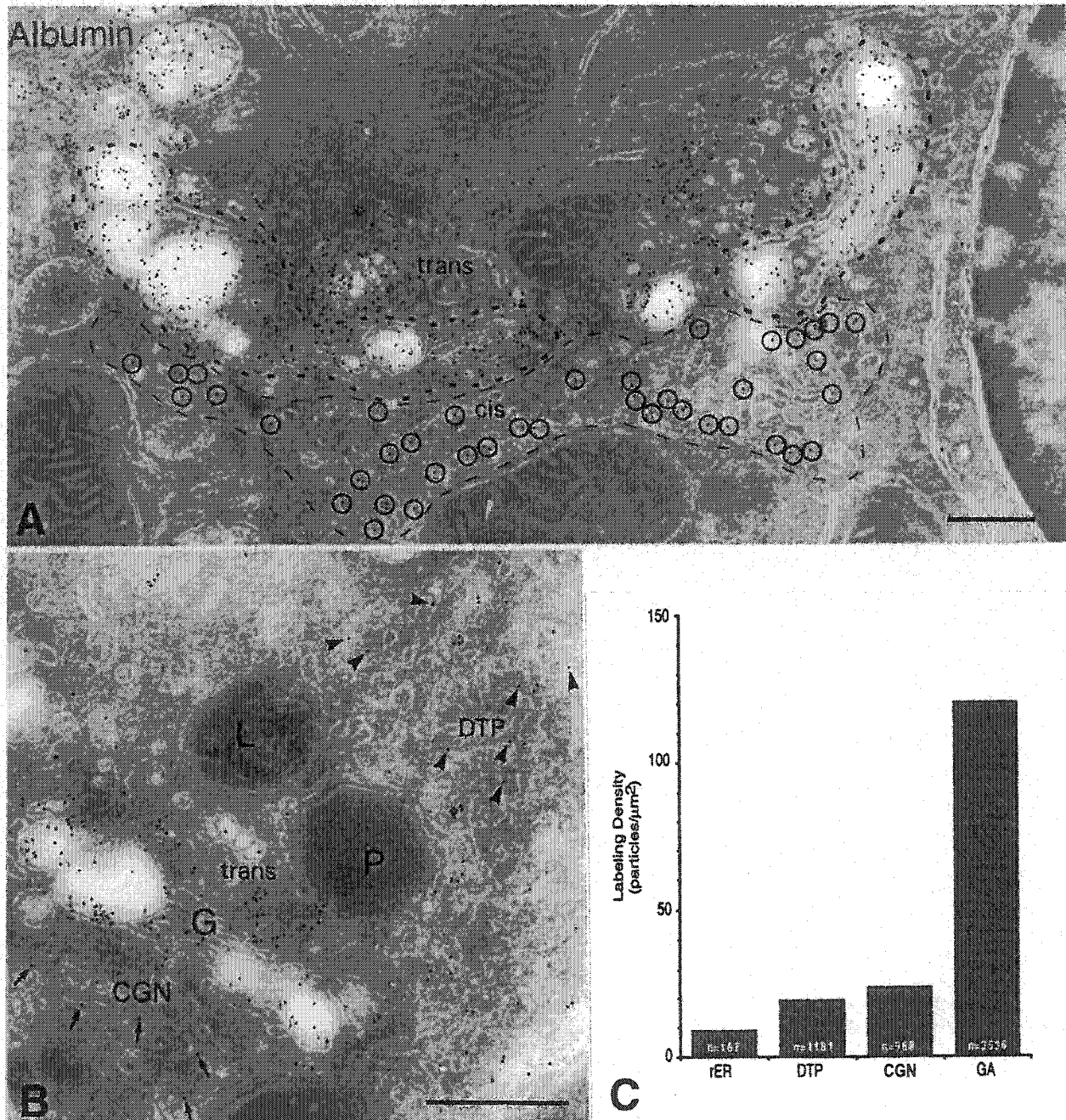


Figure 4.3.

Figure 4.4. *In situ* distribution of albumin and β -COP within liver hepatocyte Golgi apparatus. A. Rat liver cryosections were labeled for albumin with 10nm gold particles. Albumin immunoreactivity is concentrated within Golgi stacked saccules (*). Small vesicular profiles at the edge of the stack are mostly devoid of albumin labeling (*large arrowheads*). **B-D.** Sections were double immunolabeled for albumin and β -COP with 10 and 5 nm gold particles, respectively. The stacked cisternae of the Golgi apparatus (*) are labeled for albumin throughout their lumen. Small vesicular profiles, 50-80 nm in diameter about the peripheral rims of Golgi stacks are indicated by *arrowheads*; vesicular profiles harboring β -COP are indicated by *arrows*. Notably, albumin immunoreactivity is undetectable in these vesicular profiles. *Bar*, 400 nm for panel A, 200 nm for panels B-D.

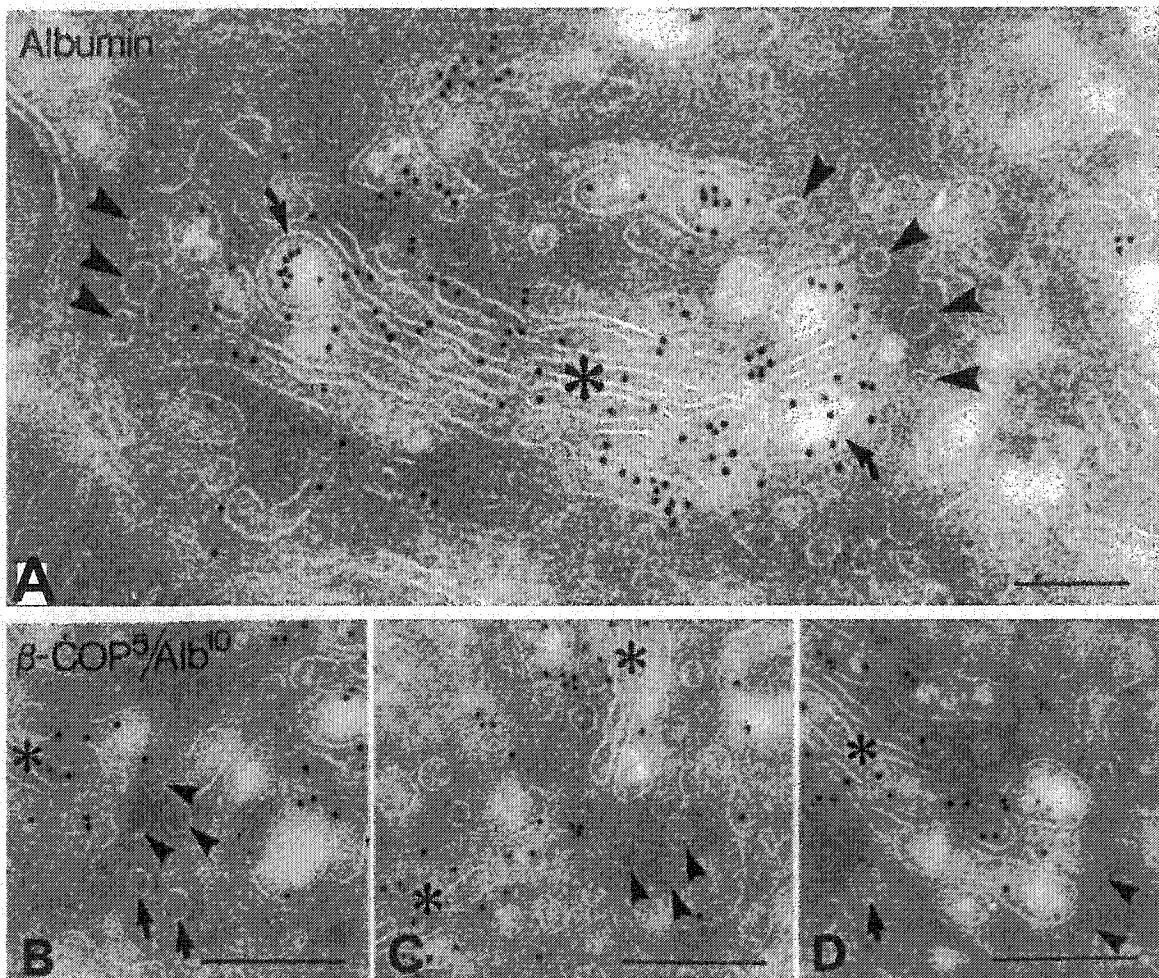


Figure 4.4.

Figure 4.5. Distribution of albumin, β -COP, and p24 α 2 in a purified rat liver Golgi fraction. Cryosections of the WNG fraction (Dominguez *et al.*, 1999) were immunolabeled with antibodies against albumin, β -COP, rp24 α 2, or the KDEL receptor, ERD2. **A.** A cryosection of the WNG Golgi fraction reveals that it consists predominantly of intact, stacked Golgi cisternae (Gs) with few small vesicles (*arrowheads*). Fuzzy coats can also be seen at the delimiting membrane of many of the Golgi-associated structures. **Inset:** Tannic acid treatment of an Epon-embedded fraction reveals some of the vesicular profiles to be coated (clathrin coats indicated with *arrowheads*, possible COPI coats are indicated by *arrows*). **B** and **C.** Albumin can be detected mostly throughout the stacked cisternae (Gs) Detectable but weak immunoreactivity can be found over tubular-vesicular profiles (*arrowheads*) at the lateral edges of stacked Golgi cisternae. **D** and **E.** In sections labeled for β -COP (*small arrows*) gold particle labeling is predominantly found in Golgi-associated tubular-vesicular profiles (*arrowheads*). **F-I.** Like β -COP, rp24 α 2 (**F** and **G**) and ERD2 (**H** and **I**) immunoreactivity is mainly present within small tubular-vesicular profiles (*arrowheads*) about Golgi stacks (Gs). The latter reveal low immunoreactivity for β -COP, p24 α 2, and ERD2. *Bars*, 200 nm.

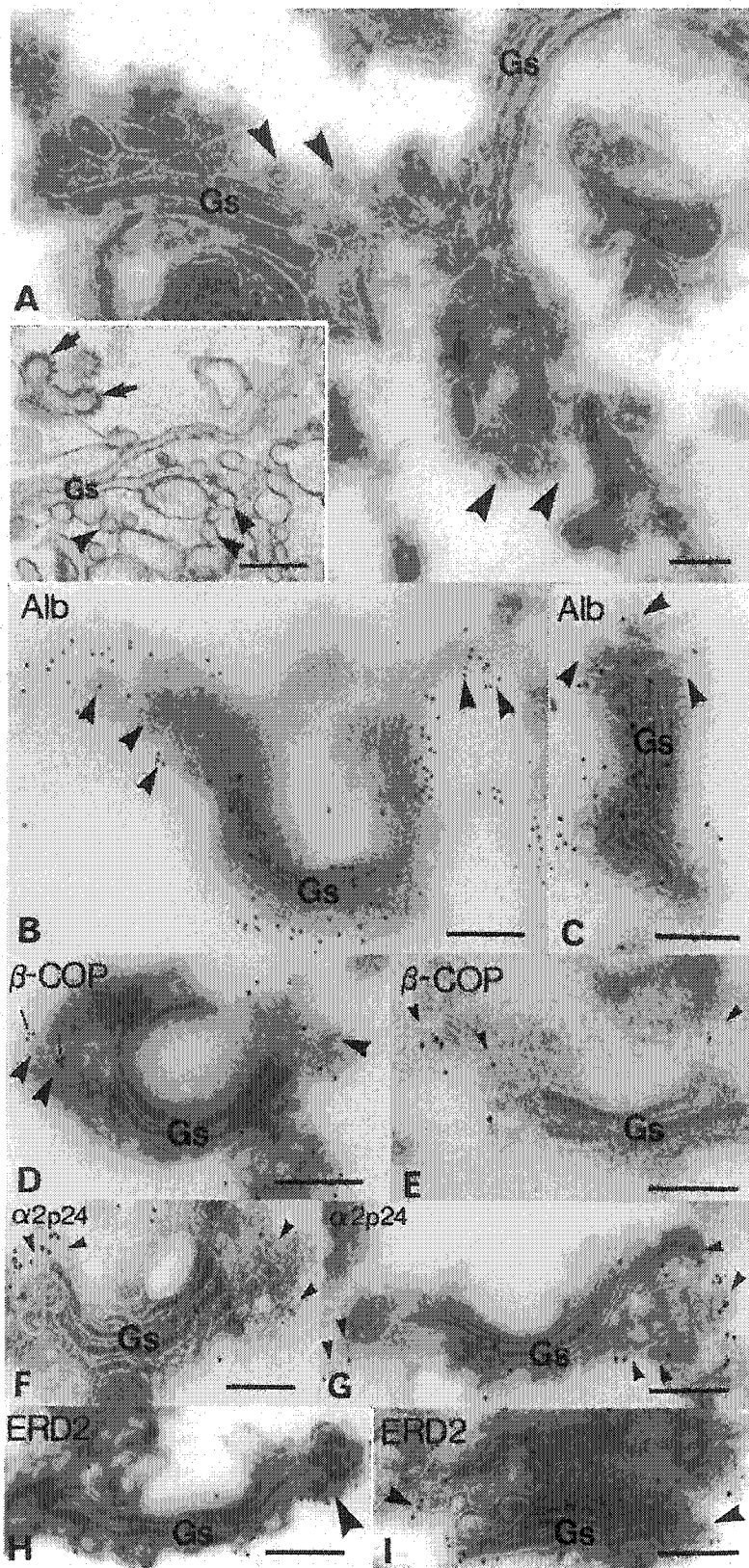


Figure 4.5.

Figure 4.6. Percent distribution of β -COP, p24 α 2, ERD2 and albumin in the WNG Golgi fraction. **A.** Golgi flattened cisternae and vesicular-tubular profiles within approximately 750 nm from Golgi stacks were examined for gold particle labeling in cryosections of the WNG Golgi fraction single-labeled for β -COP (n=17 Golgi apparatus profiles), ERD2 (n=10), rp24 α 2 (n=16), or albumin (n=19) as shown in Figure 4.5. **B-I.** β -COP, ERD2 and p24 α 2 are enriched within the CGN compartment relative to the Golgi flattened cisternae. In contrast, albumin is predominantly found within Golgi cisternae. **B.** Cryosections of the WNG Golgi fraction double-labeled for β -COP and albumin were evaluated for the gold particle labeling density of these antigens (n=10 Golgi apparatus profiles; 378 and 53 gold particles were scored for albumin and β -COP, respectively) in the two compartments. **C.** Representative micrograph used for the labeling density quantitation of albumin and β -COP shown in Panel B. Gold particle labeling for albumin (*arrows*) is concentrated within the Golgi apparatus and also present within the CGN (CGN, encircled by the *thin broken line*). β -COP is localized in majority within the CGN compartment. The *thick broken line* indicates the delimitation between the Golgi apparatus and the TGN (TGN) which included secretory vesicles (sv). Bar, 400 nm.

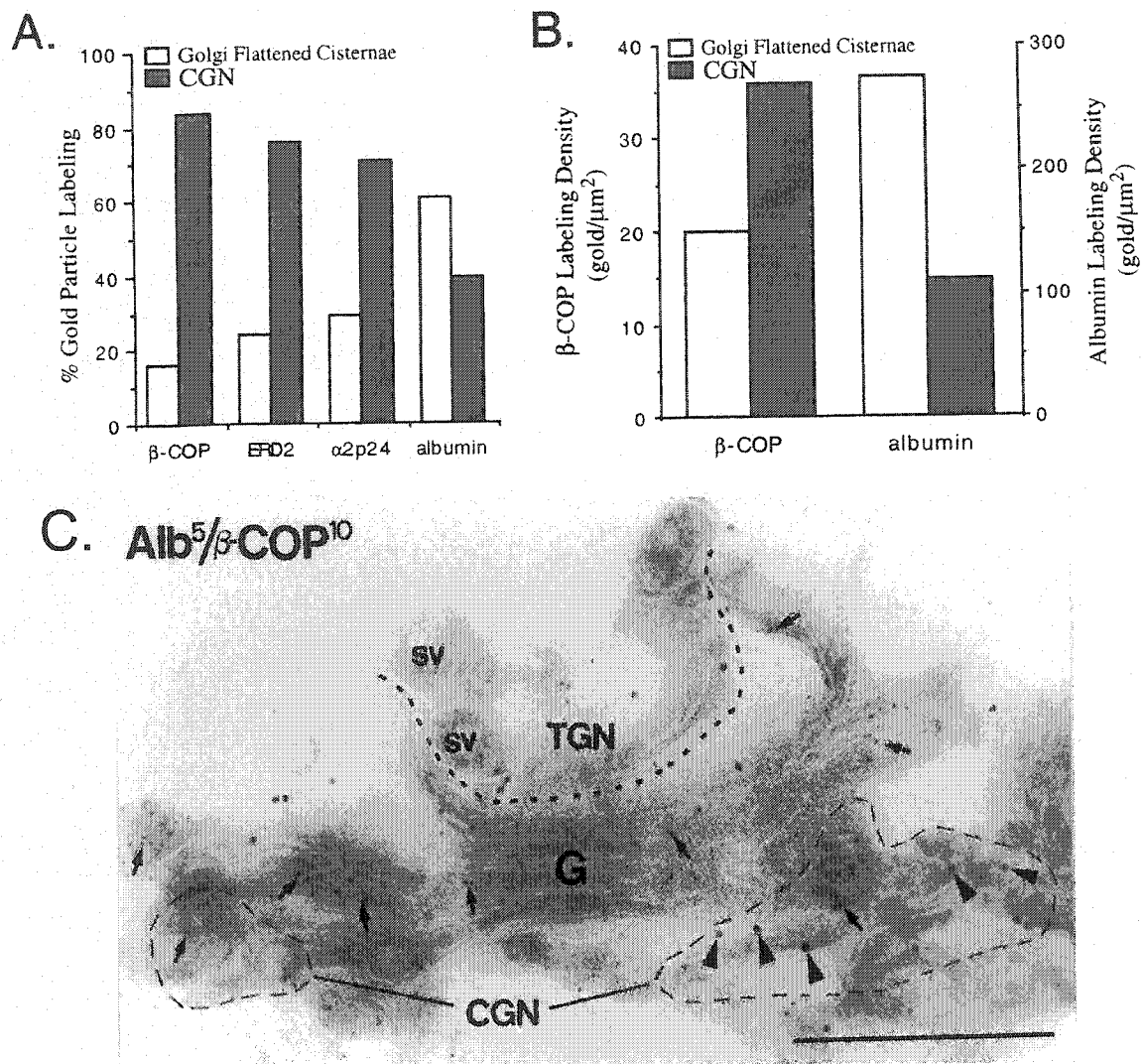


Figure 4.6.

4.6. Discussion

The first study described in this chapter identifies a novel Golgi protein, GPP34, by analyzing a purified Golgi fraction. This was done by isolating the membrane proteins from the Golgi fraction through phase partitioning followed by protein characterization from one-dimensional SDS-PAGE by Edman degradation and mass spectrometry. In fact, 81 proteins were identified through the use of this method (Bell *et al.*, 2001). This type of analysis identifies novel proteins as well as establishes the total protein constituents of the organelle. Indeed, a surprisingly high number of Rabs and low number of SNAREs were identified in this study (Bell *et al.*, 2001).

The second study involved the assessment of protein concentration in rat liver. Isolated Golgi fractions as well as *in situ* work revealed that there is a concentration of cargo that occurs in the secretory pathway. In fact, our *in situ* work has identified that this occurs in two steps. The first step occurs between the rough and smooth ER, while the second concentration step occurs just before the stacked Golgi cisternae. In addition, this study revealed that β -COP and the cargo protein albumin were not present in the same vesicular profiles. Indeed, most of the β -COP labeling was found in the CGN, while albumin was concentrated in the Golgi stacks. Our data are consistent with cargo being concentrated during transport between the ER and Golgi apparatus by exclusion from retrograde-directed (COPI-positive) recycling carriers as put forward by Martinez-Menarguez *et al.* (1999) and Shima *et al.* (1999). Lanoix *et al.*, (1999) have also documented depletion of anterograde-directed cargo in COPI-dependent vesicles derived *in vitro* from the starting hepatic Golgi fraction. The vesicles were enriched in Golgi-resident enzymes, thereby supporting a recycling model. In summary, the low abundance of anterograde-directed cargo in vesicles between Golgi cisternae, the uniform labeling of albumin throughout the Golgi apparatus, as well as the gated transport between the CGN and Golgi-stacked cisternae

(deduced from the concentration step differences) represent significant *in situ* evidence to support the continuous network model of secretion (Griffiths, 2000).

4.7. Materials and Methods

4.7.1. Isolation of Golgi Fractions

The WNG fraction was isolated exactly as described by Dominguez *et al.* (1999) and characterized for protein yield and galactosyl transferase marker enzyme enrichment also as described by Dominguez *et al.* (1999). Galactosyl transferase relative specific activity was 122 ± 32 -fold ($n = 3$) enrichment over the homogenate. The protein in the fraction corresponded to $0.043 \pm 0.018\%$ of the original homogenate protein.

4.7.2. Antibodies

Rabbit anti-peptide antibodies were raised against a peptide sequence (LKDREGYTSFWNDC) derived from the human GPP34 sequence. The peptide was coupled via the C-terminal cysteine residue to keyhole limpet hemacyanin using *m*-maleimidobenzoyl-*N*-hydroxysuccinimide ester as the cross-linker. An initial subcutaneous injection of an emulsion of peptide in complete Freund's adjuvant was followed by four boosts of peptide (100 mg each) in incomplete adjuvant. Total IgG was purified by protein A-Sepharose affinity chromatography (Harlowe and Lane, 1988). Rabbit antiserum was also raised to a bacterial recombinant GST chimera of the human GPP34. Polymerase chain reaction products encoding GPP34 cDNA (amplified from IMAGE clone 664740, GB number AA232616, Research Genetics) were purified by agarose gel electrophoresis, ligated into pGEX2T (Amersham Pharmacia Biotech) and pTrcHisA (Invitrogen) using *EcoRI/BamHI* as restriction sites, and transformed into *Escherichia coli* DH 5. Positive clones were identified by polymerase chain reaction, and expression of the fusion protein was confirmed by SDS-PAGE and Coomassie R-250 staining. His-tagged GPP34 and GST-GPP34 were purified from isopropyl-1-thio- β -D-galactopyranoside-induced bacterial cultures and affinity-purified according to the manufacturer's instructions on NiNTA resin

(Qiagen) or glutathione-Sepharose beads (Amersham Pharmacia Biotech), respectively. Antibodies were raised as above, employing complete Freund's adjuvant. Anti-GST-GPP34 antibodies were further purified by affinity chromatography employing His-tagged GPP34 bound to Sepharose 4B (Amersham Pharmacia Biotech), as described by Harlow and Lane (1988).

Rabbit-anti rat albumin was from Cappel Laboratories (West Chester, PA). E5A3 was generously supplied by Dr. T.E. Kreis (University of Geneva, Switzerland). ERD2 antibodies were a kind gift of H.-D. Söling (Majoul *et al.*, 1998). Antibodies against luminal domain peptides of rp24 α 2 have been described previously (Dominguez *et al.*, 1998). Goat anti-rabbit and goat anti-mouse IgG gold conjugate secondary antibodies were obtained from Sigma Chemical CO. (St. Louis, MO).

4.7.3. EM Immunolocalization and Morphometry

Freshly prepared Golgi fractions were incubated with primary antibodies and processed for EM immunolocalization as described by Lavoie *et al.* (1999). In the case of GPP34, cryosections of Golgi fractions were prepared using the protocol description in Lavoie *et al.* (1999) and incubated with the anti-peptide antibodies to GPP34.

4.7.4. Preparation of Liver Samples for Cryoimmune EM.

Liver samples were prepared essentially as described previously (Dahan *et al.*, 1994). Cryosectioning of liver tissue samples was based on procedures of Tokuyasu (1980), Griffiths *et al.* (1984, 1993) and Geuze *et al.* (1984) and was carried out as described in Dahan *et al.* (1994). Section thickness was determined to be 50.4 ± 8.8 nm by the fold method of Small (1968) as described in Weibel (1979).

The WNG fraction was prepared as described by Dominguez *et al.* (1999). Following isolation, the fraction was fixed with 4% paraformaldehyde/0.5% glutaraldehyde (final concentrations) for 2 hr on ice. The membranes were centrifuged for 10 min at 10000Xg and the supernatant was discarded. The pellet was washed 3 times with 0.1 M cacodylate buffer and equilibrated in 2.3 M sucrose for 2-3 hrs. The pellet, which slowly floated to the top of the sucrose, was then cut into small pieces which were placed on nickel stubs and quick-frozen in liquid N₂.

The immunolabeling procedure and staining was carried out as described in Dahan *et al.* (1994). Sections were viewed in a Philips 400 T electron microscope, operating at 80 kV.

4.7.5. Antibody Dilutions.

Antibodies were diluted as follows for the immunolabeling of WNG fraction cryosections: 1:100 for rabbit anti-albumin: 1:5 for rabbit anti-rat p24 α 2, 1:10 for mouse anti- β -COP, and 1:10 for anti-ERD2.

Double-labeling experiments were conducted only with antibodies raised in different species. In this case both primary antibodies were incubated together in one step, and both secondary antibodies (conjugated to different size gold particles) were also incubated in a single step. Controls where the primary antibodies were omitted revealed negligible labeling (not shown)

4.7.6. Analysis of Gold Label.

Quantitation of gold particle density was carried out as described by Griffiths and Hoppeler (1986) and Dahan *et al.* (1994). Liver stubs from at least three animals were used for the quantitative analysis of albumin and β -COP *in*

situ. Hepatocyte Golgi regions which had well-preserved morphology and in which secretory vesicles were clearly visualized (to discern *cis* from *trans* sides of the Golgi apparatus), were photographed randomly at a primary magnification of 14500X. Gold particles were scored on micrographs printed at a final magnification of 37800X over the following compartments: Golgi apparatus flattened stacked cisternae, Golgi-associated tubules within 750 nm from a Golgi stack (*i.e.*, tubular networks at the *cis* side and at the peripheral edges of Golgi apparatus) termed CGN (*cis*-Golgi network), rough ER cisternae, smooth tubular networks (at least 750 nm away from Golgi stacks) termed DTP (distal tubular profiles), mitochondria, and peroxisomes. Gold particle labeling density over these compartments was evaluated by scoring the total number of gold particles in a given compartment and dividing by the total profile area (in μm^2) of that compartment in all micrographs. Profile area was obtained by placing micrographs on the measuring tablet of a Zeiss MOP-3 digitizer (Carl Zeiss Inc., Don Mills, Ontario). For the β -COP labeling only gold particles within 20 nm of a membrane were counted. Gold aggregates (defined as 2 or more gold particles separated by less than one gold particle diameter (*i.e.*, separated by less than 10 nm)) were counted as a single 'hit'. Background labeling for albumin and β -COP in *in situ* cryosections (over mitochondria and peroxisomes) was subtracted from gold labeling obtained over secretory pathway compartments for each respective antigen.

CHAPTER 5.

Morphological Analysis of p24 Mutants

5.1. Introduction

The secretory pathway of *Saccharomyces cerevisiae* is a morphologically simple and compact system. Unlike the organelles of mammalian secretory cells, the yeast endoplasmic reticulum (ER) is not an extensive labyrinth and there is no stacked Golgi apparatus. Rather the cell has single strands of ER weaving through the cytoplasm and below the plasma membrane. The Golgi apparatus consists of single cisternae dispersed throughout the cell. The general mechanisms and protein composition of this system, however, are conserved among eukaryotes. Yeast have been touted as model organisms for study due to the ease of mutational analysis, facility of growth and conserved homology to higher eukaryotes. Indeed many cellular components have been identified in yeast (Novick *et al.*, 1980).

The roles of several proteins of the secretory pathway have been identified using mutational analysis (Novick *et al.*, 1980; Wuestehube *et al.*, 1996; Click *et al.*, 2002). By deleting or mutating a gene one can determine first and foremost if the gene is essential. If the cells with the mutation are viable, one can analyze the cells in order to determine what effect, if any, the mutation has. If there is a change in the cell, whether in morphology, protein secretion or otherwise, one can predict what role the protein plays in the cell. Alternatively, one can over express a gene to discover the order in which proteins effect their roles, the function of a protein or even discrete differences between similar proteins. For example the over expression of Golgi v-SNAREs in yeast can suppress the temperature sensitive mutation of *uso1-1*. In particular, the over expression of two of the SNAREs is able to suppress the full *usoΔ* mutation, indicating that these SNAREs act downstream of *Uso1p* (Sapperstain *et al.*, 1996). The over expression of *cRac1B* in primary neurons increases the number of neurites per neuron as well as increasing neurite branching (Albertinazzi *et al.*, 1998). The over expression of two HMG-CoA isozymes (*Hmg1p* and *Hmg2p*) leads to different types of membrane proliferation indicative to the localization of the particular isozyme

(Wright *et al.*, 1988; Koning *et al.*, 1996). This chapter proposes to analyze the function of a set of proteins (the p24 family) through deletion and over expression studies.

The p24 proteins are integral membrane proteins of the early secretory pathway. These proteins were identified as constituents of COPI and COPII vesicles (Stamnes *et al.*, 1995; Sohn *et al.*, 1996; Belden and Barlowe, 1996). In addition, p24 deletion strains exhibited a delay in the kinetics of the secretion of Gas1p and periplasmic invertase with an increase in Kar2p and Pdi1p secretion (Schimmöller *et al.*, 1995, Elrod-Erickson and Kaiser, 1996; Belden and Barlowe, 1996). This strain also induces a slight unfolded protein response (UPR) (Belden and Barlowe, 2001b). The unfolded protein response is a signal transduction pathway induced by a stress in the ER. When there is an accumulation of unfolded proteins or other stress in the ER, Hac1p signals to the nucleus to induce the expression of ER chaperones (reviewed in Patil and Walter, 2001).

The p24 were first identified in 1991 (Wada *et al.*, 1991), however, no clear role has been assigned to these proteins after over a decade of work. Thus far, it has been shown that the p24s cycle through the secretory pathway (Fullekrüg *et al.*, 1999), form complexes with other p24 proteins (Dominguez *et al.*, 1998; Marzioch *et al.*, 1999; Fullekrüg *et al.*, 1999) and bind to various components of the secretory pathway including COPs, GRASPs, ArfGAP1 and ARF1 (Dominguez *et al.*, 1998; Weidler *et al.*, 2000; Barr *et al.*, 2001; Majoul *et al.*, 2001; Lanoix *et al.*, 2001; Gommel *et al.*, 2001). For this study we used electron microscopy to study each p24 knock out to determine if there was any change in the morphology of the secretory pathway. In addition, the p24s were over expressed in yeast and the morphology was analyzed. Protein localization studies were also performed using cryo-immuno techniques.

5.2. Results

5.2.1. The p24 Family

The p24 proteins are small (~24kDa) type I transmembrane proteins with a short cytosolic tail and a larger luminal domain. The transmembrane domain is generally 10-12 amino acids long. Since the discovery of the first p24 protein in 1991 (Wada *et al.*, 1991), the number of p24 proteins identified has increased dramatically. Access to a multitude of genomic and proteomic databases have allowed the sequence comparisons of known p24 genes with these databases. This study identifies 54 different species that contain at least one p24 gene (Table 5.1). As a result, it is obvious that the p24 proteins are found in a wide range of organisms, with multiple p24 proteins in many organisms. The yeast *Saccharomyces cerevisiae* has eight (8) p24 proteins (Marzioch *et al.*, 1999), humans have eight (8) p24 genes identified to date, *C. elegans* have five (5) (Wen and Greenwald, 1999; Kuiper and Martens, 2000), *Mus musculus* have twelve (12), while *Drosophila melanogaster* have six (6). The species identified in Table 5.1. include nineteen (19) vertebrates, nine (9) of them being mammalian, and thirty-six (36) invertebrates.

The alignment of the p24 cytosolic domains reveals common motifs conserved among the species (Figure 5.1.). The cytoplasmic tail of each p24 protein has either a double phenylalanine motif (FF), a di-lysine motif (K(X)KXX), or both. These motifs are involved in the binding of the p24s to COPII, COPI and ArfGAP1 (Dominguez *et al.*, 1998, Cosson and Letourneur, 1994; Belden and Barlowe, 2001c; Lanoix *et al.*, 2001).

Figure 5.1. Alignment of the tails of p24 proteins. The published sequences of p24 genes were used to execute BLAST searches to identify p24 genes in various databases. Proteins sequences from 57 p24 genes were used to perform analysis with a Pattern-Induced Multi-sequence Alignment (PIMA) algorithm. Only the C-terminal portions of the proteins are represented in this figure. Most p24 proteins have a K(X)K (light grey) or FF (black) motif in their cytoplasmic tail. The conserved arginine residue (R) is indicated in blue, the conserved serine (S) in yellow, and the conserved glutamine (Q) is in bold face.

	211	225 226	240 241	255 256	270
1 ERP2	REWRNMSTVNSTESR	LTWLSILIIIIIIIAVI	SIAQVLLIQFLFTGR	QKNYV-----	215
2 ERP4	REWRNMYTVSSTESR	LTWLSLLIMGVMMGI	SIVQALIIQFFFTSR	QKNYV-----	207
3 CGI-100	FEARDRNIQESNFDK	VNFWSMVNLVMMVVV	SAIQVYMLKSLFEDK	RKSRT-----	229
4 BAB29390	FEARDRNIQESNFDK	VNFWSVNNLMVMVVV	SAIQVYTLKSLFEDK	RKSRT-----	229
5 ILILILIG	FEARDRNLQEGNLER	VNFWSAVNVAVLLLV	AVLQVCTLRFFQDK	RPVPT-----	227
6 LY841/AAC52472/MMU41805	FEARDRNLQEDNLER	VNFWSAANVAVLLLV	AVLQVCTLRFFHDK	RPVPT-----	222
7 BAB25099	REAQDRARAEDLNLR	VSYWSVGETIALFVV	SFSQVLLLKSFTEK	RPVNRVHVS--	221
8 BAB233	REAQDRARAEDLNLR	VSYWSVGETIALFVV	SFSQVLLLKSFTEK	RPVNRVHVS--	221
9 BAB22292	REAQDRARAEDLNLR	VSYWSVGETIALFVV	SFSQVLLLKSFTEK	RPVNRVHVS--	221
10 P24B	REAQDRARAEDLNLR	VSYWSVGETIALFVV	SFSQVLLLKSFTEK	RPISRAVHS--	217
11 CGI-109	REAQGRSRAEDLNLR	VAYWSVGEALILLV	SIGQVFLKSFTEK	RTTTRVGS--	215
12 AAB96722/F57B10.5	REATGRKRAEELNER	VMIWSLQGSAAVVFI	GIGQVFLKSFTEK	RTRY-----	203
13 AAF48102/CG1967	REAQGRKRAEDLNLR	VMVWSLQEAIVIVI	GLVQIMVLRNFFTD	KPSQAHYGR--	210
14 SID394/p24a	RERIHRRAINNTNSR	VVLWSFFFEALVLVAM	TLGQIYYLKRFFEV	RVV-----	201
15 RN.22775/CAA63068	RERIHRRAINNTNSR	VVLWSFFFEALVLVAM	TLGQIYYLKRFFEV	RVV-----	201
16 RNP24	RERIHRRAINNTNSR	VVLWSFFFEALVLVAM	TLGQIYYLKRFFEV	RVV-----	201
17 CHOp24	RERIHRRAINNTNSR	VVLWSFFFEALVLVAM	TLGQIYYLKRFFEV	RVV-----	196
18 AAF45951/CG3564	RDKIHRSVNENTNSR	VVLWSTFEALVLVLM	TVGQVYYLKRFFEV	RVV-----	208
19 AAD17445	REEEMQELNRSNTSR	MAWLSFVSLVCLSV	AGLQFVHLKTFEKK	KLI-----	213
20 F16A1423	REEEMHNLNIATNSK	MAWLSFVSLAVCLSV	AGLQFVHLKTFEKK	KLI-----	221
21 C073178_25	REEEMQDLNRSTNTK	MAWLSVLSFFVCIGV	AGMQFLHLKTFEKK	KVI-----	204
22 T24P137v	REEEMQNLNRATNSK	MAWLSFVSLVCLGV	AGMQFVHLKTFEKK	KVI-----	214
23 BAB02949	REREMQELNRSNTSR	MAALSLLSFVVTMSV	AGLQRLHLKSFLEK	KLL-----	225
24 AAG12126	REAEMRIVSEKTNSE	VAWYSIMSLGICIVV	SGLQILYLKQYFEKK	KLI-----	212
25 AAF19571	REAYMRINEKTNSTR	VNQLGLMSLGVAIVV	SISQVLYLKRFFLEK	KLI-----	217
26 S31111125	REEEMRDTNESTNTR	VLYFSIFSMLCLIGL	ATWQVYFLRRFFKAK	KLIE-----	213
27 S31111125	REEEMRDTNESTNTR	VLYFSIFSMLCLIGL	ATWQVYFLRRFFKAK	KLIE-----	213
28 TMP21	REEEMRDTNESTNTR	VLYFSIFSMLCLIGL	ATWQVYFLRRFFKAK	KLIE-----	203
29 TMP21-I/p23	REEEMRDTNESTNTR	VLYFSIFSMLCLIGL	ATWQVYFLRRFFKAK	KLIE-----	219
30 BAB22932	REEEMRDTNESTNTR	VLYFSIFSMLCLIGL	ATWQVYFLRRFFKAK	KLIE-----	219
31 BHKp23/TMP21	REEEMRDTNESTNTR	VLYFSIFSMLCLIGL	ATWQVYFLRRFFKAK	KLIE-----	219
32 TMP21/p23	REEEMRDTNESTNTR	VLYFSIFSMLCLIGL	ATWQVYFLRRFFKAK	KLIE-----	219
33 TMP21/p23/S31111125	REEEMRDTNESTNTR	VLYFSIFSMLCLIGL	ATWQVYFLRRFFKAK	KLIE-----	219
34 p24delta	REEEMRDTNESTNTR	VLYFSIFSMLCLIGL	ATWQVYFLRRFFKAK	KLIE-----	207
35 CAA62103	REEEMRDTNESTNTR	VLYFSIFSMLCLVAL	ATWQVYFLRRFFKAK	KLIE-----	205
36 AAF56382/CG11785	REEEMRDTNEKTNSE	VLFSSIFSMLCLLGL	ATWQVYFLRRFFKAK	KLIE-----	195
37 CAA98480/CEF47G9	REEEMRDTNEKTNSE	VLYFSIFSMLCLLGL	AIWQVFLRNYFFKSK	KLID-----	204
38 CAC18232	REQKLRTDNESTNTR	VKWFQMATTFLLIAL	WGQWIMYLRAFFRV	FPSSGANGFSY	223
39 ERV25	REERLRTDNESTNTR	VRNFSILVIVLSSL	GVWQVNYLKNFFTK	HII-----	211
40 HSGP25L2G	REERFRQTSESTNQR	VLWWSILQTLILVAI	GVWQMRHLKSFPEAK	KLIV-----	214
41 AAH01123	REERFRQTSESTNQR	VLWWSILQTLILVAI	GVWQMRHLKSFPEAK	KLIV-----	214
42 BAB26802	REERFRQTSESTNQR	VLWWSILQTLILVAI	GVWQMRHLKSFPEAK	KLIV-----	214
43 CAB60397/CEY60A3A	REERFRQTSESTNTR	VFYWSIAQVVVLAIT	GAWQMRHLRGFFEAK	KLIV-----	211
44 BAB31517	REENFRITSEDTNRN	VLWAFQAQILIFISV	GIFQMKHLKDFPIAK	KLIV-----	215
45 BAB25000	REENFRITSEDTNRN	VLWAFQAQILIFISV	GIFQMKHLKDFPIAK	KLIV-----	215
46 gp251	REENFRITSEDTNSN	VLWAFQAQTLIFIAI	GIFQMKSLKNFFIAK	KLIV-----	215
47 ERP1	REATFRDASEAVNSR	AMWWIVIQILVLAVT	CGWQMKHLKGFVVK	KIL-----	219
48 ERP6	REESFRDISESVNSR	AMWWIVTQVTLIIII	CVWQMKSLRFFVVK	KVL-----	216
49 lbrA	REATHRNTAESTNTR	VVWWSIFEALILVAM	SAWQIYYLRRFFEVK	RAV-----	206
50 ERV25/CAB11658/SPAC23H4	REARFRNTNESTNER	VKNPAYLTFFISLFLV	VIWQILYLRFFQDK	HLIP-----	216
51 ERP5	KEAEFRNQSESANSK	IMTWSVVFQLLILLGT	CAFQRLRYLKNFFVK	KVV-----	212
52 CAA92683/CEK08E4	HEARDRAVMSANFDR	VTFWSVVHTLVMMGV	AGVQVFMIRSLFEEN	SKIGKVLRRGK	232
53 EMP24/CAB76226/SPCC24B10	RERIHRNTAESTNDR	VKWWISILQTVILSV	CVFQIFYLKRLFEVK	RVV-----	199
54 EMP24	RERTHRNTAESTNDR	VKWWISIFQLGVVIAN	SLFQIYYLRRFFEV	SLV-----	203
55 CAB16901/SPBC16E9	REMTFRDTSSESANSR	VVRWTIVQIVVLLVT	CIWQLSHLQRFVKE	KLIV-----	215
56 CAB11508/SPAC17A5	REHRNSTVKSTQAR	IFWFSLAESIMVVAL	SALQVFIIVKTFPKRS	GRRGV-----	210
57 ERP3	RNTRNHHTVCSTEHR	IVMFSIYGILLIIGM	SCAQIAILEFIFRES	RKHN-----	225

Figure 5.1.

Table 5.1. Species Containing p24 Genes

<i>Anguilla anguilla</i>	<i>Entamoeba histolytica</i>	<i>Pichia angusta</i>
<i>Ancylostoma caninum</i>	<i>Fugu rubripes</i>	<i>Pichia farinosa</i>
<i>Arabidopsis thaliana</i>	<i>Gallus gallus</i>	<i>Pleurotus ostreatus</i>
<i>Bombyx mori</i>	<i>Gossypium arboreum</i>	<i>Pneumocystis carinii</i>
<i>Bos taurus</i>	<i>Halocynthia roretzi</i>	<i>Polysphondylium pallidum</i>
<i>Botryllus schlosseri</i>	<i>Homo sapiens</i>	<i>Rattus norvegicus</i>
<i>Botrytis cinerea</i>	<i>Kluyveromyces lactis</i>	<i>Saccharomyces bayanus</i>
<i>Brugia malayi</i>	<i>Kluyveromyces maxianus</i>	<i>Saccharomyces cerevisiae</i>
<i>Caenorhabditis elegans</i>	<i>Kluyveromyces thermotolerans</i>	<i>Saccharomyces kluyveri</i>
<i>Canis familiaris</i>	<i>Medicago truncatula</i>	<i>Saccharomyces servazzii</i>
<i>Ceratopteris richardii</i>	<i>Mesocricetus auratus</i>	<i>Salmo salar</i>
<i>Ciona intestinalis</i>	<i>Metarhizium anisopliae</i>	<i>Schistosoma japonicum</i>
<i>Cricetulus griseus</i>	<i>Mus musculus</i>	<i>Schistosoma mansoni</i>
<i>Cypinus carpio</i>	<i>Neurospora crassa</i>	<i>Schizosaccharomyces pombe</i>
<i>Danio rerio</i>	<i>Oryctolagus cuniculus</i>	<i>Strongyloides stercoralis</i>
<i>Debaryomyces hansenii</i>	<i>Oryzias latipes</i>	<i>Sus crofa</i>
<i>Dictyostelium discoideum</i>	<i>Penaeus monodon</i>	<i>Takifugu rubripes</i>
<i>Drosophila melanogaster</i>	<i>Paralichthys olivaceus</i>	<i>Xenopus laevis</i>

54 different species have been identified with at least one p24 gene. Searches for p24 genes were effected by performing BLAST searches of the known p24s in various databases.

5.2.2. Morphological Analysis of p24 Mutants

Previous studies have shown that none of the p24s in *Saccharomyces cerevisiae* are essential (Schimmöller *et al.*, 1995; Belden and Barlowe, 1996; Elrod-Erickson and Kaiser, 1996; Marzioch *et al.*, 1999; Springer *et al.*, 2000). However, selective cargo defects have been detected in a subset of proteins, namely, Gas1p and invertase when one or more of the p24 proteins are deleted (Schimmöller *et al.*, 1995; Belden and Barlowe, 1996; Elrod-Erickson and Kaiser, 1996; Marzioch *et al.*, 1999). In addition, the increased secretion of Kar2p and Pdi1p has been detected and a mild unfolded protein response (UPR) is elicited in deletion strains (Elrod-Erickson and Kaiser, 1996; Schimmöller *et al.*, 1995; Belden and Barlowe, 1996; Marzioch *et al.*, 1999; Belden and Barlowe, 2001b). The deletion of a p24 gene, however, does not lead to any dramatic morphological changes (Figure 5.2.). In fact, a complete deletion has been shown to provide no morphological abnormalities (Springer *et al.*, 2000). We have analyzed all eight single deletion strains, eight double deletion strains and two quadruple deletion strains, none of which had in any morphological abnormalities (data not show).

5.2.3. Morphological Analysis of p24 Overexpressors

It has been previously reported in mammalian systems that over expression of a p24 family member induces the formation of membrane systems (Rojo *et al.*, 2000). This finding was attributed a morphogenic property of the p24 proteins. To test this in yeast, the increased expression of ERV25, one of the δ family members was examined. It has a cytosolic tail with a YF motif and a **KXKXXX** motif: KNYFKTKHIL. ERV25 was expressed under a GALL promoter and cultures were grown in 3% galactose media at 30°C. Cells were then harvested and processed for electron microscopy as described in Material and Methods. Here we report the first identification of a novel membrane structure when a p24 protein is over expressed in yeast. Figure 5.3. shows the dramatic

morphological change in the membrane system of a yeast over expressing ERV25.

The membrane structure that is found in the overexpressors is composed of long regular cisternae that are interconnected and continuous with the nuclear envelope. In addition, there is a region that contains tubules and vesicles that is closely opposed to long cisternae. These membrane structures have also been identified in cells over expressing EMP24 and ERP1 (data not shown). In addition, over expression of two p24s (EMP24 and ERV25, EMP24 and ERP1 or ERV25 and ERP1) also results in the same type of membrane structure (data not shown). This result confirms that the p24s have a morphogenic property in yeast.

The membrane structure appears to be endoplasmic reticulum, due to its continuity with the nuclear envelope (Figure 5.3.). The tubular/vesicular area may be a type of transitional ER or intermediate compartment. This type of compartment has been previously described in yeast where the cells were subjected to various blocks in protein synthesis or temperature shifts in order to identify the post-ER membrane compartments (Morin-Ganet *et al.*, 2000). Specifically, the first post-ER compartment is described as a cluster of small vesicles that rapidly bridge to form tubules, resulting in a cluster of tubules and vesicles. Indeed, these vesicular-tubular clusters (VTCs) are reminiscent of what is seen in the ERV25 over expressing system. No Golgi stacks were seen to accumulate in cells. The occurrence of the large membrane structures may be attributed to a *de novo* formation elicited by the increase amount of a p24. Alternatively, this membrane structure may be a consequence of a block/delay in membrane movement or an increase in retrograde retrieval. It is also possible that there may be a disruption of the p24 protein complexes due to the increase of only one of the p24s (Rojo *et al.*, 1997; Dominguez *et al.*, 1998; Fullekrüg *et al.*, 1999) that has lead to a segregation of the excess p24 into a new compartment.

Figure 5.2. Morphological Analysis of the p24 deletion strains of *Saccharomyces cerevisiae*. Samples from a wild type strain (A), single deletion strain *erv25Δ* (B), and quadruple deletion strain *erv25Δemp24Δer1pΔerp2Δ* (C) were processed for routine electron microscopy as describe in the Material and Methods section. Electron micrographs were obtained with a Philips 400 electron microscope. Nucleus (N), vacuole (V), mitochondrion (m), endoplasmic reticulum (ER). The bar represents 250 nm.

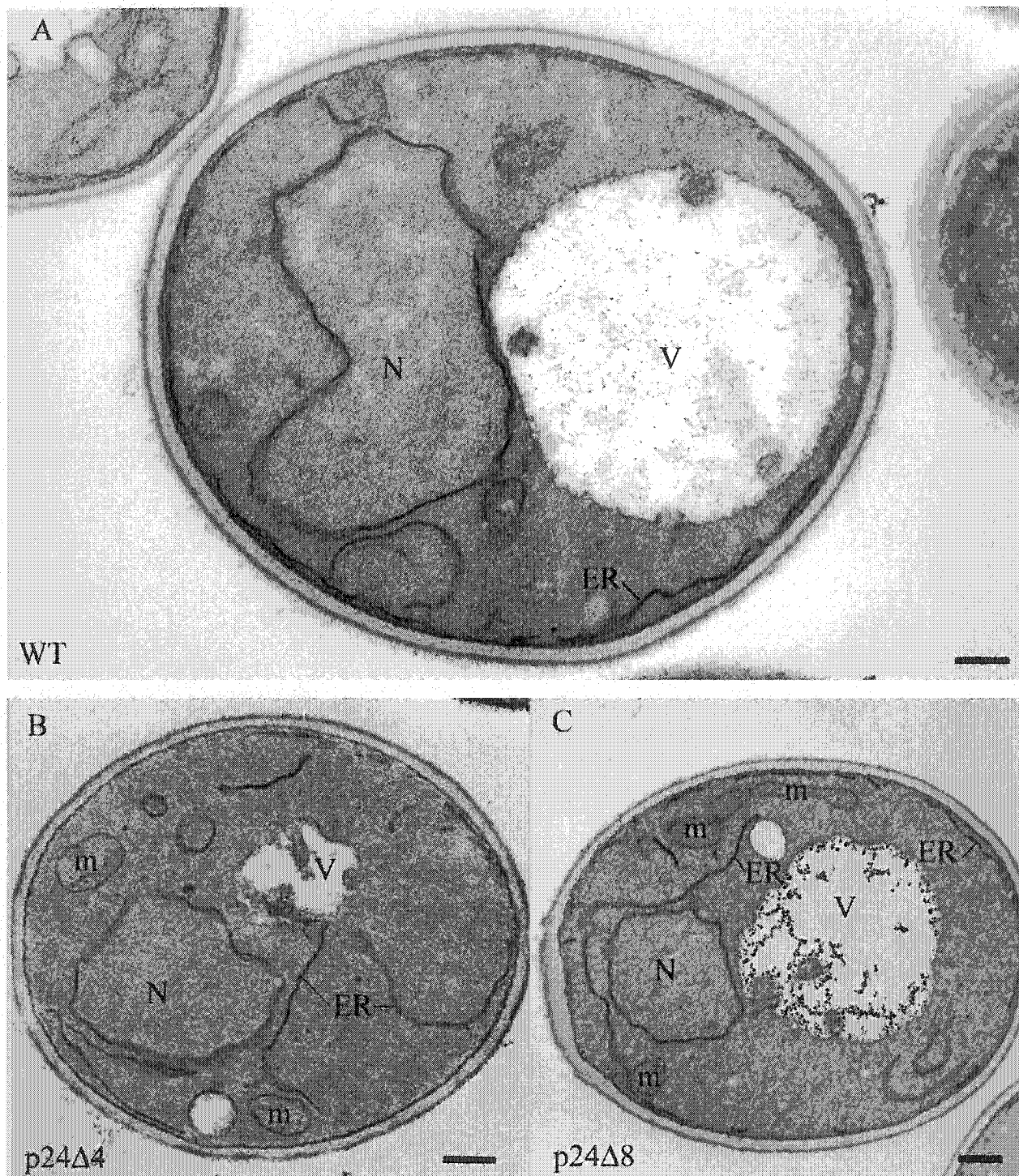


Figure 5.2.

Figure 5.3. Morphological Analysis of *S. cerevisiae* Over expressing ERV25.

Cells expressing the p426-ERV25 plasmid were grown in glucose and subsequently transferred to galactose (A and B). The cells were then processed for routine electron microscopy as describe in the Material and Methods section. Electron micrographs were obtained with a Philips 400 electron microscope. Nucleus (N), mitochondrion (m), endoplasmic reticulum (ER), small arrows indicate budding structures, arrowheads indicate possible vesicular profiles, np indicates the nuclear pores in the nuclear envelope, pER refers to the peripheral ER, large arrows indicate the continuities between the new membrane system and the nuclear envelope and the peripheral ER. The bar represents 250 nm.

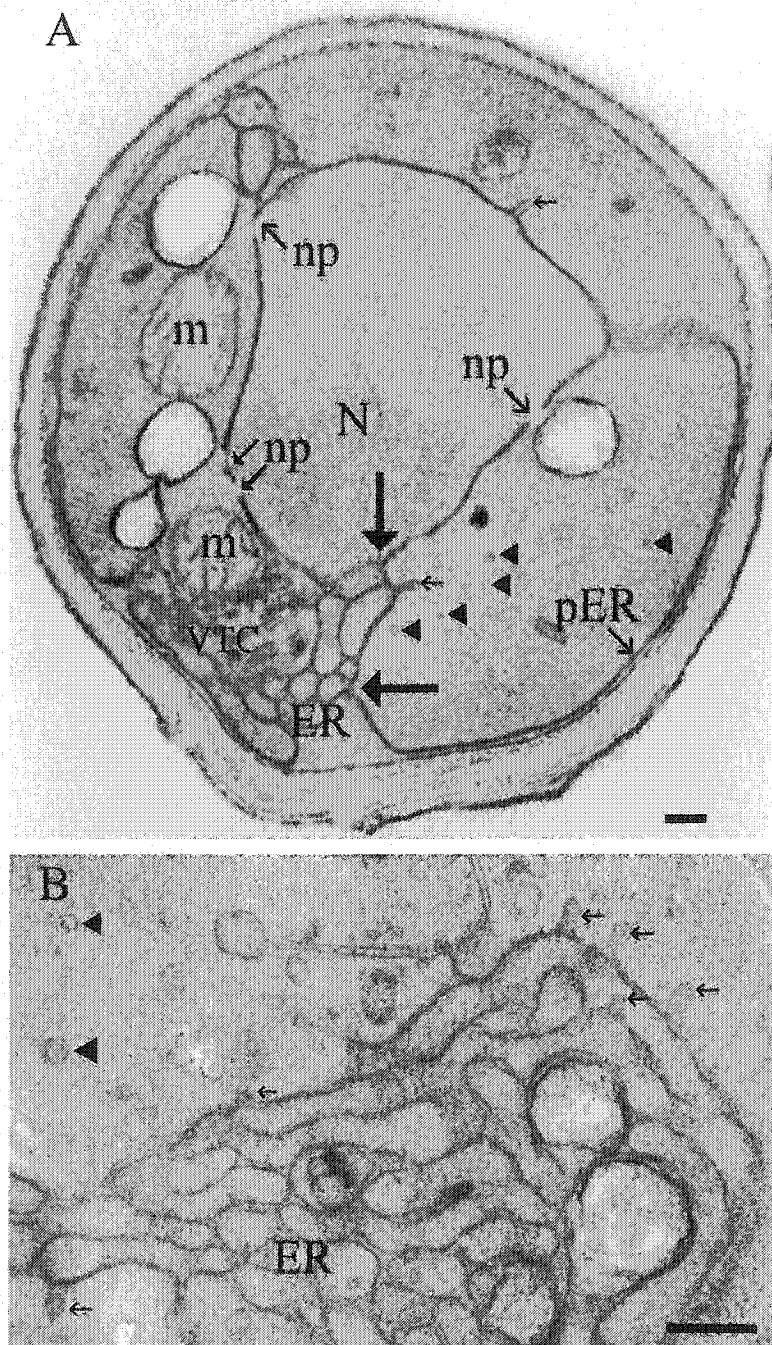


Figure 5.3.

5.2.4. Cryo-immunolabeling of Overexpressors with Anti-Erv25p

To first identify where Erv25p was located, immunolocalization studies were carried out in the ERV25 overexpressor. Frozen sections of the ERV25 overexpressors were first labeled with a primary antibody followed by a secondary antibody conjugated to 10 nm gold particles in order to visualize the staining pattern through electron microscopy (as described in Materials and Methods). Immunolocalization studies revealed that Erv25p was localized almost exclusively to the vesicular/tubular area of the cell, with some of gold particles on the large membrane network, peripheral ER and nuclear envelope (Figure 5.4. and Figure 5.6.C). Cryoimmunolabeling studies were also carried out with an antibody to another p24 protein (Erp1p) in order to determine the effect that the over expression of ERV25 has on the other p24s. The labeling study with anti-Erp1p revealed a low level of labeling, consistent with endogenous level in WT cells (data not shown). This indicates that the protein level of Erp1p is most likely not increased in conjunction with Erv25p.

5.2.5. Cryo-immunolabeling Analysis of the Overexpressors

In order to determine if the large membrane structures contained other constituents of the secretory pathway or if they were a consequence of a mechanism of the cell to segregate the over expressed membrane protein, further cryo-immunolabeling studies were performed. Kar2p is an ER protein that has many different roles. Kar2p is best known as an ER chaperone and for its role in protein folding; however, it is also involved in protein translocation, the ER-associated degradation (ERAD) pathway and the maintenance of a permeability barrier between the ER and cytosol (Matlack *et al.*, 1999; Gething, 1999; Hamman *et al.*, 1998). Antibodies against Kar2p were used to label the cells

expressing the p426-GALL-ERV25 vector. The gold labeling was detected over the large ER structures as well as in concentrated areas that are reminiscent of BiP bodies (Nishikawa *et al.*, 1994) (Figure 5.5. A). BiP bodies are a phenomenon that is seen when secretion is blocked, whether by deletion or over expression of a protein that is involved in the secretory pathway (Nishikawa *et al.*, 1994). The localization of Kar2p to the new membrane structures indicates that these large membrane structures are indeed ER.

Sar1p is a small soluble GTP-binding protein that is involved in COPII vesicle formation. Sar1p-GDP is recruited to the cytosolic side of the ER membrane by the Sec12p membrane protein. There, Sar1p-GDP is activated by a guanine nucleotide exchange to Sar1p-GTP (Barlowe and Schekman, 1993). The activated form of Sar1p then recruits the Sec23p-Sec24p complex and the Sec13-Sec31p complex to form the COPII coat (Barlowe *et al.*, 1994). Cells expressing the p426-GALL-ERV25 vector were labeled with antibodies raised against Sar1p. Again, the gold particle distribution was detected over the large membrane structures (Figure 5.6. B). This result further confirms that the membranes are ER and that the sites labeled with anti-Sar1p are possible recruitment sites for COPII vesicle formation.

We then looked at a component of the COPI coat. Sec27p is the beta prime subunit of the COPI complex. Antibodies to this protein were found on the extensive ER membranes as well as on the VTCs and cytoplasm (Figure 5.6.C.). In addition, anti-Sec27p labeling was found in the nucleus, which is an area where high background labeling generally occurs (not shown).

Bos1p is a v-SNARE that is necessary for transport from the endoplasmic reticulum to the Golgi (Lian *et al.*, 1993; Ossipov *et al.*, 1999). Gold particles were found over both the VTCs and ER when labeling was carried out with anti-Bos1p (Figure 5.6.D.).

Sed5p is also involved in vesicular transport between the ER and Golgi (Hardwick *et al.*, 1992). Labeling with anti-Sed5p revealed gold particle labeling over the VTCs (not shown) and the ER (Figure 5.6.E.).

Thus far we, have identified protein constituents that are involved in cargo protein processing and cargo transport. In order to identify if cargo proteins are present we immunolabeled with antibodies to prepro-alpha-factor. Alpha-factor is a peptide pheromone that is involved in the mating process of *Saccharomyces cerevisiae*. The precursor to this protein, prepro-alpha-factor, is translocated into the endoplasmic reticulum for glycosylation (Waters *et al.*, 1988). The protein then passes through the secretory pathway and is eventually secreted. Labeling studies revealed that prepro-alpha-factor is in the cytoplasm, the extensive ER network (Figure 5.6.F.) and the VTC (not shown). This data indicates that the ER membranes contain different protein constituents that are involved in this pathway. The occurrence of BiP bodies and the accumulation of vesicular tubular profiles may indicate that there is a block in secretion.

5.2.6. Plasmid Instability

Once transferred to galactose, the doubling time of the cells expressing the p426-ERV25 plasmid is longer than that of wild type cells. Even control cells with the p426 plasmid had an increased doubling time (not shown). This may be due to a variety of factors including the carbon source. In order to determine if the plasmid was having an effect on the cells, we investigated the stability of the plasmid. The plasmid used for these studies (p426) contains a galactokinase (GALL) promoter (a deletion variant of the GAL1 promoter) and a URA3 selection marker. Under experimental conditions, cells are grown in a -URA medium to render the plasmid essential, thus ensuring the retention of the plasmid. Cells were grown in galactose media to induce the expression of the ERV25 gene. In order to test for the plasmid stability, transformed strains were grown overnight in a standard 2% dextrose media (YPD) or a 2% galactose media

(YP-GAL). Dilutions were then plated onto YPD agar. After two days of growth, colonies were replica plated onto -URA agar plates with either glucose or galactose. Cells with the p426 expression vector had a 29%-32% rate of loss of the plasmid when grown in YPD followed by either glucose or galactose (-URA agar plates) (Table 5.2.). Cells expressing the p426 vector and that had initially been grown on YP-Gal (inducible condition) followed by glucose or galactose had a 50%-52% rate of plasmid loss. Cells that had the p426-ERV25 plasmid that were grown in YPD (non inducible condition) had a 39%-50% rate of plasmid loss when transferred to either glucose or galactose. Significantly, those cells with the p426-ERV25 plasmid that were grown in galactose, and thus ERV25 was over expressed, had a 100% rate of plasmid loss. This indicates that given the opportunity to lose the plasmid, 100% of the cells will 'spit out' the plasmid as opposed to expressing an increased amount of Erv25p. This indicates that increased levels of Erv25p are detrimental to the cell, whether through a direct or indirect mechanism.

5.2.7. Quantitation of ERV25 Overexpressors

One of the characteristics of electron microscopy is that each image represents a section of the cell and not the entire cell. As expected, we did not see our phenotype in 100% of the cell sections. Owing to the fact that increased levels of Erv25p are detrimental to the cell we decided to quantify the incidence of the extensive membrane systems. Quantitation of the number of sections exhibiting these profiles revealed that 39% of the total EM sections had irregular membrane structures (Figure 5.6.A), while 46% of the cell sections had membrane systems consistent with control cells (Figure 5.6.B). As mentioned, the sample populations that were analyzed are not whole cells, but rather thin sections (29 nm). It is thus possible that cells that appear to have normal membrane morphology actually do exhibit irregular membrane formations, but that these structures are not seen due to the plane of section. For comparison, the number of cell sections that had nuclei was assessed on the same population of cells. $64\% \pm 3\%$ of the cell

sections had a nucleus while $36\% \pm 3\%$ of the cells did not (Figure 5.8.). This indicates that even a cellular structure as large as the nucleus will only be seen in 64% of the cell sections. Thus it is possible that the number of cells with irregular membrane systems was underestimated. As a control, Epon sections of cells expressing the empty vector (p426) had no membrane accumulation (Figure 5.6.B).

We then assessed the gold particle distribution of anti-Erv25p labeling in cells expressing the p426-ERV25 plasmid. Quantitation of the immunolocalization studies revealed that Erv25p was localized almost exclusively to the vesicular/tubular area of the cell, with some of gold particles on the large membrane network, peripheral ER and nuclear envelope (Figure 5.4. and Figure 5.6.C). Quantitation was also carried out on the sections that did not exhibit the membrane proliferation (Figure 5.6.D. and Figure 5.7.). It is clear that the majority of the gold labeling for anti-Erv25p is contained within the vesicular/tubular profiles and the extensive ER networks. Cell sections not showing this area of the cell have low levels of labeling for anti-Erv25p, reminiscent of endogenous level. Indeed, the immunolocalization studies on wild type (DHY9 or W303-1a) strains with anti-Erv25p or anti-Erp1p were very weak due to the low exogenous level of the p24s (data not show). It is not clear if the sections without membrane abnormalities are a consequence of plane of section, loss of plasmid, mutation (possibly in the endogenous ERV25 gene) or if different cells express a different number of plasmids and thus have different levels of Erv25p expression (with only those cells with high levels of Erv25p producing abnormal membrane morphologies).

Figure 5.4. Erv25p localization in ERV25 expressing cells. Cells expressing GALL-p426-ERV25 were grown in galactose media and processed for cryo-electron microscopy as described in Materials and Methods. Immunolabeling of ultrathin cryosections with antibodies to Erv25p revealed gold particle labeling to be most concentrated over vesicular tubular clusters (VTCs) (A-D). The VTCs are indicated by a broken line in A and D. Erv25p labeling was also seen on the nuclear envelope (E). ER, endoplasmic reticulum; m, mitochondrion; N, nucleus, np, nuclear pore; VTC, vesicular tubular clusters. Arrows in panel D indicate labeling on ER network. Arrowheads in panel E indicate labeling on nuclear membrane. The magnification bars represent 250 nm.

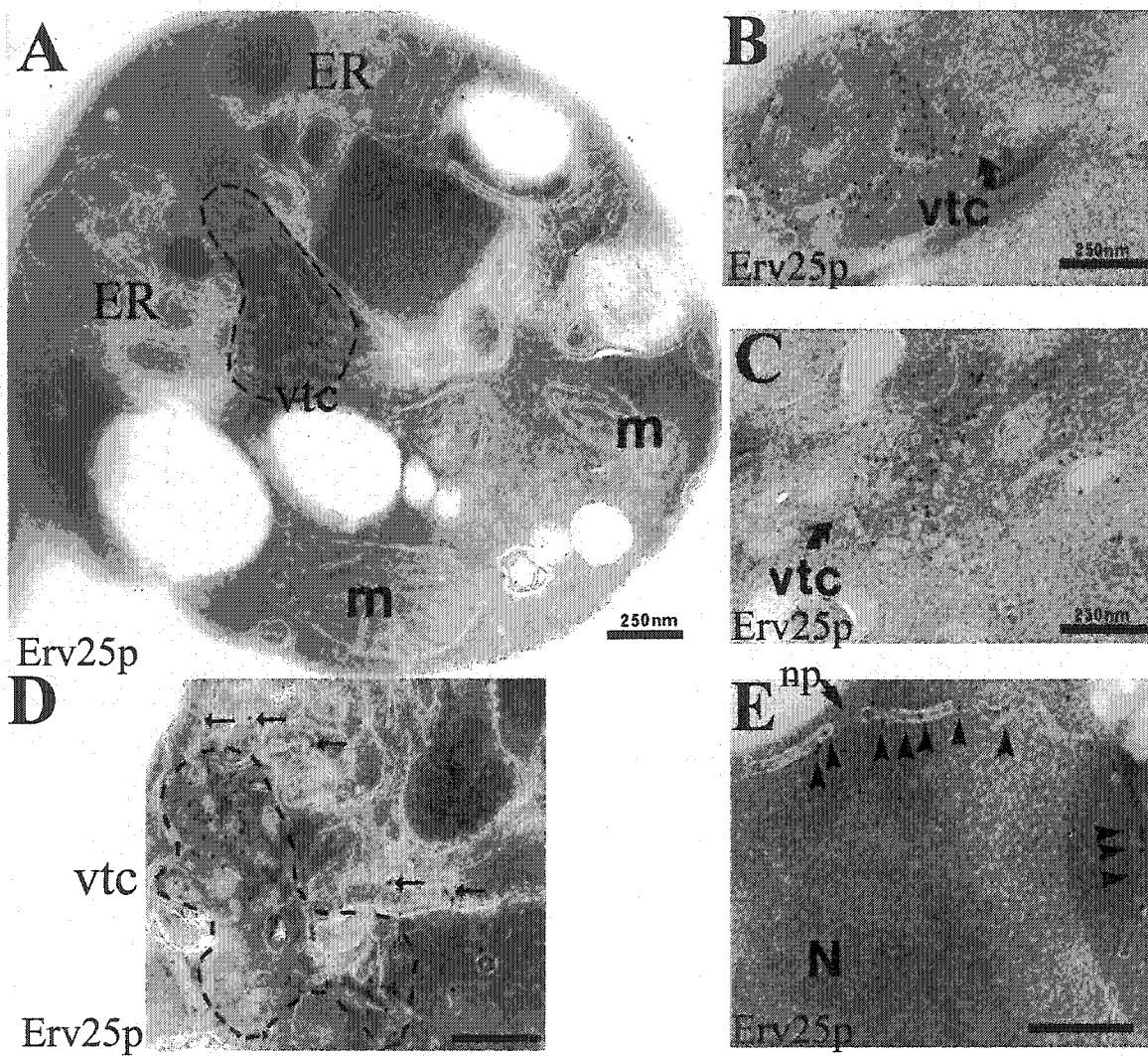


Figure 5.4.

Figure 5.5. Immunolabeling of ER profiles in ERV25 over expressing cells. Cells expressing GALL-p426-ERV25 were grown in galactose media and processed for cryo-electron microscopy as described in Materials and Methods. Cells were then labeled with antibodies to Kar2p (A), Sar1p (B), Sec27p (C), Bos1p (D), Sed5p (E), and prepro-alpha-factor (F). Some of the gold particle labeling is indicated by arrows or arrowheads. Arrowheads indicate labeling in the VTCs; black arrows represent labeling over the ER profiles; white arrows indicate labeling in the cytoplasm. Magnification bars represent 250nm.

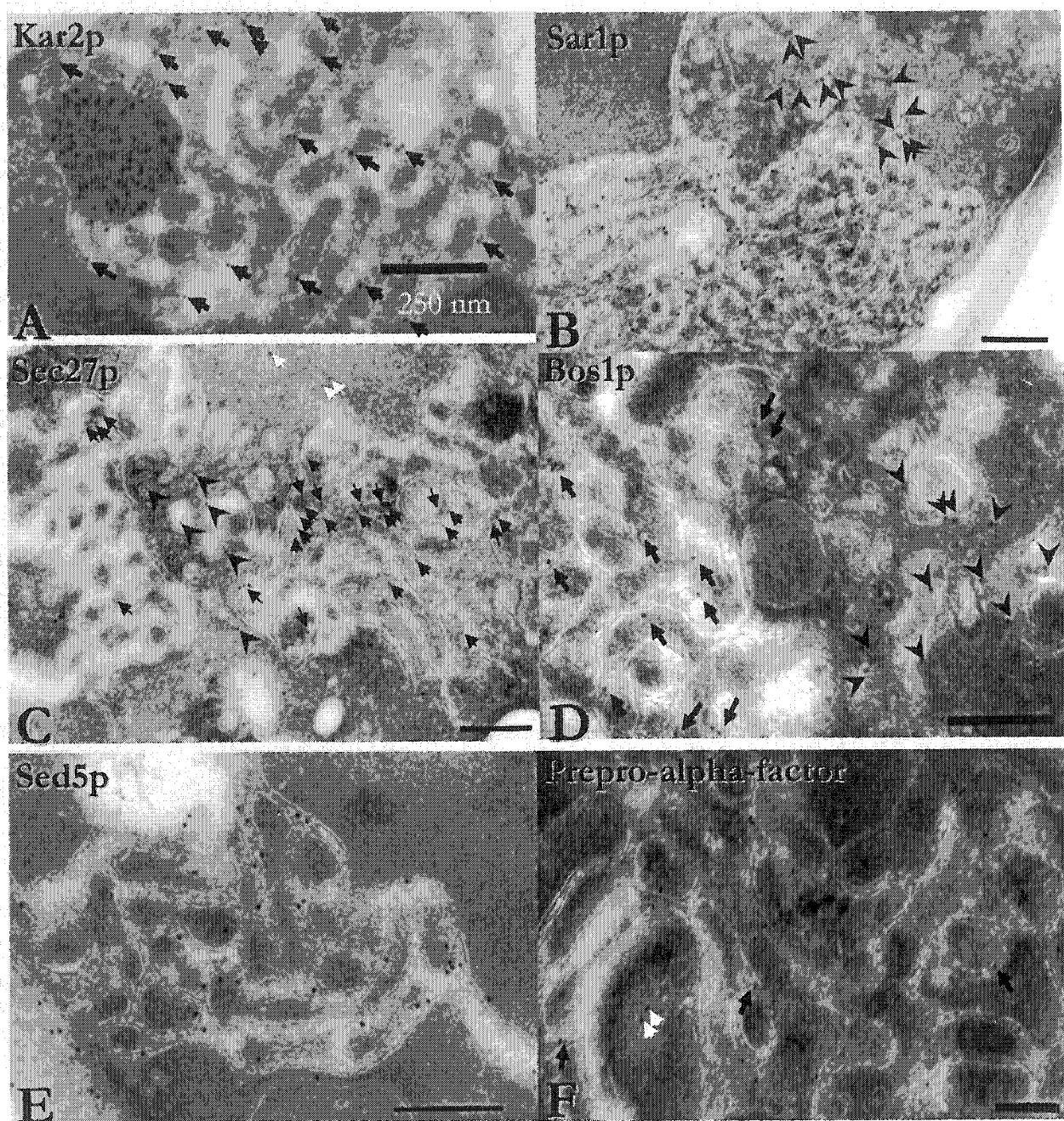


Figure 5.5.

Table 5.2. Stability of the p426-ERV25 plasmid.

Strain	Plasmid ^a	Growth medium ^b	Sugar ^c	% URA3+ (±SD)
W303-1A	p426	YPD	Glucose	71 ± 1.5
			Galactose	68 ± 1.0
	p426	YPGal	Glucose	50 ± 3.0
			Galactose	48 ± 3.2
	p426-ERV25	YPD	Glucose	61 ± 4.1
			Galactose	50 ± 2.6
	p426-ERV25	YPGal	Glucose	0 ± 0
			Galactose	0 ± 0

^a Cells were transfected with either the empty plasmid (p426) or the ERV25-containing plasmid (p426-ERV25) as described in Materials and Methods.

^b Transfected cells were grown overnight in either YPD or YPGal medium. Dilutions were then plated onto YPD agar plates. At this stage, if the plasmid is detrimental to the cell, the cell will be more likely to lose the plasmid.

^c Colonies were replica plated onto –URA plates containing either glucose or galactose in order to detect those cells that retained the plasmid.

Figure 5.6. Quantitation of ER membrane proliferation and Erv25p labeling.

Cells expressing GALL-p426-ERV25 were grown in galactose media and processed for routine or cryo-electron microscopy as described in Materials and Methods. Epon sections were used to quantify the occurrence of the proliferated ER (A, B). No membrane proliferations were detected in control cells (p426) while cells expressing ERV25 revealed membrane proliferation in 39% of the cells (histograms represents mean \pm SD of 3 separate experiments with 134, 130 and 101 cells counted). In cryosections (C, D) gold particles were prominent only on VTCs and large ER structures (C). Sections not revealing the phenotype had negligible gold particle labeling (D) which was also negligible in control cells (not shown). Categories for quantitation of Epon sections are as follows: *Extensive ER/VTCs* represents cell sections that had an abnormal or extensive amount of ER or VTCs; *Normal membrane morphology* represents sections that had membrane morphology consistent with wild type cells; *Poor morphology* represents cells whose membrane morphology was not preserved during the processing for EM; *vesiculated cells* represent a population of cells whose membrane systems have deteriorated into vesicular structures, mostly likely representative of cell death. Categories for quantitation of cryo-sections are as follows: *pER*, is the ER that is at the periphery of the cell; *ER*, includes the extensive ER network and ER cisternae that are located within the cytoplasm; *V&T*, are vesicular/tubular profiles; *NE*, nuclear envelope; *Nucleus*, nucleus not including the nuclear membrane; *Cell Wall/PM*, the cell wall and the plasma membrane; *Other*, this category includes mitochondria, vacuoles, cytoplasm and all other parts of the cell not mentioned, in particular it also includes those sections of the cell whose morphology has not been preserved and thus limiting the identification of membrane systems (see Figure 5.7. bad morphology - bm).

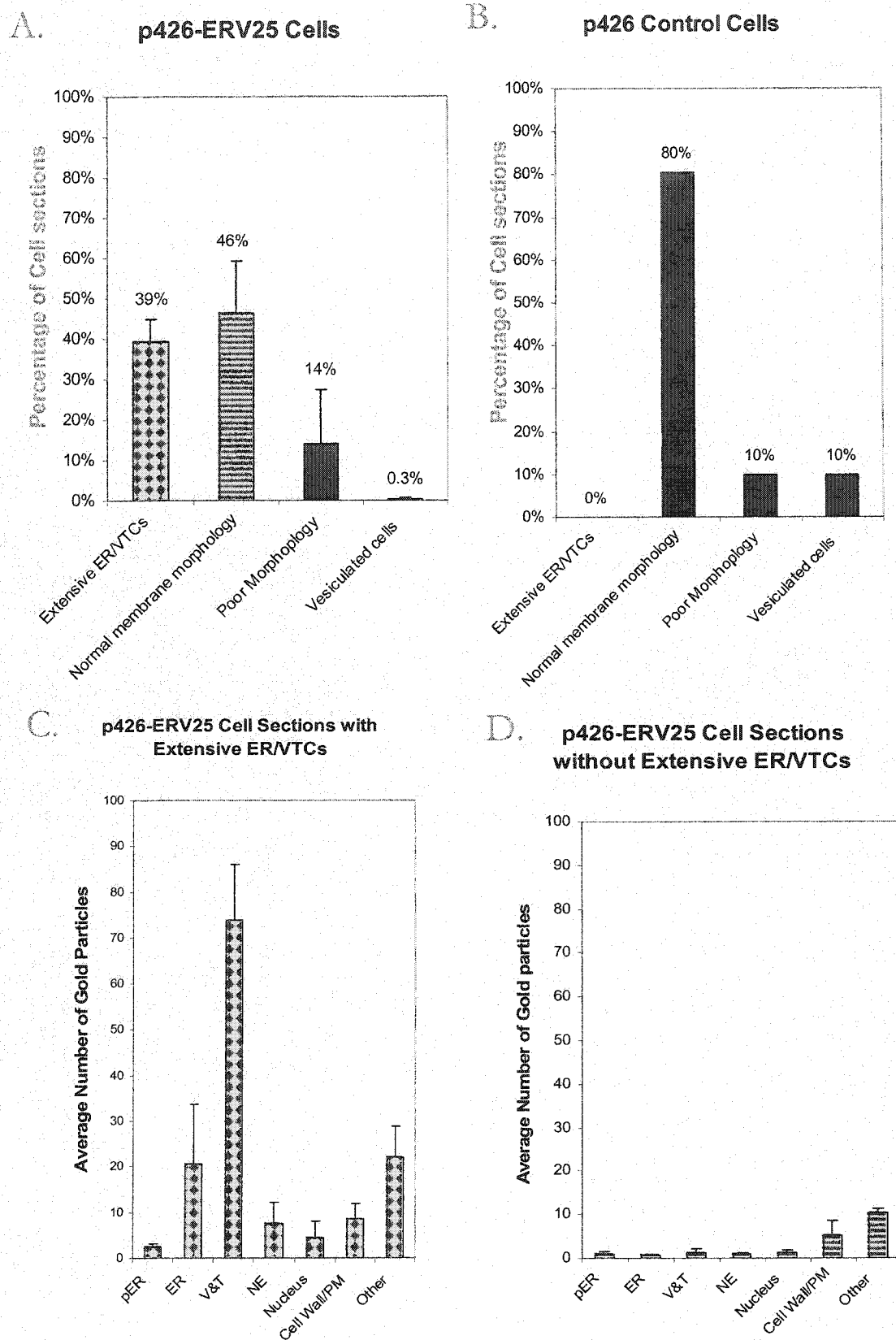


Figure 5.6.

Figure 5.7. Cell section without membrane network. Micrograph of a section of a cell that expresses the p426-ERV25 plasmid and that has been grown in galactose media. No extensive or abnormal membrane system is present in this cell section. Circles indicate the gold particles that label the cell. N, nucleus; ER, endoplasmic reticulum; PM, the plasma membrane is indicated between the two arrows; m, mitochondrion; V, vacuole; bm, represents an area of bad morphology. Magnification bar represents 250nm.

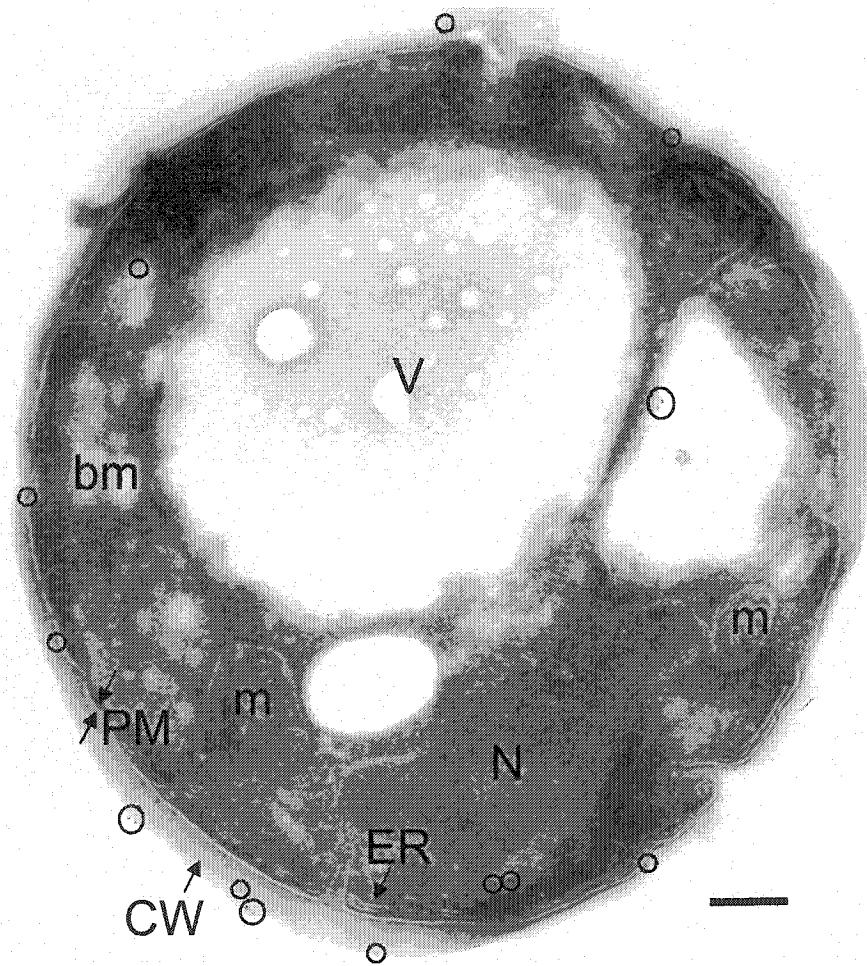


Figure 5.7.

Figure 5.8. Quantitation of the incidence of nuclei in cell section. Cells sections were quantified by electron microscopy to determine the number of sections that exhibited nuclei. This was done for $n=3$ (>300 cell sections analyzed). The data is presented as a percentage of cell sections where nuclei are apparent or not apparent in a section. The standard deviation for both categories is 3%.

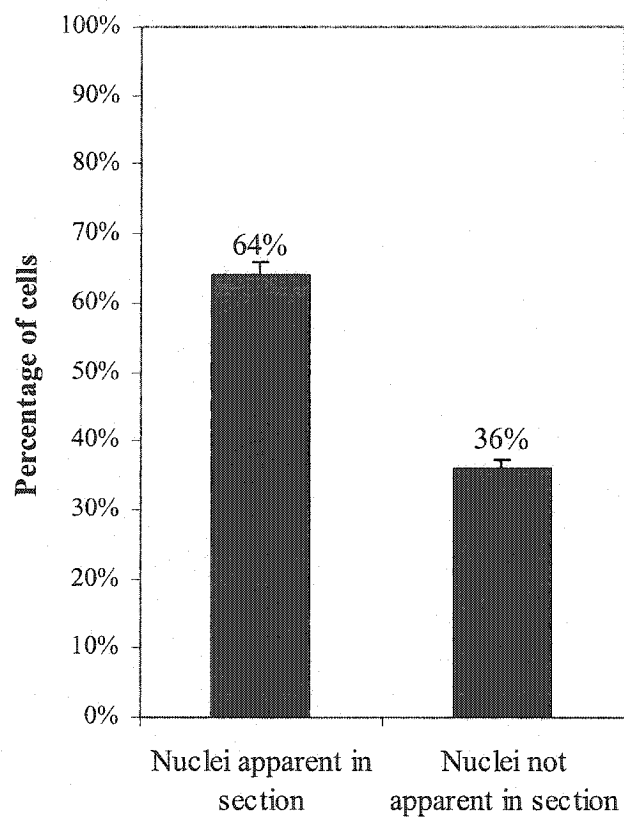


Figure 5.8.

5.3. Discussion

Yeast have long been used as tools to identify the role of proteins (Novick *et al.*, 1980). This chapter looks at mutations and over expression studies of the p24 genes. The p24 family of genes has been associated with the early secretory pathway but no clear role has been proven. Morphological assessment of the cells confirmed past studies that the deletion of the p24 genes, whether single, double or quadruple, does not alter the morphology of the yeast cell. Over expression of one of three or two of three of the p24 proteins, namely ERV25, EMP24 or ERP1, produces dramatic changes to the morphology of the yeast cell. The large membrane structure is usually seen to be continuous with the nuclear membrane. This fact alone indicates that the large membranes are endoplasmic reticulum. The ER membrane system is interconnected and consists of several tubular elements. A cross section of the membranes has a honey comb shaped appearance, while a longitudinal section exhibits a set of parallel strands of membrane cisternae. There are also vesicular/tubular and budding areas associated with this membrane structure. Cryo-immunogold techniques revealed that the ER membranes are labeled for Erv25p, however, the protein is most highly concentrated in the tubular/vesicular areas. This indicates that there is a distinct segregation or sorting of Erv25p. Labeling studies with anti-Erp1p antibodies did not show a significant increase in Erp1p in the ERV25 overexpressors indicating that the increase in expression of one of the p24 family members does not induce an increase in another.

Membrane structures similar to those seen in the p24 overexpressors were also observed in systems where SEC12 was over expressed (Nishikiawa *et al.*, 1994), where ARF1 was over expressed in an $\Delta arf1 \Delta arf2$ background (Deitz *et al.*, 2000), where Sec24p was depleted (Kuirihara *et al.*, 2000) and where the prosequence-deleted form of RNAP-I was expressed (Umebayashi *et al.*, 1997). The ER chaperone, Kar2p, exhibited high labeling on the large ER networks of

the ERV25 overexpressors. Kar2p was also found in large concentrations of what appeared to be BiP bodies (Nishikawa *et al.*, 1994). BiP bodies are also detected when Sec12p is over expressed under a GAL1 promoter. Sec12p over expression blocks ER-to-Golgi transport. Likewise, sec mutants that also inhibit ER-to-Golgi transport also exhibit BiP bodies. In contrast, over expression of other ER proteins that induce membrane formation, such as HMG-CoA reductase or Sec4p, does not produce BiP bodies (Nishikawa *et al.*, 1994). This indicates that since BiP bodies are present in the ERV25 overexpressors with the large ER structures there may be a perturbation in ER-to-Golgi transport in these cells. The accumulation of the vesicular/tubular structures may indicate that a block may be occurring in a post-ER compartment.

The COPII GTPase, Sar1p, also showed high labeling in the ERV25 overexpressors with large membrane structures. The majority of the gold particles were seen over the large membrane system. Sar1p has been localized to the ER membrane (Nishikawa and Nakano, 1991) further confirming that the large membrane system is ER. Sar1p, however, was not found to any great extent on the tubular/vesicular areas. This indicates that these areas are indeed post-ER compartments since COPII vesicles shed their coat as Sar1p-GTP is hydrolyzed and the COPII subunits disassociate. The COPI beta prime subunit (Sec27p) was also found on the ER membranes as well as over the VTCs and cytosol. The trafficking proteins Sed5p and Bos1p, likewise, were found over the ER and VTCs. In addition, the cargo protein prepro-alpha-factor was found in the ER. This indicates that this membrane compartment contains many of the constituents of the secretory pathway.

The data collected in this study confirms that deletion of the p24 proteins does not affect the morphology of the cell. It has also emphasized the low endogenous level of this protein in yeast. An increase in expression of one of the p24 protein (whether Erv25p, Erp1p or Emp24p) has a dramatic effect on the cell morphology. Indeed, we have shown that cells expressing increased amounts of

Erv25p have a large ER membrane system in the cell. This is accompanied by a vesicular/tubular area, where most of the Erv25p protein is concentrated. This latter compartment appears to be a post-ER compartment as it is not highly labeled with Sar1p. The appearance of BiP bodies also tends to indicate that there is a block in secretion in the cells and that the ER membrane structure is due to a block in secretion as opposed to a de novo synthesis of ER membranes.

5.4. Materials and Methods

5.4.1. Strains, Plasmids and Growth Media

The yeast strains used in this study are found in Table 5.1. Deletion (DHY4 and RSY1888) and wild type (DHY9) strains were grown in YDP media at 30°C and harvested during logarithmic phase. Cells over expressing ERV25 and control cells were grown in 2% glucose and transferred to 3% galactose for 6, 12, 24 and 36 hours. Over expression of the yeast p24 (ERV25) was effected by expressing the p426-ERV25 plasmid. Control cells contained the p426 plasmid alone. The plasmids were obtained from A. Rowley (GlaxoSmithKline). Briefly, the p24 gene was cloned behind the GALL promoter in the p426 plasmid containing a URA3 selection marker (Mumberg *et al.*, 1994; Mumberg *et al.*, 1995).

5.4.2. Antibodies

Goat anti-rabbit gold conjugated antibodies (5nm or 10nm) were obtained from Sigma Chemical Company (St. Louis, MO, USA). The antibodies directed against Erv25p (Belden and Barlowe, 1996), Kar2p (Brodsky et al., 1993), Sar1p (Barlowe et al., 1993) and Bos1p (Cao and Barlowe, 2000) have been described. The antibodies to prepro-alpha-factor were generously provided by Dr. R. Schekman. The antibodies to Sec27p were generously provided by Dr. C. Barlowe.

5.4.3. Yeast Transfection

Cells were transfected with the p426 and p426-ERV25 plasmid as described by Chen *et al.* (1992). Briefly, cells were grown to stationary phase. 0.2 ml of cells were pelleted and suspended in 0.1 ml of One-Step-Buffer (0.2 ml 1M LiAc, 0.8 ml 50% PEG 3400, 15 mg DTT, 25 µg ssDNA). 2-10 µg of

transforming DNA were added and the cells were incubated for 60 min at 45°C. The mixture was then plated on –URA/SD agar plates.

5.4.4. Routine Electron Microscopy

Cells were harvested and fixed with 1.5 % potassium permanganate for 20 minutes. The cells were then washed with water and post-fixed with 2% uranyl acetate overnight at 4°C. The samples were washed, dehydrated in a graded series of ethanol followed by propylene oxide and embedded in Epon (M.E.C.A. Ltée, Montreal, Quebec). Thin sections of 100 nm were cut with an ultracut E microtome (Reichert Jung) and placed on copper grids. Sections were viewed with a Philips 400 transmission electron microscope. For cells over expressing ERV25, both the W303-1a and DHY9 were transfected and examined. Both exhibited the same characteristic morphological features attributed to the over expression of a p24.

5.4.5. Cryoimmune Electron Microscopy

The strain W303-1a expressing the p426 or p426-ERV25 plasmid was used for cryoimmune experiments. Cells were fixed and processed as described in Dahan *et al.*, 1994. Briefly, cells were fixed in 4% paraformaldehyde and 0.5% glutaraldehyde in 0.1 M phosphate buffer (pH 7.4) at 4°C. Cells were washed in 4% sucrose in 0.1M phosphate buffer (pH 7.4) and cryo-protected in 2.3 M sucrose (Tokuyasu, 1980). Samples were mounted onto nickel stubs and frozen in liquid nitrogen. 29 nm sections were cut with an ultracut E microtome with FC4D attachment and placed onto copper grids. Sections were blocked with BCO (2% bovine serum albumin 2% casein 0.5% ovalbumin) for 10 minutes followed by 0.02M glycine for 10 minutes. The sections were then incubated with antibody for 30 minutes followed by a washing in Delbosco's PBS (six times 5 minutes). The sections were then incubated with secondary gold-conjugated antibodies for 30 minutes. Another washing was done, consisting of six times 5 minutes DPBS and

six times 5 minutes double distilled water. Sections were then treated with 2% uranyl acetate 0.15M oxalic acid pH 7 for 5 minutes followed by two 2.5 minute washes in water. Sections were protected with methyl cellulose.

5.4.6. Plasmid Stability

Stability of the plasmid under study was tested as described by Whiteway *et al.* (1990). Cells were grown in YPD or YPGal medium overnight and then plated on YPD plates (at ~1,000-fold dilution). After a two-day incubation at 30°C, colonies were replica plated on -URA plates (with either glucose or galactose) in order to detect cells that maintained the plasmid (p426-GALL plasmid contains a URA3 selectable marker).

Table 5.3. Yeast Strains

Strain	Genotype	Source
DHY9 (wild type)	<i>MATα</i> <i>ura3-52 lys2-801 ade2-101 trp1-Δ1 his3-Δ200 leu2-Δ1</i> (derivative of YPH274, ATCC)	A. Rowley
DHY4 (<i>erv25Δ</i>)	DHY9, <i>Δerv25::HIS3</i>	A. Rowley
ARY90 (p24 Δ 4)	DHY9, <i>Δemp24::HIS3 Δerv25::HIS3 Δerp1::TRP1 Δerp2::HIS3</i>	A. Rowley
RSY1888 (p24 Δ 8)	DHY9, <i>Δemp24::HIS3 Δerv25::HIS3 Δerp1::TRP1 Δerp2::HIS3 Δerp3::loxP Δerp4::loxP Δerp5::loxP Δerp6::loxP-Kan^r-loxP</i>	R. Schekman
W303-1a	<i>Mata ade2-1 his3-11,15 leu2-3,112 ura3-1 trp1-1 can1-100</i>	M. Whiteway

CHAPTER 6.

Genetic Expression Profiles of p24 Mutants

6.1. Introduction

The p24s are abundant protein constituents of COPII vesicles in yeast (Belden and Barlowe, 1996). The deletion of these genes in yeast does not appear to affect the morphology of the secretory pathway or the bulk of protein secretion. There are however, some effects on the kinetics of the secretion of certain proteins (Gas1p and invertase) and the retention of others (Kar2p and Pdi1p) (Schimmöller *et al.*, 1995; Belden and Barlowe, 1996; Marzioch *et al.*, 1999). The p24 deletions also elicit a mild unfolded protein response (Belden and Barlowe, 2001b). The UPR is classically associated with an accumulation of unfolded proteins in the endoplasmic reticulum. In the case of the p24 deletion strains, the lack of retention in the ER or poor retrieval of escaped proteins may have caused the response. That is, due to the increased secretion of several ER resident proteins the cell must compensate by producing more of these chaperones, which also occurs in the UPR (Patil and Walter, 2001).

The over expression of p24 proteins creates an entirely different response. A dramatic increase in one or two of the p24 genes generates a large membranous structure in the cells. The occurrence of this membrane network coincides with the increase in Erv25p labeling within the cell (mainly on tubular structures, vesicles and ER). The cells also exhibit BiP bodies and an increase in Sar1p and Kar2p labeling on the ER membranes.

To further study these two systems, we used DNA microarrays. The microarrays were used to study the genetic profile of the different cell types. This tool provides detailed information about the changes in gene expression of a cell and reveals the genes that are changed as a consequence of the over expression or deletion of a gene. Having obtained a novel phenotype for the p24 overexpressors, we wanted to further understand the mechanisms behind the formation of the membranes. This technique was used to distinguish whether the large ER membranes were due to an accumulation of membranes due to a block in

secretion or a result of de novo biogenesis of ER, in which case a vast number of genes would need to be activated. In addition, analysis of the deletion strains by this method provided further insight into the level that a p24 deletion affects the cell.

6.2. Results

The advent of DNA microarray technology has provided a powerful tool that has allowed scientist to use genomes on another level: to simultaneously examine the entire genomic expression of an organism. This study focuses on the budding yeast, *Saccharomyces cerevisiae* and changes in genomic expression when a p24 gene is deleted or the expression is increased. In order to assure a high standard of data several quality control steps were set in place and much statistical analysis was performed on the data. Below is a description of the DNA microarrays, the quality control steps used throughout an experiment, the tools and software used to analyze the data, as well as the statistical analysis and genetic profiles.

6.2.1. Yeast ORF Microarrays

The Yeast ORF microarrays used in this study were the Yeast Arrays 6.4k obtained through the Microarray Centre at University Health Network, Ontario Cancer Institute (Toronto, Canada). These arrays have the entire genome of *Saccharomyces cerevisiae* spotted onto a glass slide in duplicate. In addition there are control spots (*Arabidopsis thaliana* genes) and blank spots. The microarray slide consists of 32 subarrays in a four by eight configuration. Each subarray is composed of 400 (20 by 20) spots, for a total of 12,800 spots per microarray slide. The spot to spot distance is 200 micrometers. The probe DNA for each spot is immobilized (or spotted) onto CMT-GAPS slides (Corning Inc.) with a high-precision micro-robotics technology.

6.2.2. The DNA Microarray System

RNA must be isolated from control and experimental cells (Figure 6.1. A and Figure 6.2.). The RNA is used to transcribe cDNA that is labeled with either a

Cyanine-3 or Cyanine-5 labeled deoxy-cytosine triphosphate (dCTP) fluorescent nucleotide analogue (Figure 6.1. C). The large difference in the emission peaks between the cyanine dyes makes them ideal for multicolor detection (the Cy5 emission maximum is 660-670 nm while the Cy3 is emission maximum 570-580 nm). In addition, the cyanine dyes produce a bright signal and are incorporated in a relatively consistent manner as compared to other dyes pairs. However, since there are some differences in the rates of incorporation of the two nucleotide conjugated cytofloures, reciprocal labeling is always done to account for discrepancies.

cDNA from the control cells is labeled with one dye and the cDNA from the experimental cells is labeled with the other dye. The labeled cDNA from the control and experimental cells is combined and hybridized to the glass microarray slide (Figure 6.1. D). The gene expression for the control and mutant strains are detected using a confocal laser scanner that scans for each cytofloures separately, producing a TIFF image for both experimental and control (Figure 6.1. E). Figure 6.3. depicts two scans obtained for one chip. The image on the left is the Cy3 scan of the wild type and the image on the right is the Cy5 scan of the *erv25Δ*. The TIFF images contain valuable information about the expression of each gene. The TIFF files are used to produce data sets that will reveal the genomic expression levels.

Figure 6.1. Schematic representation of the preparation of DNA microarrays.

RNA must be isolated from both control and experimental cell lines (A). Poly-A RNA is obtained (B) for reverse transcription reactions to produce cDNA that is either labeled with Cy3- or Cy5-conjugated nucleotides (C). The cDNA is then hybridized to a glass microarray slide (D). Images are detected using a confocal scanner (E).

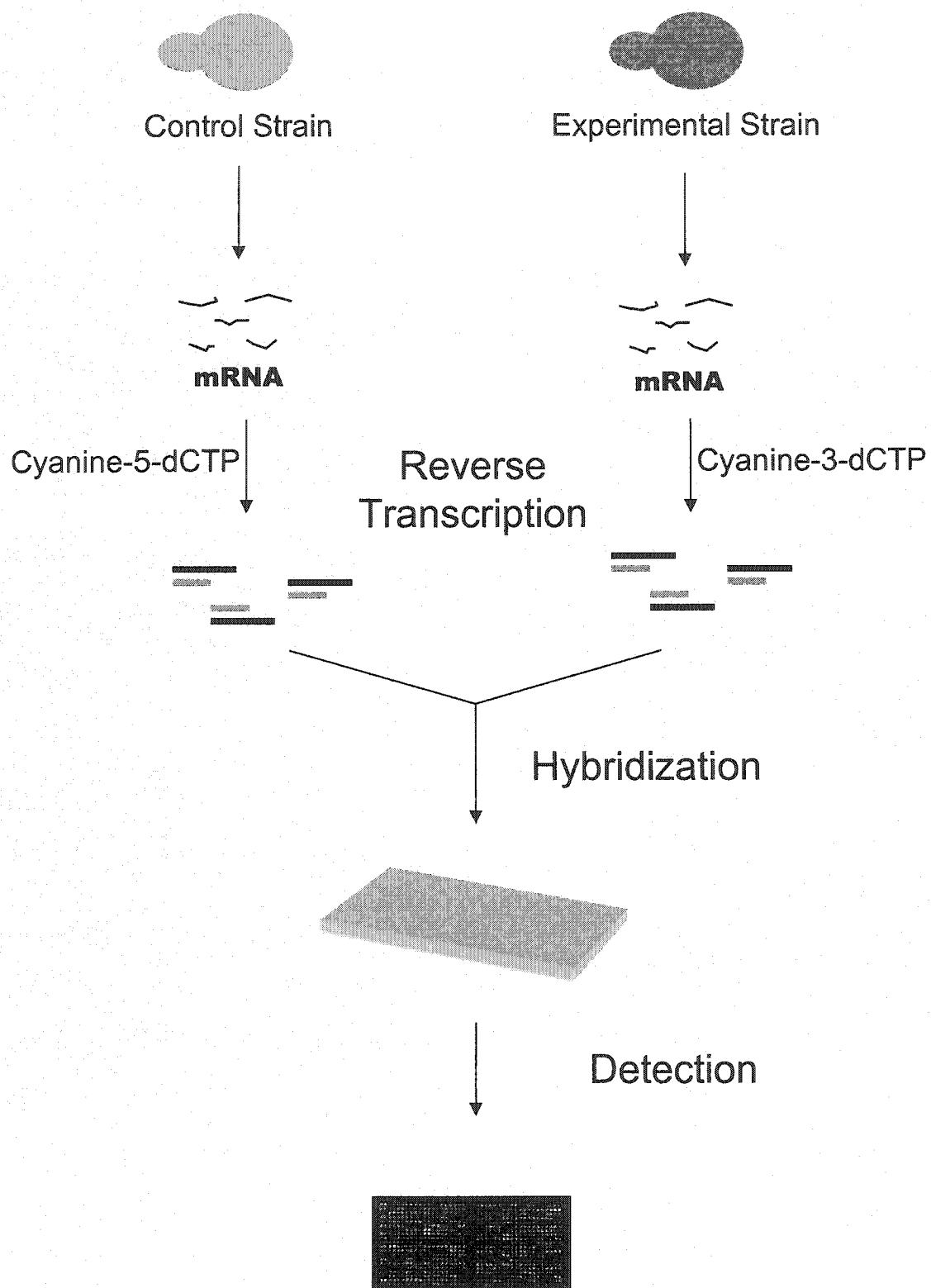


Figure 6.1.

Figure 6.2. RNA isolation for gene expression analysis. 1% agarose gel with 2 µg of total RNA isolated from control cells (lane 2) and GALL-ERV25 expressing cells (24h) (lane 3). 1 µg of polyA⁺ RNA that was isolated from the RNA of control cells and GALL-ERV25 expressing cells were electrophorized in lanes 3 and 4, respectively. Molecular weight standards were electrophorized in lane 1.

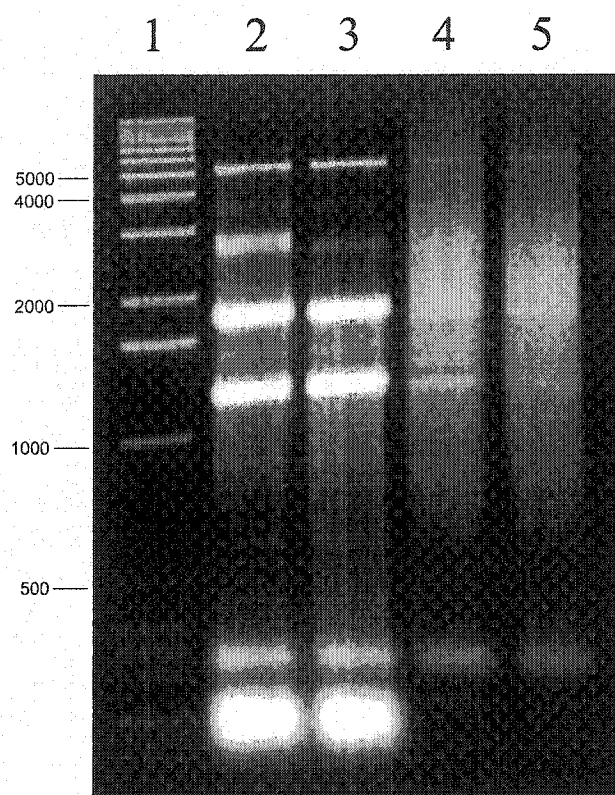
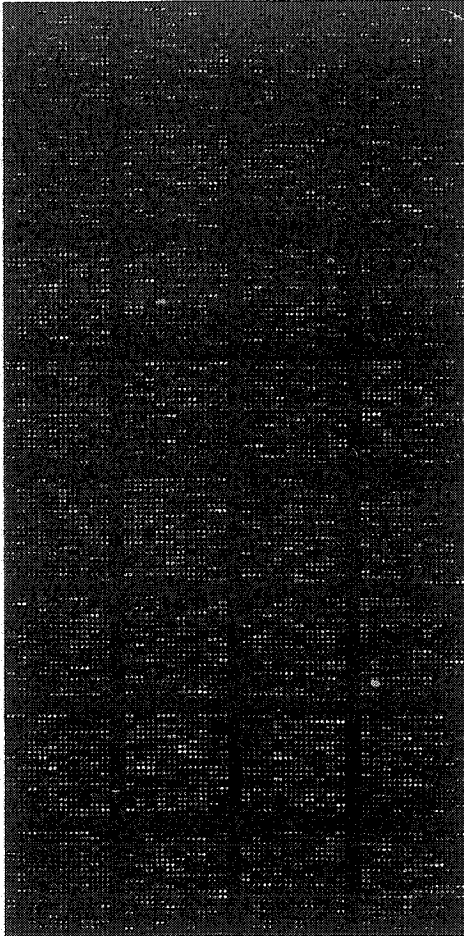


Figure 6.2.

Figure 6.3. Confocal laser image of a DNA microarray. DNA microarray was scanned with a GSI lumonics confocal scanner. TIFF files were obtained for both the cyanine-3 (Cy3) and cyanine-5 (Cy5) cytofluores.

Cy3 WT



Cy5 *erv25*Δ

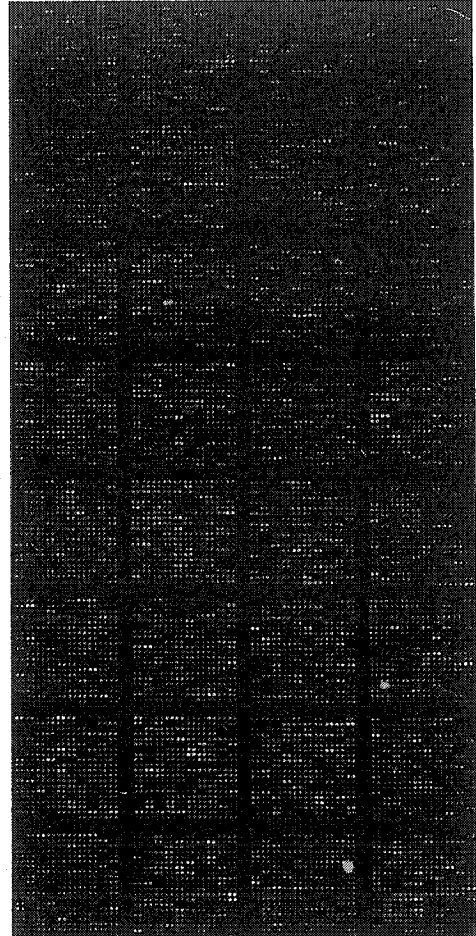


Figure 6.3

6.2.3. Quality Control and Statistical Analysis

In order to achieve high quality and reproducible data, each experimental condition was repeated many times, starting from cell culture. From the microarrays obtained from the various experiments, the best (most statistically significant) chips are selected, with a minimum of 3 chips for each condition (Table 6.1). Each experiment was subjected to an intense amount of quality control, beginning with the RNA, which is visualized on 1% agarose to check the purity (Figure 6.2). Once chips are produced for an experiment, they are scanned by the confocal laser (Figure 6.3). Data is obtained from the scanned images and analyzed (Figure 6.4). The original TIFF images (Figure 6.3) are imported into the QuantArray software program, which converts the Cy3 image to green and the Cy5 image to red (Figure 6.5). The differences in gene expression are visualized by overlapping the two images. Figure 6.5. shows the wild type (Cy3) expression pattern in green and the *erv25Δ* (Cy5) expression pattern in red. When the two images are overlapped, a yellow spot denotes the same level of expression of that particular gene in both samples. A red spot indicates a greater amount of expression in the *erv25Δ* (Cy5 labeled) sample as compared to the wild type (Cy3 labeled) sample, while a green spot would indicate a greater expression of that particular gene in the wild type (Cy3) sample. Figure 6.6. is a close up of the top left subarray of the overlapped image of a microarray for the 24h time point of ERV25 over expression (control is green, experimental is red). The arrows indicate the spots that represent the ERV25 gene (in duplicate). The red color indicates that the expression of this gene is greater in the ERV25 overexpressor than in the control, as expected.

The QuantArray program also provides the medium for visual quality control where erroneous spots can be eliminated. The program analyses each pixel of the scanned TIFF file and assigns numerical values to each spot, including background levels. A spreadsheet with values assigned to each spot is produced.

This data is imported into an Excel spreadsheet where the data is analyzed. The linear range of the data is first established by visually analyzing the distribution of the data. This is done by plotting the intensity of the experimental condition to the intensity of the control (Figure 6.7). The signal to noise ratio (the intensity of the signal minus half a STD must be greater than the intensity of the background plus half STD) is then calculated to eliminate non-significant spots. Background subtractions and experiment to reference ratios are performed. The ratios are denoted in Log2 values and normalization of the spots is effected by dividing by the median of the Log2 ratios of a particular subarray. The duplicate variability is then assessed and finally, an average of duplicate spots is produced. This analysis is repeated for each chip. The data is compiled and Student-t tests are performed to compare the variation in each condition. The data is then imported into a data analysis software program (GeneSpring, Silicon Genetics) and various graphical and cluster analyses are effected. The GeneSpring software program provides various tools and links to databases in order to examine the data to determine what genetic changes have occurred in the cells.

For this particular study, various internal controls were available, namely, the p24 proteins. The expression of these genes was observed in the deletion strains and through the over expression time course. The ERV25, EMP24, ERP5 and ERP4 mRNA are expressed at a moderate ectopic level and behaved as expected and in a statistically significant manner. However, due to the low expression of the other p24s (ERP1, ERP2, ERP3, and ERP6), they do not appear to behave in the manner that is expected. Specifically, they do not exhibit a dramatic decrease in the quadruple deletion (p24 Δ 4) or the complete deletion (p24 Δ 8) (Figure 6.8). In order to confirm that the genes were in fact deleted, the genomic DNA was isolated and PCRs were carried out on the deletion strains. As shown in Figure 6.9, the appropriate p24 genes were deleted from each strain.

Due to many factors, including incorporation of dyes, variations in RNA purity, slight differences in hybridization, amount of DNA spotted onto the slide,

there is an inherent variability in each microarray experiment. To test this inherent variability several experiments were carried out with wild type expression being compared to wild type expression. For these experiments wild type RNA was used for both Cy3 and Cy5 reverse transcription reactions, the cDNA was combined and then hybridized to a chip. Eleven chips were analyzed and the data is represented graphically in Figure 6.10. The majority of the genes (92% or 5834/6330) have a fold variation that is within the range of 0.5-2 fold variation (Figure 6.10). Those few genes that exhibit a higher variability did not reveal a significant change in expression in the other experimental conditions and are thus accounted for.

Table 6.1. Number of RNA preparations and DNA microarrays.

	RNA Preparations	Microarrays
WT	5	11
erv25 Δ	3	5
p24 Δ 4	3	5
p24 Δ 8	3	4
ERV25 12h	3	3
ERV25 24h	3	3
ERV25 36h	2	4

Figure 6.4. Schematic representation of data analysis. DNA microarrays are scanned with a GSI Lumonics scanner to obtain TIFF files (A). The TIFF files are imported to a QuantArray software program and file are represented in either green (Cy3) or red (Cy5) (B). Data obtained from the analysis produced by the QuantArray software is imported into a spreadsheet (C). Various statistical analyses are performed (D). Data is imported into the GeneSpring software program where further statistical analysis and data mining can occur (E).

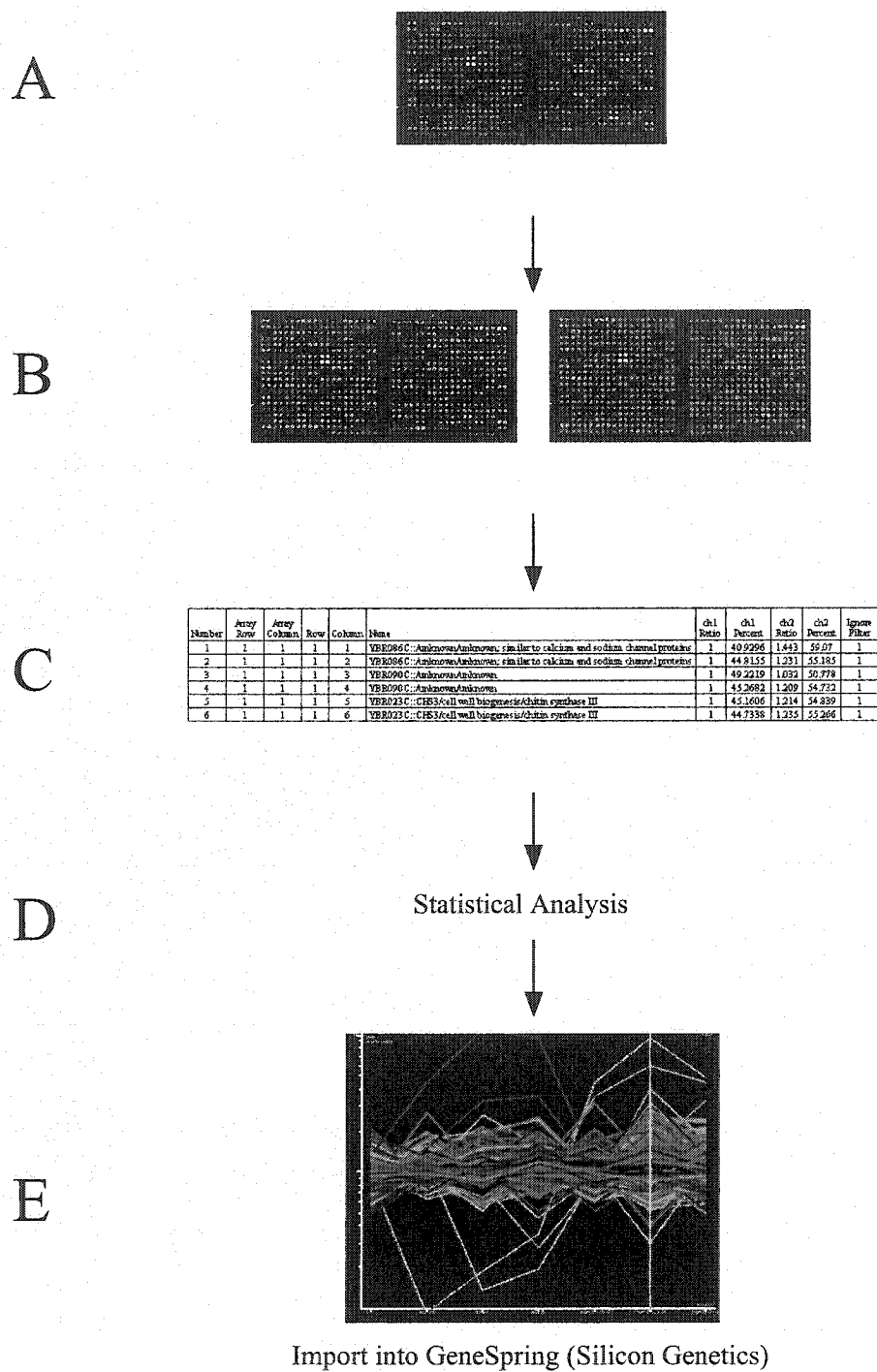


Figure 6.4.

Figure 6.5. QuantArray Image of DNA Microarrays. Images of microarray scans for the Cy3 (green) and Cy5 (red) are shown. The QuantArray software program is used to overlap the images to identify the differences in signal intensity between the control and experimental conditions. Genes that have the same intensity with respect two control and experimental are shown in yellow. Genes that are modulated appear in red (if up regulated in the experimental condition) or green (if down regulated in the experimental condition).

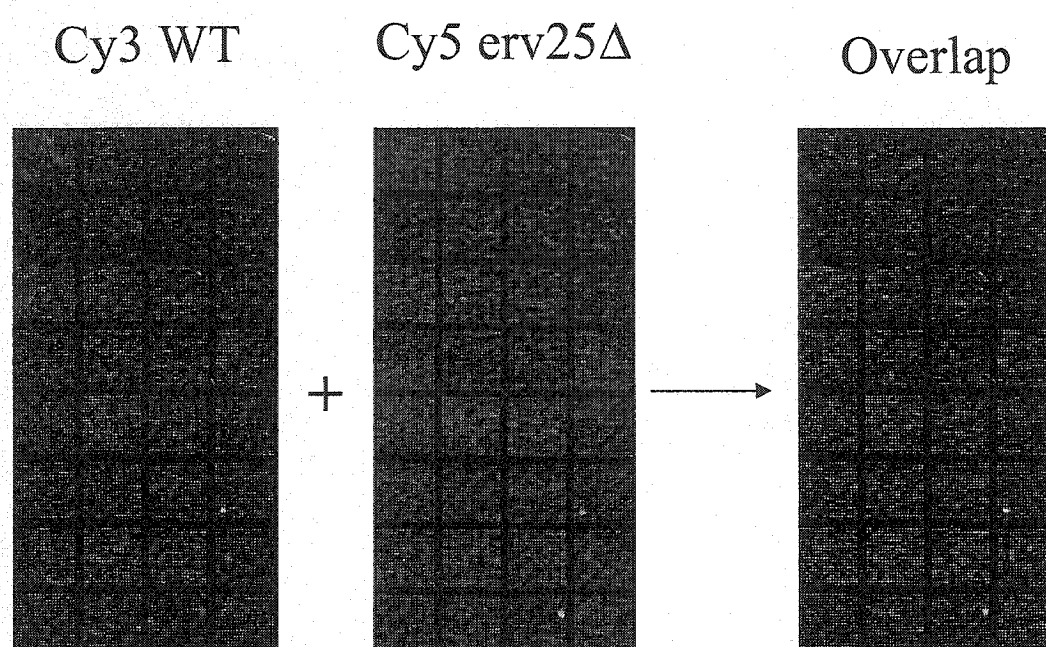


Figure 6.5.

Figure 6.6. Enlarged image of subarray. Image represents an enlarged view of the top left subarray of the microarray chip. The microarray was produced for the ERV25 overexpressor (24h time point). The yellow spots represent genes whose intensity is the same in both control and experimental conditions. The two red spots are the duplicate spots of the ERV25 gene. The spots are in red, indicating that the gene is up regulated in the ERV25 overexpressor (Cy5 or red) with respect to the control (Cy3 or green).

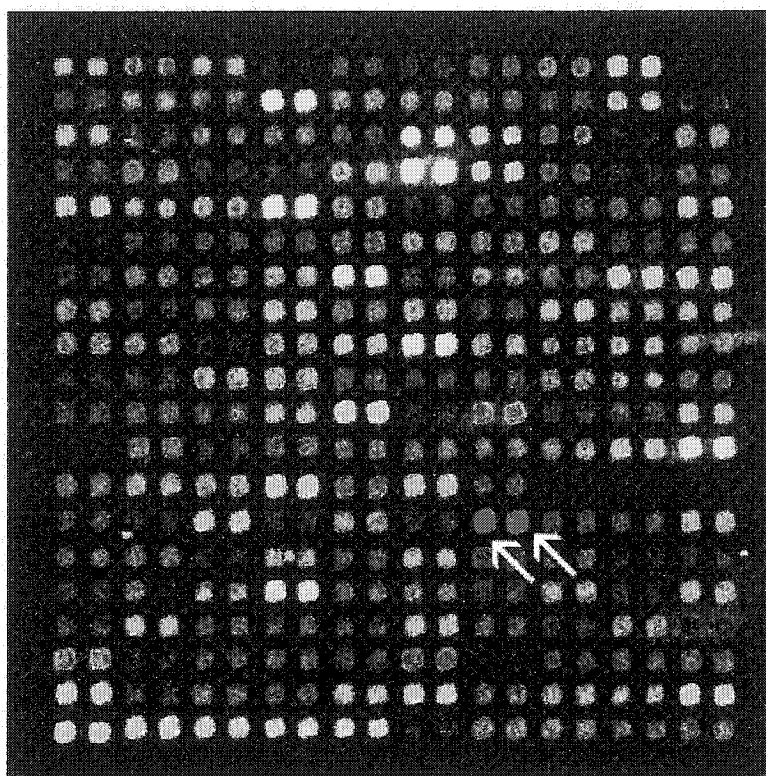


Figure 6.6.

Figure 6.7. Intensity Scatter Plot of ERV25 Overexpressor (36h). The intensity scatter plot demonstrates the amount of scatter of the genes that occurs at the various intensities. The lower the intensity value, the more inherent variability and scatter there is among the genes. This type of graph demonstrates the linear range of the data and indicates the cut off point for minimum and maximum intensity values for further statistical analysis. Each diamond (◆) represents an individual gene.

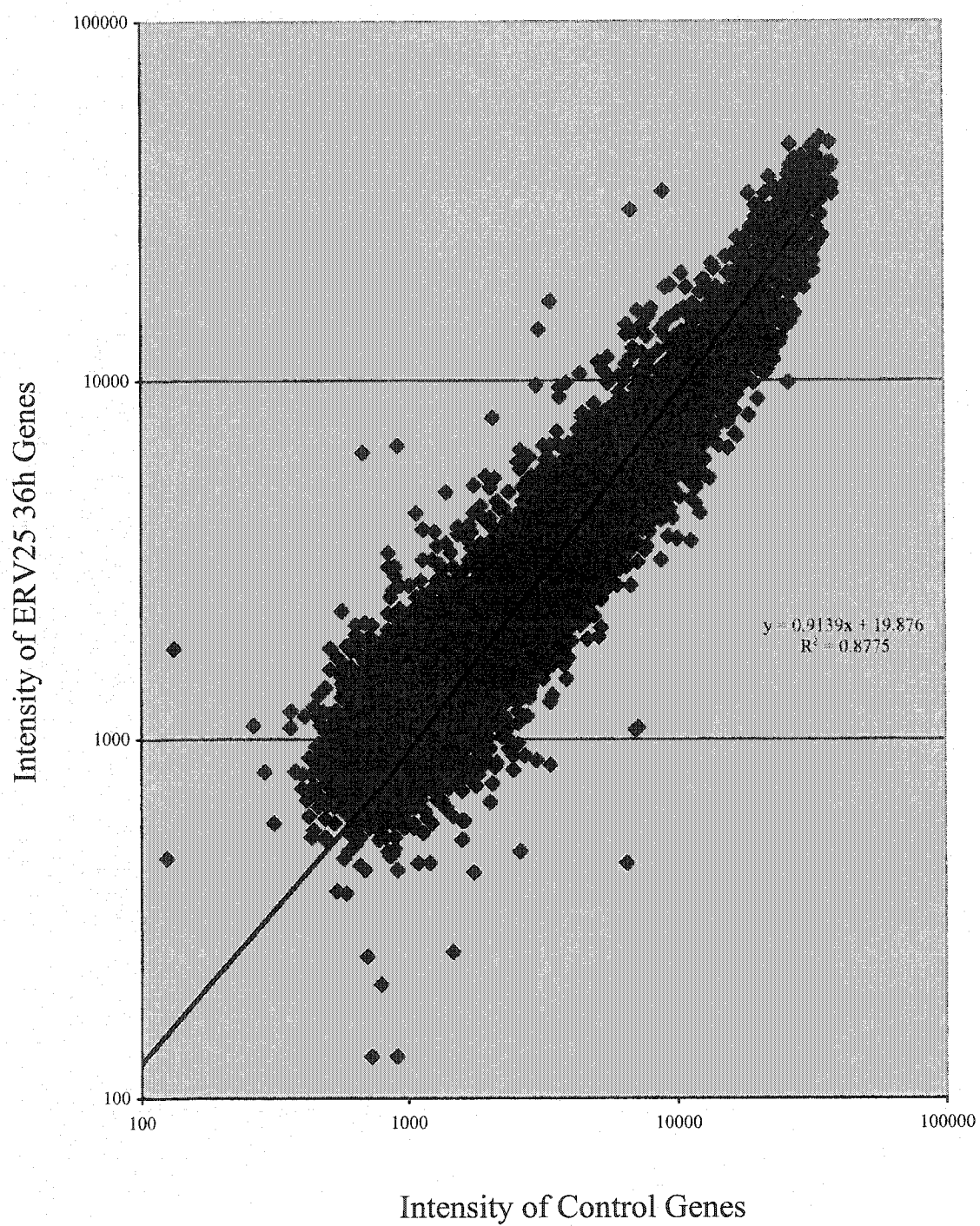


Figure 6.7.

Figure 6.8. Expression profiles of the p24 genes. The expression profiles for the p24 genes (ERV25, EMP24, ERP1-6) are shown for each experimental condition. The y-axis of the graphs represents the ratio of logarithm base 2 of the intensity of the p24 genes (experimental versus control). The x-axis is the intensity of gene expression in the control. Graphs were produced with the GeneSpring software program.

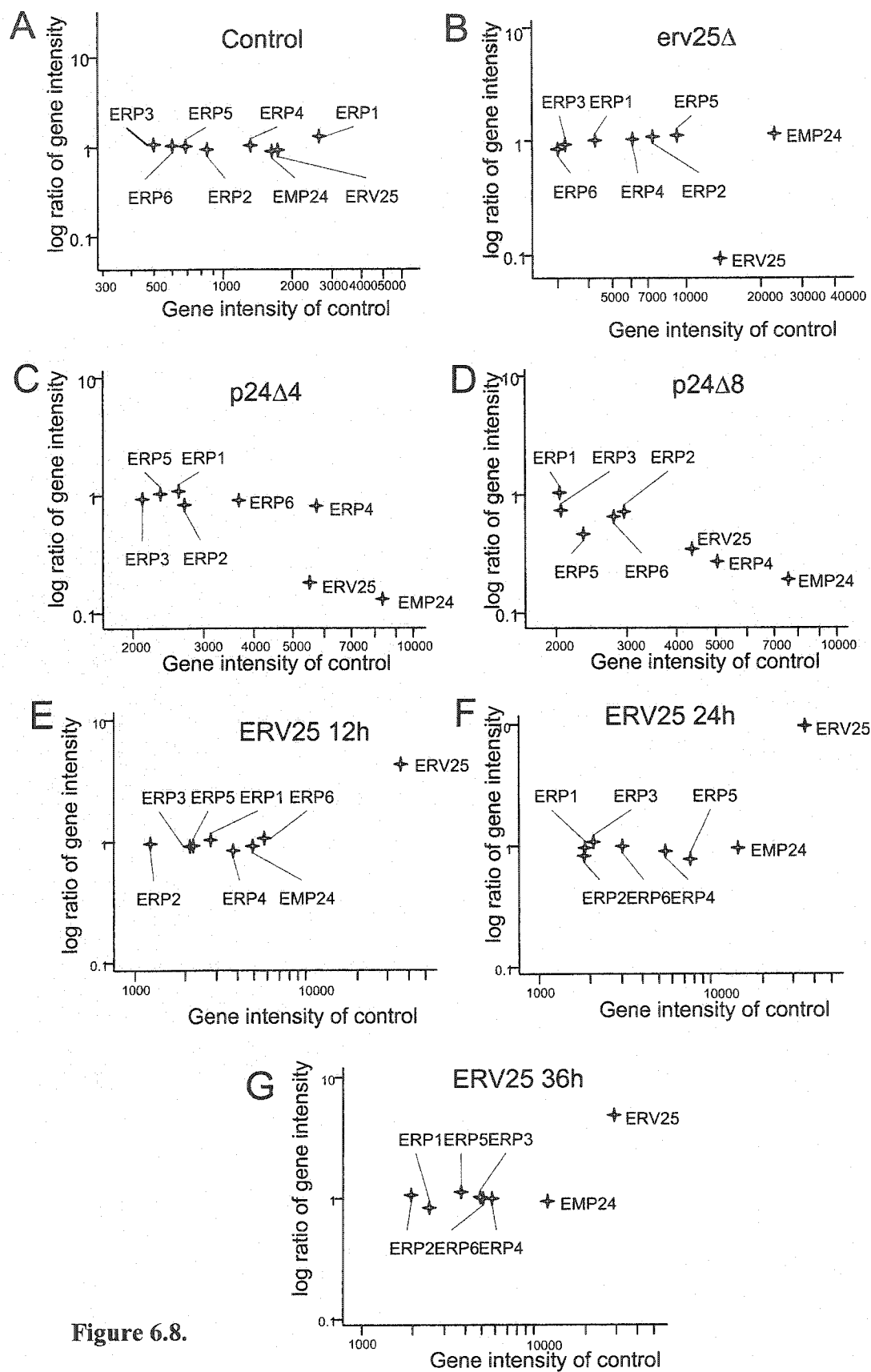


Figure 6.8.

Figure 6.9. PCR analysis of the p24 deletion strains. cDNA was extracted from wild-type (DHY9) and knockout (RSY1888, ARY90, DHY4) yeast cultures and subjected to PCR using primer pairs specific for the p24 proteins. Shown are 2% agarose gels stained with ethidium bromide. The single *erv25*Δ strain (B), the quadruple deletion strain (A) and the complete deletion strain (C) are shown. M, molecular weight marker (1kb ladder, Stratagene); WT, wild-type; KO, Knockout

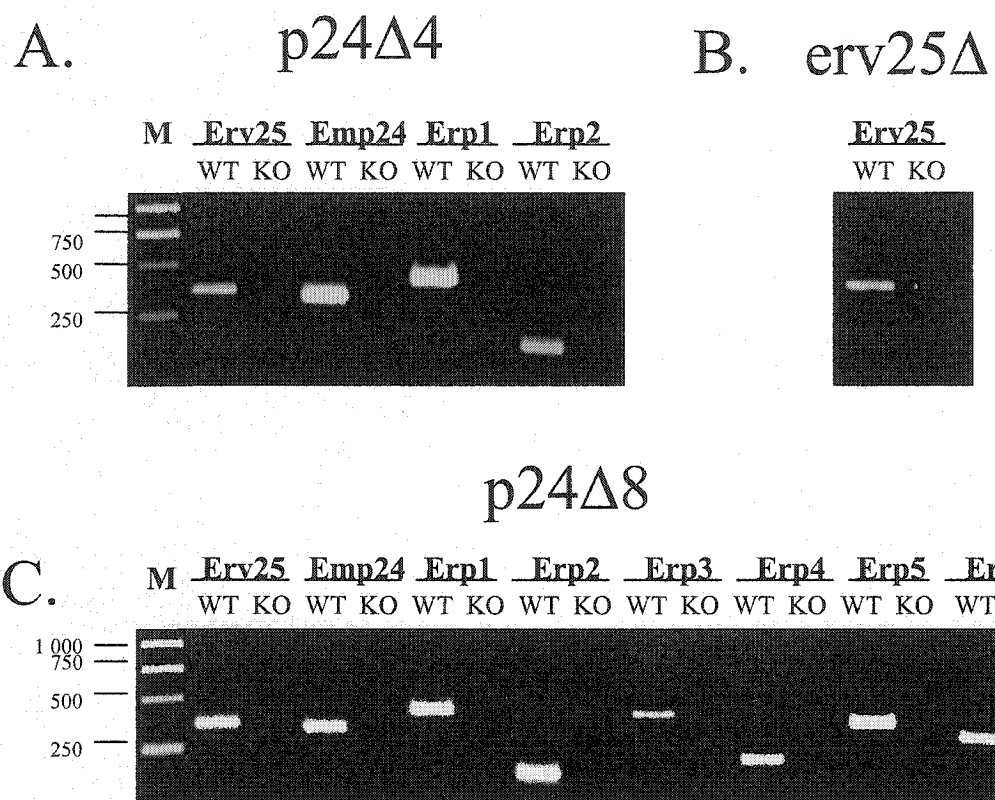


Figure 6.9.

Figure 6.10. Inherent variability in DNA microarrays. In order to test for the inherent variability in the DNA microarray system, control microarrays were produced comparing wild type cells with wild type cells. The y-axis indicates the normalized intensity in a Log2 scale. The x-axis indicates individual chip experiments. Each gene is depicted as a line. The color of the genes are referenced with respect to the first microarray experiment (15 nov 207997). Genes with increase intensity are in red while those that have a decreased intensity are in green. The majority of the genes (92%) fall within a 2-fold range of variation. The graph was produced using the GeneSpring software program.

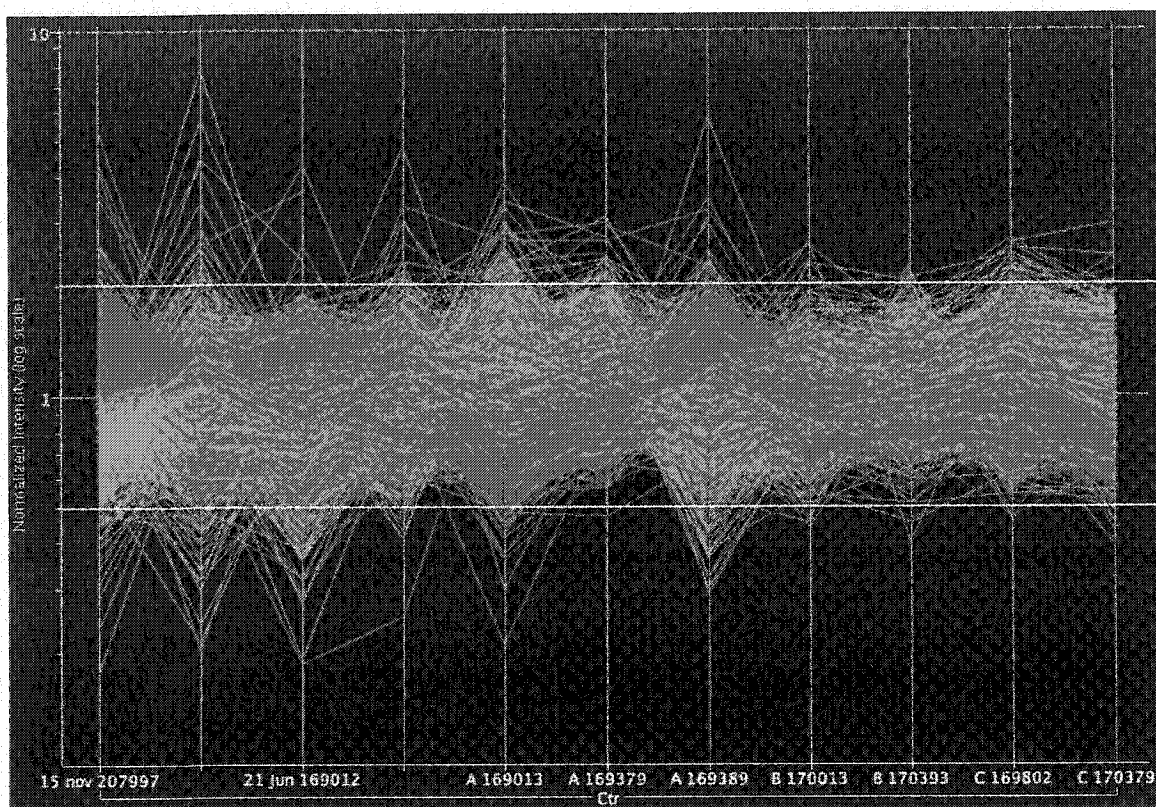


Figure 6.10.

6.2.4. Microarray Analysis

The variation in gene expression as a consequence of p24 gene deletion or over expression is summarized in Figure 6.11.A. This figure shows only those gene whose expression was modulated at least 1.5 fold above or below that of control cells with a P value of 0.05 or better. This corresponds to 160 genes out of ~6300 genes on the DNA arrays. The graph is color-coded with respect to the 24h time point of ERV25 over expression. Genes that are up regulated at the 24h time point are colored red while the genes that are down regulated at the 24h time point are in green (Figure 6.11.A). Although several genes were modulated by single or multiple p24 gene disruptions, the most dramatic changes were seen following ERV25 over expression.

It has been reported that the *erv25Δ* leads to a minor unfolded response. More specifically, a cluster of genes, including KAR2, consistently increased their expression whether p24 genes were deleted or ERV25 was over expressed. However, global comparison of all the genes previously shown to be affected by the UPR pathway (Travers *et al.*, 2000) or the environmental stress response pathway (Gasch *et al.*, 2001) revealed little overlap (data not shown). Surprisingly, a correlation was found between the over expression of ERV25 and the expression of activated form of the Rho GTPase (Figure 6.11.B) (Roberts *et al.*, 2000). Many of the genes that are common to both systems have no assigned function. We propose that they may be involved in a general stress response.

Hierarchical clustering analysis (Eisen *et al.*, 1998) identified groups of genes with similar changes in transcript abundance over the entire dataset (Figure 6.12.). This analysis also revealed the similarities between the quadruple and complete deletion strains as well as the effects of expressing ERV25 for 24 or 36 hours (Figure 6.12). Of the 160 modulated genes, 70 had putative transmembrane domains of which 29 had no known function. The number of predicted

transmembrane domains is indicated in the #TM column while the gene names are indicated on the right. The modulated genes are listed in Tables 6.2 and 6.3. The genes that appear in more than one experimental condition are indicated in red.

The modulated genes were subjected to further analysis to identify transcripts that encode proteins whose sequence is conserved in the proteome of other species. 59 of the 160 encoded proteins were found to be conserved in the yeast *Candida albicans* (C), the plant *Arabidopsis thaliana* (A), the nematode *Caenorhabditis elegans* (N), the fruit fly *Drosophila melanogaster* (F) or humans (H) (Figure 6.12 and Table 6.4.). Eight of these highly conserved proteins were of unknown function. A list of the gene names indicated in Figure 6.12. has been reproduced in Table 6.5. in larger print.

Figure 6.11. GeneSpring Analysis. (A) Modulation of gene expression by the p24 family. Expression profiles of 160 genes that show a significant change in transcript abundance in control experiments (Ctr), following the deletion of *erv25* alone (*erv25*Δ), the deletion of *erv25*, *emp24*, *erp1* and *erp2* (p24Δ4), the deletion of all 8 members of the p24 family (p24Δ8) or following the over expression of ERV25 for 12, 24 or 36 hours. Each gene is represented by a single line that is colored according the change in expression in the quadruple deletion strain (p24Δ4) Up regulated genes are colored red while down regulated genes are colored green. (B) Scatter plots showing the change in gene expression following the over expression of ERV25 after 24h and 36h compared to the expression of an activated form of Rho GTPase. There is significant correlation (P value 2×10^{-19}) between the genes that were induced by these treatments. Among the 31 genes induced by ERV25 and Rho1, 18 are part of the Environmental Stress Response while 3 are enzymes of the Glyoxylate Pathway.

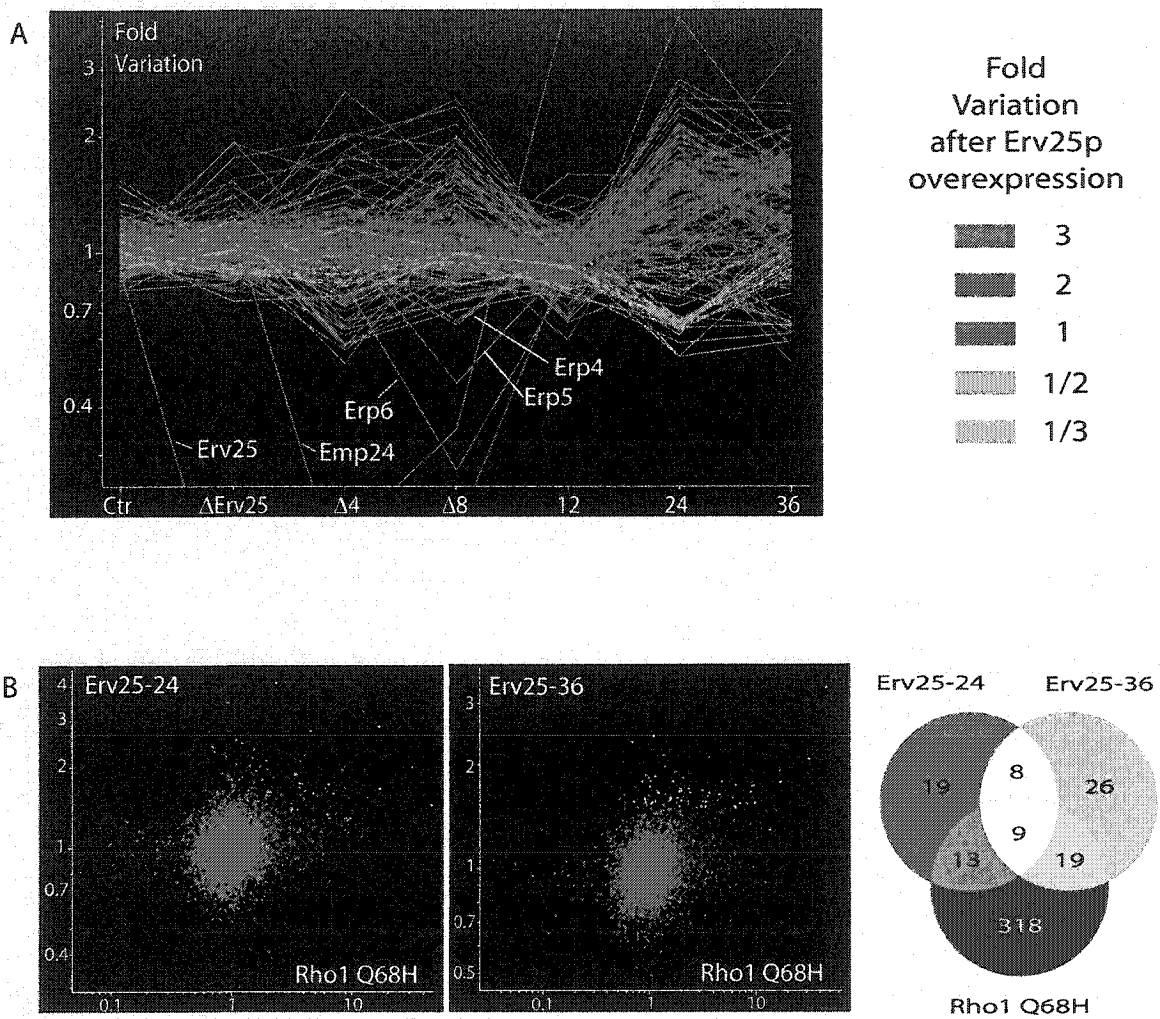


Figure 6.11.

Figure 6.12. Hierarchical clustering of 160 p24-modulated genes. The 6 columns on the left represent experimental conditions (defined in Figure 6.11.) with the changes in expression of each genes represented on a red-green color scale with up regulated genes colored red while down regulated genes are colored in green. The genes were clustered according to the similarity in their expression profile such that genes with a similar response over the entire data set are positioned in proximity to each other. The dendrogram on the y-axis represents the extent of profile similarities. In the x-axis, the gene expression profiles under the six experimental conditions were also clustered according to their similarity. The next column (column 6) indicates the number of transmembrane domains for each gene. Yellow indicates 1 transmembrane domain, light orange is 2 to 5, dark orange is 6 to 9 and red is 10-20. No color (white) indicates no transmembrane domain was predicted for that gene. The last 5 columns represents the conservation in amino acid sequence between the *S. cerevisiae* protein and its closest homolog in the fungi *Candida albicans* (C), the plant *Arabidopsis thaliana* (A), the nematode *Caenorhabditis elegans* (N), the fruit fly *Drosophila melanogaster* (F) and humans (H). Sequence homology, represented as the BlastP E-value, is color-coded on a blue-red scale. The position of genes discussed in the text is indicated. The gene names are indicated on the far the right. Table 6.5. is a reproduction of this list of gene names in a larger font.

Table 6.2. Genes Modulated in the Deletion Strains

	erv25Δ		p24Δ4		p24Δ8	
Categories	UP	DOWN	UP	DOWN	UP	DOWN
ER genes	KAR2 ERO1		KAR2 ERO1 MPD1 LHS1		KAR2 ERO1 MPD1 LHS1	
Metabolism - amino acid			LYS9 TRP1	ARG1	LYS9	
- carbohydrate					GLK1	
- glyoxylate cycle				CIT2		
- TCA cycle				ACO1		
Stress			HSP12		HSP12 TSL1	
Transport - phosphate transp. - zinc transport - p24s		ERV25		PHO84 ZRT1 EMP24 ERV25		EMP24 ERP4 ERP5 ERP6
Others	POR1		STF2	SHM2 IDH1 CHA1 DLD3 DIP5 CIT1	ALD4 PET56 YLR123C LAS21	ECM11
Cytosolic			YDL124W	YOL015W YOR050C	YDL124W YCL042W YHR087W YDR516C YJL207C YHL021C YDL023C	
Membrane	YML131W			YIL121W	YFL032W	
Membrane with signal peptide			SPI1 YMR040W			

Table 6.3. Genes Modulated in the ERV25 Overexpressors

	12h		24h		36h	
Categories	UP	DOWN	UP	DOWN	UP	DOWN
ER genes			KAR2 PDI1 HSP42		KAR2 ERO1 PDI1	
Protein degrad.					PRB1 RPN4	
Metabolism						
-gluconeogenesis			PCK1 FBP1		MDH2 CIT2	
-gluoxylate			ICL1 MDH2 CIT2			
-amino acid			CPA1			
-vitamin biosyn.			THI12		PCK1 ICL1 ACS1	SAM2
-carbohydrate					THI5	SOL1
					OYE2	INO1 CHO1
-lipid					PDE1	
-energy			THI11		CAT2 CRC1	
-carnitine						
Stress			AHP1		HSP26 HAC1 RCN1	
					CUP1-2 HOR7	
Transport	ERV25		ERV25		ERV25	
- vesicular					AUT7 PEP12	
- iron facilitator			FIT3			
- hexose transp.			HXT5 HXT2		HXT2	
- a.a. transp.				SAM3		
- myo-inositol				ITR1		
Others			GAT1 CUP9 BUR6	WTM2	BTN2 YPL088W	RPS9A
			PIR3 SPS100 STF2	TRP4 ADO1	RNA14 PCL5 PIR3	RPL18B
			CUP1-1 YPS3 YET1	PPT1 FAA3	CHS6 SED1	RPL2B
			COX7 YPT6 SGA1	PRO2		RPL9A
			PRE1	AAP1'		
				PCM1		
Cytosolic		YBR281C	YEL074W YMR181C	YGL218W	YDL124W	YOR111W
			YMR184W YHR097C	YFR044C	YHR087W YEL074W	YPL141C
			YMR295C YML039W	YIL137C	YMR181C YHR097C	DIG2
			YMR294W-A	YJL211C	YGR146C YJL144W	
			YNL157W YPR151C		YMR191W BDF2	
			YBL073W		YMR003W YDR070C	
					YGR043C YPR158W	
					YOR338W	
					YMR185W YJL103C	
					YBR281C YGL121C	
Membrane				YHR133C	YFL032W YML072C	YEL017W
					YBR004C FUN34	
Secretory			YLR194C YDR230W		YLR194C YOR383C	
			PRY2		PST1	
Membrane with signal peptide			YHR138C YBR005W	YBR224W	YBR005W YLR414C	
			YLR414C YDR366C	YBR220C	OM45	
			YNL114C YMR173W-A			

Table 6.4. Degree of Conservation of the Modulated Genes

Functional categories	Modulated under all conditions	Conserved Genes	No homology
ER genes			
- folding	KAR2, ERO1	KAR2, ERO1, MPD1, PDI1	
-translocation	RPN4	LHS1	
Metabolism			
- gluconeogenesis		FBP1	
- amino acid		LYS9, CPA1, SAM2	
- carbohydrate		GLK1	
- glyoxylate cycle	CIT2	CIT2, MDH2	
- TCA cycle		ACO1	
- nucleotide		ACS1	
- carnitine dependent		CRC1	
- lipid		INO1	
Stress			RCN1, HOR7
Transport			
- vesicular		AUT7	
- phosphate transp.		PHO84	
- myo-inositol		ITR1	
- hexose transporter		HXT2, HXT5	
- p24s		ERP5-6, EMP24,	
Others	STF2	POR1, SHM2, IDH1, CHA1, DLD3, CIT1, ALD4, LAS21, ADO1, PPT1, FAA3, PRO2, AAP1', PCM1, YPS3, YPT6, CUP9, PRE1, BUR6, YPL088W, RNA14, RPS9A, RPL18BRPL2B	YLR123C, SPS100, BTN2, SED1
Cytosolic	YDL124W, YHR087W,	YDL124W, YDR516C, YIL137C, YGR043C, BDF2, YBL049W, YPL141C, RTS2	YJL211C, YOR050C, YPR158W, YGL218W, YCL042W, YBL073W, YPR151C, YOL015W, YMR003W, YGL121C, YMR191W, YMR294W-A, YGR146C, YMR184W, YEL074W, YDR070C, YJL144W, YMR181C
Membrane	YFL032W	YML072C	YFL032W
Secretory Protein		PRY2	YDR230W, YLR194C, YOR383C
Membrane & signal peptide			YBR224W, YNL114C, YDR366C, SPI1,

Table 6.5. Gene list from Figure 6.12.

1 YNLO55C POR1	41 YGR146C	81 YMR294W-A	121 YDR354W TRP4
2 YOR374W ALD4	42 YPL088W	82 YHR096C HXT5	122 YJL105W ADO1
3 YJL063W LAS21	43 YMR191W	83 YHR053C CUP1-1	123 YOR323C PRO2
4 YPR158W	44 YDR055W PST1	84 YPR151C	124 YIL137C
5 YLR058C SHM2	45 YBR004C	85 YLR377C FBP1	125 YEL058W PCMI
6 YOL015W	46 YKL163W PIR3	86 YOR383C	126 YDR497C ITR1
7 YNL037C IDH1	47 YGL121C	87 YNL332 THI12	127 YFR044C
8 YPL265W DIP5	48 YOR036W PEP12	88 YLR262C YPT6	128 YBR224W
9 YNR001C CIT1	49 YDR070C	89 YMR295C	129 YJL211C
10 YLR304C AC01	50 YDR077W SED1	90 YER012W PRE1	130 YHR133C
11 YCR005C CIT2	51 YIL136W OM45	91 YBR005W	131 YHR047C AAP1'
12 YEL071W DLD3	52 YBR072W HSP26	92 YER159C BUR6	132 YGL218W
13 YML131W	53 YJL099W CHS6	93 YDR366C	133 YOR229W WTM2
14 KAR2	54 YGL248W PDE1	94 YHR071W PCL5	134 YIL009W FAA3
15 YDL124W	55 YDL020C RPN4	95 YOR100C CRC1	135 YGR123C PPT1
16 ERO1	56 YEL060C PRB1	96 YOR303W CPA1	136 YEL017W
17 YHR087W	57 YHR179W OYE2	97 YMR256C COX7	137 YBR220C
18 YMR040W	58 YGR043C	98 YLR109W AHP1	138 YPL081W RPS9A
19 YHL021C RPS27B	59 YBL078C AUT7	99 YALO54C ACS1	139 YER026C CHO1
20 PDI1	60 YOR338W	100 YJR156C THI11	140 YIL018W RPL2B
21 YFL021W GAT1	61 YML072C	101 YPL177C CUP9	141 YNL301C RPL18B
22 YFL014W HSP12	62 YMR003W	102 YKLO65C YET1	142 YJL153C INO1
23 YGR008C STF2	63 YMR061W RNA1	103 YMR184W	143 YDR502C SAM2
24 YER150W SPI1	64 YKL159C RCN1	104 YMR173W-A	144 YNR034W SOL1
25 YFL032W	65 YMR185W	105 YBL073W	145 YPL141C
26 HAC1	66 YDL070W BDF2	106 YNL114C	146 YOR077W RTS2
27 YJL103C	67 YDL037C	107 YHR139C SPS100	147 YGL147C RPL9A
28 YNR002C FUN34	68 YBL049W	108 ERV25	148 YOR111W
29 YDR171W HSP42	69 YKR097W PCK1	109 YML123C PHO84	149 MPD1
30 YMR251W-A HOF	70 YML039W	110 YIL121W	150 LHS1
31 YGR142W BTN2	71 YER065C ICL1	111 YOL058W ARG1	151 LYS9
32 YJL144W	72 YMR011W HXT2	112 EMP24	152 YCL042W
33 YML042W CAT2	73 YHR138C	113 YOR050C	153 YDR516C
34 YHR055C CUP1-2	74 YDR230W	114 YCL064C CHA1	154 YCL040W GLK1
35 YBR281C	75 YKR013W PRY2	115 YGL255W ZRT1	155 YDL023C
36 YEL074W	76 YLR194C	116 YDR446W ECM1	156 YML100W TSL1
37 YMR181C	77 YNL157W	117 ERP3	157 YOR201C PET56
38 YFL058W THI5	78 YOL126C MDH2	118 ERP4	158 YLR123C
39 YLR121C YPS3	79 YHR97C	119 ERP5	159 YJL207C
40 YLR414C	80 YIL099W SGA1	120 YPL274W SAM3	160 YDR007W TRP1

6.2.5. Gene Deletion Analysis

Seven genes were up regulated in at least two of the three deletion strains (Table 6.2.). Four of these genes are involved in protein folding (*KAR2*, *ERO1*, *MPD1*, and *LHS1*). Kar2p (BiP) is an ER chaperone. Lhs1p (luminal Hsp seventy) is also an ER chaperone and shares 24% amino acid identity with KAR2 (Baxter *et al.*, 1996; Hamilton *et al.*, 1999). In fact, Lhs1p appears to have overlapping functions with Kar2p (Craven *et al.*, 1996; Baxter *et al.*, 1996) as both proteins interact with each other and have been implicated in increasing the efficiency of protein translocation across the ER membrane (Craven *et al.*, 1996; Baxter *et al.*, 1996; Tyson and Stirling, 2000; Uetz *et al.*, 2000). Mpd1p is a protein disulfide isomerase (Tachikawa *et al.*, 1995; Norgaard *et al.*, 2001). The *MPD1* gene, although nonessential, can itself complement the essential phenotype of *PDII*. Ero1p is the oxidase of Pdi1p. The *KAR2* and *ERO1* transcripts were both consistently more abundant in all three of the deletion strains. Belden and Barlowe have previously documented that the *erv25* deletion leads to a partial unfolded protein response with an increase in secretion of Kar2p (Belden and Barlowe, 2001b). This study indicates that only a very small subset of UPR-induced genes changes due to a deletion of p24 genes (Table 6.2).

LYS9, *HSP12* and *YDL124W* had increased transcript levels in the quadruple (p24 Δ 4) and complete (p24 Δ 8) deletion strains. Lys9p is involved in lysine biosynthesis. The increase in expression of this gene may be due to an activation of the GCN pathway (Harding *et al.*, 2002). *HSP12* encodes one of the two major small heat shock proteins. Its expression is affected by stresses such as heat shock, entry into stationary phase, high levels of salt (osmostress), oxidative stress, high concentrations of alcohol, and glucose depletion (Praekelt *et al.*, 1990; Varela *et al.*, 1992; Varela *et al.*, 1995; de Groot *et al.*, 2000). The *YDL124W* gene encodes a protein predicted to be cytosolic.

The remaining gene products listed in Table 6.2. were genes seen in only one of the knockout conditions, with a preponderance of novel genes modulated in the complete (p24 Δ 8) deletion. Figures 6.13 to 6.15 indicate the predicted subcellular location of the modulated genes.

6.2.6. Over expression of *ERV25*

By gene cluster analysis (Figure 6.11.A; Table 6.3), 125 genes were shown to be modulated in response to *ERV25* over expression at 24h and 36h with little change seen at 12h. The gene analysis has initially focused on twelve genes whose expression varied at both the 24h and 36h time points of *ERV25* over expression. Six of these genes encode proteins of known functions, while the other six have no identified functional role.

Similar to the deletion strains, *KAR2* was consistently up regulated in the *ERV25* overexpressor. A protein disulfide isomerase was also up regulated in the overexpressors. However, rather than *MPD1*, it was *PDH1*. Like the p24 gene deletions, a mild unfolded protein response was likely a consequence the change in expression of the p24 gene. Two genes required for gluconeogenesis were consistently up regulated, *PCK1* and *ICL1*. *PCK1* is involved in the rate limiting enzyme in gluconeogenesis; *ICL1* is an isocitrate lyase. *MDH2* (malate dehydrogenase), like *ICL1* functions in the glyoxylate cycle. These genes are likely linked to the GCN pathway (Scheuner *et al.*, 2001). *PIR3* is a member of the *HSP150* family and may be related to a stress response to the increase in *ERV25* expression (Toh-e *et al.*, 1993).

By far the greatest number of genes whose expression changed consequent to *ERV25* over expression were 54 genes of unknown function. Of these, only 6 were modulated at both 24 and 36h following *ERV25* over expression. Three genes were predicted to encode cytosolic proteins. A single soluble protein of the secretory pathway, *YLR194C*, was modulated by *ERV25* over expression. The

predicted gene product has a cleaved signal sequence but no ER localization sequence. Two gene products whose expression increased were integral membrane proteins. *YBR005W*, a predicted type II transmembrane protein and *YLR414C*, with a cleaved N-terminal signal sequence and 3 predicted transmembrane domains. The remaining genes in Table 6.3, whose expression changed significantly in either the 24h or 36h experiment, did not reveal any mechanistic insight into the effects of the increase in expression of ERV25. Figure 6.16 and Figure 6.17 describe the predicted subcellular location of the modulated genes for the 24h time point.

Figure 6.13. Diagram representing the genes modulated for the *erv25Δ* strain. Gene names in green represent down regulated genes, while those in red are up regulated.

erv25Δ

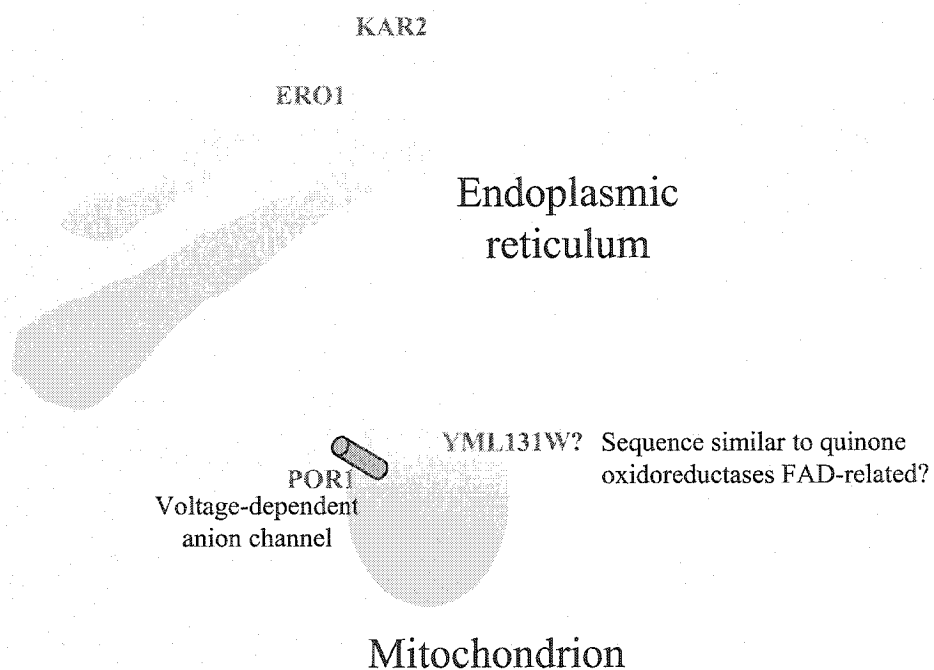


Figure 6.13.

Figure 6.14. Diagram representing the genes modulated for the p24 Δ 4 strain.
Gene names in green represent down regulated genes, while those in red are up regulated.

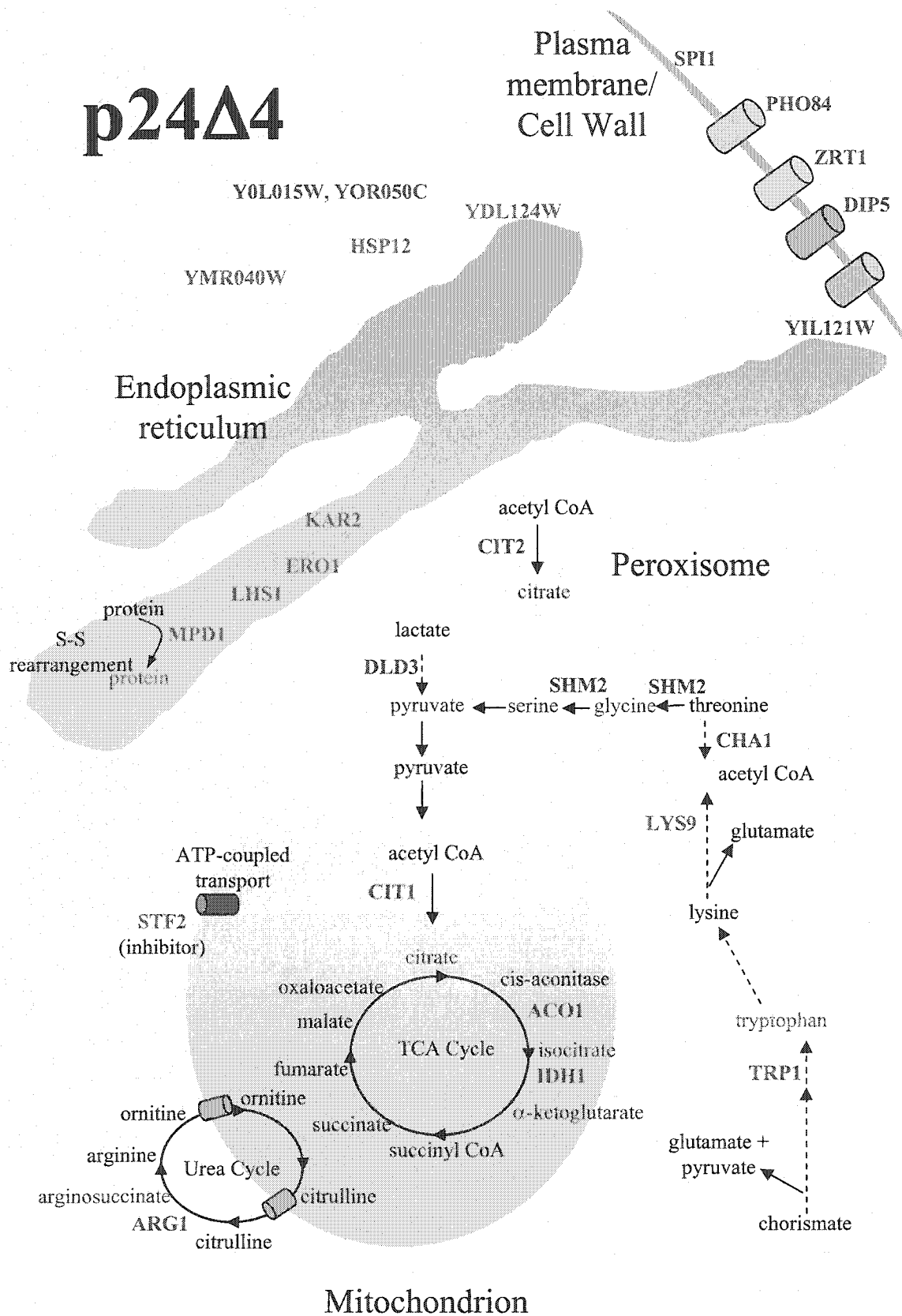


Figure 6.14.

Figure 6.15. Diagram representing the genes modulated for the p24Δ8 strain.
Gene names in green represent down regulated genes, while those in red are up regulated.

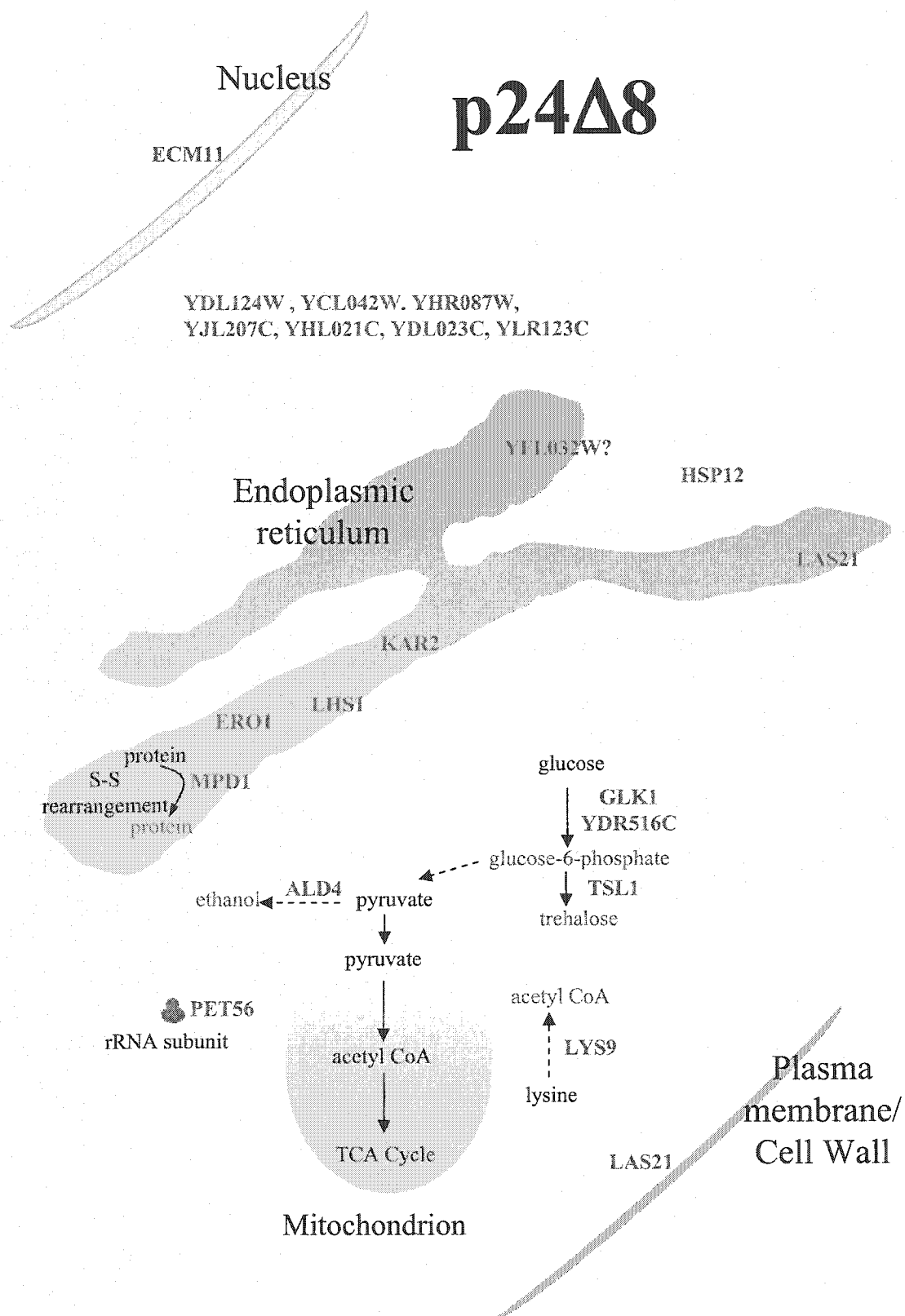


Figure 6.15.

Figure 6.16. Diagram representing the genes modulated for the ERV25 overexpressor at the 24h time point. Gene names in green represent down regulated genes, while those in red are up regulated.

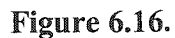
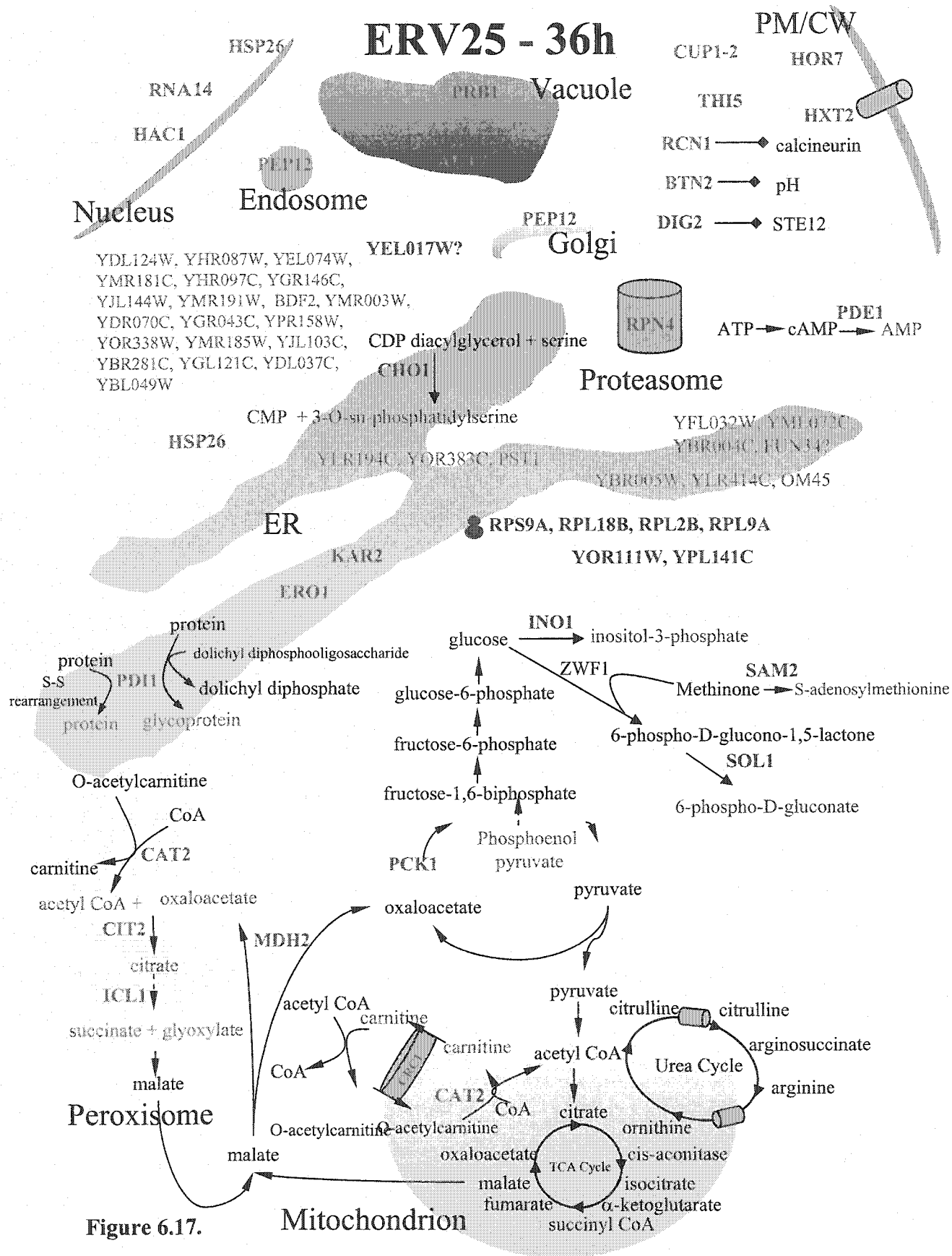


Figure 6.17. Diagram representing the genes modulated for the ERV25 overexpressor at the 24h time point. Gene names in green represent down regulated genes, while those in red are up regulated.



6.3. Discussion

The detailed analysis of the genetic expression patterns of p24 deletion strains and cells over expressing ERV25 revealed several genes encoding ER luminal proteins and an unexpectedly large number of unknown genes (42%).

The complete p24 deletion strain (p24 Δ 8) showed changes in the expression of some ER proteins thus confirming the mild UPR response observed in the *erv25* Δ (Belden and Barlowe, 2001b) (Figure 6.13). In addition, metabolic genes were affected possibly as an attempt to maintain homeostasis. Novel cytoplasmic genes (6) were also modulated which may be relevant to a machinery involved in cargo exit or cargo segregation in the absence of the p24s (Muniz *et al.*, 2001; Kaiser, 2000). It is noteworthy that *LAS21*, which encodes a protein involved in the attachment of GPI anchors, was up regulated, possibly due to the fact that the p24s are involved in the selective packaging of GPI linked proteins into COPII vesicles (Muniz *et al.*, 2000).

Several novel ER genes were found to have increased transcript levels after 24 hours of *ERV25* over expression. These were predicted to be located herein because of the presence of membrane spanning domains and/or cleaved signal peptide. The large number of novel cytosolic proteins (20) may again be a consequence of molecular machinery attempting to coordinate ER cargo exit in such a morphologically perturbed cell. The increase in plasma membrane proteins and metabolic enzymes may be to coordinate the entry of nutrients and metal ions to maintain homeostasis. The increase in expression of the proteasome subunit *PRE1* is likely in order to deal with the over expressed ERV25.

What is the significance of the phenotype of ERV25 over expression? Firstly, the expression of ERV25 leads to the generation of a toxic level of the Erv25p protein (Table 5.2.). Whether this is due to Erv25p itself or one of the

modulated genes remains to be demonstrated. Secondly, the phenotype shown here is similar to that seen when the same p24 family member (mammalian p23) was over expressed in mammalian cells (Rojo *et al.*, 2000). Therefore, both in mammalian cells and yeast, this p24 family member is a morphogenic gene.

The large number of novel genes (Figure 6.14.) whose expression is increased predicts that they are relevant to the phenotype and with particular emphasis on the ten conserved genes of unknown function found to be expressed in mammalian cells (Table 6.4).

Taken together, these results demonstrate an expansion of ER and VTCs consequent to ERV25 over expression. The morphogenic property of the p24s is predicted to be linked to the expression of the genes of unknown function whose expression was modulated consequent to ERV25 over expression. These genes are for the first time linked to the phenotype shown here.

Similar phenotypes have been observed for strains over expressing SEC12, the Sar1p guanyl-nucleotide exchange factor (GEF) (Nishikawa *et al.*, 1994). Over expression of ARF1 also showed a similar phenotype as well as when the essential genes for COPII (SEC24 and SEC31), COPI (SEC26 and RET1), the conserved oligomeric Golgi transport complex (COG2 and COG3), and the v-SNARE BOS1 were depleted (Deitz *et al.*, 2000; Kuirihara *et al.*, 2000; Duden *et al.*, 1994; Wuestehube *et al.*, 1996). Sec12p, Arf1p, Sec24p, Sec31p, Sec26p, Ret1p, Cog2p (Sec35p), Cog3p (Sec34p) and Bos1p (Sec32p) are all located and implicated in ER cargo exit as are the p24s (Kaiser, 2000). It will be noteworthy to compare the genes whose expression is altered by these above genes.

6.4. Materials and Methods

6.4.1. Strains, Plasmids and Growth Media

As described in Chapter 5 and Table 5.1.

6.4.2. Microarrays

Yeast ORF microarray slides were obtained from the Ontario Cancer Institute (Canada).

6.4.3. Cell Cultures for RNA Isolation

Knock outs and control strains were grown on YPD at 30°C. Single colonies were inoculated into 3 ml to 5 ml volumes of YPD media and grown overnight to stationary phase. Cells were then transferred to 50 ml volumes and grown overnight to an OD_{600nm} of approximately 1 A. Cells were then diluted to 0.1 A in 100 ml of YPD. Cells were harvested at an optical density (600 nm) of approximately 0.5 A.

Single colonies of the overexpressors and control cells were inoculated into 10 ml volumes of 2% glucose (-uracil) media and allowed to grow to stationary phase. Cells were then transferred to 300 ml of 2% glucose (-uracil) media and grown overnight until an OD_{600nm} of about 1A was reached. Cells were then centrifuged, washed with sterile water and transferred to 3% galactose (-uracil) for 6h, 12h, 24h or 48 hours.

For all experimental conditions a control culture was grown at the same time and under the same conditions.

6.4.4. RNA Isolation for DNA Microarrays

RNA isolation was essentially carried out as described by Koehrer and Domdey (1991). All nonsterile solutions were treated with 0.1% diethyl pyrocarbonate and autoclaved. Materials were sterilized as appropriate for RNA work. Cells were grown as above, harvested and frozen at -80°C . Cell pellets were suspended in 10 ml of 50 mM sodium acetate 10 mM EDTA pH 5 (SAB) and transferred to a tube with 1.2x the volume of hot SAB equilibrated phenol and 1/10 volume of 10% sodium dodecyl sulfate (SDS). Samples were vortexed 5x 30 seconds, returning the tube to a 65°C water bath between vortexing. Samples were cooled to room temperature on ice and centrifuged at 3700 rpm for 10 minutes. The lower organic phase was discarded and a fresh volume of equilibrated phenol was added. The phenol extraction was repeated. The upper aqueous phase was then transferred to a new tube with an equal volume of chloropane (50% phenol equilibrated with 50 mM sodium acetate 100 mM sodium chloride 1 mM EDTA pH 6 and 50% chloroform). Samples were vortexed for 2 minutes and centrifuged. The upper aqueous phase was transferred to a new tube with an equal volume of 24:1 chloroform-isoamyl alcohol. Samples were vortexed for 2 minutes and centrifuged. The upper aqueous phase was once again transferred to a new tube and 3x volume of 95% ethanol and 1/10 volume of 3M sodium acetate pH 5.3 were added. The samples were allowed to precipitate overnight at -20°C . The RNA was then collected by centrifugation at 4°C for 20-30 minutes. The pellet was washed with ice cold 70% ethanol, dried briefly and suspended in 0.3-1 mL of diethyl pyrocarbonate (DEPC) treated water. 3x volume of 95% ethanol and 1/10 volume of 3 M sodium acetate pH 5.3 were added and the samples were allowed to precipitate for 20 minutes at -80°C . The precipitate was centrifuged at 14,000g for 15 minutes. The pellet was washed with ice cold 70% ethanol, dried briefly and suspended in 100-200 μL of DEPC water. Quantitation of RNA was carried out using the RiboGreenTM RNA Quantitation Kit (Molecular Probes Inc.).

mRNA isolation was effected using the Micro-Fast Track™ 2.0 (Invitrogen Living Science, USA) isolation kit. Total RNA and mRNA samples were run on a 1% agarose gels to visualize the RNA (Figure 8). RNA from control and deletion or overexpressing strains was always isolated at the same time.

6.4.5. cDNA Synthesis and Hybridization of Microarrays

cDNA synthesis and generation of microarrays were essentially carried out as per the protocol provided by P. Jorgensen and T. Goh of the Ontario Cancer Institute (Canada). 2-3 µg of mRNA were combined on ice with 8 µl of 5x First Strand Buffer (Gibco Life Sciences), 1.5 µl of AncT mRNA primer (T20VN, 100 pmol/µl), 3 µl 20 mM dNTPs – dCTP, 1 µl 2 mM dCTP, 2 µl of either Cyanine-3 dCTP or Cyanine-5 dCTP (NEN, Perkin Elmer Life Sciences), 4 µl of 0.1 M DTT (Gibco) and 1 µl of *Arabidopsis thaliana* mRNA (2 ng/µl). The volume was made up to 40 µl with DEPC water. Reciprocal labeling was also done. cDNA was synthesized (in reciprocal) for both control and experimental conditions. The incubation mixes were incubated at 65°C for 5 minutes and then at 42°C for 5 minutes. 2 µl of SuperScript II (GIBCO) were added to each reaction and incubated for 2 hours at 42°C. The reaction was stopped by adding 5 µl of 50 mM EDTA pH 8.0, 2 µl of 10 N NaOH and incubating for 20 minutes at 65°C. 4 µl of 5 M acetic acid and one volume of isopropanol were added to the mixture. The cDNA was precipitated for 1 hour at –20°C. The cDNA was centrifuged for 30-60 minutes at 4°C at 13,000 rpm. The pellet was washed 2-3 times with very cold 70% ethanol. The pellet was then suspended in 3 µl of water.

Microarray slides were prehybridized at 37°C with 50 µl of 1:1:20 baker's yeast tRNA (10mg/mL)/ssDNA (10 mg/mL)/filtered DIG EASY HYB (Boehringer Mannheim, Germany) for at least 1 hour. Slides were washed in 0.1x SSC before the hybridization mixture was added. 3 µl of labeled cDNA from the deletion or over expression strains were combined with 3 µl of labeled cDNA

from control cells and 46 μ l of 1:1:20 tRNA/ssDNA/DIG EASY HIB. This mixture was applied to the slide and incubated for a minimum of 12 hours at 37°C. Slides were then washed 3 x 15 minutes in 0.1x SSC 0.1% SDS at 37°C followed by 3 x 0.1x SSC at room temperature and 70% ethanol. Slides were dried through centrifugation (8 minutes at 700 rpm).

6.4.6. Scanning of Microarray Slides and Analysis

The microarray slides were scanned with a ScanArray 5000 microarray biochip confocal scanner using the ScanArray software program (Perkin Elmer). TIFF images were quantified in QuantArray software version 2.0 (Perkin Elmer). The data that was obtained from this program was imported into an Excel spreadsheet program and computations and analyses were effected as described previously (Cowen *et al.*, 2002). Data was then imported in GeneSpring software (Silicon Genetics) for graphical and clustering analyses.

Discussion

Several years ago, the vesicular model neatly summarized protein transport through the secretory pathway (Rothman, 1994). This model described a system whereby all transport of cargo proteins occurred via small vesicular intermediates, namely, COPI and COPII vesicles. In an attempt to resolve some of the mechanisms of this system we attempted to study a group of abundant protein constituents of COPI and COPII vesicles, the p24 family of transmembrane proteins. In doing so, our work, coincident with the work of many of our colleagues, has led us to question the dogma that was the vesicular model (reviewed in Storrie and Nilsson, 2002).

The vesicular model has dominated the field of the secretory pathway for decades. However, many studies have put this model into question (Nilsson *et al.*, 1993; Dahan *et al.*, 1994; Lin *et al.*, 1999; Bonfanti *et al.*, 1998; Lanoix *et al.*, 1999; Martinez-Menarguez *et al.*, 2001). In fact, a paradigm shift has occurred and the maturation model has once again come to the forefront. The work in this thesis supports the cisternal maturation model, where membrane systems are dynamic and have the ability to be transformed. Our work does not support a model where organelles are stable, static entities and where protein transport occurs solely through small membrane bound vesicles. The objective of this thesis is to resolve some of the mechanisms of the secretory pathway through the analysis of p24 proteins.

The p24 proteins: from the ER to the Golgi and back

The p24s are distributed throughout the early secretory pathway, from the ER to the Golgi (Wada *et al.*, 1991; Rojo *et al.*, 1997; Dominguez *et al.*, 1998; Blum *et al.*, 1999; Gommel *et al.*, 1999; Fullekrüg *et al.*, 1999). The α or p25 subfamily is found mainly in the ER, the δ or p23 subfamily and γ or p26/p27

subfamily are found predominantly in the IC/CGN, and the β or p24 subfamily is found in the Golgi (Wada *et al.*, 1991; Blum *et al.*, 1999; Fullekrüg *et al.*, 1999; Emery *et al.*, 2000).

The Endoplasmic Reticulum

Although the p24 proteins have been shown to concentrate in the intermediate compartment/cis-Golgi network (Blum *et al.*, 1996; Dominguez *et al.*, 1998; Fullekrüg *et al.*, 1999) the presence of the p24s in the ER is significant. Chapter 1 of this thesis describes the association of the p24s with the ribosome. This is essentially the very beginning of the secretory pathway: where polypeptides are formed and enter the secretory pathway. Indeed, the first p24 to be identified was co-isolated with calnexin, TRAP α and TRAP β from an isolated ER fraction (Wada *et al.*, 1991). By studying the associations of calnexin and rp24 α 2 (gp25L) in isolated ER microsomes, we discovered that both proteins have an association with the ribosome. While calnexin appears to bind directly to the ribosome, the association of rp24 α 2 is abrogated by puromycin (Chevet *et al.*, 1999). This indicates that the association of rp24 α 2 with the ribosome is dependent on the presence of the nascent polypeptide chain. The dependence on the peptide chain further suggests that rp24 α 2 does not associate directly with the ribosome, but may in fact associate with the nascent polypeptide chain or some effector molecule. One could speculate that rp24 α 2 is a cargo sensor. Thus it is able to sense the presence of newly synthesized proteins and may do one of several things: (1) rp24 α 2 remains with the cargo and is involved in a sorting process; (2) rp24 α 2 remains with the cargo and is involved in moving the cargo to the ER exit sites; (3) rp24 α 2 dissociated from the ribosomal complex and begins to organize cargo exit sites; and (4) rp24 α 2 is involved in a signaling pathway to recruit machinery for cargo exit.

Although we have shown a clear link between ribosomes and at least one of the p24s, the majority of the data collected to date indicate that the p24 proteins have a functional role that is carried out somewhere between the ER cargo exit sites and the CGN (Sohn *et al.*, 1996; Dominguez *et al.*, 1998; Emery *et al.*, 2000). Indeed, four of the eight yeast p24 proteins (Emp24p, Erv25p, Erp1p and Erp2p) have been identified as abundant constituents of COPII-coated vesicles generated from an in vitro budding reaction (Schimmöller *et al.*, 1995; Belden and Barlowe, 1996; Otte *et al.*, 2001). In fact, Emp24p has been identified as a gene that negatively regulates COPII vesicle formation (Elrod-Erickson and Kaiser, 1996). It can thus be extrapolated that the p24 proteins must be concentrated at the ER exit sites, where COPII buds are forming. Thus the function of the p24s may very well begin in the endoplasmic reticulum, when ribosomes are threading through polypeptide chains, however their functional role extends far beyond the translocon.

Exit from the Endoplasmic Reticulum

Chapter 2 indicates the need for rp24 α 2 in membrane morphogenesis. We showed that low-density microsomes can be used to reconstitute a system of both rough endoplasmic reticulum and smooth endoplasmic reticulum domains. In fact, in addition to the morphological divisions, the protein constituents of this membrane system are sorted and concentrated into their respective compartments (Lavoie *et al.*, 1999; Roy *et al.*, 2000; Chapter 2). The smooth endoplasmic reticulum portion of the reconstituted membranes was identified as transitional endoplasmic reticulum. The addition of cytosol transforms the transitional endoplasmic reticulum into vesicular tubular clusters (VTCs) (Lavoie *et al.*, 1999). Our data has shown that antibodies to rp24 α 2 abrogate the formation of both transitional endoplasmic reticulum and vesicular tubular clusters (Lavoie *et al.*, 1999). Thus the p24s are clearly involved in membrane morphology. What is not clear is the mechanisms through which this is achieved. It is possible that the p24s are able to recruit factors (e.g., COPI, COPII or GAPs), which themselves

can create subdomains and alter the membrane topology (Presley *et al.*, 2002). The new membrane domains that are created by this machinery are the cargo exit sites that will produce COPII vesicles. These will then carry the cargo and the p24s to the intermediate compartment.

Indeed this data indicates that low-density microsomes can reconstitute rough endoplasmic reticulum and transitional endoplasmic reticulum, which can then be transformed into vesicular tubular clusters. This clearly shows the dynamic nature of these membranes and is inconsistent with a model for stable, static organelles.

The Intermediate Compartment

We have also clearly shown that the p24s are in the intermediate compartment. Chapter 3 details the immunoprecipitation of the p23 (delta) compartment. Antibodies raised against the p23 protein were conjugated to magnetic beads. These were then used to immunoprecipitate the p23 compartment from a Golgi enriched fraction. We isolated a smooth tubular membrane system that was occasionally seen to be associated with Golgi cisternae. This clearly indicates that p23 is highly enriched in the intermediate compartment and early Golgi membranes. Indeed we have also shown that VSV-G proteins are glycosylated in the p24 compartment (Lin *et al.*, 1999). In addition, we have shown that the cell free Golgi assay that had once proven the vesicular model (Balch *et al.*, 1984) was actually misinterpreted. We have indicated that this assay reconstitutes the retrograde cycling of Golgi enzymes to the intermediate compartment, where cargo proteins (VSV-G) become glycosylated. These data are also inconsistent with the vesicular model.

The Golgi Apparatus

Not only is the p24 compartment the site of glycosylation, it is also the site of cargo concentration (Chapter 4). We have shown that the p24s reach as far as the Golgi through the detection of p24s in a purified Golgi fraction (Bell *et al.*, 2001). The p24 proteins, along with Golgi resident proteins and other proteins involved in trafficking, make up the abundant portion of membrane proteins of the Golgi apparatus (Dominguez *et al.*, 1998; Bell *et al.*, 2001). This indicates that the p24s are a major protein of the Golgi apparatus. When p24 is over expressed in mammalian cells, it relocates to the endoplasmic reticulum and the morphology of the Golgi apparatus is disrupted (Rojo *et al.*, 2000; Emery *et al.*, 2000). Similarly, the heterozygous p23 deletion in mice, which has reduced expression levels of p23, also have morphological disruptions to the Golgi apparatus (Denzel *et al.*, 2000). Indeed, several p24s (alpha, beta and delta subfamilies) have been shown to interact with the Golgi matrix proteins (Barr *et al.*, 2001). This indicates a clear structural or morphological requirement for the p24s by the Golgi membrane system.

For the immunocytochemical analysis of the Golgi apparatus, we used antibodies raised against the rat p24 α 2 protein. We have found that rp24 α 2, β COP and ERD2 (the KDEL receptor) are all concentrated in the CGN (Chapter 4). We have also determined that cargo undergoes a two-step concentration. The first step occurs between the endoplasmic reticulum and the Golgi associated tubular compartment (or intermediate compartment), while the second concentration of cargo occurs between the Golgi associated tubular compartment and the Golgi apparatus (Chapter 4). This indicates that there is a selection for cargo in the endoplasmic reticulum. It also indicates that the intermediate compartment may cycle ER components backwards to concentrate cargo, which is again inconsistent with the vesicular model. Alternatively, COPI anterograde vesicles may select exclusively for cargo and deliver these cargo proteins to the

Golgi apparatus. However, we did not detect albumin in β COP decorated vesicular profiles found along the edges of the Golgi stack (Chapter 4).

Saccharomyces cerevisiae

From our data and those of our colleagues it is clear that the p24s are somehow involved in membrane morphogenesis and the COPI/COPII complexes. In order to further investigate their role we used the budding yeast *Saccharomyces cerevisiae* to study the morphology and gene expression profiles of strains whose p24 genes had been manipulated (whether through disruption or over expression) (Chapters 5 and 6).

Deletion of the p24 genes in yeast creates a kinetic defect in the transport of a subset of proteins (Schimmöller *et al.*, 1995; Belden and Barlowe, 1996; Marzioch *et al.*, 1999). Needless to say, the p24s are not essential genes and deletion only causes a minor defect in the cells. What is interesting about the deletion of some of the p24s is that they bypass the requirement for the COPII subunit Sec13p. This data implies that the p24s are involved in COPII protein transport. What is also relevant is that these cells have no major morphological phenotype. Thus there is no essential requirement for the p24s by the yeast membrane system nor for the protein transport machinery. This indicates that the p24s are not direct effectors of membrane morphogenesis or protein transport, but rather are involved in recruiting, modulating or regulating the proteins that are. Thus without the p24s, morphogenesis and protein transport will still occur (since the cell still contains the machinery for these processes), however, the membrane morphogenesis and protein transport do not unfold as smoothly, efficiently or with as much regulation as when the p24s are present.

This regulation may be effected at several levels. p24 β_1 (beta/p24 subfamily) is able to bind to ArfGAP1, the GTPase-activating protein for Arf1 (Lanoix *et al.*, 2001). In fact, binding of the p24s to ArfGAP1 mediates the sorting of the proteins into COPI-vesicles (Lanoix *et al.*, 2001). The p24s have also been shown to bind to Sec23p, the GAP for the Sar1p GTPase involved in COPII vesicle formation (Dominguez *et al.*, 1998). In addition, a delta (p23)

subfamily member has been shown to bind to and recruit ARF1-GDP to Golgi membranes (Gommel *et al.*, 2001). Thus one member of the p24 family is involved in recruiting ARF1-GDP, while the other recruits the ARF-GAP, creating a favorable location for coatamer to polymerize.

Over expression of the p24 in yeast, as in mammalian cells, causes the formation of large membrane structures that are continuous with the ER (Chapter 5, Rojo *et al.*, 2000). This is consistent with our model, where the p24s are able to recruit effectors that create membrane subdomains.

Microarray analysis of these yeast strains have revealed: (1) these strains are accessing general stress response pathway. (2) Several ER luminal proteins are being up regulated. (3) In the overexpressor, ER chaperones are being up regulated (UPR genes) while inositol response (IR) genes are being down regulated. Thus the cell is able to accommodate the need for UPR, while sensing the abundance of ER and thus down regulating the IR. (4) We have identified many unknown genes that are also modulated during other types of stress, and are thus general stress response genes. (5) We have identified many unknown genes that are not modulated during other types of stress and are thus postulated to be involved in the role of the p24s. YDL124W in particular was seen to be up regulated in many of the experimental conditions. Indeed, the genes of unknown function can now be linked to a response to ERV25 over expression.

Proposed Role of the p24 Proteins

The model we propose for the p24s is one where the p24 proteins are involved in the recruitment/regulation of factors essential for membrane morphogenesis and protein transport. Essentially, we predict that they are involved in the recruitment of the COPI and COPII protein complexes and/or the GAPs/GTPases associated with these complexes. Since the association/dissociation of coatamer has been shown to be rapid (Presley *et al.*, 2002), we do not believe that the p24s are COPI-receptors, instead we believe that the p24s are able to bind to the COP complexes, but that it is not a strong/tight association. In addition, we propose that the alpha subfamily of p24s is able to sense cargo as it enters the ER lumen.

We have shown that the p24 alpha subfamily is able to associate with the ribosome only when a nascent polypeptide chain is present (Chevet *et al.*, 1999; Chapter 1). The alpha subfamily has also been shown to be present in the endoplasmic reticulum (Wada *et al.*, 1991; Chevet *et al.*, 1999; Lavoie *et al.*, 1999; Emery *et al.*, 2000). In addition, the alpha subfamily has been detected in COPII vesicles and binds to both COPI and COPII subunits (Otte *et al.*, 2001; Dominguez *et al.*, 1998). The tails of the alpha subfamily contain a COPII binding motif (FF) and an ER retrieval/COPI binding motif (K(X)KXX). Taken together, these data indicate that the alpha subfamily detects cargo entry into the endoplasmic reticulum and is somehow involved in cargo exit through COPII vesicles. The alpha p24s along with the other subfamily members (beta, gamma and delta) are at the ER exit sites, possibly through p24 interactions or interaction with cargo. COPII is recruited via the FF motif on the cytoplasmic domains of the p24s. COPII vesicles are formed, travel to the intermediate compartment and fuse with the IC. The alpha subfamily members recruit COPI via their K(X)KXX motif. The alpha p24s return to the endoplasmic reticulum via COPI retrograde vesicles, taking some of the other subfamily members with them. Indeed, the alpha p24 family member was found to be the most abundant in isolated COPI

vesicle, followed by the gamma and delta subfamily members (the beta subfamily was not analyzed) (Lanoix *et al.*, 1999). Alternatively, it may be the beta family members that modulate the ArfGAP1 activity for sorting of the p24s into COPI vesicles (Lanoix *et al.*, 2001).

How cargo and the p24s progress from this point is unclear. Recycling of resident ER proteins and membranes through retrograde COPI vesicles would produce a concentration of cargo in the CGN. What is not clear is how the distinction between anterograde and retrograde COPI vesicles is made. Campbell and Schekman have shown that by altering the ratios of the machinery required for COPII vesicle formation (i.e., Sar1p, Sec13/Sec31p and Sec23p/Sec24p) you can achieve selective packaging into vesicles (Campbell and Schekman, 1997). Specifically, when Sar1p is titrated, the COPII vesicles have drastically different protein composition. For example, the cargo protein glycosylated pro- α -factor ($gp\alpha f$) is incorporated into COPII vesicles in a way that is almost independent of Sar1p levels. Conversely, for Emp24p and Bos1p to be incorporated into COPII vesicles they need a much greater amount of Sar1p. Bet1p and Sec22p are intermediary to $gp\alpha f$ and Emp24p/Bos1p (Campbell and Schekman, 1997). Thus the titration of transport factors, or alternatively the recruitment of factors, can greatly affect the protein constituents of a COPII vesicle. Reizman and colleagues have found that GPI linked proteins (Gas1p and Yps1p) are sorted into different vesicular carriers than those for other cargo proteins (Gap1p, $gp\alpha f$, ALP) (Muniz *et al.*, 2001). This group has also demonstrated that Gas1p interacts with p24s and that p24 proteins are required for the efficient packaging of Gas1p into vesicles (Muniz *et al.*, 2000).

It is interesting to note that the guanine nucleotide exchange factor (GEF) for the GTPase Sar1p is Sec12p (d'Enfert *et al.*, 1991a; Barlowe and Schekman, 1993). When SEC12 is over expressed it produces a membrane system that is very similar to that produced when p24s are over expressed (Nishikawa *et al.*, 1994;

Chapter 5). In addition, these membranes are enriched in Sar1p (d'Enfert *et al.*, 1991a; Campbell and Schekman, 1997; Chapter 5). Along a similar vein, depletion of Sec24p (a COPII subunit) also creates a membrane system reminiscent of the Sec12p and Erv25p overexpressors (Kurihara *et al.*, 2000; Nishikawa *et al.*, 1994; Chapter 5). In addition, an *arf1Δarf2Δ* strain expressing pGAL::ARF1 also exhibits the same ultrastructural changes in the ER (Deitz *et al.*, 2000). These data implicate the p24s, Sec12p, Sec24p and ARF in the mechanisms of membrane morphogenesis. In addition to the fact that there is a physical link between these proteins, they also appear to act along the same pathway since the membranes produced by these three systems are reminiscent of one another and distinct from other types of membrane proliferation (Kurihara *et al.*, 2000; Nishikawa *et al.*, 1994; Chapter 5; Wright *et al.*, 1988; Koning *et al.*, 1996). We have previously shown that COPI has a role in membrane morphogenesis and others have indicated a role for COPI in membrane domain formation (Lavoie *et al.*, 1999; Presley *et al.*, 20002). Indeed, COPII also seems to be involved in membrane morphogenesis. This creates a link between the p24s and proteins transport/membrane morphogenesis through the COPI and COPII complexes.

Conclusions

In summary, all of the different p24 family members have been detected in each of the compartments of the early secretory pathway (Sohn *et al.*, 1996; Dominguez *et al.*, 1998; Fullekrüg *et al.*, 1999; Chevet *et al.*, 1999; Lavoie *et al.*, 1999; Lin *et al.*, 1999; Emery *et al.*, 2000; Bell *et al.*, 2001; Otte *et al.*, 2001; Lanoix *et al.*, 2001; Chapters 1-4). This is not surprising since these proteins form complexes with one another and have been shown to cycle through the secretory pathway (Dominguez *et al.*, 1998; Fullekrüg *et al.*, 1999; Marzioch *et al.*, 1999; Emery *et al.*, 2000). There is, however, a clear concentration of the various p24 subfamilies in the different secretory compartments (Emery *et al.*, 2000). This indicates that the p24 complexes may be dynamic and alter their ratios as they progress through the pathway. This correlates with the signal sequences found on the cytoplasmic tails of the p24s. For example, the alpha subfamily members have a COPII binding motif (FF) and an ER retrieval/COPI binding motif (K(X)KXX). Indeed, a member of the alpha subfamily has been detected in COPII vesicles and was found to be located in the ER (Wada *et al.*, 1991; Otte *et al.*, 2001; Emery *et al.*, 2000). None of the other p24 subfamily members contain true ER retrieval motifs, which may be why these family members tend to be distributed in the intermediate compartment and Golgi apparatus (Dominguez *et al.*, 1998; Emery *et al.*, 2000; Lanoix *et al.*, 2001).

Thus the p24s may not be true COPI receptors, however, they may facilitate or regulate the binding of the COP complexes to the membrane through GAPs (Lanoix *et al.*, 2001). They may also be involved in the titration of factors that are involved in vesicle budding, thus having the capacity to regulate vesicle content. Indeed, different types of ER vesicles have been detected in yeast and a link between the p24s and sorting has been made (Muniz *et al.*, 2000; Muniz *et al.*, 2001). What is still unclear is if and how the p24s interact with cargo. Specifically, how the p24s are able to sense the nascent polypeptide chain in the ribosome, and how mutations in the p24s can allow a misfolded protein to escape

the ER (Chevet *et al.*, 1999; Wen and Greenwald, 1999). Further work is needed to identify the nature of the association of the p24 proteins with the ribosome and nascent peptide chain. In addition, several novel genes in yeast have now been linked to the phenotype of the increase in expression of ERV25. These genes may be part of a molecular machinery that may provide insight into the functional and mechanistic roles of the p24 proteins.

Original Contributions

This body of work characterizes the p24 proteins in yeast and mammalian systems. Cell culture, in vitro reconstitution, proteomics, quantitative immunoelectron microscopy and DNA microarray technology were used for this characterization. The following are original contribution to the existing scientific data:

1. The characterization of the morphology of canine pancreatic rough microsomes treated with KCl, puromycin , EDTA , as well as untreated microsomes. Specifically, the identification of the abundance of ribosome on the membranes under the various protocols.
2. Identified of a sorting of constituents of the secretory pathway in reconstituted membrane systems through the use of cryo-immunolabeling studies with antibodies to albumin, transferrin, rp24 α 2 , p58 , ribophorin, syntaxin 5 and calnexin.
3. The first isolation and morphological analysis of the p23 compartment.
4. Quantitation of the contaminating organelles by the point hit method in the WNG fraction. This characterization identified the purity of this Golgi fraction.
5. The first immunolocalization of the novel protein GPP34 in the Golgi fraction by cryoimmune electron microscopy.
6. The comprehensive immunocytochemical and quantitative analysis of albumin, β -COP, rp24 α 2, ERD2 in rat liver hepatocytes and in Golgi fractions revealing two cargo concentration steps and the relative distribution of the various constituents of the secretory pathway. This

study has also confirmed the depletion of albumin in COPI labeled structures.

7. We have performed the first morphological analysis of p24 overexpressing cells in yeast with a morphological phenotype.
8. We have performed the first immunolabeling studies on p24 overexpressing yeast. We have identified a concentration of Erv25p, an accumulation of Kar2p in BiP bodies, as well as the localization of Sar1p, Sec27p and prepro-alpha-factor in the proliferating ER of the ERV25 overexpressors.
9. We have performed the first microarray analysis of p24 mutants. We have identified a number of genes with no assigned function that are associated with the p24 proteins. Thereby indicating the first functional significance in a link to p24 induced membrane proliferation. We have also identified a number of genes that are involved in the secretory pathway that have been modulated by p24 overexpression or deletion.

References

- Adelman, M.R., G. Blobel, and D.D. Sabatini. 1973. An improved cell fractionation procedure for the preparation of rat liver membrane-bound ribosomes. *J Cell Biol.* 56:191-205.
- Albertinazzi, C., D. Gilardelli, S. Paris, R. Longhi, and I. de Curtis. 1998. Over expression of a neural-specific rho family GTPase, cRac1B, selectively induces enhanced neuritogenesis and neurite branching in primary neurons. *J Cell Biol.* 142:815-25.
- Amar-Costesec, A., H. Beaufay, M. Wibo, D. Thines-Sempoux, E. Feytmans, M. Robbi, and J. Berthet. 1974. Analytical study of microsomes and isolated subcellular membranes from rat liver. II. Preparation and composition of the microsomal fraction. *J Cell Biol.* 61:201-12.
- Anderson, R.G., L. Orci, M.S. Brown, L.M. Garcia-Segura, and J.L. Goldstein. 1983. Ultrastructural analysis of crystalloid endoplasmic reticulum in UT-1 cells and its disappearance in response to cholesterol. *J Cell Sci.* 63:1-20.
- Aridor, M., and W.E. Balch. 1996. Principles of elective transport. *Trends Cell Biol.* 6:315-320.
- Aridor, M., and W.E. Balch. 1999. Integration of endoplasmic reticulum signaling in health and disease. *Nat Med.* 5:745-51.
- Baker, L.A., and R.A. Gomez. 2000. Tmp21-I, a vesicular trafficking protein, is differentially expressed during induction of the ureter and metanephros. *J Urol.* 164:562-6.
- Balch, W.E., W.G. Dunphy, W.A. Braell, and J.E. Rothman. 1984. Reconstitution of the transport of protein between successive compartments of the Golgi measured by the coupled incorporation of N-acetylglucosamine. *Cell.* 39:405-16.
- Balch, W.E., J.M. McCaffery, H. Plutner, and M.G. Farquhar. 1994. Vesicular stomatitis virus glycoprotein is sorted and concentrated during export from the endoplasmic reticulum. *Cell.* 76:841-52.

- Ballou, L., L.M. Hernandez, E. Alvarado, and C.E. Ballou. 1990. Revision of the oligosaccharide structures of yeast carboxypeptidase Y. *Proc Natl Acad Sci U S A.* 87:3368-72.
- Bankaitis, V.A., J.R. Aitken, A.E. Cleves, and W. Dowhan. 1990. An essential role for a phospholipid transfer protein in yeast Golgi function. *Nature.* 347:561-2.
- Bannykh, S.I., and W.E. Balch. 1997. Membrane dynamics at the endoplasmic reticulum-Golgi interface. *J Cell Biol.* 138:1-4.
- Bannykh, S.I., T. Rowe, and W.E. Balch. 1996. The organization of endoplasmic reticulum export complexes. *J Cell Biol.* 135:19-35.
- Barlowe, C. 1998. COPII and selective export from the endoplasmic reticulum. *Biochim Biophys Acta.* 1404:67-76.
- Barlowe, C., L. Orci, T. Yeung, M. Hosobuchi, S. Hamamoto, N. Salama, M.F. Rexach, M. Ravazzola, M. Amherdt, and R. Schekman. 1994. COPII: a membrane coat formed by Sec proteins that drive vesicle budding from the endoplasmic reticulum. *Cell.* 77:895-907.
- Barlowe, C., C. d'Enfert, and R. Schekman. 1993. Purification and characterization of Sar1p, a small GTP-binding protein required for transport vesicle formation from the endoplasmic reticulum. *J. Biol. Chem.* 268, 873-879.
- Barlowe, C., and R. Schekman. 1993. SEC12 encodes a guanine-nucleotide-exchange factor essential for transport vesicle budding from the ER. *Nature.* 365:347-9.
- Barlowe, C., and R. Schekman. 1995. Expression, purification, and assay of Sec12p: a Sar1p-specific GDP dissociation stimulator. *Methods Enzymol.* 257:98-106.
- Baron, J., J.A. Redick, and F.P. Guengerich. 1982. Effects of 3-methylcholanthrene, beta-naphthoflavone, and phenobarbital on the 3-methylcholanthrene-inducible isozyme of cytochrome P-450 within centrilobular, midzonal, and periportal hepatocytes. *J Biol Chem.* 257:953-7.

- Barr, F.A., C. Preisinger, R. Kopajtich, and R. Korner. 2001. Golgi matrix proteins interact with p24 cargo receptors and aid their efficient retention in the Golgi apparatus. *J Cell Biol.* 155:885-91.
- Barz, W.P., and P. Walter. 1999. Two endoplasmic reticulum (ER) membrane proteins that facilitate ER-to-Golgi transport of glycosylphosphatidylinositol-anchored proteins. *Mol Biol Cell.* 10:1043-59.
- Basson, M.E., M. Thorsness, and J. Rine. 1986. *Saccharomyces cerevisiae* contains two functional genes encoding 3-hydroxy-3-methylglutaryl-coenzyme A reductase. *Proc Natl Acad Sci U S A.* 83:5563-7.
- Baudhuin, P., and J. Berthet. 1967. Electron microscopic examination of subcellular fractions. II. Quantitative analysis of the mitochondrial population isolated from rat liver. *J Cell Biol.* 35:631-48.
- Baudhuin, P., P. Evrard, and J. Berthet. 1967. Electron microscopic examination of subcellular fractions. I. The preparation of representative samples from suspensions of particles. *J Cell Biol.* 32:181-91.
- Baxter, B.K., P. James, T. Evans, and E.A. Craig. 1996. SSI1 encodes a novel Hsp70 of the *Saccharomyces cerevisiae* endoplasmic reticulum. *Mol Cell Biol.* 16:6444-56.
- Beams, H.W., and R.G. Kessel. 1968. The Golgi apparatus: structure and function. *Int Rev Cytol.* 23:209-76.
- Becker, B., B. Bolinger, and M. Melkonian. 1995. Anterograde transport of algal scales through the Golgi complex is not mediated by vesicles. *Trends Cell Biol.* 5: 305-307
- Becker, B., and M. Melkonian. 1996. The secretory pathway of protists: spatial and functional organization and evolution. *Microbiol Rev.* 60:697-721.
- Becker, F., L. Block-Alper, G. Nakamura, J. Harada, K.D. Wittrup, and D.I. Meyer. 1999. Expression of the 180-kD ribosome receptor induces membrane proliferation and increased secretory activity in yeast. *J Cell Biol.* 146:273-84.
- Bednarek, S.Y., M. Ravazzola, M. Hosobuchi, M. Amherdt, A. Perrelet, R.

- Schekman, and L. Orci. 1995. COPI- and COPII-coated vesicles bud directly from the endoplasmic reticulum in yeast. *Cell*. 83:1183-96.
- Belden, W.J., and C. Barlowe. 1996. Erv25p, a component of COPII-coated vesicles, forms a complex with Emp24p that is required for efficient endoplasmic reticulum to Golgi transport. *J Biol Chem*. 271:26939-46.
- Belden, W.J., and C. Barlowe. 2001a. Role of Erv29p in collecting soluble secretory proteins into ER-derived transport vesicles. *Science*. 294:1528-31.
- Belden, W.J., and C. Barlowe. 2001b. Deletion of yeast p24 genes activates the unfolded protein response. *Mol Biol Cell*. 12:957-69.
- Belden, W.J., and C. Barlowe. 2001c. Distinct Roles for the Cytoplasmic Tail Sequences of Emp24p and Erv25p in Transport between the Endoplasmic Reticulum and Golgi Complex. *J Biol Chem*. 276:43040-43048.
- Bell, A.W., M.A. Ward, W.P. Blackstock, H.N. Freeman, J.S. Choudhary, A.P. Lewis, D. Chotai, A. Fazel, J.N. Gushue, J. Paiement, S. Palcy, E. Chevet, M. Lafreniere-Roula, R. Solari, D.Y. Thomas, A. Rowley, and J.J. Bergeron. 2001. Proteomics characterization of abundant Golgi membrane proteins. *J Biol Chem*. 276:5152-65.
- Benachour, A., G. Sipos, I. Flury, F. Reggiori, E. Canivenc-Gansel, C. Vionnet, A. Conzelmann, and M. Benghezal. 1999. Deletion of GPI7, a yeast gene required for addition of a side chain to the glycosylphosphatidylinositol (GPI) core structure, affects GPI protein transport, remodeling, and cell wall integrity. *J Biol Chem*. 274:15251-61.
- Bergeron, J.J., J.H. Ehrenreich, P. Siekevitz, and G.E. Palade. 1973. Golgi fractions prepared from rat liver homogenates. II. Biochemical characterization. *J Cell Biol*. 59:73-88.
- Bingham, E.W., H.M. Farrell, Jr., and J.J. Basch. 1972. Phosphorylation of casein. Role of the golgi apparatus. *J Biol Chem*. 247:8193-4.
- Blobel, G., and B. Dobberstein. 1975. Transfer to proteins across membranes. II. Reconstitution of functional rough microsomes from heterologous components. *J Cell Biol*. 67:852-62.

- Block, M.R., B.S. Glick, C.A. Wilcox, F.T. Wieland, and J.E. Rothman. 1988. Purification of an N-ethylmaleimide-sensitive protein catalyzing vesicular transport. *Proc Natl Acad Sci U S A*. 85:7852-6.
- Blum, R., P. Feick, M. Puype, J. Vandekerckhove, R. Klengel, W. Nastainczyk, and I. Schulz. 1996. Tmp21 and p24A, two type I proteins enriched in pancreatic microsomal membranes, are members of a protein family involved in vesicular trafficking. *J Biol Chem*. 271:17183-9.
- Blum, R., F. Pfeiffer, P. Feick, W. Nastainczyk, B. Kohler, K.H. Schafer, and I. Schulz. 1999. Intracellular localization and in vivo trafficking of p24A and p23. *J Cell Sci*. 112 (Pt 4):537-48.
- Bolender, R.P., and E.R. Weibel. 1973. A morphometric study of the removal of phenobarbital-induced membranes from hepatocytes after cessation of threathment. *J Cell Biol*. 56:746-61.
- Bonfanti, L., A.A. Mironov, Jr., J.A. Martinez-Menarguez, O. Martella, A. Fusella, M. Baldassarre, R. Buccione, H.J. Geuze, A.A. Mironov, and A. Luini. 1998. Procollagen traverses the Golgi stack without leaving the lumen of cisternae: evidence for cisternal maturation. *Cell*. 95:993-1003.
- Braakman, I., J. Helenius, and A. Helenius. 1992. Manipulating disulfide bond formation and protein folding in the endoplasmic reticulum. *Embo J*. 11:1717-22.
- Bremser, M., W. Nickel, M. Schweikert, M. Ravazzola, M. Amherdt, C.A. Hughes, T.H. Sollner, J.E. Rothman, and F.T. Wieland. 1999. Coupling of coat assembly and vesicle budding to packaging of putative cargo receptors. *Cell*. 96:495-506.
- Brigance, W.T., C. Barlowe, and T.R. Graham. 2000. Organization of the yeast Golgi complex into at least four functionally distinct compartments. *Mol Biol Cell*. 11:171-82.
- Broadie, K., A. Prokop, H.J. Bellen, C.J. O'Kane, K.L. Schulze, and S.T. Sweeney. 1995. Syntaxin and synaptobrevin function downstream of vesicle docking in *Drosophila*. *Neuron*. 15:663-73.
- Brodsky, J.L., S. Hamamoto, D. Feldheim, R. and Schekman. 1993.

- Reconstitution of protein translocation from solubilized yeast membranes reveals topologically distinct roles for BiP and cytosolic Hsc70. *J. Cell Biol* 120, 95-102.
- Brown, R.M., Jr. 1969. Observations on the relationship of the golgi apparatus to wall formation in the marine chrysophycean alga *Pleurochrysis scherffellii* Pringsheim. *J Cell Biol.* 41:109-23.
- Bruni, C. and K.R. Porter. 1965. The fine structure of the parenchymal cell of the normal rat liver. *Am. J. Pathol.* XLVI:691-755.
- Campbell, J.L., and R. Schekman. 1997. Selective packaging of cargo molecules into endoplasmic reticulum-derived COPII vesicles. *Proc Natl Acad Sci U S A.* 94:837-42.
- Cannon, K.S., and A. Helenius. 1999. Trimming and readdition of glucose to N-linked oligosaccharides determines calnexin association of a substrate glycoprotein in living cells. *J Biol Chem.* 274:7537-44.
- Cao, X. and C. Barlowe
- . 2000. Asymmetric requirements for a Rab GTPase and SNARE proteins in fusion of COPII vesicles with acceptor membranes. *J. Cell Biol.* 149, 55-65
- Cao, X., N. Ballew, and C. Barlowe. 1998. Initial docking of ER-derived vesicles requires Usa1p and Ypt1p but is independent of SNARE proteins. *Embo J.* 17:2156-65.
- Chavrier, P., R.G. Parton, H.P. Hauri, K. Simons, and M. Zerial. 1990. Localization of low molecular weight GTP binding proteins to exocytic and endocytic compartments. *Cell.* 62:317-29.
- Chen, D.C., B.C. Yang, and T.T. Kuo. 1992. One-step transformation of yeast in stationary phase. *Curr Genet.* 21:83-4.
- Chen, Y.A., and R.H. Scheller. 2001. SNARE-mediated membrane fusion. *Nat Rev Mol Cell Biol.* 2:98-106.
- Chen, Y.G., A. Siddhanta, C.D. Austin, S.M. Hammond, T.C. Sung, M.A. Frohman, A.J. Morris, and D. Shields. 1997. Phospholipase D stimulates release of nascent secretory vesicles from the trans-Golgi network. *J Cell*

Biol. 138:495-504.

- Chevet, E., P.H. Cameron, M.F. Pelletier, D.Y. Thomas, and J.J. Bergeron. 2001. The endoplasmic reticulum: integration of protein folding, quality control, signaling and degradation. *Curr Opin Struct Biol.* 11:120-4.
- Chevet, E., H.N. Wong, D. Gerber, C. Cochet, A. Fazel, P.H. Cameron, J.N. Gushue, D.Y. Thomas, and J.J. Bergeron. 1999. Phosphorylation by CK2 and MAPK enhances calnexin association with ribosomes. *Embo J.* 18:3655-66.
- Chin, D.J., K.L. Luskey, R.G. Anderson, J.R. Faust, J.L. Goldstein, and M.S. Brown. 1982. Appearance of crystalloid endoplasmic reticulum in compactin-resistant Chinese hamster cells with a 500-fold increase in 3-hydroxy-3-methylglutaryl-coenzyme A reductase. *Proc Natl Acad Sci U S A.* 79:1185-9.
- Cho, J.H., Y. Noda, and K. Yoda. 2000. Proteins in the early golgi compartment of *Saccharomyces cerevisiae* immunoisolated by Sed5p. *FEBS Lett.* 469:151-4.
- Cho, R.J., M.J. Campbell, E.A. Winzeler, L. Steinmetz, A. Conway, L. Wodicka, T.G. Wolfsberg, A.E. Gabrielian, D. Landsman, D.J. Lockhart, and R.W. Davis. 1998. A genome-wide transcriptional analysis of the mitotic cell cycle. *Mol Cell.* 2:65-73.
- Ciufo, L.F., and A. Boyd. 2000. Identification of a luminal sequence specifying the assembly of Emp24p into p24 complexes in the yeast secretory pathway. *J Biol Chem.* 275:8382-8.
- Clary, D.O., I.C. Griff, and J.E. Rothman. 1990. SNAPs, a family of NSF attachment proteins involved in intracellular membrane fusion in animals and yeast. *Cell.* 61:709-21.
- Clermont, Y., A. Rambourg, and L. Hermo. 1994. Connections between the various elements of the cis- and mid-compartments of the Golgi apparatus of early rat spermatids. *Anat Rec.* 240:469-80.
- Click, E.S., T. Stearns, and D. Botstein. 2002. Systematic Structure-Function Analysis of the Small GTPase Arf1 in Yeast. *Mol Biol Cell.* 13:1652-64.

- Connolly, T., P.J. Rapiejko, and R. Gilmore. 1991. Requirement of GTP hydrolysis for dissociation of the signal recognition particle from its receptor. *Science*. 252:1171-3.
- Cosson, P., C. Demolliere, S. Hennecke, R. Duden, and F. Letourneur. 1996. Delta- and zeta-COP, two coatomer subunits homologous to clathrin-associated proteins, are involved in ER retrieval. *Embo J*. 15:1792-8.
- Cosson, P., and F. Letourneur. 1994. Coatomer interaction with di-lysine endoplasmic reticulum retention motifs. *Science*. 263:1629-31.
- Cowen, L.E., A. Nantel, M.S. Whiteway, D.Y. Thomas, D.C. Tessier, L.M. Kohn, and J.B. Anderson. 2002. Population genomics of drug resistance in *Candida albicans*. *Proc Natl Acad Sci U S A*. 99:9284-9.
- Cowles, C.R., S.D. Emr, and B.F. Horazdovsky. 1994. Mutations in the VPS45 gene, a SEC1 homologue, result in vacuolar protein sorting defects and accumulation of membrane vesicles. *J Cell Sci*. 107:3449-59.
- Cowles, C.R., G. Odorizzi, G.S. Payne, and S.D. Emr. 1997. The AP-3 adaptor complex is essential for cargo-selective transport to the yeast vacuole. *Cell*. 91:109-18.
- Cox, J.S., R.E. Chapman, and P. Walter. 1997. The unfolded protein response coordinates the production of endoplasmic reticulum protein and endoplasmic reticulum membrane. *Mol Biol Cell*. 8:1805-14.
- Craven, R.A., M. Egerton, and C.J. Stirling. 1996. A novel Hsp70 of the yeast ER lumen is required for the efficient translocation of a number of protein precursors. *Embo J*. 15:2640-50.
- Dahan, S., J.P. Ahluwalia, L. Wong, B.I. Posner, and J.J. Bergeron. 1994. Concentration of intracellular hepatic apolipoprotein E in Golgi apparatus saccular distensions and endosomes. *J Cell Biol*. 127:1859-69.
- Dascher, C., R. Ossig, D. Gallwitz, and H.D. Schmitt. 1991. Identification and structure of four yeast genes (SLY) that are able to suppress the functional loss of YPT1, a member of the RAS superfamily. *Mol Cell Biol*. 11:872-85.
- de Groot, E., J.P. Bebelman, W.H. Mager, and R.J. Planta. 2000. Very low

- amounts of glucose cause repression of the stress-responsive gene HSP12 in *Saccharomyces cerevisiae*. *Microbiology*. 146 (Pt 2):367-75.
- Deitz, S.B., A. Rambourg, F. Kepes, and A. Franzusoff. 2000. Sec7p directs the transitions required for yeast Golgi biogenesis. *Traffic*. 1:172-83.
- d'Enfert, C., C. Barlowe, S. Nishikawa, A. Nakano, and R. Schekman. 1991. Structural and functional dissection of a membrane glycoprotein required for vesicle budding from the endoplasmic reticulum. *Mol Cell Biol*. 11:5727-34.
- d'Enfert, C., L.J. Wuestehube, T. Lila, and R. Schekman. 1991. Sec12p-dependent membrane binding of the small GTP-binding protein Sar1p promotes formation of transport vesicles from the ER. *J Cell Biol*. 114:663-70.
- Denzel, A., F. Otto, A. Girod, R. Pepperkok, R. Watson, I. Rosewell, J.J. Bergeron, R.C. Solari, and M.J. Owen. 2000. The p24 family member p23 is required for early embryonic development. *Curr Biol*. 10:55-8.
- Depierre, J.W., and G. Dallner. 1975. Structural aspects of the membrane of the endoplasmic reticulum. *Biochim Biophys Acta*. 415:411-72.
- Doering, T.L., and R. Schekman. 1996. GPI anchor attachment is required for Gas1p transport from the endoplasmic reticulum in COP II vesicles. *Embo J*. 15:182-91.
- Dominguez, M., K. Dejgaard, J. Fullekrug, S. Dahan, A. Fazel, J.P. Paccaud, D.Y. Thomas, J.J. Bergeron, and T. Nilsson. 1998. gp25L/emp24/p24 protein family members of the cis-Golgi network bind both COP I and II coatomer. *J Cell Biol*. 140:751-65.
- Dominguez, M., A. Fazel, S. Dahan, J. Lovell, L. Hermo, A. Claude, P. Melancon, and J.J. Bergeron. 1999. Fusogenic domains of golgi membranes are sequestered into specialized regions of the stack that can be released by mechanical fragmentation. *J Cell Biol*. 145:673-88.
- Donaldson, J.G., D. Cassel, R.A. Kahn, and R.D. Klausner. 1992. ADP-ribosylation factor, a small GTP-binding protein, is required for binding of the coatomer protein beta-COP to Golgi membranes. *Proc Natl Acad Sci USA*. 89:6408-12.

- Droscher, A. 1998. Camillo Golgi and the discovery of the Golgi apparatus. *Histochem Cell Biol.* 109:425-30.
- Duden, R., G. Griffiths, R. Frank, P. Argos, and T.E. Kreis. 1991. Beta-COP, a 110 kd protein associated with non-clathrin-coated vesicles and the Golgi complex, shows homology to beta-adaptin. *Cell.* 64:649-65.
- Duden, R., M. Hosobuchi, S. Hamamoto, M. Winey, B. Byers, and R. Schekman. 1994. Yeast beta- and beta'-coat proteins (COP). Two coatomer subunits essential for endoplasmic reticulum-to-Golgi protein traffic. *J Biol Chem.* 269:24486-95.
- Dunphy, W.G., and J.E. Rothman. 1985. Compartmental organization of the Golgi stack. *Cell.* 42:13-21.
- Echard, A., F. Jollivet, O. Martinez, J.J. Lacapere, A. Rousselet, I. Janoueix-Lerosey, and B. Goud. 1998. Interaction of a Golgi-associated kinesin-like protein with Rab6. *Science.* 279:580-5.
- Eisen, M.B., P.T. Spellman, P.O. Brown, and D. Botstein. 1998. Cluster analysis and display of genome-wide expression patterns. *Proc Natl Acad Sci U S A.* 95:14863-8.
- Ekins, R., and F.W. Chu. 1999. Microarrays: their origins and applications. *Trends Biotechnol.* 17:217-8.
- Elgersma, Y., L. Kwast, M. van den Berg, W.B. Snyder, B. Distel, S. Subramani, and H.F. Tabak. 1997. Overexpression of Pex15p, a phosphorylated peroxisomal integral membrane protein required for peroxisome assembly in *S.cerevisiae*, causes proliferation of the endoplasmic reticulum membrane. *Embo J.* 16:7326-41.
- Elgersma, Y., L. Kwast, M. van den Berg, W.B. Snyder, B. Distel, S. Subramani, and H.F. Tabak. 1997. Overexpression of Pex15p, a phosphorylated peroxisomal integral membrane protein required for peroxisome assembly in *S.cerevisiae*, causes proliferation of the endoplasmic reticulum membrane. *Embo J.* 16:7326-41.
- Ellgaard, L., M. Molinari, and A. Helenius. 1999. Setting the standards: quality control in the secretory pathway. *Science.* 286:1882-8.

- Elrod-Erickson, M.J., and C.A. Kaiser. 1996. Genes that control the fidelity of endoplasmic reticulum to Golgi transport identified as suppressors of vesicle budding mutations. *Mol Biol Cell*. 7:1043-58.
- Emery, G., M. Rojo, and J. Gruenberg. 2000. Coupled transport of p24 family members. *J Cell Sci*. 113 (Pt 13):2507-16.
- Englund, P.T. 1993. The structure and biosynthesis of glycosyl phosphatidylinositol protein anchors. *Annu Rev Biochem*. 62:121-38.
- Esmon, B., P.C. Esmon, and R. Schekman. 1984. Early steps in processing of yeast glycoproteins. *J Biol Chem*. 259:10322-7.
- Espenshade, P., R.E. Gimeno, E. Holzmacher, P. Teung, and C.A. Kaiser. 1995. Yeast SEC16 gene encodes a multidomain vesicle coat protein that interacts with Sec23p. *J Cell Biol*. 131:311-24.
- Fang, M., M.P. Rivas, and V.A. Bankaitis. 1998. The contribution of lipids and lipid metabolism to cellular functions of the Golgi complex. *Biochim Biophys Acta*. 1404:85-100.
- Farquhar, M.G. 1985. Progress in unraveling pathways of Golgi traffic. *Annu Rev Cell Biol*. 1:447-88.
- Fasshauer, D., R.B. Sutton, A.T. Brunger, and R. Jahn. 1998. Conserved structural features of the synaptic fusion complex: SNARE proteins reclassified as Q- and R-SNAREs. *Proc Natl Acad Sci U S A*. 95:15781-6.
- Ferro-Novick, S., and R. Jahn. 1994. Vesicle fusion from yeast to man. *Nature*. 370:191-3.
- Fitting, T., and D. Kabat. 1982. Evidence for a glycoprotein "signal" involved in transport between subcellular organelles. Two membrane glycoproteins encoded by murine leukemia virus reach the cell surface at different rates. *J Biol Chem*. 257:14011-7.
- Frand, A.R., J.W. Cuozzo, and C.A. Kaiser. 2000. Pathways for protein disulphide bond formation. *Trends Cell Biol*. 10:203-10.
- Franke, W.W., D.J. Morre, B. Deumling, R.D. Cheetham, J. Kartenbeck, E.D. Jarasch, and H.W. Zentgraf. 1971. Synthesis and turnover of membrane proteins in rat liver: an examination of the membrane flow hypothesis. *Z*

- Franzusoff, A., K. Redding, J. Crosby, R.S. Fuller, and R. Schekman. 1991. Localization of components involved in protein transport and processing through the yeast Golgi apparatus. *J Cell Biol.* 112:27-37.
- Fries, E., L. Gustafsson, and P.A. Peterson. 1984. Four secretory proteins synthesized by hepatocytes are transported from endoplasmic reticulum to Golgi complex at different rates. *Embo J.* 3:147-52.
- Fujiwara, T., K. Oda, S. Yokota, A. Takatsuki, and Y. Ikehara. 1988. Brefeldin A causes disassembly of the Golgi complex and accumulation of secretory proteins in the endoplasmic reticulum. *J Biol Chem.* 263:18545-52.
- Fullekrug, J., and T. Nilsson. 1998. Protein sorting in the Golgi complex. *Biochim Biophys Acta.* 1404:77-84.
- Fullekrug, J., T. Suganuma, B.L. Tang, W. Hong, B. Storrie, and T. Nilsson. 1999. Localization and recycling of gp27 (hp24gamma3): complex formation with other p24 family members. *Mol Biol Cell.* 10:1939-55.
- Gagnon, E., S. Duclos, C. Rondeau, E. Chevet, P.H. Cameron, O. Steele-Mortimer, J. Paiement, J.J. Bergeron, and M. Desjardins. 2002. Endoplasmic reticulum-mediated phagocytosis is a mechanism of entry into macrophages. *Cell.* 110:119-31.
- Garin, J., R. Diez, S. Kieffer, J.F. Dermine, S. Duclos, E. Gagnon, R. Sadoul, C. Rondeau, and M. Desjardins. 2001. The phagosome proteome: insight into phagosome functions. *J Cell Biol.* 152:165-80.
- Gasch, A.P., M. Huang, S. Metzner, D. Botstein, S.J. Elledge, and P.O. Brown. 2001. Genomic expression responses to DNA-damaging agents and the regulatory role of the yeast ATR homolog Mec1p. *Mol Biol Cell.* 12:2987-3003.
- Gaynor, E.C., and S.D. Emr. 1997. COPI-independent anterograde transport: cargo-selective ER to Golgi protein transport in yeast COPI mutants. *J Cell Biol.* 136:789-802.
- Gaynor, E.C., T.R. Graham, and S.D. Emr. 1998. COPI in ER/Golgi and intra-Golgi transport: do yeast COPI mutants point the way? *Biochim Biophys*

Acta. 1404:33-51.

- Gaynor, E.C., S. te Heesen, T.R. Graham, M. Aebl, and S.D. Emr. 1994. Signal-mediated retrieval of a membrane protein from the Golgi to the ER in yeast. *J Cell Biol*. 127:653-65.
- Gething, M.J. 1999. Role and regulation of the ER chaperone BiP. *Semin Cell Dev Biol*. 10:465-72.
- Geuze, H.J., J.W. Slot, G.J.A.M. Strous, J. Peppard, K.M. Figura, A. Hasilik, and A.L. Schwartz. 1984. Intracellular receptor sorting during endocytosis: Comparative immunoelectron microscopy of multiple receptors in rat liver. *Cell*. 37:195-204.
- Gimeno, R.E., P. Espenshade, and C.A. Kaiser. 1995. SED4 encodes a yeast endoplasmic reticulum protein that binds Sec16p and participates in vesicle formation. *J Cell Biol*. 131:325-38.
- Gimeno, R.E., P. Espenshade, and C.A. Kaiser. 1996. COPII coat subunit interactions: Sec24p and Sec23p bind to adjacent regions of Sec16p. *Mol Biol Cell*. 7:1815-23.
- Gommel, D., L. Orci, E.M. Emig, M.J. Hannah, M. Ravazzola, W. Nickel, J.B. Helms, F.T. Wieland, and K. Sohn. 1999. p24 and p23, the major transmembrane proteins of COPI-coated transport vesicles, form heterooligomeric complexes and cycle between the organelles of the early secretory pathway. *FEBS Lett*. 447:179-85.
- Gommel, D.U., A.R. Memon, A. Heiss, F. Lottspeich, J. Pfannstiel, J. Lechner, C. Reinhard, J.B. Helms, W. Nickel, and F.T. Wieland. 2001. Recruitment to Golgi membranes of ADP-ribosylation factor 1 is mediated by the cytoplasmic domain of p23. *Embo J*. 20:6751-60.
- Gonatas, N.K., J.O. Gonatas, and A. Stieber. 1998. The involvement of the Golgi apparatus in the pathogenesis of amyotrophic lateral sclerosis, Alzheimer's disease, and ricin intoxication. *Histochem Cell Biol*. 109:591-600.
- Gorlich, D., S. Prehn, E. Hartmann, K.U. Kalies, and T.A. Rapoport. 1992. A mammalian homolog of SEC61p and SECYp is associated with ribosomes and nascent polypeptides during translocation. *Cell*. 71:489-503.

- Graham, T.R., and S.D. Emr. 1991. Compartmental organization of Golgi-specific protein modification and vacuolar protein sorting events defined in a yeast sec18 (NSF) mutant. *J Cell Biol.* 114:207-18.
- Graham, T.R., and S.D. Emr. 1991. Compartmental organization of Golgi-specific protein modification and vacuolar protein sorting events defined in a yeast sec18 (NSF) mutant. *J Cell Biol.* 114:207-18.
- Grasse, P.P. 1957. Ultrastructure polarite et reproduction de l'appareil de Golgi. *C.R. Acad. Sci. Paris.* 245:1278-81.
- Griff, I.C., R. Schekman, J.E. Rothman, and C.A. Kaiser. 1992. The yeast SEC17 gene product is functionally equivalent to mammalian alpha-SNAP protein. *J Biol Chem.* 267:12106-15.
- Griffiths, G. 2000. Gut thoughts on the Golgi complex. *Traffic.* 1:738-45.
- Griffiths, G., R. Pepperkok, J.K. Locker, and T.E. Kreis. 1995. Immunocytochemical localization of beta-COP to the ER-Golgi boundary and the TGN. *J Cell Sci.* 108:2839-56.
- Griffiths, G. 1993. Fine structure immunocytochemistry. Springer Verlag, Berlin.
- Griffiths, G., and K. Simons. 1986. The trans Golgi network: sorting at the exit site of the Golgi complex. *Science.* 234:438-43.
- Griffiths, G., and H. Hoppeler. 1986. Quantitation in immunocytochemistry: Correlation of immunogold labeling to absolute number of membrane antigens. *J. Histochem. Cytochem.* 34:1389-1398.
- Griffiths, G., A. McDowall, R. Back, and J. Dubochet. 1984. On the preparations of cryosections for immunocytochemistry. *J. Ultrastruct. Res.* 89:65-78.
- Hamilton, T.G., T.B. Norris, P.R. Tsuruda, and G.C. Flynn. 1999. Cer1p functions as a molecular chaperone in the endoplasmic reticulum of *Saccharomyces cerevisiae*. *Mol Cell Biol.* 19:5298-307.
- Hamman, B.D., L.M. Hendershot, and A.E. Johnson. 1998. BiP maintains the permeability barrier of the ER membrane by sealing the luminal end of the translocon pore before and early in translocation. *Cell.* 92:747-58.
- Hammond, C., I. Braakman, and A. Helenius. 1994. Role of N-linked oligosaccharide recognition, glucose trimming, and calnexin in

- glycoprotein folding and quality control. *Proc Natl Acad Sci U S A.* 91:913-7.
- Harding, H.P., M. Calton, F. Urano, I. Novoa, and D. Ron. 2002. Transcriptional and translational control in the Mammalian unfolded protein response. *Annu Rev Cell Dev Biol.* 18:575-99.
- Hardwick, K.G., M.J. Lewis, J. Semenza, N. Dean, and H.R. Pelham. 1990. ERD1, a yeast gene required for the retention of luminal endoplasmic reticulum proteins, affects glycoprotein processing in the Golgi apparatus. *Embo J.* 9:623-30.
- Hardwick, K.G., and H.R. Pelham. 1992. SED5 encodes a 39-kD integral membrane protein required for vesicular transport between the ER and the Golgi complex. *J Cell Biol.* 119:513-21.
- Harlow, E., and D. Lane. 1988. *Antibodies: A Laboratory Manual*, Cold Spring Harbor Laboratory, Cold Spring Harbor, NY.
- Harter, C., and F.T. Wieland. 1998. A single binding site for dilysine retrieval motifs and p23 within the gamma subunit of coatamer. *Proc Natl Acad Sci U S A.* 95:11649-54.
- Hauri, H.P., and A. Schweizer. 1992. The endoplasmic reticulum-Golgi intermediate compartment. *Curr Opin Cell Biol.* 4:600-8.
- Hausler, A., L. Ballou, C.E. Ballou, and P.W. Robbins. 1992. Yeast glycoprotein biosynthesis: MNT1 encodes an alpha-1,2-mannosyltransferase involved in O-glycosylation. *Proc Natl Acad Sci U S A.* 89:6846-50.
- Hegde, R.S., and V.R. Lingappa. 1999. Regulation of protein biogenesis at the endoplasmic reticulum membrane. *Trends Cell Biol.* 9:132-7.
- Helms, J.B., K.J. de Vries, and K.W. Wirtz. 1991. Synthesis of phosphatidylinositol 4,5-bisphosphate in the endoplasmic reticulum of Chinese hamster ovary cells. *J Biol Chem.* 266:21368-74.
- Hermo, L., H. Green, and Y. Clermont. 1991. Golgi apparatus of epithelial principal cells of the epididymal initial segment of the rat: structure, relationship with endoplasmic reticulum, and role in the formation of secretory vesicles. *Anat Rec.* 229:159-76.

- Hermo, L., and C.E. Smith. 1998. The structure of the Golgi apparatus: a sperm's eye view in principal epithelial cells of the rat epididymis. *Histochem Cell Biol.* 109:431-47.
- Herrmann, J.M., P. Malkus, and R. Schekman. 1999. Out of the ER--outfitters, escorts and guides. *Trends Cell Biol.* 9:5-7.
- Herscovics, A., and P. Orlean. 1993. Glycoprotein biosynthesis in yeast. *Faseb J.* 7:540-50.
- Hicke, L., and R. Schekman. 1989. Yeast Sec23p acts in the cytoplasm to promote protein transport from the endoplasmic reticulum to the Golgi complex in vivo and in vitro. *Embo J.* 8:1677-84.
- Hicke, L., T. Yoshihisa, and R. Schekman. 1992. Sec23p and a novel 105-kDa protein function as a multimeric complex to promote vesicle budding and protein transport from the endoplasmic reticulum. *Mol Biol Cell.* 3:667-76.
- Hirschberg, C.B., P.W. Robbins, and C. Abeijon. 1998. Transporters of nucleotide sugars, ATP, and nucleotide sulfate in the endoplasmic reticulum and Golgi apparatus. *Annu Rev Biochem.* 67:49-69.
- Holthuis, J.C., M.C. van Riel, and G.J. Martens. 1995. Translocon-associated protein TRAP delta and a novel TRAP-like protein are coordinately expressed with pro-opiomelanocortin in *Xenopus* intermediate pituitary. *Biochem J.* 312:205-13.
- Hosobuchi, M., T. Kreis, and R. Schekman. 1992. SEC21 is a gene required for ER to Golgi protein transport that encodes a subunit of a yeast coatomer. *Nature.* 360:603-5.
- Hunt, J.M., K. Bommert, M.P. Charlton, A. Kistner, E. Habermann, G.J. Augustine, and H. Betz. 1994. A post-docking role for synaptobrevin in synaptic vesicle fusion. *Neuron.* 12:1269-79.
- Hurtley, S.M., and A. Helenius. 1989. Protein oligomerization in the endoplasmic reticulum. *Annu Rev Cell Biol.* 5:277-307.
- Huse, J.T., K. Liu, D.S. Pijak, D. Carlin, V.M. Lee, and R.W. Doms. 2002. Beta-secretase processing in the trans-Golgi network preferentially generates truncated amyloid species that accumulate in Alzheimer's disease brain. *J*

Biol Chem. 277:16278-84.

- Hwang, C., A.J. Sinskey, and H.F. Lodish. 1992. Oxidized redox state of glutathione in the endoplasmic reticulum. *Science*. 257:1496-502.
- Jackson, M.R., T. Nilsson, and P.A. Peterson. 1993. Retrieval of transmembrane proteins to the endoplasmic reticulum. *J Cell Biol.* 121:317-33.
- Jamieson, J.D. 1998. The Golgi complex: perspectives and prospectives. *Biochim Biophys Acta*. 1404:3-7.
- Jamieson, J.D., and G.E. Palade. 1967b. Intracellular transport of secretory proteins in the pancreatic exocrine cell. I. Role of the peripheral elements of the Golgi complex. *J Cell Biol.* 34:577-96.
- Jamieson, J.D., and G.E. Palade. 1967a. Intracellular transport of secretory proteins in the pancreatic exocrine cell. II. Transport to condensing vacuoles and zymogen granules. *J Cell Biol.* 34:597-615.
- Jamieson, J.D., and G.E. Palade. 1968. Intracellular transport of secretory proteins in the pancreatic exocrine cell. 3. Dissociation of intracellular transport from protein synthesis. *J Cell Biol.* 39:580-8.
- Jelsema, C.L., and D.J. Morre. 1978. Distribution of phospholipid biosynthetic enzymes among cell components of rat liver. *J Biol Chem.* 253:7960-71.
- Jenks, B.G., A.P. Overbeeke, and B.F. McStay. 1977. *Can J Zoo.* 55:922-927.
- Jergil, B., and R. Sundler. 1983. Phosphorylation of phosphatidylinositol in rat liver Golgi. *J Biol Chem.* 258:7968-73.
- Jones, A.L., and D.W. Fawcett. 1966. Hypertrophy of the agranular endoplasmic reticulum in hamster liver induced by phenobarbital (with a review on the functions of this organelle in liver). *J Histochem Cytochem.* 14:215-32.
- Jungmann, J., and S. Munro. 1998. Multi-protein complexes in the cis Golgi of *Saccharomyces cerevisiae* with alpha-1,6-mannosyltransferase activity. *Embo J.* 17:423-34.
- Kaiser, C. 2000. Thinking about p24 proteins and how transport vesicles select their cargo. *Proc Natl Acad Sci U S A.* 97:3783-5.
- Kalies, K.U., D. Gorlich, and T.A. Rapoport. 1994. Binding of ribosomes to the rough endoplasmic reticulum mediated by the Sec61p-complex. *J Cell*

Biol. 126:925-34.

- Karnovsky, M.J. 1971. Use of ferrocyanide-reduced osmium tetroxide in electron microscopy. *J. Cell Biol.*, 51:146a.
- Kaufman, R.J. 1999. Stress signaling from the lumen of the endoplasmic reticulum: coordination of gene transcriptional and translational controls. *Genes Dev.* 13:1211-33.
- Kawabe, Y., T. Enomoto, T. Morio, H. Urushihara, and Y. Tanaka. 1999. LbrA, a protein predicted to have a role in vesicle trafficking, is necessary for normal morphogenesis in *Polysphondylium pallidum*. *Gene*. 239:75-9.
- Keenan, T.W., and D.J. Morre. 1970. Phospholipid class and fatty acid composition of golgi apparatus isolated from rat liver and comparison with other cell fractions. *Biochemistry*. 9:19-25.
- Kelleher, D.J., G. Kreibich, and R. Gilmore. 1992. Oligosaccharyltransferase activity is associated with a protein complex composed of ribophorins I and II and a 48 kd protein. *Cell*. 69:55-65.
- Klis, F.M. 1994. Review: cell wall assembly in yeast. *Yeast*. 10:851-69.
- Kochevar, D.T., and R.G. Anderson. 1987. Purified crystalloid endoplasmic reticulum from UT-1 cells contains multiple proteins in addition to 3-hydroxy-3-methylglutaryl coenzyme A reductase. *J Biol Chem*. 262:10321-6.
- Kohrer, K., and H. Domdey. 1991. Preparation of high molecular weight RNA. *Methods Enzymol.* 194:398-405.
- Koning, A.J., C.J. Roberts, and R.L. Wright. 1996. Different subcellular localization of *Saccharomyces cerevisiae* HMG-CoA reductase isozymes at elevated levels corresponds to distinct endoplasmic reticulum membrane proliferations. *Mol Biol Cell*. 7:769-89.
- Kornfeld, R., and S. Kornfeld. 1985. Assembly of asparagine-linked oligosaccharides. *Annu Rev Biochem*. 54:631-64.
- Kuge, O., C. Dascher, L. Orci, T. Rowe, M. Amherdt, H. Plutner, M. Ravazzola, G. Tanigawa, J.E. Rothman, and W.E. Balch. 1994. Sar1 promotes vesicle budding from the endoplasmic reticulum but not Golgi compartments. *J*

Cell Biol. 125:51-65.

- Kuiper, R.P., G. Bouw, K.P. Janssen, J. Rotter, F. van Herp, and G.J. Martens. 2001. Localization of p24 putative cargo receptors in the early secretory pathway depends on the biosynthetic activity of the cell. *Biochem J.* 360:421-9.
- Kuiper, R.P., and G.J. Martens. 2000. Prohormone transport through the secretory pathway of neuroendocrine cells. *Biochem Cell Biol.* 78:289-98.
- Kuiper, R.P., H.R. Waterham, J. Rotter, G. Bouw, and G.J. Martens. 2000. Differential induction of two p24delta putative cargo receptors upon activation of a prohormone-producing cell. *Mol Biol Cell.* 11:131-40.
- Kuismanen, E., and J. Saraste. 1989. Low temperature-induced transport blocks as tools to manipulate membrane traffic. *Methods Cell Biol.* 32:257-74.
- Kurihara, T., S. Hamamoto, R.E. Gimeno, C.A. Kaiser, R. Schekman, and T. Yoshihisa. 2000. Sec24p and Iss1p function interchangeably in transport vesicle formation from the endoplasmic reticulum in *Saccharomyces cerevisiae*. *Mol Biol Cell.* 11:983-98.
- Ladinsky, M.S., D.N. Mastronarde, J.R. McIntosh, K.E. Howell, and L.A. Staehelin. 1999. Golgi structure in three dimensions: functional insights from the normal rat kidney cell. *J Cell Biol.* 144:1135-49.
- LaMantia, M., T. Miura, H. Tachikawa, H.A. Kaplan, W.J. Lennarz, and T. Mizunaga. 1991. Glycosylation site binding protein and protein disulfide isomerase are identical and essential for cell viability in yeast. *Proc Natl Acad Sci U S A.* 88:4453-7.
- Lanoix, J., J. Ouwendijk, C.C. Lin, A. Stark, H.D. Love, J. Ostermann, and T. Nilsson. 1999. GTP hydrolysis by arf-1 mediates sorting and concentration of Golgi resident enzymes into functional COP I vesicles. *Embo J.* 18:4935-48.
- Lanoix, J., J. Ouwendijk, A. Stark, E. Szafer, D. Cassel, K. Dejgaard, M. Weiss, and T. Nilsson. 2001. Sorting of Golgi resident proteins into different subpopulations of COPI vesicles: a role for ArfGAP1. *J Cell Biol.* 155:1199-212.

- Lavoie, C., J. Lanoix, F.W. Kan, and J. Paiement. 1996. Cell-free assembly of rough and smooth endoplasmic reticulum. *J Cell Sci.* 109:1415-25.
- Lavoie, C., J. Paiement, M. Dominguez, L. Roy, S. Dahan, J.N. Gushue, and J.J. Bergeron. 1999. Roles for alpha(2)p24 and COPI in endoplasmic reticulum cargo exit site formation. *J Cell Biol.* 146:285-99.
- Ledford, B.E., and D.F. Davis. 1983. Kinetics of serum protein secretion by cultured hepatoma cells. Evidence for multiple secretory pathways. *J Biol Chem.* 258:3304-8.
- Letourneur, F., E.C. Gaynor, S. Hennecke, C. Demolliere, R. Duden, S.D. Emr, H. Riezman, and P. Cosson. 1994. Coatamer is essential for retrieval of dilysine-tagged proteins to the endoplasmic reticulum. *Cell.* 79:1199-207.
- Li, L., B.R. Ernstring, M.J. Wishart, D.L. Lohse, and J.E. Dixon. 1997. A family of putative tumor suppressors is structurally and functionally conserved in humans and yeast. *J Biol Chem.* 272:29403-6.
- Lian, J.P., and S. Ferro-Novick. 1993. Bos1p, an integral membrane protein of the endoplasmic reticulum to Golgi transport vesicles, is required for their fusion competence. *Cell.* 73:735-45.
- Lin, C.C., H.D. Love, J.N. Gushue, J.J. Bergeron, and J. Ostermann. 1999. ER/Golgi intermediates acquire Golgi enzymes by brefeldin A-sensitive retrograde transport in vitro. *J Cell Biol.* 147:1457-72.
- Lippincott-Schwartz, J. 2001. The secretory membrane system studied in real-time. Robert Feulgen Prize Lecture, 2001. *Histochem Cell Biol.* 116:97-107.
- Lippincott-Schwartz, J., L.C. Yuan, J.S. Bonifacino, and R.D. Klausner. 1989. Rapid redistribution of Golgi proteins into the ER in cells treated with brefeldin A: evidence for membrane cycling from Golgi to ER. *Cell.* 56:801-13.
- Littleton, J.T., R.J. Barnard, S.A. Titus, J. Slind, E.R. Chapman, and B. Ganetzky. 2001. SNARE-complex disassembly by NSF follows synaptic-vesicle fusion. *Proc Natl Acad Sci U S A.* 98:12233-8.
- Lodish, H.F. 1988. Transport of secretory and membrane glycoproteins from the

- rough endoplasmic reticulum to the Golgi. A rate-limiting step in protein maturation and secretion. *J Biol Chem.* 263:2107-10.
- Lodish, H.F., N. Kong, M. Snider, and G.J. Strous. 1983. Hepatoma secretory proteins migrate from rough endoplasmic reticulum to Golgi at characteristic rates. *Nature.* 304:80-3.
- Loftus, T.M., Y.H. Nguyen, and E.J. Stanbridge. 1997. The QM protein associates with ribosomes in the rough endoplasmic reticulum. *Biochemistry.* 36:8224-30.
- Lucocq, J., G. Warren, and J. Pryde. 1991. Okadaic acid induces Golgi apparatus fragmentation and arrest of intracellular transport. *J Cell Sci.* 100 (Pt 4):753-9.
- Lucocq, J.M., J.G. Pryde, E.G. Berger, and G. Warren. 1987. A mitotic form of the Golgi apparatus in HeLa cells. *J Cell Biol.* 104:865-74.
- Lussier, M., A.M. Sdicu, A. Camirand, and H. Bussey. 1996. Functional characterization of the YUR1, KTR1, and KTR2 genes as members of the yeast KRE2/MNT1 mannosyltransferase gene family. *J Biol Chem.* 271:11001-8.
- Lyko, F., B. Martoglio, B. Jungnickel, T.A. Rapoport, and B. Dobberstein. 1995. Signal sequence processing in rough microsomes. *J Biol Chem.* 270:19873-8.
- Majoul, I., K. Sohn, F.T. Wieland, R. Pepperkok, M. Pizza, J. Hillemann, and H.D. Soling. 1998. KDEL receptor (Erd2p)-mediated retrograde transport of the cholera toxin A subunit from the Golgi involves COPI, p23, and the COOH terminus of Erd2p. *J Cell Biol.* 143:601-12.
- Majoul, I., M. Straub, S.W. Hell, R. Duden, and H.D. Soling. 2001. KDEL-cargo regulates interactions between proteins involved in COPI vesicle traffic: measurements in living cells using FRET. *Dev Cell.* 1:139-53.
- Malhotra, V., T. Serafini, L. Orci, J.C. Shepherd, and J.E. Rothman. 1989. Purification of a novel class of coated vesicles mediating biosynthetic protein transport through the Golgi stack. *Cell.* 58:329-36.
- Marchi, F., and C.P. Leblond. 1984. Radioautographic characterization of

- successive compartments along the rough endoplasmic reticulum-Golgi pathway of collagen precursors in foot pad fibroblasts of [3H]proline-injected rats. *J Cell Biol.* 98:1705-9.
- Martinez-Menarguez, J.A., H.J. Geuze, J.W. Slot, and J. Klumperman. 1999. Vesicular tubular clusters between the ER and Golgi mediate concentration of soluble secretory proteins by exclusion from COPI-coated vesicles. *Cell.* 98:81-90.
- Martinez-Menarguez, J.A., R. Prekeris, V.M. Oorschot, R. Scheller, J.W. Slot, H.J. Geuze, and J. Klumperman. 2001. Peri-Golgi vesicles contain retrograde but not anterograde proteins consistent with the cisternal progression model of intra-Golgi transport. *J Cell Biol.* 155:1213-24.
- Marzioch, M., D.C. Henthorn, J.M. Herrmann, R. Wilson, D.Y. Thomas, J.J. Bergeron, R.C. Solari, and A. Rowley. 1999. Erp1p and Erp2p, partners for Emp24p and Erv25p in a yeast p24 complex. *Mol Biol Cell.* 10:1923-38.
- Matlack, K.E., B. Misselwitz, K. Plath, and T.A. Rapoport. 1999. BiP acts as a molecular ratchet during posttranslational transport of prepro- α factor across the ER membrane. *Cell.* 97:553-64.
- McGee, T.P., H.B. Skinner, E.A. Whitters, S.A. Henry, and V.A. Bankaitis. 1994. A phosphatidylinositol transfer protein controls the phosphatidylcholine content of yeast Golgi membranes. *J Cell Biol.* 124:273-87.
- Melancon, P., B.S. Glick, V. Malhotra, P.J. Weidman, T. Serafini, M.L. Gleason, L. Orci, and J.E. Rothman. 1987. Involvement of GTP-binding "G" proteins in transport through the Golgi stack. *Cell.* 51:1053-62.
- Meldolesi, J. 1974. Dynamics of cytoplasmic membranes in guinea pig pancreatic acinar cells. I. Synthesis and turnover of membrane proteins. *J Cell Biol.* 61:1-13.
- Meldolesi, J., and T. Pozzan. 1998. The heterogeneity of ER Ca^{2+} stores has a key role in nonmuscle cell signaling and function. *J Cell Biol.* 142:1395-8.
- Melkonian, M., B. Becker, and D. Becker. 1991. Scale formation in algae. *J Electron Microsc Tech.* 17:165-78.

- Minard, K.I., G.T. Jennings, T.M. Loftus, D. Xuan, and L. McAlister-Henn. 1998. Sources of NADPH and expression of mammalian NADP⁺-specific isocitrate dehydrogenases in *Saccharomyces cerevisiae*. *J Biol Chem.* 273:31486-93.
- Mollenhauer, H.H., and D.J. Morre. 1991. Perspectives on Golgi apparatus form and function. *J Electron Microsc Tech.* 17:2-14.
- Morin-Ganet MN, Rambourg A, Deitz SB, Franzusoff A, Kepes F. Morphogenesis and dynamics of the yeast Golgi apparatus. *Traffic*. 2000 Jan;1(1):56-68.
- Morre, D.J., and L. Ovtracht. 1977. Dynamics of the Golgi apparatus: membrane differentiation and membrane flow. *Int Rev Cytol Suppl*:61-188.
- Morre, D.J. and T.W. Keenan. 1997. Membrane flow revisited: what pathways are followed by membrane molecules moving through the Golgi apparatus? *BioScience* 47:489-498.
- Mumberg, D., R. Muller, and M. Funk. 1994. Regulatable promoters of *Saccharomyces cerevisiae*: comparison of transcriptional activity and their use for heterologous expression. *Nucleic Acids Res.* 22:5767-8.
- Mumberg, D., R. Muller, and M. Funk. 1995. Yeast vectors for the controlled expression of heterologous proteins in different genetic backgrounds. *Gene*. 156:119-22.
- Muniz, M., P. Morsomme, and H. Riezman. 2001. Protein sorting upon exit from the endoplasmic reticulum. *Cell*. 104:313-20.
- Muniz, M., C. Nuoffer, H.P. Hauri, and H. Riezman. 2000. The Emp24 complex recruits a specific cargo molecule into endoplasmic reticulum-derived vesicles. *J Cell Biol.* 148:925-30.
- Munro, S., and H.R. Pelham. 1987. A C-terminal signal prevents secretion of luminal ER proteins. *Cell*. 48:899-907.
- Naik, R.R., and E.W. Jones. 1998. The PBN1 gene of *Saccharomyces cerevisiae*: an essential gene that is required for the post-translational processing of the protease B precursor. *Genetics*. 149:1277-92.
- Nakamura, N., S. Yamazaki, K. Sato, A. Nakano, M. Sakaguchi, and K. Mihara.

1998. Identification of potential regulatory elements for the transport of Emp24p. *Mol Biol Cell*. 9:3493-503.
- Nakano, A., D. Brada, and R. Schekman. 1988. A membrane glycoprotein, Sec12p, required for protein transport from the endoplasmic reticulum to the Golgi apparatus in yeast. *J Cell Biol*. 107:851-63.
- Nakayama, K., T. Nagasu, Y. Shimma, J. Kuromitsu, and Y. Jigami. 1992. OCH1 encodes a novel membrane bound mannosyltransferase: outer chain elongation of asparagine-linked oligosaccharides. *Embo J*. 11:2511-9.
- Neutra, M., and C.P. Leblond. 1966. Radioautographic comparison of the uptake of galactose-H and glucose-H3 in the golgi region of various cells secreting glycoproteins or mucopolysaccharides. *J Cell Biol*. 30:137-50.
- Ng, D.T., J.D. Brown, and P. Walter. 1996. Signal sequences specify the targeting route to the endoplasmic reticulum membrane. *J Cell Biol*. 134:269-78.
- Nichols, W.C., U. Seligsohn, A. Zivelin, V.H. Terry, C.E. Hertel, M.A. Wheatley, M.J. Moussalli, H.P. Hauri, N. Ciavarella, R.J. Kaufman, and D. Ginsburg. 1998. Mutations in the ER-Golgi intermediate compartment protein ERGIC-53 cause combined deficiency of coagulation factors V and VIII. *Cell*. 93:61-70.
- Nickel, W., B. Brugger, and F.T. Wieland. 1998. Protein and lipid sorting between the endoplasmic reticulum and the Golgi complex. *Semin Cell Dev Biol*. 9:493-501.
- Nilsson, T., M. Pypaert, M.H. Hoe, P. Slusarewicz, E.G. Berger, and G. Warren. 1993. Overlapping distribution of two glycosyltransferases in the Golgi apparatus of HeLa cells. *J Cell Biol*. 120:5-13.
- Nishikawa, S., A. Hirata, and A. Nakano. 1994. Inhibition of endoplasmic reticulum (ER)-to-Golgi transport induces relocalization of binding protein (BiP) within the ER to form the BiP bodies. *Mol Biol Cell*. 5:1129-43.
- Norgaard, P., V. Westphal, C. Tachibana, L. Alsoe, B. Holst, and J.R. Winther. 2001. Functional differences in yeast protein disulfide isomerases. *J Cell Biol*. 152:553-62.

- Normington, K., K. Kohno, Y. Kozutsumi, M.J. Gething, and J. Sambrook. 1989. *S. cerevisiae* encodes an essential protein homologous in sequence and function to mammalian BiP. *Cell*. 57:1223-36.
- Novick, P., C. Field, and R. Schekman. 1980. Identification of 23 complementation groups required for post- translational events in the yeast secretory pathway. *Cell*. 21:205-15.
- Novikoff, A.B. 1976. The endoplasmic reticulum: a cytochemist's view (a review). *Proc Natl Acad Sci U S A*. 73:2781-7.
- Nuoffer, C., H.W. Davidson, J. Matteson, J. Meinkoth, and W.E. Balch. 1994. A GDP-bound of rab1 inhibits protein export from the endoplasmic reticulum and transport between Golgi compartments. *J Cell Biol*. 125:225-37.
- Nuoffer, C., A. Horvath, and H. Riezman. 1993. Analysis of the sequence requirements for glycosylphosphatidylinositol anchoring of *Saccharomyces cerevisiae* Gas1 protein. *J Biol Chem*. 268:10558-63.
- Oprins, A., R. Duden, T.E. Kreis, H.J. Geuze, and J.W. Slot. 1993. Beta-COP localizes mainly to the cis-Golgi side in exocrine pancreas. *J Cell Biol*. 121:49-59.
- Orci, L., M. Amherdt, M. Ravazzola, A. Perrelet, and J.E. Rothman. 2000. Exclusion of golgi residents from transport vesicles budding from Golgi cisternae in intact cells. *J Cell Biol*. 150:1263-70.
- Orci, L., M.S. Brown, J.L. Goldstein, L.M. Garcia-Segura, and R.G. Anderson. 1984. Increase in membrane cholesterol: a possible trigger for degradation of HMG CoA reductase and crystalloid endoplasmic reticulum in UT-1 cells. *Cell*. 36:835-45.
- Orci, L., B.S. Glick, and J.E. Rothman. 1986. A new type of coated vesicular carrier that appears not to contain clathrin: its possible role in protein transport within the Golgi stack. *Cell*. 46:171-84.
- Orci, L., M. Ravazzola, P. Meda, C. Holcomb, H.P. Moore, L. Hicke, and R. Schekman. 1991. Mammalian Sec23p homologue is restricted to the endoplasmic reticulum transitional cytoplasm. *Proc Natl Acad Sci U S A*.

88:8611-5.

- Orci, L., M. Stannnes, M. Ravazzola, M. Amherdt, A. Perrelet, T.H. Sollner, and J.E. Rothman. 1997. Bidirectional transport by distinct populations of COPI-coated vesicles. *Cell*. 90:335-49.
- Ossipov, D., S. Schroder-Kohne, and H.D. Schmitt. 1999. Yeast ER-Golgi v-SNAREs Bos1p and Bet1p differ in steady-state localization and targeting. *J Cell Sci*. 112 (Pt 22):4135-42.
- Ostermann, J., L. Orci, K. Tani, M. Amherdt, M. Ravazzola, Z. Elazar, and J.E. Rothman. 1993. Stepwise assembly of functionally active transport vesicles. *Cell*. 75:1015-25.
- Otte, S., W.J. Belden, M. Heidtman, J. Liu, O.N. Jensen, and C. Barlowe. 2001. Erv41p and Erv46p: new components of COPII vesicles involved in transport between the ER and Golgi complex. *J Cell Biol*. 152:503-18.
- Ou, W.J., J.J. Bergeron, Y. Li, C.Y. Kang, and D.Y. Thomas. 1995. Conformational changes induced in the endoplasmic reticulum luminal domain of calnexin by Mg-ATP and Ca²⁺. *J Biol Chem*. 270:18051-9.
- Ou, W.J., P.H. Cameron, D.Y. Thomas, and J.J. Bergeron. 1993. Association of folding intermediates of glycoproteins with calnexin during protein maturation. *Nature*. 364:771-6.
- Paiment, J., and J.J. Bergeron. 1983. Localization of GTP-stimulated core glycosylation to fused microsomes. *J Cell Biol*. 96:1791-6.
- Paiment, J., F.W. Kan, J. Lanoix, and M. Blain. 1988. Cytochemical analysis of the reconstitution of endoplasmic reticulum after microinjection of rat liver microsomes into *Xenopus* oocytes. *J Histochem Cytochem*. 36:1263-73.
- Palade, G. 1975. Intracellular aspects of the process of protein synthesis. *Science*. 189:347-58.
- Palmer, D.J., J.B. Helms, C.J. Beckers, L. Orci, and J.E. Rothman. 1993. Binding of coatomer to Golgi membranes requires ADP-ribosylation factor. *J Biol Chem*. 268:12083-9.
- Parlati, F., J.A. McNew, R. Fukuda, R. Miller, T.H. Sollner, and J.E. Rothman.

2000. Topological restriction of SNARE-dependent membrane fusion. *Nature*. 407:194-8.
- Partaledis, J.A., and V. Berlin. 1993. The FKB2 gene of *Saccharomyces cerevisiae*, encoding the immunosuppressant-binding protein FKBP-13, is regulated in response to accumulation of unfolded proteins in the endoplasmic reticulum. *Proc Natl Acad Sci U S A*. 90:5450-4.
- Patil, C., and P. Walter. 2001. Intracellular signaling from the endoplasmic reticulum to the nucleus: the unfolded protein response in yeast and mammals. *Curr Opin Cell Biol*. 13:349-55.
- Pelham, H.R. 1989. Control of protein exit from the endoplasmic reticulum. *Annu Rev Cell Biol*. 5:1-23.
- Pelham, H.R. 1994. About turn for the COPs? *Cell*. 79:1125-7.
- Pelham, H.R. 1995. Sorting and retrieval between the endoplasmic reticulum and Golgi apparatus. *Curr Opin Cell Biol*. 7:530-5.
- Pelham, H.R. 2001. SNAREs and the specificity of membrane fusion. *Trends Cell Biol*. 11:99-101.
- Pelletier L, Stern CA, Pypaert M, Sheff D, Ngo HM, Roper N, He CY, Hu K, Toomre D, Coppens I, Roos DS, Joiner KA, Warren G. 2002. Golgi biogenesis in *Toxoplasma gondii*. *Nature*. 418:548-52.
- Pepperkok, R., J. Scheel, H. Horstmann, H.P. Hauri, G. Griffiths, and T.E. Kreis. 1993. Beta-COP is essential for biosynthetic membrane transport from the endoplasmic reticulum to the Golgi complex in vivo. *Cell*. 74:71-82.
- Pepperkok, R., J.A. Whitney, M. Gomez, and T.E. Kreis. 2000. COPI vesicles accumulating in the presence of a GTP restricted *arf1* mutant are depleted of anterograde and retrograde cargo. *J Cell Sci*. 113 (Pt 1):135-44.
- Pereira-Leal, J.B., and M.C. Seabra. 2000. The mammalian Rab family of small GTPases: definition of family and subfamily sequence motifs suggests a mechanism for functional specificity in the Ras superfamily. *J Mol Biol*. 301:1077-87.
- Peter, F., H. Plutner, H. Zhu, T.E. Kreis, and W.E. Balch. 1993. Beta-COP is essential for transport of protein from the endoplasmic reticulum to the

- Golgi in vitro. *J Cell Biol.* 122:1155-67.
- Pfeffer, S.R. 2001. Rab GTPases: specifying and deciphering organelle identity and function. *Trends Cell Biol.* 11:487-91.
- Pfeffer, S.R., A.B. Dirac-Svejstrup, and T. Soldati. 1995. Rab GDP dissociation inhibitor: putting rab GTPases in the right place. *J Biol Chem.* 270:17057-9.
- Pfeffer, S.R., and J.E. Rothman. 1987. Biosynthetic protein transport and sorting by the endoplasmic reticulum and Golgi. *Annu Rev Biochem.* 56:829-52.
- Pind, S.N., C. Nuoffer, J.M. McCaffery, H. Plutner, H.W. Davidson, M.G. Farquhar, and W.E. Balch. 1994. Rab1 and Ca²⁺ are required for the fusion of carrier vesicles mediating endoplasmic reticulum to Golgi transport. *J Cell Biol.* 125:239-52.
- Porter, K.R., A. Claude, and E.F. Fullam. 1945. A Study of Tissue Culture Cells by Electron Microscopy. *J. Exp. Med.* 81:233-246.
- Praekelt, U.M., and P.A. Meacock. 1990. HSP12, a new small heat shock gene of *Saccharomyces cerevisiae*: analysis of structure, regulation and function. *Mol Gen Genet.* 223:97-106.
- Presley, J.F., N.B. Cole, T.A. Schroer, K. Hirschberg, K.J. Zaal, J. Lippincott-Schwartz. 1997. ER-to-Golgi transport visualized in living cells. *Nature.* 389:81-5.
- Presley, J.F., T.H. Ward, A.C. Pfeifer, E.D. Siggia, R.D. Phair, and J. Lippincott-Schwartz. 2002. Dissection of COPI and Arf1 dynamics in vivo and role in Golgi membrane transport. *Nature.* 417:187-93.
- Preuss, D., J. Mulholland, A. Franzusoff, N. Segev, and D. Botstein. 1992. Characterization of the *Saccharomyces* Golgi complex through the cell cycle by immunoelectron microscopy. *Mol Biol Cell.* 3:789-803.
- Preuss, D., J. Mulholland, C.A. Kaiser, P. Orlean, C. Albright, M.D. Rose, P.W. Robbins, and D. Botstein. 1991. Structure of the yeast endoplasmic reticulum: localization of ER proteins using immunofluorescence and immunoelectron microscopy. *Yeast.* 7:891-911.
- Pryer, N.K., L.J. Wuestehube, and R. Schekman. 1992. Vesicle-mediated protein

- sorting. *Annu Rev Biochem.* 61:471-516.
- Rabouille, C., N. Hui, F. Hunte, R. Kieckbusch, E.G. Berger, G. Warren, and T. Nilsson. 1995. Mapping the distribution of Golgi enzymes involved in the construction of complex oligosaccharides. *J Cell Sci.* 108 (Pt 4):1617-27.
- Rambourg, A., and Y. Clermont. 1990. Three-dimensional electron microscopy: structure of the Golgi apparatus. *Eur J Cell Biol.* 51:189-200.
- Rambourg, A., Y. Clermont, and L. Hermo. 1979. Three-dimensional architecture of the golgi apparatus in Sertoli cells of the rat. *Am J Anat.* 154:455-76.
- Rambourg, A., Y. Clermont, and F. Kepes. 1993. Modulation of the Golgi apparatus in *Saccharomyces cerevisiae* sec7 mutants as seen by three-dimensional electron microscopy. *Anat Rec.* 237:441-52.
- Rambourg, A., Y. Clermont, J.M. Nicaud, C. Gaillardin, and F. Kepes. 1996. Transformations of membrane-bound organelles in sec 14 mutants of the yeasts *Saccharomyces cerevisiae* and *Yarrowia lipolytica*. *Anat Rec.* 245:447-58.
- Rambourg, A., Y. Clermont, L. Ovtracht, and F. Kepes. 1995. Three-dimensional structure of tubular networks, presumably Golgi in nature, in various yeast strains: a comparative study. *Anat Rec.* 243:283-93.
- Rapoport, T.A., B. Jungnickel, and U. Kutay. 1996. Protein transport across the eukaryotic endoplasmic reticulum and bacterial inner membranes. *Annu Rev Biochem.* 65:271-303.
- Raschke, W.C., K.A. Kern, C. Antalis, and C.E. Ballou. 1973. Genetic control of yeast mannan structure. Isolation and characterization of mannan mutants. *J Biol Chem.* 248:4660-6.
- Rayner, J.C., and S. Munro. 1998. Identification of the MNN2 and MNN5 mannosyltransferases required for forming and extending the mannose branches of the outer chain mannans of *Saccharomyces cerevisiae*. *J Biol Chem.* 273:26836-43.
- Reaven, E., L. Tsai, B. Maffe, and S. Azhar. 1993. Effect of okadaic acid on hepatocyte structure and function. *Cell Mol Biol Res.* 39:275-88.
- Roberts CJ, Nelson B, Marton MJ, Stoughton R, Meyer MR, Bennett HA, He YD,

- Dai H, Walker WL, Hughes TR, Tyers M, Boone C, Friend SH. Signaling and circuitry of multiple MAPK pathways revealed by a matrix of global gene expression profiles. *Science*. 2000 Feb 4;287(5454):873-80.
- Rodwell, V.W., J.L. Nordstrom, and J.J. Mitschelen. 1976. Regulation of HMG-CoA reductase. *Adv Lipid Res*. 14:1-74.
- Rogalski, A.A., and S.J. Singer. 1984. Associations of elements of the Golgi apparatus with microtubules. *J Cell Biol*. 99:1092-100.
- Rojo, M., G. Emery, V. Marjomaki, A.W. McDowall, R.G. Parton, and J. Gruenberg. 2000. The transmembrane protein p23 contributes to the organization of the Golgi apparatus. *J Cell Sci*. 113:1043-57.
- Rojo, M., R. Pepperkok, G. Emery, R. Kellner, E. Stang, R.G. Parton, and J. Gruenberg. 1997. Involvement of the transmembrane protein p23 in biosynthetic protein transport. *J Cell Biol*. 139:1119-35.
- Rosa, P., S. Mantovani, R. Rosboch, and W.B. Huttner. 1992. Monensin and brefeldin A differentially affect the phosphorylation and sulfation of secretory proteins. *J Biol Chem*. 267:12227-32.
- Rose, J.K., and R.W. Doms. 1988. Regulation of protein export from the endoplasmic reticulum. *Annu Rev Cell Biol*. 4:257-88.
- Rose, M.D., L.M. Misra, and J.P. Vogel. 1989. KAR2, a karyogamy gene, is the yeast homolog of the mammalian BiP/GRP78 gene. *Cell*. 57:1211-21.
- Rossanese, O.W., J. Soderholm, B.J. Bevis, I.B. Sears, J. O'Connor, E.K. Williamson, and B.S. Glick. 1999. Golgi structure correlates with transitional endoplasmic reticulum organization in *Pichia pastoris* and *Saccharomyces cerevisiae*. *J Cell Biol*. 145:69-81.
- Rothman, J.E. 1987. Protein sorting by selective retention in the endoplasmic reticulum and Golgi stack. *Cell*. 50:521-2.
- Rothman, J.E. 1994. Mechanisms of intracellular protein transport. *Nature*. 372:55-63.
- Rothman, J.E., and L. Orci. 1992. Molecular dissection of the secretory pathway. *Nature*. 355:409-15.

- Rothman, J.E., and G. Warren. 1994. Implications of the SNARE hypothesis for intracellular membrane topology and dynamics. *Curr Biol.* 4:220-33.
- Rothman, J.E., and F.T. Wieland. 1996. Protein sorting by transport vesicles. *Science.* 272:227-34.
- Rotter, J., R.P. Kuiper, G. Bouw, and G.J. Martens. 2002. Cell-type-specific and selectively induced expression of members of the p24 family of putative cargo receptors. *J Cell Sci.* 115:1049-58.
- Roy, L., J.J. Bergeron, C. Lavoie, R. Hendriks, J. Gushue, A. Fazel, A. Pelletier, D.J. Morre, V.N. Subramaniam, W. Hong, and J. Paiement. 2000. Role of p97 and syntaxin 5 in the assembly of transitional endoplasmic reticulum. *Mol Biol Cell.* 11:2529-42.
- Salama, N.R., and R.W. Schekman. 1995. The role of coat proteins in the biosynthesis of secretory proteins. *Curr Opin Cell Biol.* 7:536-43.
- Salama, N.R., T. Yeung, and R.W. Schekman. 1993. The Sec13p complex and reconstitution of vesicle budding from the ER with purified cytosolic proteins. *Embo J.* 12:4073-82.
- Sapperstein, S.K., V.V. Lupashin, H.D. Schmitt, and M.G. Waters. 1996. Assembly of the ER to Golgi SNARE complex requires Usa1p. *J Cell Biol.* 132:755-67.
- Saraste, J., and E. Kuismanen. 1992. Pathways of protein sorting and membrane traffic between the rough endoplasmic reticulum and the Golgi complex. *Semin Cell Biol.* 3:343-55.
- Sata, M., J.G. Donaldson, J. Moss, and M. Vaughan. 1998. Brefeldin A-inhibited guanine nucleotide-exchange activity of Sec7 domain from yeast Sec7 with yeast and mammalian ADP ribosylation factors. *Proc Natl Acad Sci U S A.* 95:4204-8.
- Scales, S.J., R. Pepperkok, and T.E. Kreis. 1997. Visualization of ER-to-Golgi transport in living cells reveals a sequential mode of action for COPII and COPI. *Cell.* 90:1137-48.
- Scheele, G., and A. Tartakoff. 1985. Exit of nonglycosylated secretory proteins from the rough endoplasmic reticulum is asynchronous in the exocrine

- pancreas. *J Biol Chem.* 260:926-31.
- Schekman, R. 1985. Protein localization and membrane traffic in yeast. *Annu Rev Cell Biol.* 1:115-43.
- Schekman, R., and L. Orci. 1996. Coat proteins and vesicle budding. *Science.* 271:1526-33.
- Scheuner, D., B. Song, E. McEwen, C. Liu, R. Laybutt, P. Gillespie, T. Saunders, S. Bonner-Weir, and R.J. Kaufman. 2001. Translational control is required for the unfolded protein response and in vivo glucose homeostasis. *Mol Cell.* 7:1165-76.
- Schimmoller, F., B. Singer-Kruger, S. Schroder, U. Kruger, C. Barlowe, and H. Riezman. 1995. The absence of Emp24p, a component of ER-derived COPII-coated vesicles, causes a defect in transport of selected proteins to the Golgi. *Embo J.* 14:1329-39.
- Schunck, W.H., F. Vogel, B. Gross, E. Kargel, S. Mauersberger, K. Kopke, C. Gengnagel, and H.G. Muller. 1991. Comparison of two cytochromes P-450 from *Candida maltosa*: primary structures, substrate specificities and effects of their expression in *Saccharomyces cerevisiae* on the proliferation of the endoplasmic reticulum. *Eur J Cell Biol.* 55:336-45.
- Schweizer, A., J.A. Fransen, K. Matter, T.E. Kreis, L. Ginsel, and H.P. Hauri. 1990. Identification of an intermediate compartment involved in protein transport from endoplasmic reticulum to Golgi apparatus. *Eur J Cell Biol.* 53:185-96.
- Schweizer, A., K. Matter, C.M. Ketcham, and H.P. Hauri. 1991. The isolated ER-Golgi intermediate compartment exhibits properties that are different from ER and cis-Golgi. *J Cell Biol.* 113:45-54.
- Schwikowski, B., P. Uetz, and S. Fields. 2000. A network of protein-protein interactions in yeast. *Nat Biotechnol.* 18:1257-61.
- Segev, N. 2001. Ypt and Rab GTPases: insight into functions through novel interactions. *Curr Opin Cell Biol.* 13:500-11.
- Semenza, J.C., K.G. Hardwick, N. Dean, and H.R. Pelham. 1990. ERD2, a yeast gene required for the receptor-mediated retrieval of luminal ER proteins

- from the secretory pathway. *Cell*. 61:1349-57.
- Serafini, T., L. Orci, M. Amherdt, M. Brunner, R.A. Kahn, and J.E. Rothman. 1991b. ADP-ribosylation factor is a subunit of the coat of Golgi-derived COP- coated vesicles: a novel role for a GTP-binding protein. *Cell*. 67:239-53.
- Serafini, T., G. Stenbeck, A. Brecht, F. Lottspeich, L. Orci, J.E. Rothman, and F.T. Wieland. 1991a. A coat subunit of Golgi-derived non-clathrin-coated vesicles with homology to the clathrin-coated vesicle coat protein beta-adaptin. *Nature*. 349:215-20.
- Shapiro, D.J., and V.W. Rodwell. 1971. Regulation of hepatic 3-hydroxy-3-methylglutaryl coenzyme A reductase and cholesterol synthesis. *J Biol Chem*. 246:3210-6.
- Shapiro, D.J., and V.W. Rodwell. 1971. Regulation of hepatic 3-hydroxy-3-methylglutaryl coenzyme A reductase and cholesterol synthesis. *J Biol Chem*. 246:3210-6.
- Shaywitz, D.A., L. Orci, M. Ravazzola, A. Swaroop, and C.A. Kaiser. 1995. Human SEC13Rp functions in yeast and is located on transport vesicles budding from the endoplasmic reticulum. *J Cell Biol*. 128:769-77.
- Shima, D.T., S.J. Scales, T.E. Kreis, and R. Pepperkok. 1999. Segregation of COPI-rich and anterograde-cargo-rich domains in endoplasmic-reticulum-to-Golgi transport complexes. *Curr Biol*. 9:821-4.
- Siddhanta, A., J.M. Backer, and D. Shields. 2000. Inhibition of phosphatidic acid synthesis alters the structure of the Golgi apparatus and inhibits secretion in endocrine cells. *J Biol Chem*. 275:12023-31.
- Sil, A.K., P. Xin, and J.E. Hopper. 2000. Vectors allowing amplified expression of the *Saccharomyces cerevisiae* Gal3p-Gal80p-Gal4p transcription switch: applications to galactose-regulated high-level production of proteins. *Protein Expr Purif*. 18:202-12.
- Singer-Kruger, B., R. Frank, F. Crausaz, and H. Riezman. 1993. Partial purification and characterization of early and late endosomes from yeast. Identification of four novel proteins. *J Biol Chem*. 268:14376-86.

- Sipos, G., A. Puoti, and A. Conzelmann. 1995. Biosynthesis of the side chain of yeast glycosylphosphatidylinositol anchors is operated by novel mannosyltransferases located in the endoplasmic reticulum and the Golgi apparatus. *J Biol Chem.* 270:19709-15.
- Sitia, R., and J. Meldolesi. 1992. Endoplasmic reticulum: a dynamic patchwork of specialized subregions. *Mol Biol Cell.* 3:1067-72.
- Skehel, J.J., and D.C. Wiley. 1998. Coiled coils in both intracellular vesicle and viral membrane fusion. *Cell.* 95:871-4.
- Small, J.V. 1968. Measurement of section thickness. In *Proceedings of the 4th European Congress on Electron Microscopy*. Vol. 1. D.S. Bocciarelli, ed. Tipographia Poliglotta Vaticana, Rome. p 609.
- Sohn, K., L. Orci, M. Ravazzola, M. Amherdt, M. Bremser, F. Lottspeich, K. Fiedler, J.B. Helms, and F.T. Wieland. 1996. A major transmembrane protein of Golgi-derived COPI-coated vesicles involved in coatomer binding. *J Cell Biol.* 135:1239-48.
- Sollner, T., M.K. Bennett, S.W. Whiteheart, R.H. Scheller, and J.E. Rothman. 1993. A protein assembly-disassembly pathway in vitro that may correspond to sequential steps of synaptic vesicle docking, activation, and fusion. *Cell.* 75:409-18.
- Spellman, P.T., G. Sherlock, M.Q. Zhang, V.R. Iyer, K. Anders, M.B. Eisen, P.O. Brown, D. Botstein, and B. Futcher. 1998. Comprehensive identification of cell cycle-regulated genes of the yeast *Saccharomyces cerevisiae* by microarray hybridization. *Mol Biol Cell.* 9:3273-97.
- Springer, S., E. Chen, R. Duden, M. Marzioch, A. Rowley, S. Hamamoto, S. Merchant, and R. Schekman. 2000. The p24 proteins are not essential for vesicular transport in *Saccharomyces cerevisiae*. *Proc Natl Acad Sci U S A.* 97:4034-9.
- Stamnes, M.A., M.W. Craighead, M.H. Hoe, N. Lampen, S. Geromanos, P. Tempst, and J.E. Rothman. 1995. An integral membrane component of coatomer-coated transport vesicles defines a family of proteins involved in budding. *Proc Natl Acad Sci U S A.* 92:8011-5.

- Steegmaier, M., V. Oorschot, J. Klumperman, and R.H. Scheller. 2000. Syntaxin 17 is abundant in steroidogenic cells and implicated in smooth endoplasmic reticulum membrane dynamics. *Mol Biol Cell*. 11:2719-31.
- Stenbeck, G., C. Harter, A. Brecht, D. Herrmann, F. Lottspeich, L. Orci, and F.T. Wieland. 1993. beta'-COP, a novel subunit of coatamer. *Embo J*. 12:2841-5.
- Storrie, B., and T. Nilsson. 2002. The Golgi apparatus: balancing new with old. *Traffic*. 3:521-9.
- Stratford, M. 1992. Yeast flocculation: receptor definition by mnn mutants and concanavalin A. *Yeast*. 8:635-45.
- Subramaniam, V.N., E. Loh, and W. Hong. 1997. N-Ethylmaleimide-sensitive factor (NSF) and alpha-soluble NSF attachment proteins (SNAP) mediate dissociation of GS28-syntaxin 5 Golgi SNAP receptors (SNARE) complex. *J Biol Chem*. 272:25441-4.
- Sundaram, M., and I. Greenwald. 1993. Suppressors of a lin-12 hypomorph define genes that interact with both lin-12 and glp-1 in *Caenorhabditis elegans*. *Genetics*. 135:765-83.
- Sutton, R.B., D. Fasshauer, R. Jahn, and A.T. Brunger. 1998. Crystal structure of a SNARE complex involved in synaptic exocytosis at 2.4 Å resolution. *Nature*. 395:347-53.
- Sweeney, D.A., A. Siddhanta, and D. Shields. 2002. Fragmentation and re-assembly of the Golgi apparatus in vitro. A requirement for phosphatidic acid and phosphatidylinositol 4,5-bisphosphate synthesis. *J Biol Chem*. 277:3030-9.
- Swift, L.L. 1996. Role of the Golgi apparatus in the phosphorylation of apolipoprotein B. *J Biol Chem*. 271:31491-5.
- Tabas, I., and S. Kornfeld. 1979. Purification and characterization of a rat liver Golgi alpha- mannosidase capable of processing asparagine-linked oligosaccharides. *J Biol Chem*. 254:11655-63.
- Tachibana, C., and T.H. Stevens. 1992. The yeast EUG1 gene encodes an endoplasmic reticulum protein that is functionally related to protein

- disulfide isomerase. *Mol Cell Biol.* 12:4601-11.
- Tachikawa, H., Y. Takeuchi, W. Funahashi, T. Miura, X.D. Gao, D. Fujimoto, T. Mizunaga, and K. Onodera. 1995. Isolation and characterization of a yeast gene, MPD1, the overexpression of which suppresses inviability caused by protein disulfide isomerase depletion. *FEBS Lett.* 369:212-6.
- Takizawa, P.A., J.K. Yucel, B. Veit, D.J. Faulkner, T. Deerinck, G. Soto, M. Ellisman, and V. Malhotra. 1993. Complete vesiculation of Golgi membranes and inhibition of protein transport by a novel sea sponge metabolite, ilimaquinone. *Cell.* 73:1079-90.
- Tanigawa, G., L. Orci, M. Amherdt, M. Ravazzola, J.B. Helms, and J.E. Rothman. 1993. Hydrolysis of bound GTP by ARF protein triggers uncoating of Golgi- derived COP-coated vesicles. *J Cell Biol.* 123:1365-71.
- Thorne-Tjomsland, G., M. Dumontier, and J.C. Jamieson. 1998. 3D topography of noncompact zone Golgi tubules in rat spermatids: a computer-assisted serial section reconstruction study. *Anat Rec.* 250:381-96.
- Tisdale, E.J., H. Plutner, J. Matteson, and W.E. Balch. 1997. p53/58 binds COPI and is required for selective transport through the early secretory pathway. *J Cell Biol.* 137:581-93.
- Toh-e, A., S. Yasunaga, H. Nisogi, K. Tanaka, T. Oguchi, and Y. Matsui. 1993. Three yeast genes, PIR1, PIR2 and PIR3, containing internal tandem repeats, are related to each other, and PIR1 and PIR2 are required for tolerance to heat shock. *Yeast.* 9:481-94.
- Tokuyasu, K.T. 1980. Immunocytochemistry on ultrathin frozen sections. *Histochem J.* 12:381-403.
- Townsley, F.M., and H.R. Pelham. 1994. The KKXX signal mediates retrieval of membrane proteins from the Golgi to the ER in yeast. *Eur J Cell Biol.* 64:211-6.
- Travers, K.J., C.K. Patil, L. Wodicka, D.J. Lockhart, J.S. Weissman, and P. Walter. 2000. Functional and genomic analyses reveal an essential coordination between the unfolded protein response and ER-associated

- degradation. *Cell*. 101:249-58.
- Trimble, R.B., and P.H. Atkinson. 1986. Structure of yeast external invertase Man8-14GlcNAc processing intermediates by 500-megahertz ¹H NMR spectroscopy. *J Biol Chem*. 261:9815-24.
- Trombetta, E.S., and A. Helenius. 1998. Lectins as chaperones in glycoprotein folding. *Curr Opin Struct Biol*. 8:587-92.
- Trower, M.K., S.M. Orton, I.J. Purvis, P. Sanseau, J. Riley, C. Christodoulou, D. Burt, C.G. See, G. Elgar, R. Sherrington, E.I. Rogaev, P. St George-Hyslop, S. Brenner, and C.W. Dykes. 1996. Conservation of synteny between the genome of the pufferfish (*Fugu rubripes*) and the region on human chromosome 14 (14q24.3) associated with familial Alzheimer disease (AD3 locus). *Proc Natl Acad Sci U S A*. 93:1366-9.
- Tulsiani, D.R., S.C. Hubbard, P.W. Robbins, and O. Touster. 1982. alpha-D-Mannosidases of rat liver Golgi membranes. Mannosidase II is the GlcNAcMAN5-cleaving enzyme in glycoprotein biosynthesis and mannosidases Ia and IB are the enzymes converting Man9 precursors to Man5 intermediates. *J Biol Chem*. 257:3660-8.
- Tyson, J.R., and C.J. Stirling. 2000. LHS1 and SIL1 provide a luminal function that is essential for protein translocation into the endoplasmic reticulum. *Embo J*. 19:6440-52.
- Uetz, P., L. Giot, G. Cagney, T.A. Mansfield, R.S. Judson, J.R. Knight, D. Lockshon, V. Narayan, M. Srinivasan, P. Pochart, A. Qureshi-Emili, Y. Li, B. Godwin, D. Conover, T. Kalbfleisch, G. Vijayadamodar, M. Yang, M. Johnston, S. Fields, and J.M. Rothberg. 2000. A comprehensive analysis of protein-protein interactions in *Saccharomyces cerevisiae*. *Nature*. 403:623-7.
- Umebayashi K, Hirata A, Fukuda R, Horiuchi H, Ohta A, Takagi M. 1997. Accumulation of misfolded protein aggregates leads to the formation of Russell body-like dilated endoplasmic reticulum in yeast. *Yeast*. 13:1009-20.
- van Meer, G. 1993. Transport and sorting of membrane lipids. *Curr Opin Cell*

Biol. 5:661-73.

- van Meer, G. 1998. Lipids of the Golgi membrane. *Trends Cell Biol.* 8:29-33.
- Varela, J.C., U.M. Praekelt, P.A. Meacock, R.J. Planta, and W.H. Mager. 1995. The *Saccharomyces cerevisiae* HSP12 gene is activated by the high-osmolarity glycerol pathway and negatively regulated by protein kinase A. *Mol Cell Biol.* 15:6232-45.
- Varela, J.C., C. van Beekvelt, R.J. Planta, and W.H. Mager. 1992. Osmostress-induced changes in yeast gene expression. *Mol Microbiol.* 6:2183-90.
- Varki, A. 1993. Biological roles of oligosaccharides: all of the theories are correct. *Glycobiology.* 3:97-130.
- Vegh, M., and A. Varro. 1997. Phosphorylation of gastrin-related peptides: physiological casein kinase like enzyme in Golgi membranes from bovine adrenal chromaffin cells and GH3 cells. *Regul Pept.* 68:37-43.
- Vergeres, G., T.S. Yen, J. Aggeler, J. Lausier, and L. Waskell. 1993. A model system for studying membrane biogenesis. Overexpression of cytochrome b5 in yeast results in marked proliferation of the intracellular membrane. *J Cell Sci.* 106:249-59.
- Wada, I., D. Rindress, P.H. Cameron, W.J. Ou, J.J. Doherty, 2nd, D. Louvard, A.W. Bell, D. Dignard, D.Y. Thomas, and J.J. Bergeron. 1991. SSR alpha and associated calnexin are major calcium binding proteins of the endoplasmic reticulum membrane. *J Biol Chem.* 266:19599-610.
- Walter, P., and G. Blobel. 1983. Preparation of microsomal membranes for cotranslational protein translocation. *Methods Enzymol.* 96:84-93.
- Walter, P., and A.E. Johnson. 1994. Signal sequence recognition and protein targeting to the endoplasmic reticulum membrane. *Annu Rev Cell Biol.* 10:87-119.
- Wang, X.H., K. Nakayama, Y. Shimma, A. Tanaka, and Y. Jigami. 1997. MNN6, a member of the KRE2/MNT1 family, is the gene for mannosylphosphate transfer in *Saccharomyces cerevisiae*. *J Biol Chem.* 272:18117-24.
- Wanker, E.E., Y. Sun, A.J. Savitz, and D.I. Meyer. 1995. Functional characterization of the 180-kD ribosome receptor in vivo. *J Cell Biol.*

130:29-39.

- Warren, G. 1987. Protein transport. Signals and salvage sequences. *Nature*. 327:17-8.
- Waters, M.G., E.A. Evans, and G. Blobel. 1988. Prepro-alpha-factor has a cleavable signal sequence. *J Biol Chem*. 263:6209-14.
- Waters, M.G., T. Serafini, and J.E. Rothman. 1991. 'Coatomer': a cytosolic protein complex containing subunits of non- clathrin-coated Golgi transport vesicles. *Nature*. 349:248-51.
- Weibel, E. R. 1979. Stereological Methods. Practical Methods for Biological Morphometry. Academic Press, London.
- Weidler, M., C. Reinhard, G. Friedrich, F.T. Wieland, and P. Rosch. 2000. Structure of the cytoplasmic domain of p23 in solution: implications for the formation of COPI vesicles. *Biochem Biophys Res Commun*. 271:401-8.
- Weiner, J.H., B.D. Lemire, M.L. Elmes, R.D. Bradley, and D.G. Scraba. 1984. Overproduction of fumarate reductase in Escherichia coli induces a novel intracellular lipid-protein organelle. *J Bacteriol*. 158:590-6.
- Wen, C., and I. Greenwald. 1999. p24 proteins and quality control of LIN-12 and GLP-1 trafficking in Caenorhabditis elegans. *J Cell Biol*. 145:1165-75.
- Whiteway, M., L. Hougan, and D.Y. Thomas. 1990. Overexpression of the STE4 gene leads to mating response in haploid Saccharomyces cerevisiae. *Mol Cell Biol*. 10:217-22.
- Wiggins, C.A., and S. Munro. 1998. Activity of the yeast MNN1 alpha-1,3-mannosyltransferase requires a motif conserved in many other families of glycosyltransferases. *Proc Natl Acad Sci U S A*. 95:7945-50.
- Williams, D.B., S.J. Swiedler, and G.W. Hart. 1985. Intracellular transport of membrane glycoproteins: two closely related histocompatibility antigens differ in their rates of transit to the cell surface. *J Cell Biol*. 101:725-34.
- Wilson, D.W., M.J. Lewis, and H.R. Pelham. 1993. pH-dependent binding of KDEL to its receptor in vitro. *J Biol Chem*. 268:7465-8.
- Wilson, D.W., C.A. Wilcox, G.C. Flynn, E. Chen, W.J. Kuang, W.J. Henzel,

- M.R. Block, A. Ullrich, and J.E. Rothman. 1989. A fusion protein required for vesicle-mediated transport in both mammalian cells and yeast. *Nature*. 339:355-9.
- Wong, H.N., M.A. Ward, A.W. Bell, E. Chevet, S. Bains, W.P. Blackstock, R. Solari, D.Y. Thomas, and J.J. Bergeron. 1998. Conserved in vivo phosphorylation of calnexin at casein kinase II sites as well as a protein kinase C/proline-directed kinase site. *J Biol Chem*. 273:17227-35.
- Wooding, S., and H.R. Pelham. 1998. The dynamics of golgi protein traffic visualized in living yeast cells. *Mol Biol Cell*. 9:2667-80.
- Wright, R., M. Basson, L. D'Ari, and J. Rine. 1988. Increased amounts of HMG-CoA reductase induce "karmellae": a proliferation of stacked membrane pairs surrounding the yeast nucleus. *J Cell Biol*. 107:101-14.
- Wuestehube, L.J., R. Duden, A. Eun, S. Hamamoto, P. Korn, R. Ram, and R. Schekman. 1996. New mutants of *Saccharomyces cerevisiae* affected in the transport of proteins from the endoplasmic reticulum to the Golgi complex. *Genetics*. 142:393-406.
- Yip, C.L., S.K. Welch, F. Klebl, T. Gilbert, P. Seidel, F.J. Grant, P.J. O'Hara, and V.L. MacKay. 1994. Cloning and analysis of the *Saccharomyces cerevisiae* MNN9 and MNN1 genes required for complex glycosylation of secreted proteins. *Proc Natl Acad Sci U S A*. 91:2723-7.
- Young, B.P., R.A. Craven, P.J. Reid, M. Willer, and C.J. Stirling. 2001. Sec63p and Kar2p are required for the translocation of SRP-dependent precursors into the yeast endoplasmic reticulum in vivo. *Embo J*. 20:262-71.
- Zapun, A., N.J. Darby, D.C. Tessier, M. Michalak, J.J. Bergeron, and D.Y. Thomas. 1998. Enhanced catalysis of ribonuclease B folding by the interaction of calnexin or calreticulin with ERp57. *J Biol Chem*. 273:6009-12.
- Zapun, A., C.A. Jakob, D.Y. Thomas, and J.J. Bergeron. 1999. Protein folding in a specialized compartment: the endoplasmic reticulum. *Structure Fold Des*. 7:R173-82.
- Zapun, A., S.M. Petrescu, P.M. Rudd, R.A. Dwek, D.Y. Thomas, and J.J.

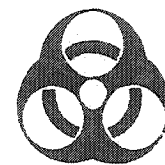
- Bergeron. 1997. Conformation-independent binding of monoglucosylated ribonuclease B to calnexin. *Cell*. 88:29-38.
- Zerial, M., and H. McBride. 2001. Rab proteins as membrane organizers. *Nat Rev Mol Cell Biol*. 2:107-17.
- Zhang, L., C.L. Ashendel, G.W. Becker, and D.J. Morre. 1994. Isolation and characterization of the principal ATPase associated with transitional endoplasmic reticulum of rat liver. *J Cell Biol*. 127:1871-83.
- Zhang, T., S.H. Wong, B.L. Tang, Y. Xu, and W. Hong. 1999. Morphological and functional association of Sec22b/ERS-24 with the pre- Golgi intermediate compartment. *Mol Biol Cell*. 10:435-53.

Appendix 1.



McGill University

University Biohazards Committee



APPLICATION TO USE BIOHAZARDOUS MATERIALS*

No project should be commenced without prior approval of an application to use biohazardous materials. Submit this application to the Chair, Biohazards Committee, one month before starting new projects or expiry of a previously approved application.

1. PRINCIPAL INVESTIGATOR: Dr. J.J.M. Bergeron TELEPHONE: _____
ADDRESS: 8 FAX NUMBER _____
DEPARTMENT: Anatomy and Cell Biology E-MAIL: _____
PROJECT TITLE: The Molecular Cytology of Membrane Dynamics

2. FUNDING SOURCE: MRC ☒ NSERC _____ NIH _____ FCAR _____ FRSQ _____
INTERNAL _____ OTHER _____ (specify) _____
Grant No.: MT 5605 Beginning date July 1, 1998 End date June 30, 2003

3. Indicate if this is
- ☐ Renewal use application: procedures have been previously approved and no alterations have been made to the protocol.
Approval End Date _____
 - ☐ New funding source: project previously reviewed and approved under an application to another agency.
Agency _____ Approval End Date _____
 - ☒ New project: project not previously reviewed or procedures and/or microorganism altered from previously approved application.

CERTIFICATION STATEMENT: The Biohazards Committee approves the experimental procedures proposed and certifies with the applicant that the experiment will be in accordance with the principles outlined in the "Laboratory Biosafety Guidelines" prepared by Health Canada and the MRC, and in the "McGill Laboratory Biosafety Manual".

Containment Level (circle 1): 1 (2)

Principal Investigator or course director: _____ date: 04 MARCH 1998
day month year

Chairperson, Biohazards Committee: _____ date: 9 March 98
day month year

Approved period: _____ beginning 9 March 98 ending 30 June 2003
day month year day month year

* as defined in the "McGill Laboratory Biosafety manual"



McGill University
Animal Use Protocol – Research
Guidelines for completing the form are available at
www.mcgill.ca/rgo/animal

Protocol #: 3920
Investigator #: 237
Approval End Date: June 30, 2003
Facility Committee: MCO

☐ Pilot ☐ New Application ☒ Renewal of Protocol # 3920

Title The Molecular Cytology of Membrane Dynamics
(must match the title of the funding source application)

1. Investigator Data:

Principal Investigator: John J.M. Bergeron Office #: _____
Department: Anatomy and Cell Biology Fax#: 398-5047
Address: _____ Email: _____

2. Emergency Contacts: Two people must be designated to handle emergencies.

Name: Pamela Cameron Work #: _____ Emergency #: _____
Name: Ali Fazal Work #: _____ Emergency #: _____

3. Funding Source:

External ☒
Source (s): Canadian Institutes of Health Research

Peer Reviewed: ☒ YES ☐ NO**

Status: ☒ Awarded ☐ Pending

Funding period: July 1, 1998 to Sept 30, 2003

Internal ☐
Source (s): _____

Peer Reviewed: ☐ YES ☐ NO**

Status: ☐ Awarded ☐ Pending

Funding period: _____

ACTION	✓	DATE
P.I.	✓	Oct 16 03
FACC	✓	7
RGD	✓	7
VET	✓	1
DB		
Approved		

** All projects that have not been peer reviewed for scientific merit by the funding source require 2 Peer Review Forms to be completed.
e.g. Projects funded from industrial sources. Peer Review Forms are available at www.mcgill.ca/fgsr/rgo/animal/

Proposed Start Date of Animal Use (d/m/y): _____ or ongoing ☒

Expected Date of Completion of Animal Use (d/m/y): _____ or ongoing ☒

Investigator's Statement: The information in this application is exact and complete. I assure that all care and use of animals in this proposal will be in accordance with the guidelines and policies of the Canadian Council on Animal Care and those of McGill University. I shall request the Animal Care Committee's approval prior to any deviations from this protocol as approved. I understand that this approval is valid for one year and must be approved on an annual basis.

Principal Investigator's signature: _____

Date: Mar. 20/02

Approval Signatures:

Chair, Facility Animal Care Committee:

Date: 11/4/02

University Veterinarian:

Date: 21/12/02

Chair, Ethics Subcommittee(as per UACC policy):

Date: _____

Approved Period for Animal Use

Beginning: July 1, 2002

Ending: June 30, 2003

☐ This protocol has been approved with the modifications noted in Section 13.

APR 16 2002

296

McGill University Internal Radioisotope Permit

20010194

Permit Holder & Position BERGERON, JOHN DR., PROFESSOR &	Building (Office) STRATHCONA BUILDING	Building (Lab) STRATHCONA BUILDING	PLEASE POST	Date Issued 2000/09/01
Department ANATOMY & CELL BIOLOGY	Room Number(s) MZ/9	Room Number(s) MZ1-16		Expiry Date 2001/08/31

PERSON(S) APPROVED TO WORK WITH RADIOISOTOPES

Name	Cond(s)	Class(es)	Radioisotope(s)
ALI FAZEL, RESEARCH ASSISTANT	1, 2, 4	4, 2, 3	P-32, I-125, S-35, C-14, H-3
PAMELA CAMERON, TECHNICIAN	1, 2, 4	4, 2, 3	P-32, I-125, S-35, C-14, H-3, Ca-45
J.J.M. BERGERON, PROFESSOR	1, 2, 4	1	P-32, I-125, S-35, H-3, Ca-45, C-14
ERIC CHEVET, POST-DOC	1, 2, 4	4, 2, 3	P-32, I-125, S-35, C-14, Ca-45, H-3
SEAN TAYLOR, STUDENT	1, 2, 4	1, 3, 4	P-32, I-125, S-35, C-14, H-3, Ca-45
JENNIFER GUSHUE, STUDENT	1, 2, 4	2, 3, 4	P-32, I-125, S-35, C-14, H-3, Ca-45
MARY DEBINA, LAB ASSISTANT	6	6	
SANDRINE PALCY, POST DOC	1, 2, 4	3, 4	P-32, S-35, C-14, H-3, I-125, Ca-45
LINE ROY, RESEARCH ASSISTANT	1, 2, 4	3, 4	P-32, S-35, C-14, H-3, I-125, Ca-45
BENJAMIN THOMSON, GRADUATE STUDENT	1, 2, 4	3, 4	P-32, S-35, C-14, H-3, I-125, Ca-45
BRETT BURSTEIN, STUDENT	6	6	
SEAN MORAN, STUDENT	1, 2, 4	2, 3, 4	P-32, I-125, S-35, C-14, H-3, Ca-45
ETIENNE ROUSSELLE, STUDENT	1, 2, 4	2, 3, 4	P-32, I-125, S-35, C-14, H-3, Ca-45
JISHENG LIU, RESEARCH ASSISTANT	1, 2, 4	2, 3, 4	P-32, I-125, S-35, C-14, H-3, Ca-45
ROXANA ATANASIU, RESEARCH ASSISTANT	1, 2, 4	2, 3, 4	P-32, I-125, S-35, C-14, H-3, Ca-45

GENERAL LICENCE CONDITIONS (OPEN AND/OR SEALED SOURCES)

- The Licence must be posted in the licensee's premises.
- Handling shall be in accordance with the McGill Radiation Safety Manual and with the requirements of the McGill Radiation Safety Committee.
- The licensee must ensure that all persons mandated to work with radioisotopes be properly trained in radiation safety.
- Laboratories where both radioactive and non-radioactive work are done must have separate areas set aside and clearly identified with radiation warning signs.
- Smoking, eating, drinking, storage of foods or drink and the application of cosmetics and contact lenses are prohibited in areas where radioisotopes are used.
- All procedures involving radioactive materials should be carried out on spill trays or on benches lined with disposable absorbent material.
- Procedures that might produce airborne radioactive contamination should be carried out in a fume hood which is of optimal efficiency. (i.e. free, and to some extent bound I-125)
- When hand or clothing contamination is possible, protective gloves and clothing must be worn.
- After handling radioactive material and especially before leaving the laboratory, personnel must ensure that all parts of their clothes are not contaminated.
- Purchase and disposal of radioisotopes must be documented in a log book.
- For disposal of radioactive waste, consult the McGill Radiation Safety Manual.
- Wipe tests must be made on surfaces and equipment likely to become contaminated with radioactive material. Records of the tests must be properly documented and kept in a log book.
- The Licence must reflect the exact conditions under which radioactive material is used. If changes must be made, contact the Environmental Safety Office at 398-4563.
- The device(s) containing the sealed source(s) listed in this Licence must have an identification label bearing the name and telephone number of the responsible user. A radiation symbol should also be affixed to each device.
- Leak tests must be performed on sealed sources equal to or greater than 50 MBq (1.35mCi).

Approved Unsealed Radioisotope(s) and Location(s)

Isotope	Possession Limit	Stored	Handled
P-32	< 4 GBq (108 mCi)	MZ1, MZ2	MZ1, MZ3, 1/34
I-125	< 400 MBq (11 mCi)	MZ1, MZ2	MZ1, MZ3, MZ11, COLD
S-35	< 4 GBq (108 mCi)	MZ2	MZ1, MZ3, 1/34
C-14	< 40 MBq (1.1 mCi)	MZ2	MZ1, MZ3
H-3	< 4 GBq (108 mCi)	MZ2, MZ3, COLD ROOM	MZ1, MZ3
Ca-45	< 40 MBq (1.1 mCi)	MZ1	MZ1, MZ3

Approved Sealed Radioisotope(s) and Location(s)

Permanently Housed Source(s)				Accessible Source(s)			
Isotope	Activity	Stored	Handled	Isotope	Activity	Stored	Handled
Cs-137	30 uCi	MZ12	MZ12				

Personnel Conditions

- Must be submitted to monthly thyroid bioassays
- Must wear a whole-body film badge.
- Must wear an extremity film badge (ex. ring or wrist)
- Classified as Radiation Worker
- Classified as Atomic Radiation Worker
- Does not work with any isotopes but may be indirectly exposed

Workload Classes

- Work load < 10MBq (270 uCi) of unsealed radioisotopes in open areas.
- Work load < 10MBq (270 uCi) of unsealed radioisotopes in a fume hood.
- Work load > 10MBq (270 uCi) of unsealed radioisotopes in open areas.
- Work load > 10 MBq (270 uCi) of unsealed radioisotopes in a fume hood.
- Work with sealed sources.
- Individual does not work with radioactive sources but normal working conditions involve presence in a room where radioactive material is used or stored.

Joseph V. Piccoli
RSO & Occupational Hygienist
McGill Environmental Safety Office

For: Dr. Pierre Belanger, Chairman
McGill Radiation Safety Committee
Dean and Vice Principal (Research)

Oct 24/2000
Date



ERT TABOR

The Journal of Biological Chemistry

October 24, 2002

Dr Jennifer Gushue
McGill University
Strathcona Anatomy and Dentistry Building
Montreal, Quebec H3A 2B2

Dear Dr. Gushue:

Please note your recent request for copyright permission has been granted for the following:

Vol	Page	Year
276	5152-5165	2001

For future requests, we can be contacted by e-mail at jbc@asbmb.faseb.org. If you have any questions, please contact us at 301-530-7150.

Sincerely yours,

PERMISSION GRANTED
contingent upon obtaining that of the author

for the copyright owner
THE AMERICAN SOCIETY FOR BIOCHEMISTRY
AND MOLECULAR BIOLOGY

The Rockefeller
University Press
1114 First Avenue, 3rd Floor

October 23, 2002

Dr. Jennifer Gushue
3640 University Street
Strathcona Anatomy and Dentistry Bldg.
McGill University
Montreal, Quebec H3A 2B2
CANADA

Dear Dr. Gushue:

We will grant you permission for the print reproduction of JCB-vol:147(7),1457-1472,1999-article; JCB-vol:146(2),285-299,1999-article as referred to in your letter dated October 18, 2002.

Permission is granted for one time use only. Please write to us each time for permission concerning future editions and translations, as we do not grant blanket permissions.

Since you are one of the authors, a credit line is our only requirement.

Please give suitable acknowledgment to the source in the following manner: Reproduced from **The Journal of Cell Biology**, year, vol., pp. by copyright permission of The Rockefeller University Press.

Sincerely yours,

THE JOURNAL OF
CELL BIOLOGY

 Lynette N. Henry
Permissions Coordinator

MOLECULAR BIOLOGY OF THE CELL

PUBLICATIONS OFFICE

EDITOR-IN-CHIEF

Keith Yamamoto

EDITORS

Landy Schekman

Amela Silver

ASSOCIATE EDITORS

Rick Assoian

Lori Bargmann

Mary C. Beckerle

Elizabeth H. Blackburn

Juan Bonifacio

David Botstein

Anthony Bretscher

Elizabeth Craig

Peter N. Devreotes

David Drubin

Thomas D. Fox

Joseph Gall

Reid Gilmore

Mark Ginsberg

Guido Guidotti

Carl-Henrik Heldin

Tim Hunt

Tony Hunter

Richard Hynes

Chris Kaiser

Douglas Koshland

Monty Krieger

Keith Mostov

Vivek Malhotra

Paul T. Matsudaira

J. Richard McIntosh

Elliot Meyerowitz

Marc Mumby

Hugh R.B. Pelham

Suzanne R. Pfeffer

Thomas D. Pollard

John Pringle

Martin Raff

Howard Riezman

Ted Salmon

Martin Schwartz

Mark J. Solomon

Allan Spradling

Tim Stearns

Harold E. Varmus

Peter Walter

Marvin P. Wickens

Mitsuhiro Yanagida

ESSAY EDITORS

Bruce M. Alberts

Thomas D. Pollard

COVER EDITOR

Jennifer Lippincott-Schwartz

VIDEO EDITOR

Jennifer Lippincott-Schwartz

November 5, 2002

Ms. Jennifer Gushue

3640 University Street

Strathcona Anatomy and Dentistry Building

McGill University

Montreal, Quebec

H3A 2B2

Canada

Dear Dr. Gushue:

We are pleased to grant you permission to reprint the article "Role of p97 and syntaxin 5 in the assembly of transitional endoplasmic reticulum", which was published in *Molecular Biology of the Cell*. We require acknowledgment as follows: "Reprinted from *Molecular Biology of the Cell*, (2000, volume 11, pgs. 2529-2542), with permission by the American Society for Cell Biology".

Sincerely,

Liz Haberkorn

Editorial Assistant

Jennifer Gushue
3640 University Street
Strathcona Anatomy and Dentistry Building
McGill University
Montreal, Quebec
H3A 2B2

Dear Ms Gushue

RE: EMBO Journal, Vol. 18: 13, 1999, pp. 3655-66

Chevet et al, 'Phosphorylation by CK2 and MAPK enhances...'

Thank you for your email dated 18th October 2002, requesting permission to reprint the above material. Our permission is granted without fee to reproduce the material, as you are the original author.

Use of the **article** is restricted to republication in your doctoral thesis, available in *print* format only, to be used only in the *English* Language. This permission is limited to this particular use and does not allow you to use it elsewhere or in any other format other than specified above.

Please include a credit line in your publication citing full details of the Oxford University Press publication which is the source of the material and by permission of Oxford University Press or the sponsoring society if this is a society journal.

If the credit line or acknowledgement in our publication indicates that material including any illustrations/figures etc was drawn or modified from an earlier source it will be necessary for you to also clear permission with the original publisher. If this permission has not been obtained, please note that this material cannot be included in your publication/photocopies.

Please do not hesitate to contact me if I can be of any further assistance.

Yours sincerely,

Chris Payne
Journals Rights Assistant
(on behalf of Fiona Willis, Journals Rights Sales Manager)

For an online permissions forms visit our web site at:
<http://www3.oup.co.uk/jnls/permissions/>